An investigation into the transcriptional control of the Schwann cell during differentiation, demyelination and disease.

Peter Arthur-Farraj

A Thesis Submitted for the Degree of Doctor of Philosophy

2008

Department of Cell & Developmental Biology

UCL

ProQuest LLC
789 East Eisenhower Parkway
P.O. Box 1346
Ann Arbor, MI 48106-1346

I, Peter Arthur-Farraj, confirm that the work presented in this thesis is my own. Where information has been derived from other sources, I confirm that this has been indicated in the thesis.

To my parents, Clare and Dler.

ABSTRACT

The generation of mature myelinating and non-myelinating Schwann cells from immature Schwann cells is regulated by signals from the axon. In the absence of axonal signals, for example during nerve injury, Schwann cells will return to an immature-like phenotype. However, Schwann cells retain the ability to re-differentiate after injury, demonstrating remarkable plasticity throughout adult life. Although these cellular transformations are normally beneficial, during diseases of the peripheral nervous system, they are often disrupted producing negative consequences.

In this thesis, I have demonstrated a synergistic relationship between two signals, cyclic adenosine monophosphate (cyclic AMP) and β-neuregulin-1 (NRG1) in inducing myelin differentiation in cultured mouse Schwann cells. Furthermore, I found that the cyclic-AMP response element binding protein (CREB) family of transcription factors are required for this differentiation. Second, I have investigated the role of the transcription factor c-Jun in controlling Schwann cell responses after nerve injury. Using *in vivo* and *in vitro* approaches, I have found that c-Jun is an axonal-regulated injury factor that controls Schwann cell demyelination and dedifferentiation. Furthermore, Schwann cell derived c-Jun is crucial for adequate nerve regeneration and repair after injury. Finally, I investigated the functional properties of a mutant form of the myelin-related transcription factor Egr2 (Krox-20), which leads to severe congenital hypomyelinating neuropathy in humans. I found that mutant Egr2 is not transcriptionally inactive but retains residual wild-type Egr2 functions. More importantly, mutant Egr2 also demonstrates aberrant effects in Schwann cells, enhancing DNA synthesis, both in the presence and absence of the putative axonal mitogen, β-neuregulin 1. This is in stark contrast to wild-type Egr2, which causes withdrawal from the cell cycle.

TABLE OF CONTENTS

LIST OF FIGURES

CHAPTER 1: GENERAL INTRODUCTION

CHAPTER 3: β-neuregulin-1 and cyclic-AMP synergise to induce myelin differentiation in mouse Schwann cells.

CHAPTER 4: The role of c-Jun in the Schwann cell response to peripheral nerve injury.

CHAPTER 5: Investigation of the functional properties of a mutant form of Egr2 (S382R/D383Y) in Schwann cells.

CHAPTER 6: General Discussion

ABBREVIATIONS

ADS	Antibody diluting solution
AP-1	Activator protein-1
AraC	Cytosine arabinoside
ATF	Activating transcription factor
BDNF	Brain-derived neurotrophic factor
β-gal	β-galactosidase
BrdU	Bromodeoxyuridine
BSA	Bovine serum albumin
CAM	Cell adhesion molecule
CHN	Congenital hypomyelinating neuropathy
CMT	Charcot-Marie-Tooth disease
CMV	Cytomegalovirus
CNS	Central nervous system
CNTF	Ciliary neurotrophic factor
CREB	Cyclic AMP response element binding protein
Cx32	Connexin 32
Cyclic AMP	Cyclic adenosine monophosphate
dbcAMP	2'-*O*-dibutyryladenosine 3':5'-cyclicAMP
DM	Defined Medium
DMEM	Dulbecco's modified Eagles medium
DRG	Dorsal root ganglion
ECM	Extracellular matrix
E day	Embryonic day
EGR	Early growth response
Epac	Exchange protein directly activated by cyclic AMP
ERK	Extracellular signal-related kinase
FCS	Foetal calf serum
FGF	Fibroblast growth factor
Gal-C	Galactocerebroside
GAPDH	Glyceraldehyde-3-phosphate dehydrogenase

GDNF	Glial derived neurotrophic factor
GFP	Green fluorescent protein
HS	Horse serum
ICC	Immunocytochemistry
IGF	Insulin-like growth factor
IHC	Immunohistochemistry
IL	Interleukin
iNOS	Inducible Nitric oxide synthase
IP	Intraperitoneal
IPL	Interperiod line
JNK	c-Jun N-terminal kinase
LIF	Leukaemia inhibitory factor
MAG	Myelin associated glycoprotein
MAPK	Mitogen-activated protein kinase
MBP	Myelin basic protein
MCP	Macrophage chemoattractant protein
MDL	Major dense line
MMP	Matrix metalloprotease
NCAM	Neural-cell adhesion molecule
NGF	Nerve growth factor
NRG1	β–Neuregulin 1
NT	Neurotrophin
P_0	Myelin protein zero
p38MAPK	p38 mitogen-activated protein kinase
$p75^{NTR}$	p75 neurotrophin receptor
PBS	Phosphate buffered saline
PCR	Polymerase chain reaction
P day	Postnatal day
PDGF	Platelet derived growth factor
PDL	Poly-D-lysine
PF	Paraformaldehyde
PI3K	Phosphatidylinositol 3-kinase

PKA	Protein kinase A
PLL	Poly-L-lysine
PMP22	Peripheral myelin protein 22
PNS	Peripheral nervous system
SLI	Schmidt Lantermann Incisure
TGF	Transforming growth factor
TNF	Tumour necrosis factor
TUNEL	terminal deoxynucleotidyl transferase-mediated dUTP-biotin nick end labeling
WB	Western blotting
Wld^S	Wallerian degeneration slow

UNITS

bp	base pair
°C	degrees Celcius
kb	kilobase
kDa	kilo Dalton
s	second
g	gram
mg	milligram
µg	microgram
L	litre
ml	millilitre
µl	microlitre
mm	millimetre
µm	micrometre
nm	nanometre
M	molar
mM	millimolar
µM	micromolar

The conventions used in the text

The name of a gene or mRNA appears in *italics* in the text whereas the protein product is written in normal script.

CHAPTER 1: GENERAL INTRODUCTION

1.1 Schwann cells and their origins in peripheral nervous system development.

Schwann cells constitute the major form of glial cell in the mammalian peripheral nervous system (PNS). Other forms of glial cell in the PNS include, satellite cells found in dorsal root ganglia (DRG) and ganglia of the sympathetic and parasympathetic nervous system, olfactory ensheathing cells that associate with axons of the olfactory nerve, terminal glia (teloglia) which are present at the neuromuscular junction, enteric glia of the enteric nervous system and specialised glia that accompany sensory nerve endings in the skin, such as Pacinian corpuscles (Jessen and Mirsky, 2005).

In the adult mammalian PNS nerve trunks there are two forms of Schwann cell, the myelinating Schwann cell, which associates in a 1:1 relationship and wraps a myelin sheath around axons greater than 1μm in diameter and, non-myelinating Schwann cells that associate with a variable number of small calibre axons (less than 1μM in diameter) that form troughs in its cytoplasm (Jessen and Mirsky, 2005).

Schwann cells in the spinal nerves are derived from migratory neural crest cells, which originate from the tips of the neural folds during neural tube formation (Le Douarin et al., 1991; Anderson, 1997). In contrast, a majority of Schwann cells in the dorsal and ventral roots are derived from Boundary cap cells, which themselves are derived from neural crest cells, and are positioned at the dorsal and ventral root entry and exit points to the spinal cord early during development (Maro et al., 2004).

The generation of myelinating and non-myelinating Schwann cells from neural crest cells occurs via two intermediary cellular stages. Firstly, Schwann cell precursors are formed from neural crest cells and are present around embryonic day

(E) 14-15 in rat peripheral nerves. Schwann cell precursors in turn lead to the generation of immature Schwann cells by E17-18 (Jessen et al., 1994; Dong et al., 1995). In murine peripheral nerves, these developmental transitions occur two days earlier, thus Schwann cell precursors are present at E12-13 and immature Schwann cells at E15/16 (Dong et al., 1999). These two cell types are phenotypically distinct from one another, in terms of antigenic expression, survival mechanisms, morphology and relationship to the axons and the extracellular matrix (Fig.1.1) (Woodhoo et al., 2004; Jessen and Mirsky, 2005).

1.1.1. The Schwann cell precursor

Neural crest cells are specified to be Schwann cell precursors through the process of gliogenesis. The transcription factor Sox-10 is crucial in regulating this process, since a targeted mutation in Sox-10 leads to a complete lack of Schwann cells and satellite cells in the PNS whereas neurogenesis is initially unaffected (Britsch et al., 2001).

At E14, rat Schwann cell precursors are identified generally at the periphery but sometimes within the developing nerve, surrounding large bundles of small diameter axons. These cells usually extended processes deep into the axon bundles that contact processes from other Schwann cell precursors. Nerves at this time point contain little extracellular matrix (ECM) and no apparent connective tissue or blood vessels (Jessen et al., 1994; Jessen and Mirsky, 2005). Furthermore, *in vitro* Schwann cell precursors demonstrate a radically different appearance to immature Schwann cells, often forming groups of cells and adopting a flattened shape as opposed to a bi- or tripolar morphology seen with cultured Schwann cells (Jessen et al., 1994). In addition, Schwann cell precursors appear to require β-neuregulin-1 (NRG1) signalling (see

section 1.5.2 for summary) through its receptors erbB2 and erbB3 in order to survive both in *vitro and in vivo* (Dong et al., 1995; Meyer and Birchmeier, 1995; Riethmacher et al., 1997; Woldeyesus et al., 1999; Morris et al., 1999; Garrat et al., 2000). Additionally, in mice lacking both type I and type II NRG1 isoforms Schwann cell precursors develop normally whereas mice lacking NRG1 type III have severely reduced numbers of Schwann cell precursors (Meyer et al., 1997; Wolpowitz et al., 2000). The source of NRG1 type III during development appears to be the motor and sensory neurons, which are present in the nerve at the same time as the Schwann cell precursors (Ho et al., 1995; Meyer et al., 1997; Yang et al., 1998; Wanner et al., 2006a). In summary this data suggests that Schwann cell precursors rely on NRG1 type III expressed on growing axons for their survival during PNS development.

There are several known functions of Schwann cell precursors in PNS development. Firstly, they provide the source of progenitors from which immature Schwann cells and endoneurial fibroblasts are generated (Joseph et al., 2004; Jessen and Mirsky, 2005). They also appear to support the survival of growing neurons since in mouse mutants that lack Schwann cell precursors there is substantial death of both motor and sensory neurons (Riethmacher et al., 1997; Woldeyesus et al., 1999; Britsch et al., 2001; Sonnenberg-Riethmacher et al., 2001). In addition, Schwann cell precursors appear important for axon fasciculation and nerve compaction, forming a tight cellular cluster around advancing growth cones of neurons before they innervate their targets (Woldeyesus et al., 1999; Morris et al., 1999; Wolpowitz et al., 2000; Wanner et al., 2006a).

Figure 1.1 Antigenic and phenotypic profile of cells in the Schwann cell lineage during embryogenesis.

Yellow box – antigens present in the whole of the early Schwann cell lineage; *Blue box* – antigens present only in crest cells and Schwann cell precursors; *Purple box* – antigens present only in Schwann cell precursors; *Grey box* – antigens present in Schwann cell precursors and Schwann cells; *Brown box* – antigens present only in Schwann cells. Adapted from Mirsky et al., (2008).

1.1.2 Regulation of the Schwann cell precursor to Schwann cell transition

As mentioned above, immature Schwann cells will have been generated from Schwann cell precursors by E17/18 in the rat and E15/16 in the mouse PNS. This transition is marked by many changes, particularly in antigenic profile, proliferative and survival responses and motility (Fig.1.1) (Jessen et al., 1994; Dong et al., 1995; Meier et al., 1999; Jessen and Mirsky, 2005). Moreover, many aspects of this cellular transition can be faithfully recapitulated *in vitro* using Schwann cell precursors from E14 rats or E12 mice cultured in medium containing NRG-1 (Jessen et al., 1994; Dong et al., 1995, 1999). The fact that these experiments use NRG-1 demonstrates that NRG-1 is sufficient for both precursor survival and maturation *in vitro* (Dong et al., 1995, 1999). Additionally, fibroblast growth factor 2 (FGF2) can accelerate precursor maturation in the presence of NRG-1 (Dong et al., 1995). Furthermore, endothelin acting through endothelin B receptors and overexpression of the transcription factor AP-2α appears to antagonize NRG-1 induced precursor differentiation (Brennan et al., 2000; Stewart et al., 2001). Interestingly, in growth factor deficient medium, expression of the anti-apoptotic gene, bcl-2, in Schwann cell precursors, in order to promote survival, is sufficient to allow the generation of immature Schwann cells after 4 days in culture (V.Sahni, unpublished observations). This suggests that there may be cell intrinsic mechanisms for Schwann cell precursor maturation.

In vivo, loss of endothelin B receptors in the *spotting lethal* rat leads to generation of Schwann cells ahead of schedule, confirming a role for endothelin in antagonizing Schwann cell precursor maturation (Brennan et al., 2000). Additionally, mutation of components of the Notch pathway demonstrates its requirement for the

correct timing of Schwann cell generation from precursors (A. Woodhoo, unpublished observations).

1.1.3 The immature Schwann cell

The generation of immature Schwann cells at E17/18 in the rat and E15/16 in the mouse PNS correlates with changes in the cytoarchitecture of the nerve including the development of fibroblasts, connective tissue and blood vessels within the endoneurium and the development of a well-defined perineurial sheath surrounding the nerve (Jessen and Mirsky, 2005). At this time point Schwann cells are associated with discrete compact bundles of axons similar to 'axon-Schwann cell families' observed in newborn rat nerves. These axon-Schwann cell units also demonstrate a noticeable basal lamina with associated collagen fibrils (Webster and Favilla, 1984; Jessen and Mirsky, 2005). Additionally, at this stage there is control over overall numbers of Schwann cells, through proliferation and survival mechanisms, presumably to match the numbers of Schwann cells with the numbers of axons before myelination (Webster, 1973; Jessen and Mirsky, 2005).

1.1.3.1 Mechanisms of Schwann cell proliferation.

Cell proliferation is a characteristic of both the Schwann cell precursor and the immature Schwann cell. However, the peak of proliferation, measured by BrdU incorporation, occurs at the immature Schwann cell stage, E18/E19 in the rat and E15 in the mouse sciatic nerve (Stewart et al., 1993; Yu et al., 2005). As Schwann cells begin to myelinate they drop out of the cell cycle (Webster et al., 1973; Stewart et al., 1993), hence proliferation rates in the sciatic nerve fall sharply after birth, although

cells destined to become non-myelinating Schwann cells continue to proliferate into the second postnatal week (Asbury, 1967; Stewart et al., 1993).

Direct contact with axons, *in vitro*, or treatment of Schwann cells with axon-enriched fractions can induce Schwann cell proliferation (Salzer et al., 1980a, 1980b). The mitogen that mediates the majority of this proliferation *in vitro* was identified as NRG1 (Morrissey et al., 1995), yet, crucially, definitive evidence from *in vivo* studies demonstrating that NRG1 is a Schwann cell mitogen is still lacking. In zebrafish, mutation of erbB3 or pharmacologically blocking NRG1/erbB signalling reduced both Schwann cell precursor and immature Schwann cell proliferation (Lyons et al., 2005). However, conditional mutation of the mouse erbB2 receptor in Schwann cells actually lead to an increase in postnatal Schwann cell proliferation, most probably due to the delay in myelination seen in these mice (see section 1.5.2.1), although embryonic proliferation levels were not assessed (Garratt et al., 2000).

Another mitogen that has been shown to play a role in Schwann cell proliferation is Transforming growth factor β (TGFβ). Addition of TGFβ to cultured Schwann cells can augment NRG1 induced proliferation and conditional mutation of TGF-β receptor type II in mouse Schwann cells reduces proliferation rates at E18 in the sciatic nerve (D'Antonio et al., 2006b). Additionally, laminin (a component of the basal lamina, see section 1.5.1) also appears to regulate developmental Schwann cell proliferation. Mice lacking the laminin γ_1 chain specifically in Schwann cells or mice lacking both laminin α_2 and α_4 chains show substantially reduced levels of immature Schwann cell proliferation embryonically and during the postnatal period (Yu et al., 2005; Yang et al., 2005). Interestingly proliferation at E13, the Schwann cell precursor stage, was normal in laminin γ_1 mutant embryos demonstrating that laminin does not affect precursor proliferation (Yu et al., 2005; Jessen and Mirsky, 2005).

The intracellular signalling mechanisms involved in regulating developmental Schwann cell proliferation are only beginning to be identified. Recently, two studies identified a requirement for focal adhesion kinase (FAK) and a member of the RhoGTPase family, cdc42, *in vivo*, in embryonic and perinatal Schwann cell division (Grove et al., 2007; Benninger et al., 2007). Furthermore, another study showed that cyclin dependent kinase 4 (cdk4) was required for postnatal but not embryonic Schwann cell proliferation at E18 demonstrating that there may be subtle mechanistic differences in the two types of proliferation (Atanasoski et al., 2008).

1.1.3.2 Mechanisms of Schwann cell survival and death

During PNS development there appears to be significant levels of apoptotic Schwann cell death at late time points during embryogenesis and also perinataly (Syroid et al., 1996; Grinspan et al., 1996; D'Antonio et al., 2006b). Whereas Schwann cell precursors cannot survive in the absence of axons or NRG1 (see section 1.1.1), the majority of immature Schwann cells survive after loss of axonal contact by either culturing or nerve transection (Grinspan et al., 1996). NRG1, however, can still act as a survival signal for immature Schwann cells because exogenous NRG1 application can reduce the percentage of apoptotic Schwann cells in uninjured and transected neonatal nerves and at denervated neuromuscular junctions (Grinspan et al., 1996; Trachtenberg and Thompson, 1996). Laminin also acts as a survival signal for immature Schwann cells, since there is a considerable increase in apoptotic Schwann cell death, marked by TUNEL labelling, in *laminin* γ_1 mutant mice (Yu et al., 2005). Identification of autocrine survival circuits that contribute to survival of immature Schwann cells but not precursors in culture is likely to be an important mechanism of how immature Schwann cells survive in the absence of axons (Meier

et al., 1999). Schwann cell survival is also likely to depend upon the activity of the Ets and Stat, particularly Stat3, family of transcription factors (Parkinson et al., 2002; C. Davis, unpublished observations).

In addition to survival signals, signals that initiate Schwann cell death have also been identified. TGFβ can induce death in neonatal Schwann cells in culture and conditional mutation of the TGF-β receptor type II reduces Schwann cell death rates at E18 in the developing nerve and after neonatal nerve transection (Parkinson et al., 2001; D'Antonio et al., 2006b). Nerve growth factor (NGF) acting through the $p75^{NTR}$ receptor has also been shown to induce Schwann cell death in culture (Soilu-Hanninen *et al.*, 1999). However, $p75^{NTR}$ does not play a role in developmental Schwann cell death as levels of apoptosis in control and $p75^{NTR}$ null mice were equivalent (Syroid et al., 2000). $p75^{NTR}$ may play a role in Schwann cell death after nerve injury, though, since there was a significant reduction in the number of apoptotic cells after nerve transection in both neonatal and adult $p75^{NTR}$ null mice compared to controls (Ferri and Bisby, 1999; Syroid et al., 2000).

1.2 Postnatal Schwann cell differentiation

1.2.1 Myelination

In the newborn rodent sciatic nerve axons are present in axon 'Schwann cell families', which, as mentioned previously are axon bundles surrounded by Schwann cells and a continuous basal lamina (Webster and Favilla, 1984; Jessen and Mirsky, 2005). Axons to be myelinated (>1μm in diameter) appear at the edge of these axon bundles and are enveloped by a radial Schwann cell process, eventually associating in a 1:1 relationship with the Schwann cell and its basal lamina. This process has been termed radial sorting (Webster, 1971; Webster et al., 1973; Webster and Favilla,

1984). However the precise mechanism behind how only axons above 1μM are selected and myelinated is still largely unknown. Schwann cells destined to myelinate can be identified by expression of galactocerebroside (gal-C) from E19, in the rat sciatic nerve (Jessen et al., 1985). Although gal-C is eventually expressed by non-myelinating Schwann cells (see section 1.2.2) antibodies to gal-C can block myelination in Schwann cell/DRG cocultures at the 1:1 stage, before myelin is formed (Ranscht et al., 1987; Owens et al., 1990). Myelin sheath formation is then believed to occur through the inner Schwann cell mesaxon or process spiralling around the axon to generate successive myelin wraps (Webster, 1971; Bunge et al., 1989). The process of myelination is strongly correlated with the cessation of cell division. Although it has been shown that Schwann cells do not proliferate once compact myelin formation begins, it is likely that Schwann cells cease proliferation at the 1:1 stage since proliferating Schwann cells are seldom seen in 1:1 association with axons (Martin and Webster, 1973; Webster et al., 1973; Stewart et al., 1993).

The formation of myelinating Schwann cells is accompanied by an extensive change in gene expression. Genes required for the formation of the myelin sheath, such as Krox-20, Protein zero (P_0) and many genes associated with lipid and cholesterol biosynthesis are upregulated whereas expression of molecules that characterise the immature Schwann cell, like L1, $p75^{NTR}$ and NCAM are downregulated (Fig.1.2)(Nagarajan et al., 2002; Verheijen et al., 2003; Jessen and Mirsky, 2005).

Figure 1.2: Antigenic profile of immature, myelinating and non-myelinating Schwann cells.

White box – antigens present in immature Schwann cells and mature myelinating and non-myelinating Schwann cells; Blue box – antigens expressed by mature non-myelinating Schwann cells; Orange box – antigens present in immature and non-myelinating Schwann cells but downregulated in myelinating Schwann cells; Green box – antigens expressed only in mature myelinating Schwann cells. Notice that gal-C is expressed by both mature myelinating and non-myelinating Schwann cells. Adapted from Mirsky et al., (2008).

1.2.2 Non-myelinating Schwann cell differentiation

In contrast to myelinating Schwann cells, non-myelinating Schwann cells maintain expression of most immature Schwann cell genes, however they do downregulate basal expression of the P_0 gene, which is seen in precursors and immature Schwann cells (Fig.1.2)(Lee et al., 1997; Jessen and Mirsky, 2005). Non-myelinating Schwann cells also upregulate expression of galactocerebroside (gal-C) 3 weeks after birth, shortly before they form mature Remak fibres characterised by small calibre axons lying in troughs in the Schwann cell cytoplasm (Diner et al., 1965; Jessen et al., 1985). One marker that appears to be exclusively expressed by non-myelinating Schwann cells in normal adult nerves is $\alpha_1\beta_1$ integrin (Stewart et al., 1997).

1.3 The general structure of a myelinated fibre.

Myelination of axons is likely to have evolved to allow the advantage of rapidity of action potential signalling while minimizing the size of the axon (Colman et al., 2001). Myelinated axons are completely insulated by myelin sheaths apart from at Nodes of Ranvier, gaps of less than 1μm, where axons are exposed to the extracellular environment. These nodes are rich in voltage gated sodium channels and in combination with the reduced capacitance or increased resistance provided by the internodal myelin sheath, facilitate salutatory conduction of action potentials between nodes of Ranvier (Arroyo and Scherer, 2000; Sherman and Brophy, 2005).

Each Schwann cell internode is divided into two distinct domains, compact myelin and non-compact myelin, usually with the nucleus in the centre of the internode. Compact myelin accounts for the majority of the internode, appearing as a lamellar structure of alternating dark and light lines with a periodicity of about 13 –

19 nm using electron microscopy (Kirschner and Sidman, 1976; Kirschner and Hollingshead, 1980). The dark major dense lines (MDL) are 2.5 nm thick and are separated from each other by the light interperiod lines (IPL). The MDL consists of two intracellular lipid bilayers fused together whereas the IPL represents the fusion of the two opposed extracellular surfaces of the Schwann cell plasma membrane. Compact myelin is highly specialised containing many proteins and lipids required for its maintenance (see section 1.4).

Non-compact myelin consists of the Schmidt Lantermann incisures (SLI), internodal cytoplasmic channels that connect the abaxonal membrane (which is in contact with the basal lamina) with the adaxonal membrane (which is contact with the axon), and the paranodal loops (Fig.1.3, A and B). The paranodal loops are situated adjacent to the node of Ranvier, where the MDL opens up to accommodate cytoplasm. These loops or glial end feet are attached by septate like junctions to the axonal membrane. Heterodimers of contactin and Caspr (contactin associated protein) expressed on the axonal membrane are likely to bind Neurofascin 155, expressed on the glial end feet to form these junctions (Sherman and Brophy, 2005). These junctions have been suggested to anchor the myelin membrane to the axon and also provide a diffusion barrier into the periaxonal space (Arroyo and Scherer, 2000). Beyond the paranodal loops, Schwann cell microvilli project from the abaxonal membrane to contact the axolemma (Fig.1.3, B). Next to the paranodal loops is the juxtaparanodal region (Fig.1.3, B), which is anchored by homophilic interaction of the cell adhesion molecule TAG-1, expressed on both the glial and axonal membrane. In addition TAG-1 binds in cis to Caspr-2 on the axonal juxtaparanodal membrane (Traka et al., 2002, 2003). The axonal membrane in this region contains K^+ channels, which are mainly thought to dampen excitability of myelinated fibres preventing

ectopic impulses. In addition the juxtaparanodal Schwann cell membrane also contains K^+ channels, which have been suggested to act to remove accumulations of periaxonal potassium ions (Arroyo and Scherer, 2000).

1.4 The molecular composition of PNS myelin.

Myelin membrane is composed of about 70-80% lipids and 20-30% proteins. Cholesterol accounts for about 20-30% of the total lipids in PNS myelin. Other significant lipid constituents of PNS myelin are the galactolipids, gal-C and galactosulfatide (Sgal-C) accounting for 15-20% and phospholipids account for between 50-60% of total myelin lipids (Garbay et al., 2000). The major protein constituents of PNS compact myelin are P_0 (50-70% of total PNS myelin protein), myelin basic protein (MBP, 5-15% of total PNS myelin protein) and peripheral myelin protein 22 (PMP22, 2-5% of total PNS myelin protein)(Garbay et al., 2000). P_0 is a 28kDa integral membrane glycoprotein with an Ig-like extracellular domain that acts as the major adhesion molecule of the IPL and potentially contributes to the formation of the MDL too, since Schwann cells in mice lacking P_0 form membrane spirals around axons but the majority of myelin does not compact (Giese et al., 1992; Martini et al., 1995a). Individual P_0 molecules were shown to be likely to form tetramers in cis and then these tetramers bind each other in trans, demonstrating how P_0 contributes to cell membrane adhesion (Shapiro et al., 1996). Interestingly, P_0 null mice also lack SLIs. Furthermore, replacing Proteolipid protein (PLP/DM20) with P_0 in central nervous system (CNS) myelin, which normally lacks SLIs, is sufficient to induce SLI formation. This data suggests that P_0 is important in instructing SLI formation, though the mechanism is unknown (Yin et al., 2008). MBP is a cytoplasmic protein that is also involved in myelin compaction and the formation of

the MDL (Martini et al., 1995b; Nave, 2001). Four main isoforms are expressed in the PNS, with apparent sizes of 21.5, 18.5, 17 and 14kDa. The naturally occurring mouse mutant *shiverer*, which lacks expression of all MBP isoforms (Roach et al., 1983; Molineaux et al., 1986), does not show any major abnormalities in PNS myelin compaction though homozygous *shiverer* mutant nerves do contain twice the number of SLIs compared to wild-type nerves (Rosenbluth, 1980; Gould et al., 1995). However, mice lacking both P_0 and MBP are unable to form any compact myelin demonstrating the requirement for both of these proteins in myelin sheath compaction (Martini et al., 1995b). PMP22 is an intrinsic membrane 22kDa glycoprotein that is crucial for correct peripheral nerve myelination (Adlkofer et al., 1995). Furthermore numerous mutations in the human *PMP22* gene have been shown to be responsible for a variety of different inherited peripheral neuropathies (Suter and Scherer, 2003; see section 1.7.1). Despite this relatively little is known about how PMP22 contributes to myelin formation with roles suggested in cell adhesion, proliferation and basal lamina integrity (Zoidl et al., 1995; Nave, 2001; Amici et al., 2006). Other proteins that are found in PNS compact myelin are P2 (1-10% of total PNS myelin protein), PLP/DM20 (<0.5% of total PNS myelin protein) and myelin and lymphocyte protein (MAL/MVP17) (Garbay et al., 2000; Nave, 2001).

The main protein constituents of non-compact myelin are myelin associated glycoprotein (MAG), connexin 32 (Cx32), periaxin, E-cadherin and nectin-like (Necl) proteins (Garbay et al., 2000; Maurel et al., 2007; Spiegel et al., 2007). MAG is a 100kDa glycoprotein with two isoforms and bears substantial homology to other cell adhesion molecules such as L1 and neural cell adhesion molecule (NCAM). MAG is found mainly in the periaxonal Schwann cell membrane but also in the paranodal loops, the external and internal mesaxons and the SLIs. MAG deficient mice show

minimal myelin abnormalities but do demonstrate an axonal phenotype consisting of reduced axonal calibres, neurofilament phosphorylation and spacing (Montag et al., 1994; Li et al., 1994; Yin et al., 1998). This may identify a role for MAG in glial axon signalling. Cx32 is a gap junction protein and is located in Schwann cell paranodal loops and SLIs, probably forming gap junctions between adjacent myelin lamellae (Scherer et al., 1995a). Periaxin is a 170kDa glycoprotein that is localised at the adaxonal membrane in the mature myelin sheath (Gillespie et al., 1994; Scherer et al., 1995b; Dytrych et al., 1998). It is attached to the dystroglycan complex through dystrophin related protein-2 (DRP-2) and thus is able to link laminin-2 in the basal lamina to the actin cytoskeleton (Sherman et al., 2001). Normally this complex is located at appositions between the abaxonal surface of the Schwann cell and the myelin sheath, leading to the formation of cytoplasmic channels between these appositions, called 'Cajal bands'. Periaxin is required for the formation of these Cajal bands and also appears necessary for internodal elongation, as the nerve is stretched postnataly by limb growth (Court et al., 2004). E-cadherin, a Ca^{2+}-dependent adhesion molecule is located in the inner and outer mesaxon, SLIs and paranodal loops (Fannon et al., 1995). E-cadherin forms adherens junctions in non-compact myelin by binding homophilically to itself in trans on the apposing membrane thus stabilizing the myelin sheath (Shapiro et al., 1995; Arroyo and Scherer, 2000; Garbay et al., 2000). Necl proteins, through heterophilic interactions with other Necl family members, have recently been identified to play a role in axon-glia interactions during myelination. Necl4 is expressed by myelinating Schwann cells along the length of the internode in apposition to Necl1, which is expressed on the internodal surface of the axon. Necl1 and 4 have been shown to interact and inhibition of Necl4 expression in Schwann

cells can block myelination in Schwann cell/DRG cocultures (Maurel et al., 2007; Spiegel et al., 2007).

In addition, Schwann cell microvilli present over the node of Ranvier also demonstrate molecular specialisations. Gliomedin, which is a type II transmembrane protein is cleaved from the surface of the Schwann cell microvilli and incorporated as a multimer into the extra-cellular matrix (ECM). There it mediates interactions between the Schwann cell microvilli and the axonally expressed cell adhesion molecules (CAMs), Neurofascin 186 and NrCAM (Eshed et al., 2005, 2007). Gliomedin is required for proper node formation *in vitro* (Eshed et al., 2005). Addtionally, dystroglycan and laminin, both components of the basal lamina (see section 1.5.1) are required for proper microvilli organisation and Sodium channel clustering at the node, *in vivo* (Saito et al., 2003; Occhi et al., 2005). Furthermore, ERM proteins (ezrin-radixin-meosin) are expressed at the microvilli, colocalise with actin filaments and are thought to be important in the formation of the microvilli (Melandez-Vasquez et al., 2001; Scherer et al., 2001; Gatto et al., 2003).

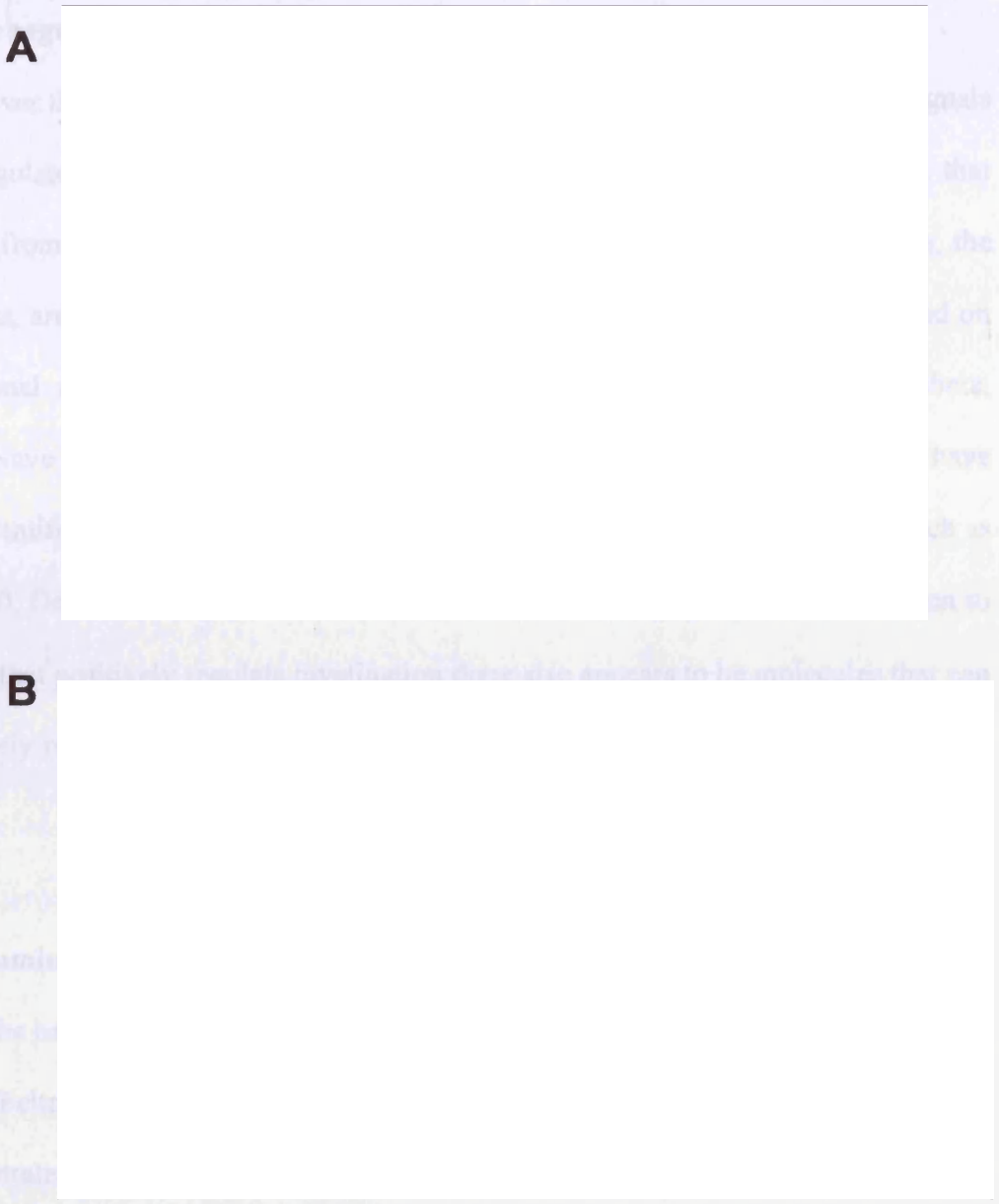

Figure 1.3: Representation of a Schwann cell internode and node.

(A) A myelinating Schwann cell unravelled demonstrating the various cellular domains that constitute the compact myelin, and non-compact myelin. *Blue* – area on axon occupied by node of Ranvier; *Red* – area on axon occupied by the paranodal loops; *Green* – area on axon occupied by the juxtaparanodal region; *yellow* – refers to gap junctions in SLIs and paranodal loops; *purple* – adherens junctions in paranodal myelin. (B) A representation of the node of Ranvier, paranode and juxtaparanode. Adapted from Arroyo and Scherer, (2000).

1.5 The regulation of myelination.

Over the last fifteen years major advances have been made in identifying signals that regulate Schwann cell myelination. Recent evidence has demonstrated that signals from the basal lamina, which include laminins binding to their receptors, the integrins, are crucial in regulating radial sorting whereas NRG1 type III expressed on the axonal membrane regulates myelin membrane wrapping (Feltri and Wrabetz, 2005; Nave and Salzer, 2006). Furthermore, a number of transcription factors have been identified that control Schwann cell gene expression during myelination, such as Krox-20, Oct-6 (Pou3f1), Sox10 and NFκB (Jessen and Mirsky, 2005). In addition to signals that positively regulate myelination there also appears to be molecules that can negatively regulate myelin differentiation too (Jessen and Mirsky, 2005; see Chapter 4).

1.5.1 Laminins, integrins, Rho GTPases and downstream pathways.

The basal lamina forms a continuous tube around the internodes of a myelinated axon (Feltri and Wrabetz, 2005). Schwann cell/DRG co-culture experiments demonstrated that the formation but not the maintenance of the basal lamina by Schwann cells was reliant on axonal contact (Bunge et al., 1982; Clark and Bunge, 1989). Whereas, basal lamina formation appears not to be a prerequisite for myelin formation either *in vitro* (Podratz et al., 1998, 2001) or *in vivo* (Madrid et al., 1975; Nakagawa et al., 2001), laminin, a major constituent of the basal lamina, is required for myelination (Yu et al., 2005; Yang et al., 2005). Laminins are a family of extracellular matrix proteins that exist as trimers made up of an α–, β–, and γ-subunit, with each subunit encoded by a different gene. There are five α–subunits, four β–subunits and three γ–subunits (Feltri and Wrabetz, 2005). In the PNS, both laminin 2

(composed of the subunits $\alpha_2\beta_1\gamma_1$) and laminin 8 (composed of the subunits $\alpha_4\beta_1\gamma_1$) are expressed in the endoneurial basal lamina during development, in the adult nerve and also after injury (Wallquist et al., 2002). In addition, laminin α_5 (potentially forming laminin 10) is present at the nodes of Ranvier and *laminin* γ_3 (potentially forming laminin 12) mRNA is upregulated in Schwann cells after nerve injury (Wallquist et al., 2002; Feltri and Wrabetz, 2005).

The role of laminins 2 and 8 during Schwann cell development has been discerned through studying mice with spontaneous mutations or genetic inactivation of various laminin subunits. *Dystrophic* mice that are homozygous for the *Lama2*^{dy} allele do not produce the α_2-subunit and hence laminin-2 (merosin)(Feltri and Wrabetz, 2005). These mice develop a peripheral neuropathy characterized by the presence of unsorted bundles of naked axons, which are more commonly observed in the proximal compared to the distal PNS, particularly in the ventral roots (Bradley and Jenkison, 1973; Stirling, 1975). They also demonstrate other myelin abnormalities such as shorter internodes and widened Nodes of Ranvier (Bradley et al., 1977; Jaros and Jenkison, 1983). In addition, mice with targeted inactivation of the *Lama2* gene (that produces the α_2-subunit) have thinner myelin sheaths, predominantly in the nerve roots, but show fewer amyelinated or unsorted axons compared to the *dystrophic* mouse mutant (Nakagawa et al., 2001). This may be due to differential expression of the α_5-subunit in the ventral roots of *dystrophic* and *Lama2* null mice (Nakagawa et al., 2001). Mice lacking expression of laminin 8 due to targeted inactivation of the *Lama4* gene showed similar myelin abnormalities in the tibial nerve, such as unsorted axons, to a mouse strain which lacks functional laminin 2 (*dy2J*) (Wallquist et al., 2005; Yang et al., 2005). However, whereas mice without laminin 2 show a more severe phenotype in the spinal roots *Lama4* null mice

demonstrated a very mild phenotype. This is potentially explained by a greater requirement for laminin2 than laminin8 in axonal sorting and myelination of the ventral root (Yang et al., 2005). Importantly, mice lacking expression of both laminin2 and 8, produced by generating *Lama2*, *Lama4* double knockout mice, or mice with Schwann cell specific ablation of the laminin-γ_1 subunit demonstrated markedly reduced axonal sorting and myelination in the nerves and their roots (Chen and Strickland, 2003; Yu et al., 2005; Yang et al., 2005).

Inactivation of laminin receptors also leads to axonal sorting and myelination defects (Feltri and Wrabetz, 2005). There are two types of laminin receptor expressed on Schwann cells, integrins and dystroglycan (DG). Integrins are dimers consisting of an α– and β–transmembrane subunits whereas DG consists of an extracellular α–subunit and a β–transmembrane subunit (Feltri and Wrabetz, 2005). Schwann cell precursors and immature Schwann cells express $\alpha_6\beta_1$-, $\alpha_2\beta_1$- and $\alpha_3\beta_1$-integrins (Hsiao *et al.*, 1991; Milner et al., 1997; Previtali *et al.*, 2003a) whereas $\alpha_6\beta_4$-integrin and DG appear during the pro-myelin stage (when Schwann cells associate in 1:1 ratio with axons) at birth (Previtali *et al.*, 2003a), and $\alpha_7\beta_1$-integrin is expressed later by mature myelinating Schwann cells (Previtali *et al.*, 2003c). As mentioned previously, mature non-myelinating Schwann cells express the dual collagen/laminin receptor, $\alpha_1\beta_1$-integrin (Stewart et al., 1997). Conditional inactivation of *β_1-integrin* in Schwann cells leads to the majority of Schwann cells being unable to sort and hence myelinate axons (Feltri et al., 2002). Similarly, function blocking antibodies to β_1-integrin block myelination in Schwann cell/DRG cocultures (Fernandez-Valle et al., 1994). Schwann cells without DG or β_4-integrin hardly show any sorting defects but do demonstrate abnormally folded myelin sheaths, which is more severe in DG conditionally-null mice and characterised by a late onset neuropathy (Saito et al.,

2003; Nodari et al., 2008). In contrast, mice lacking α_7-integrin in Schwann cells do not appear to have any deficit in axonal sorting or myelination (Previtali *et al.*, 2003c).

ECM/Integrin signalling can cooperate with growth factor signalling in many cell types to regulate, in particular, proliferation, motility and survival (ffrench-Constant and Colognato, 2004; Guo and Giancotti, 2004). The majority of integrins activate FAK and thus the Src family kinases, leading to activation of downstream effectors such as Rho GTPases and MAPK pathways, which in turn regulate the actin cytoskeleton (Guo and Giancotti, 2004).

The mechanism, by which laminin-β_1-integrin signalling, in Schwann cells, acts to regulate axon sorting is only beginning to be elucidated. One study demonstrated that the failure of Schwann cells without *β_1-integrin* to extend radial lamellipodia might be linked to the failure of these Schwann cells to sort axons *in vivo* (Feltri et al., 2002; Nodari et al., 2007). In the absence of β_1-integrin, activation of the small GTPases, Rac1 and RhoA but not cdc42, is reduced (Nodari et al., 2007). Conditional inactivation of Rac1 in Schwann cells produced a similar defect to *β_1-integrin* null mice in axonal sorting and myelination (Nodari et al., 2007; Benninger et al., 2007). Furthermore, adenovirally expressed Rac1 injected into the sciatic nerve of *β_1-integrin* null mice partially rescued the phenotype of *β_1-integrin* null Schwann cells (Nodari et al., 2007). Ablation of both FAK and cdc42 in Schwann cells also produces significant axonal sorting defects although this may be in part due to the reduced Schwann cell proliferation seen in these mutants (Grove et al., 2007; Benninger et al., 2007; see section 1.1.3.1). Finally, in vitro studies from Schwann cell/DRG cocultures have also identified a potential role for the p38 mitogen activated protein kinase (p38MAPK) and phosphatidyl-inositol-3 kinase (PI3-K) pathways and the actin

cytoskeleton in Schwann cell axon ensheathment and myelination (Fernandez-Valle et al., 1997; Maurel and Salzer, 2000; Fragoso et al., 2003; Haines et al., 2008).

1.5.2 An overview of NRG1 signalling

Neuregulins are members of a family of proteins containing an epidermal growth factor (EGF)-like domain that bind to and activate membrane-associated receptor tyrosine kinases, which are related to the EGF receptor. Four NRG genes have so far been identified in vertebrates (NRG1-4) although so far, only NRG1 has been shown to be important in PNS development (Buonanno and Fischbach, 2001).

The *NRG1* gene is about 1.4 megabases long, with only 0.3% of it encoding proteins. At least 15 different NRG1 isoforms can be generated due to alternative splicing and multiple promoters. Common to all the isoforms is the EGF-like domain, which is sufficient for activation of the receptors. The differential structural characterisitics of the NRG1 isoforms that are known to be important for *in vivo* function include the type of EGF-domain (α or β) and the N-terminal sequence (type I, II, or III) and whether the protein is synthesised as a transmembrane or non-membrane protein (Fig.1.4) (Falls, 2003). Mice lacking all NRG1 isoforms with an α-type EGF-like domain do not show any abnormalities in PNS development and demonstrate normal survival and lifespan (Li et al., 2002). In addition, only loss of the NRG1 type III isoform but not type I or II isoforms demonstrates PNS defects (Meyer et al., 1997; Wolpowitz et al., 2000). Thus, it appears that the β-NRG1 type III isoform is the most important NRG isoform in PNS development (see section 1.1.1), however this does not preclude roles for NRG1 type I and type II in the postnatal or adult PNS.

NRG1 can bind the ErbB receptors, ErbB3, which does not have a kinase domain and ErbB4. Both receptors can, in turn, heterodimerize with ErbB2, which cannot directly bind NRG1 but does possess a kinase domain. In Schwann cells ErbB2-ErbB3 heterodimers are thought to be the relevant NRG1 receptor since ErbB4 expression is hardly detectable in the PNS and ErbB2 is unable to homodimerise easily (Nave and Salzer, 2006). Binding of NRG1 to ErbB3 induces ErbB2-ErbB3 heterodimerisation, receptor cross phosphorylation, recruitment of SH3-containing adaptor molecules and activation of many different downstream signalling pathways including the mitogen-activated protein kinase (MAPK), PI3-K, p38MAPK, phospholipase-Cγ (PLCγ) and Janus kinase pathways (Citri et al., 2003; Nave and Salzer, 2006).

Figure 1.4: Overview of the main neuregulin1 isoforms in the PNS.

NRG1 type I and II have a single transmembrane domain in contrast to NRG1 type III has two transmembrane domains. Cleavage by metalloproteases (MP) leads to release of type I and II from the cellular surface to signal in a paracrine fashion whereas type III remains tethered through its cysteine rich domain (CRD) and acts as a juxtacrine signal. The cytoplasmic domain can also be cleaved and may signal to the nucleus (Falls, 2003). Adapted from Nave and Salzer, (2006).

1.5.2.1 The role of NRG1/erbB signalling in myelination.

In addition to regulating embryonic Schwann cell development (see section 1.1.1), NRG1 signalling has recently been demonstrated to modulate PNS myelination (Nave and Salzer, 2006). Blocking ErbB2-ErbB3 signalling in mice, specifically in Schwann cells either using Cre-loxP technology or by expressing a dominant-negative ErbB molecule leads to delayed onset of myelination and thinner myelin sheaths (Garratt et al., 2000; Chen et al., 2006). Pharmacologically blocking ErbB signalling in zebrafish demonstrated that postmigratory Schwann cells required ErbB signalling to commit to a myelinating fate and express Krox-20 and MBP (Lyons et al., 2005). In addition, mice that are heterozygous for NRG1 type III, which are viable, have thinner myelin sheaths than control animals whereas mice heterozygous for ErbB2 had normal myelin sheaths (Garratt et al., 2000; Michailov et al., 2004; Taveggia et al., 2005). This suggests that the level of NRG1 expressed on the axon rather than the level of ErbB receptors on the Schwann cell was rate limiting (Michailov et al., 2004). In support of this, transgenic mice that overexpress NRG1 type III on peripheral axons develop thicker myelin sheaths, with a greater number of myelin wraps than control mice (Michailov et al., 2004). Importantly, although NRG1-erbB signalling is involved in regulating myelin sheath thickness, it is not required for the maintenance of myelin sheaths in the adult (Atanasoski et al., 2006).

NRG1 type III also appears to regulate axonal sorting and the enseathment fate of axons. In NRG1 type III heterozygotes there are fewer myelinated axons than in controls and larger collections of unsorted axons >1μm in diameter that would normally be myelinated (Taveggia et al., 2005). Similarly, axons in DRG cultures from NRG1 type III null embryos are not properly segregated, ensheathed or myelinated by wild-type Schwann cells *in vitro* (Taveggia et al., 2005).

Further experiments suggested that axonal NRG1 type III might be sufficient to induce Schwann cell myelination. Firstly, the level of NRG1 type III expressed on axons of different types of neuron correlates with axonal calibre and the extent to which they are myelinated. Thus, expression of NRG1 type III by lentiviral transfer into sympathetic cervical ganglion neurons, which are normally mostly unmyelinated, was sufficient to induce a small degree of myelination *in vitro* (Taveggia et al., 2005). Also NRG1 type III overexpressing mice contain a number of axons <1μm in diameter that are myelinated (Michailov et al., 2004; Nave and Salzer, 2006). However, these observations are difficult to interpret given the potential role of NRG1 in axonal sorting, ensheathment and potentially proliferation (Taveggia et al., 2005; section 1.1.3.1). It is possible that a graded level of NRG1 type III is required for initially sorting, then enseathment and subsequently myelination of axons, although this remains to be tested. It is also important to note that while NRG1 type III can promote Schwann cell myelination *in vivo* it is insufficient to induce myelin gene expression in Schwann cell monocultures suggesting that other signals are likely to be involved (Taveggia et al., 2005; see Chapter 3).

Other experiments, using a dominant-negative erbB construct have also indicated a role for NRG1 signalling in non-myelinating Schwann cell survival and consequently the survival of the C-fibre sensory axons that they ensheath (Chen et al., 2003).

1.5.3 Other signals that regulate PNS myelination.

Brain-derived neurotrophic factor (BDNF) treatment can enhance myelination in Schwann cell/DRG cocultures through binding to the $p75^{NTR}$ receptor. Furthermore lack of $p75^{NTR}$ in null animals or injection of a $p75^{NTR}$ function blocking antibody

lead to reduced myelin sheath wrapping compared to control animals (Cosgaya et al., 2002). Overexpression of BDNF *in vivo* generated thicker myelin sheaths over time, however axon calibre was also increased but to a lesser extent than myelin sheath thickness (Tolwani et al., 2004), arguing for a role for BDNF and $p75^{NTR}$ in regulating myelination. The $p75^{NTR}$ receptor has been shown to associate with the cell polarity protein, par-3, at the axo-glial interface in Schwann cells. Disruption of this asymmetric par-3 localisation was shown to inhibit myelination in Schwann cell/DRG cocultures (Chan et al., 2006), although it is unknown whether par-3 plays a role in myelination *in vivo*.

The *claw paw* phenotype in mice is due to a spontaneous mutation causing a delay in radial sorting, Krox-20 upregulation and myelination and deficits in limb posture (Henry et al., 1991; Darbas et al., 2004). The claw paw mutation was recently shown to be due to a repetitive element insertion in *Lgi4*, a member of the leucine-rich-glioma-inactivated family of genes. This mutation leads to $Lgi4^{clp}$ being retained within the endoplasmic reticulum instead of being glycosylated and secreted. Schwann cell/DRG cocultures from *claw paw* mice could not be induced to myelinate unless Lgi4 protein was added to the culture medium suggesting that the *claw paw* mutation is due to a loss of function of *Lgi4* (Bermingham et al., 2006).

Ablation of *ADAM22*, a member of the ADAM (a disintegrin and metalloproteinase domain) family of proteins leads to severe hypomyelination and ataxia in the PNS. The authors suggested that the myelination deficits seen in the absence of *ADAM22* may be due to an impairment in integrin signalling, though this remains to be tested (Sagane et al., 2005). Interestingly, ADAM22 has also been identified as a transmembrane receptor for Lgi1, regulating synaptic transmission in

the CNS (Fukata et al., 2006), suggesting that ADAM22 and Lgi4 may also potentially interact in the PNS.

Additionally, mice lacking the β-secretase, BACE1 (beta-site amyloid precursor protein-cleaving enzyme 1) develop hypomyelination in both the CNS and the PNS (Willem et al., 2006; Hu et al., 2008). BACE1 has been shown to cleave NRG1 type III, *in vitro* (Willem et al., 2006), although it remains untested whether NRG1 type III is a physiological substrate in vivo and whether its cleavage is a requirement for PNS myelination (see Fig.1.4).

1.5.4 Transcription factors that regulate myelination.

1.5.4.1 Krox-20.

Krox-20 (Egr2) is a member of a family of transcription factors called early growth response genes (Egr), which all share a highly conserved DNA binding domain consisting of three zinc fingers that recognise GC-rich sequences. In addition to Egr2, this family includes Egr1 (Krox-24), Egr3 and Egr4 (Vesque and Charnay, 1992; Crosby et al., 1992). Krox-20 was originally identified as a transcription factor that is induced upon serum treatment and G0 to G1 cell cycle transition in fibroblasts (Chavrier et al., 1988). In Schwann cells, Krox-20 expression is activated at E15.5 in the mouse sciatic nerve, judged by expression of a *lacZ* reporter gene and at E18 in the rat sciatic nerve, shown by immunohistochemistry. These time points broadly correspond to the Schwann cell precursor to immature Schwann cell transition in both species (see section 1.1)(Murphy et al., 1996; Parkinson et al., 2003). Furthermore Krox-20 expression is regulated by axonal contact *in vitro* and *in vivo*, thus after nerve injury Krox-20 expression is lost from myelinating Schwann cells (Murphy et al., 1996; Topilko et al., 1997). Control of Krox-20 expression is regulated by the

immature Schwann cell element (ISE), active in immature Schwann cells from E15.5 and the myelinating Schwann cell element (MSE), which is active in cells preparing to myelinate from E18.5 (Ghislain et al., 2002). Further studies identified that the transcription factors Sox10 and Oct-6/Brn2 can cooperate to activate the MSE element, *in vitro* (Ghislain and Charnay, 2006), suggesting that these factors are likely to regulate Krox-20 expression in myelinating Schwann cells *in vivo*. In support of this MSE activity was found to be minimal in *Oct-6* null mice demonstrating a requirement for Oct-6 in activation of the *Krox-20* MSE (Ghislain et al., 2002).

In the absence of *Krox-20*, or in $Egr2^{Lo/Lo}$ (a hypomorphic *Egr2* allele) mice, Schwann cells sort axons but arrest at the pro-myelin stage, forming a 1:1 relationship but only wrapping 1.5 times around the axon (Topilko et al., 1994; Le et al., 2005a). Moreover, *Krox-20* null or $Egr2^{Lo/Lo}$ mice do not express high levels of the 'late myelin proteins', P_0 or MBP but do express the early myelin associated proteins, MAG and periaxin (Topilko et al., 1994; Parkinson et al., 2003; Le et al., 2005a). Furthermore constant Krox-20 expression is required for Schwann cells to maintain the myelinating state in the adult PNS (Decker et al., 2006).

Adenoviral expression of Krox-20 in both cultured rat and mouse Schwann cell was sufficient to induce mRNA and protein expression of a number of myelin related genes, including P_0, PMP22, MBP, MAG, periaxin and Cx32 (Nagarajan et al., 2001; Parkinson et al., 2003). Recently, using ChIP (chromatin immunoprecipitation) assays, Krox-20 has been shown to bind to intron elements of a number of genes upregulated during PNS myelination *in vivo*, including *P_0*, *MBP*, *MAG* and *desert hedgehog* (*Dhh*)(Le Blanc et al., 2006; Jang et al., 2006). Additionally, Krox-20 was shown to directly induce P_0 expression through binding to an intron element *in vitro* (LeBlanc et al., 2006). Krox-20 has also been shown to induce expression of a

number of genes involved in lipid and cholesterol metabolism which are also highly expressed during myelination (Nagarajan et al., 2001; Nagarajan et al., 2002; Verheijen et al., 2003). In fact Krox-20 can act synergistically with the sterol regulatory element binding proteins 1 and 2 (SREBP1 and 2), which are also upregulated during myelination, to induce expression of cholesterol/lipid biosynthetic genes, such as 3-hydroxyl-3-methylglutaryl coenzyme A reductase (HMGCR)(Nagarajan et al., 2002; Verheijen et al., 2003; LeBlanc et al., 2005).

In addition to regulating genes important for myelin sheath formation, Krox-20 also demonstrates several other important functions in Schwann cells. Firstly, Krox-20 expression is sufficient to downregulate expression of many non-myelin genes or immature genes, such as L1, c-Jun and Sox-2 (Parkinson et al., 2003, 2004, 2008). Expression of these genes is normally downregulated in Schwann cells that begin to myelinate at birth, but in postnatal *Krox-20* null or $Egr2^{Lo/Lo}$ nerves they remain expressed at high levels (Parkinson et al., 2003, 2004; Le et al., 2005a). Another role for Krox-20 appears to be in arresting proliferation and promoting myelinating Schwann cell survival (Zorick et al., 1999; Parkinson et al., 2004). In *Krox-20* null or $Egr2^{Lo/Lo}$ mice postnatal Schwann cell proliferation and death are greatly elevated, even at postnatal day 12 (P12), when levels of proliferation and death are minimal in control nerves (Zorick et al., 1999; Le et al., 2005a). Furthermore, adenoviral Krox-20 expression is sufficient to inhibit NRG1 induced Schwann cell proliferation and protect Schwann cells against cell death induced by TGFβ addition or serum withdrawal (Parkinson et al., 2004).

A number of co-factors have been identified that modulate the activity of Krox-20, these include, Nab1 and 2 (NGFI-A binding 1 and 2), Ddx20 and HCF-1. Whereas Nab1/2 and Ddx20 are thought to act as corepressors of Krox-20 targets, HCF-1 is

thought to act as a co-activator (Russo et al., 1995; Svaren et al., 1996; Luciano and Wilson, 2003; Gillian and Svaren, 2004). Generation of Nab1/2 double knockout mice demonstrated a similar PNS phenotype, though not as severe, to *Krox-20* null or $Egr2^{Lo/Lo}$ mice, with hypomyelination and reduced expression of myelin genes, increased postnatal Schwann cell proliferation and arrest at the promyelinating stage (Le et al., 2005b). Further evidence to underline the importance of Krox-20/Nab1/2 interaction in PNS myelination comes from the fact that expression of a mutant form of Krox-20 (I268F), that prevents binding of Nabs to Krox-20, in both mice and humans leads to congenital hypomyelinating neuropathy, characterised by severe hypomyelination (Warner et al., 1998; Desmazières et al., 2008). Interestingly, in the absence of the Krox-20/Nab1/2 interaction there appears to be not only reduction in expression of myelin associated genes, like P_0 and *MBP* but also aberrant increased expression of other genes, such as *parathyroid hormone like peptide* (*pthrp*) and *Id-2* (inhibitor of DNA binding 2) (Le et al., 2005b; Desmazières et al., 2008). Recently, studies have demonstrated the mechanism by which Nabs may mediate repression of certain target genes in Schwann cells during myelination. Interaction between Nabs and the chromodomain helicase DNA binding protein 4 (CHD4) subunit of the nucleosome remodelling and deacetylase chromatin remodelling (NuRD) complex is required for Nabs to mediate gene repression (Srinivasan et al., 2006). Furthermore, it was shown by ChIP analysis that Krox-20, Nabs and the CHD4 subunit of the NuRD complex were all recruited to Krox-20 binding sites in the promoters of genes that were repressed during myelination, such as *Id-2* and *Rad* (Mager et al., 2008). Exactly how Krox-20/Nab1/2 interactions regulate myelin gene expression, however, has yet to be determined.

1.5.4.2 Oct-6.

The POU domain protein Oct-6 (SCIP/ Tst-1/Pou3f1) was isolated from a cDNA library from a rat sciatic nerve (Monuki et al., 1989). In the rat PNS, Oct-6 is present in Schwann cell precursors and immature Schwann cells (Blanchard et al., 1996). The peak of Oct-6 expression occurs shortly after birth, with the majority of expression occurring in Schwann cells that are at the pro-myelin or 1:1 stage and some expression in myelinating Schwann cells (Blanchard et al., 1996; Arroyo et al., 1998). Oct-6 expression is progressively downregulated after this period, being expressed in few cells by P30, though it is still detected in some non-myelinating Schwann cells (Monuki et al., 1990; Scherer et al., 1994a; Blanchard et al., 1996; Arroyo et al., 1998). Oct-6 expression has been shown to be regulated by the presence of axons, *in vitro* and *in vivo* (Scherer et al., 1994a; Mandemakers et al., 2000). A Schwann cell specific enhancer (SCE) was identified that was sufficient to drive the correct spatial and temporal expression of Oct-6 in the PNS (Mandemakers et al., 2000). Furthermore, genetic deletion of the SCE in mice was sufficient to replicate the phenotype of the *Oct-6* null mouse (Ghazvini et al., 2002).

In *Oct-6* null mice myelinating Schwann cell differentiation is arrested at the promyelin stage with limited expression of myelin genes such as P_0 and MBP although periaxin and MAG expression appeared normal (Jaegle et al., 1996; Bermingham et al., 1996). This block in differentiation is only transient, however, with myelination proceeding during the second postnatal week and nerves of surviving adult *Oct-6* null mice indistinguishable from wild-type controls (Jaegle et al., 1996). The reason why ablation of Oct-6 leads only to a delay in myelination was partly explained by the fact another POU domain protein, Brn-2, which has a similar expression pattern and virtually identical DNA binding characteristics to Oct-6, was

transiently upregulated in Oct-6 null nerves. Additionally, transgenic expression of Brn2 in Oct-6 null mice partially rescued the delay in myelination whereas ablation of both Oct-6 and Brn-2 led to a much more severe phenotype (Jaegle et al., 2003). Krox-20 appears to be a direct transcriptional target for Oct-6/Brn2, explaining how Oct-6/Brn2 is likely to contribute to myelination (Ghislain and Charnay, 2006; see section 1.5.4.1). More recent experiments have shown that constant overexpression of Oct-6 during Schwann cell development and myelination leads to a hypomyelinating phenotype and eventual axon loss (Ryu et al., 2007). This potentially demonstrates the requirement for the correct level and or the correct temporal downregulation of Oct-6 expression in order for myelination to proceed.

1.5.4.3 Sox10.

In addition to the role of Sox10 in early glial development (see section 1.1.1), more recent evidence suggests that Sox10 also plays an active role in the regulation of myelination. Firstly, some patients suffering from Waardenburg-Hirschsprung disease, due to mutations in Sox10, develop myelin abnormalities characteristic of peripheral neuropathies (Inoue et al., 2002). Furthermore, Sox10 and Krox-20 have been shown to cooperate to activate the Cx32 promoter and mutations in the Sox10 binding site have been shown to underlie some forms of X-linked Charcot-Marie-Tooth neuropathy (CMT)(Bondurand et al., 2001). Sox10 has also been shown to regulate expression of the P_0 promoter and was demonstrated to act synergistically with Krox-20 to induce very high expression levels of the *P_0 gene* through an intron element (Peirano et al., 2000; LeBlanc et al., 2006). Additionally, as mentioned above Sox10 acts in tandem with Oct-6/Brn2 to induce expression of Krox-20 through activation of the MSE (Ghislain et al., 2002; Ghislain and Charnay, 2006). Recently,

evidence from studies of mice expressing mutated forms of Sox10, with deletion of specific domains, has demonstrated a direct role for Sox10 in myelination. Deletion of the dimerization domain prevented Schwann cells from entering the pro-myelinating stage, judged by Oct-6 expression, on schedule whereas deletion of the K2 transactivation domain led to Schwann cells being able to express Oct-6 but not upregulate expression of *MBP* and P_0 mRNA at E18.5 (Schreiner et al., 2007). Thus Sox10 appears to employ different mechanisms for target gene regulation at different points in the Schwann cell lineage.

1.5.4.4 NFκB.

The transcription factor, NFκB has been shown to be highly expressed in pre-myelinating Schwann cells but is subsequently downregulated after P12 (Nickols et al., 2003; Yoon et al., 2008). Blocking the activated nuclear subunit of NFκB, phosphorylated p65 in Schwann cells, inhibited Schwann cell/DRG coculture myelination and prevented activation of Oct-6 (Nickols et al., 2003). Further work has demonstrated that the upstream activator of NFκB in Schwann cells is likely to be protein kinase A (PKA)(see chapter 3)(Yoon et al., 2008).

1.6 Injury and regeneration in the nervous system.

One of the most striking properties of the mammalian PNS is its ability to regenerate after injury. This is in sharp contrast to the mammalian CNS, which shows limited regeneration. These observations were originally detailed by Ramon y Cajal, who went on to show that even though peripheral nerves have the capacity to fully regenerate they were unable to grow through CNS tissue, such as an optic nerve graft (Cajal, 1928). Over fifty years later Aguayo and colleagues performed the converse

experiment. They showed that injured CNS axons, which are unable to grow into CNS tissue, could grow through a transplanted piece of sciatic nerve from the PNS (David and Aguayo, 1981). These results, taken together, show that the proximal stumps of severed axons, in both the PNS and the CNS, have the inherent capacity to re-grow but that only the PNS and not the CNS environment is conducive to axonal regeneration in mammals. This idea is corroborated by evidence from studies which lesion either branch of dorsal root ganglion (DRG) neurons, whose cell bodies lie outside of the CNS and send projections into the CNS (the gracile and cuneate tracts of the spinal cord) and into the PNS. Whereas injuring the CNS branch of DRG neurones does not result in axonal regeneration, lesion of the PNS branch of the same neurons will result in robust regeneration (Raivich and Makwana, 2007). Interestingly, the CNS of non-mammalian animals can regenerate after injury and it has been postulated that the loss of CNS regenerative capacity in mammals may be due to the increased morphological and cellular complexity of their neuronal circuitry (Larner et al., 1995; Pizzi and Crowe, 2007).

When an axon is severed in either the PNS or the CNS the distal stump of that axon begins to degenerate, the surrounding glia react to the injury and an inflammatory response is initiated (Stoll et al., 2002). Seminal observations by Augustus Waller of the frog glossopharyngeal and hypoglossal nerves after transection demonstrated that, using his words, there was a 'disorganization' and 'curdling of the medulla of the nerve (axons)', (Waller, 1850). The term Wallerian degeneration refers to the axonal destruction that follows nerve transection. It is sometimes also used to describe the broader cellular and biochemical events that occur when a nerve is injured.

1.6.1 Axonal Degeneration.

Axonal degeneration occurs within 24 to 48 hours after nerve insult in the rat or the mouse (Lubinska, 1977; Beirowski et al., 2005). Interestingly, the nature of how axons degenerate depends upon the type of injury. After peripheral nerve transection, axons degenerate anterogradely (Lubinska, 1977; Lunn et al., 1990; Beirowski et al., 2005) whereas after peripheral nerve crush axons degenerate retrogradely (Lunn et al., 1990; Beirowski et al., 2005). Furthermore, it appears that large diameter axons degenerate faster than small diameter axons (Ranvier, 1878; Lubinska, 1977). Early experiments demonstrated that the rate of axonal degeneration could be altered by factors such as temperature, axonal transport and calcium influx into the axon (Coleman, 2005).

The discovery that axonal degeneration is delayed by 2 to 3 weeks upon transection of either PNS or CNS nerves in the C57BL/6/Ola (referred to as, Wallerian degeneration slow, Wld^S) strain of mice (Lunn et al., 1989; Perry et al., 1991) has underlined the idea that axonal degeneration is an active process rather than being a passive atrophy of the severed distal axon. Positional cloning identified the Wld^S mutation as a 85Kb tandem triplication on mouse chromosome 4 (Lyon et al., 1993; Coleman et al., 1998). This results in the overexpression of a chimeric protein in neurons, which consists of the first 70 amino acids of the multi-ubiquitination factor, Ufd2 (ubiquitin fusion degradation protein 2a), fused to the entire coding sequence of D4Cole1e/Nmnat1 (nicotinamide mononucleotide adenylyltransferase1). In addition, the cellular retinoid-binding protein, Rbp7 is also overexpressed in Wld^S mice but appears not to be expressed in the nervous system (Conforti et al., 2000; Mack et al., 2001). Both the Nmnat1 and Ube4b (Ufd2) portions of the Wld^S protein can protect against axonal degeneration to an extent. Yet, when expressed as separate

molecules together they are insufficient to replicate the effect of Wld^S, suggesting a more complex explanation for the action of Wld^S (Zhai et al., 2003; Araki et al., 2004; Coleman, 2005; Wang et al., 2005; MacDonald et al., 2006; Conforti et al., 2007). A complete understanding of the Wld^S mechanism of action is likely to provide insight into normal axonal degeneration. At present, how Wld^S interacts with other known mechanisms of axonal degeneration, such as Ca^{2+} elevation and calpain activation is unknown (Coleman, 2005).

1.6.2 The differences between demyelination in the PNS and the CNS.

Whereas axon degeneration happens within the same timescale in the CNS as in the PNS, the clearance of myelin debris is usually completed within 7-14 days in the mammalian PNS whereas myelin debris remains for months after injury in the mammalian CNS (Stoll et al., 1989a, 1989b; Vargas and Barres, 2007). Furthermore, in addition to this there are a number of key differences in the nature of the events that occur during Wallerian degeneration between the CNS and the PNS. The majority of these differences may be attributed to the contrasting responses of the myelinating cells of the PNS, the Schwann cell, and the CNS, the oligodendrocyte to injury (Vargas and Barres, 2007). Briefly, in the PNS, Schwann cells both participate in the removal of myelin debris and proliferate in response to nerve injury. They are joined by hematogenous macrophages, which assist in myelin phagocytosis and removal (Hirata and Kawabuchi, 2002). These events are accompanied by the break down of the blood nerve barrier along the entire length of the nerve, which allows serum components to come into contact with nervous tissue. In the CNS, the oligodendrocyte is unable to clear myelin and axonal debris and instead of proliferating becomes either apoptotic or atrophic (Ludwin, 1990a, 1990b; Barres et

al., 1993). Additionally, resident CNS microglia only phagocytose small amounts of myelin debris and hematogenous macrophage influx is restricted to only the site of injury, possibly due to the fact the blood brain barrier only breaks down at the site of injury (Vargas and Barres, 2007).

1.6.3 Schwann cell demyelination.

Within minutes of nerve injury there is a retraction of paranodal myelin and a dilation of the Schmidt-Lanterman Incisures (SLIs), even at sites distal to the injury region (Williams and Hall, 1971). In teased fibre preparations of degenerating rat phrenic nerves, myelin sheaths begin to break up into myelin ovoids around 20 hours post injury for the thinnest fibres and 32 hours post injury for the thickest fibres. Within a given internode, myelin ovoid formation is seen to originate in the perinuclear cytoplasm and then move from internode to internode along a proximodistal gradient from the injury site (Lubinska, 1977). Electron microscopic analysis has demonstrated that myelin fibre fragmentation appeared to begin at sites adjacent to the SLIs (Ghabriel and Allt, 1979). It was proposed that the initial dilation of the SLIs could be a mechanical response due to the loss of tension in the nerve fibre as a result of injury or a biochemical response by the Schwann cell (Young, 1945; Williams and Hall, 1971). In addition, nodal widening and paranodal demyelination are known to occur within minutes at sites adjacent to nerve compression injuries, suggesting that mechanical forces may also be involved in their formation after nerve transection or crush (Dyck et al., 1990). Dilation of the SLIs would allow for apposition and fusion of opposing myelin membranes around a collapsing axon thus forming the closed end of a myelin ovoid (Williams and Hall, 1971; Ghabriel and Allt, 1979). These observations provide convincing evidence that

the Schwann cell initiates demyelination. Indeed, Stoll and colleagues reminded us that Cajal initially described the series of early changes in the Schwann cell and, significantly, that these events preceded the appearance of haematogenous phagocytic cells (Stoll et al., 1989b; Ramon y Cajal, 1928).

How Schwann cells process myelin after ovoid formation is not well understood. Many ideas have been proposed, based on findings from in vitro studies, but so far there has been a critical lack of in vivo evidence for many of these hypotheses. Experiments inside Millipore chambers by Beuche and Friede, in which segments of sciatic nerve were transplanted into the peritoneal cavity, to prevent infiltration of blood-born phagocytes, suggested that Schwann cells play no part in myelin digestion and instead divide away from or 'reject' their myelin sheaths (Beuche and Friede, 1984). Degeneration observed in sciatic nerve explant cultures also showed Schwann cells dividing away from their myelin sheaths and secreting myelin into the endoneurial space (Crang and Blakemore, 1986). In contrast, reduction of macrophage infiltration into injured peripheral nerves by whole body irradiation prior to surgery demonstrated that myelin removal proceeded normally for the first 5 days after injury and then proceeded at a slower rate after 5 days. This suggested that the main contribution to myelin removal by blood-born macrophages happens after 5 days and that another cell type, potentially the Schwann cell, was responsible for myelin removal before this time point (Perry et al., 1995). This idea is supported by observations from Schwann cell/DRG coculture models of Wallerian degeneration. In this system, after DRG axons have been severed, most Schwann cells are able to remove myelin debris in the absence of macrophages. Only Schwann cells associated with very large myelin sheaths appear incapable of removing all their myelin, suggesting that macrophages may assist with the removal of large myelin

sheaths (Fernandez-Valle et al., 1995). This idea is consistent with the conclusions from the early *in vivo* observations by Cajal and then the later findings by Stoll and colleagues (Stoll et al., 1989b; Cajal et al., 1928).

Electron microscopic analysis shows us that Schwann cells contain whorls of myelin debris and fat and are therefore capable of processing degenerating myelin (Stoll et al., 1989b; Reichert et al., 1994). In addition, Schwann cells show increased numbers of dense end-stage lysosomal bodies, seen in close association to myelin whorls in the cytoplasm, and demonstrate considerable acid phosphatase reactivity after nerve injury, characteristic of heightened degradative enzyme activity (Holtzman and Novikoff, 1965; Bigbee et al., 1987; Stoll et al., 1989b; Wang et al., 2004). An enzyme that is upregulated by Schwann cells after nerve injury is phospholipase A_2 (PLA_2) and blocking its action pharmacologically can delay myelin degeneration (Paul and Gregson, 1992; De et al., 2003). One of the ways PLA_2 might contribute to myelin degeneration is by production of lysophosphatidylcholine (LPC), which can act as a detergent to cause myelin breakdown (Hall and Gregson, 1971). Matrix metalloproteinases (MMPs) may also have an important role to play in myelin degeneration. MMPs, 2, 7, 9 and 12 are all upregulated by Schwann cells after nerve injury (Hughes et al., 2002; Krekoski et al., 2002) and an *MMP-9* knockout mouse shows delayed demyelination after sciatic nerve injury (Shubayev et al., 2006). Importantly, further experiments will be required to demonstrate whether the effects observed in injured nerves by inhibiting PLA_2 and MMP-9 are Schwann cell autonomous since macrophages also express these proteins.

Although Schwann cells are seen to contain myelin debris after nerve injury, how it ends up inside the Schwann cell still remains unknown. Many authors have proposed phagocytosis of myelin debris as a solution. Certainly, Schwann cells are

capable of phagocytosing myelin debris. Cultured Schwann cells treated with exogenous myelin membranes contained MBP positive phagosomes, indicating uptake and processing of myelin. Additionally, this process could be blocked with ammonium chloride, a lysosomal inhibitor (Bigbee et al., 1987). Furthermore, a galactose-specific lectin, MAC2, was identified as a potential mediator of myelin phagocytosis by Schwann cells. MAC2 is upregulated by Schwann cells after nerve injury and blocking the MAC2 receptor using the competitive inhibitors galactose and lactose slowed myelin degeneration in an in vitro nerve segment degeneration assay (Reichert et al., 1994). Alternatively, Schwann cells might internalise and digest their myelin membranes by an endosomal/ autophagic mechanism. The numerous myelin digestion vacuoles seen within Schwann cells appear to be bounded by a single membrane that derives from the myelin itself, suggesting that 'myelin may not be phagocytosed in the usual manner' (Holtzman and Novikoff, 1965). Evidently, the lack of any observation of myelin expulsion and subsequent phagocytosis by Schwann cells, in the many studies of peripheral nerve demyelination since the time of Cajal, suggests that phagocytosis may not be a common process for Schwann cell demyelination. It remains to be tested whether Schwann cells operate using an autophagic-like mechanism to demyelinate.

1.6.4 Injury induced Schwann cell proliferation.

In the uninjured adult nerve, Schwann cell proliferation is minimal but is rapidly induced after injury (Abercrombie and Johnson, 1946; Thomas, 1948). This proliferation is highest in nerves containing a majority of large myelinated fibres, peaking around 3 days after injury in mice, and lowest in nerves containing only unmyelinated fibres (Thomas, 1948; Abercrombie et al., 1959; Bradley and Asbury,

1970; Romine et al., 1976). Injury induced Schwann cell proliferation moves along a proximo-distal gradient, with the rate of proliferation for the distal nerve peaking roughly a day later than for the region closest to the injury site (Friede and Johnstone, 1967; Oaklander et al., 1987).

There is an apparent difference in proliferative behaviour to injury of myelinating Schwann cells compared to non-myelinating Schwann cells. Whereas myelinating Schwann cells all along the distal stump of an injured nerve proliferate, a crush of the unmyelinated cervical sympathetic trunk revealed that non-myelinating Schwann cells only proliferate at the injury site but not in the distal nerve (Romine et al., 1976). However non-myelinating Schwann cells do demonstrate a much higher rate of proliferation distally in a mixed nerve, like the Sciatic nerve (Romine et al., 1976; Clemence et al., 1989). Similarly, Schwann cell/DRG co-culture experiments have shown that only the Schwann cells that have elaborated a myelin sheath proliferate after the neurites have been transected. Non-myelinating Schwann cells were only induced to proliferate when directly injured in the presence of degenerating neurites (Salzer and Bunge, 1980). Furthermore, the presence of Schwann cells undergoing demyelination is sufficient to induce non-myelinating Schwann cells of neighbouring intact unmyelinated fibres to proliferate (Griffin et al., 1990; Murinson et al., 2005), suggesting that the presence of degenerating myelin may be a proliferative stimulus for all Schwann cells.

The idea that degenerating myelin may contain the stimulus for proliferation after injury has been partially tested by treating Schwann cells in culture with myelin membranes. A subset of Schwann cells will proliferate in response to endocytosis and lysosomal processing of the myelin membranes (Yoshino et al., 1984; Meador-Woodruff et al., 1985). Macrophage processing of myelin membranes can also

produce a soluble mitogenic factor for cultured Schwann cells (Baichwal et al., 1988). Furthermore, the fact that non-myelinating Schwann cells of uninjured unmyelinated axons undergo mitosis in response to neighbouring myelinated fibre degeneration suggests the existence of a diffusible mitogen, possibly released from myelin (Murinson et al., 2005).

An alternative hypothesis for injury induced Schwann cell proliferation is that the level of proliferation is related to cell-to-cell interactions within a basal lamina tube after myelin removal. Large myelinated nerves have low initial cell densities but high rates of proliferation after injury whereas nerves containing unmyeliated fibres have high initial cell densities and low levels of proliferation (Joseph et al., 1950). It has been suggested that in myelinated fibres, after myelin removal, loss of cell to cell contact could be the stimulus for Schwann cells to proliferate, as with other forms of epithelial cell (Crang and Blakemore, 1986). Thus, there is a possibility that both diffusible and direct cell-to-cell signals may be important in this process.

The intracellular mechanisms that control injury-induced Schwann cell proliferation are largely unknown but are likely to be related to mechanisms of proliferation that occur in culture in response to growth factors (Harrisingh and Lloyd, 2004). It has been shown that cyclin D1 expression is upregulated by Schwann cells after nerve injury and is required for their full mitogenic response (Kim et al., 2000; Atanasoski et al., 2001; Yang et al., 2008). In addition, *cyclin-dependent kinase 4* (*cdk4*) but not *cdk2* or *cdk6* null mice show reduced proliferation after nerve transection (Atanasoski et al., 2008) and furthermore, nerve transection also leads to the reduction in levels of the cell cycle inhibitor p27 in Schwann cells (Shen et al., 2008).

It is important to note that Schwann cell proliferation in transected nerves takes place in the absence of re-growing axons, unlike after nerve crush. Thus, Schwann cell proliferation after nerve crush during axonal regeneration may have different mechanisms to Schwann cell proliferation in transected nerves. In support of this, developmental 'axon induced' Schwann cell proliferation appears to be differently controlled in comparison to mitosis after nerve cut since embryonic cell division is normal in the *cyclin D1* and *cdk4* knockout mice (Kim et al., 2000; Atanasoski et al., 2001; Atanasoski et al., 2008; Yang et al., 2008; see section 1.1.3.1).

1.6.5 Role of macrophages in myelin clearance during peripheral nerve injury.

Although Schwann cells are involved in the clearance of myelin after nerve injury, they require assistance from heamatogenous macrophages to complete myelin removal. Crucially, macrophage entry is minimal after nerve injury in the CNS, which may be one of the main reasons why myelin clearance is so slow (Stoll et al., 1989a; Vargas and Barres, 2007).

Macrophages begin to enter the peripheral nerve from the bloodstream at the lesion site and then enter distal segments of the degenerating nerve from 3 to 4 days after injury, with numbers peaking after two weeks (Olsson and Sjöstrand, 1969; Monaco et al., 1992; Mueller et al., 2003). Prevention of macrophage entry into degenerating peripheral nerve, by placement into Millipore diffusion chambers in the peritoneal cavity of mice (Beuche and Friede, 1984; Dahlin, 1995), intra-peritoneal (IP) injection of silica dust (Beuche and Friede, 1986), whole body irradiation (Perry et al., 1995) or treatment with liposomes loaded with clodronate (Brück et al., 1996; Liu et al., 2000) can delay myelin clearance. In addition, the peripheral nerve also contains a resident population of macrophages, which proliferate after nerve injury

and also participate in removal of myelin debris (Monaco et al., 1992; Hirata et al., 1999; Mueller et al., 2001; Mueller et al., 2003).

1.6.5.1 Mechanism of recruitment of haematogenous macrophages during nerve injury.

It is widely believed that the disruption of the Schwann cell axon interface leads to macrophage recruitment, since influx does not happen after nerve injury in the Wld^S mouse (Lunn et al., 1989; Brück et al., 1995). This belief is further supported by the observation that during LPC-induced demyelination, macrophages do enter the Wld^S nerve even though the axons remain intact (Hall, 1993). In addition, conditioned medium from denervated Schwann cells induces macrophage chemotactic activity in culture (Tofaris et al., 2002).

Upon nerve injury Schwann cells upregulate production of a number of cytokines and chemokines, some of which have been shown to act as chemoattractant signals for macrophages. The chemokines, macrophage chemoattractant protein-1 (MCP-1) and macrophage inflammatory protein-1α (MIP-1α) and the cytokine interleukin-1β (IL-1β), are expressed by Schwann cells within 24 hours of nerve injury (Toews et al., 1998; Taskinen and Röyttä, 2000; Shamash et al., 2002; Perrin et al., 2005; Cheepudomwit et al., 2008). The use of blocking antibodies to MCP-1, MIP-1α and IL-1β reduces both macrophage infiltration and activation after nerve transection, implicating all three in macrophage recruitment during peripheral nerve injury (Perrin et al., 2005). Furthermore, injured peripheral nerves from *CCR2* (a MCP-1 receptor) knockout mice recruited a reduced number of macrophages and showed delayed myelin clearance (Siebert et al., 2000).

Additionally, mice lacking the cytokines tumor necrosis alpha (TNFα) or leukaemia inhibitory factor (LIF) show reduced macrophage recruitment after peripheral nerve injury (Liefner et al., 2000; Sugiura et al., 2000; Shubayev et al., 2006). *LIF* mRNA is induced predominantly in Schwann cells after nerve injury and is chemotactic for macrophages. Thus it may directly induce macrophage influx, although it may also act indirectly through induction of MCP-1 (Banner and Patterson, 1994; Sugiura et al., 2000; Tofaris et al., 2002). In the case of TNFα, it is produced by Schwann cells, fibroblasts and also by macrophages after injury although it is not required for macrophage activation (Wagner and Myers, 1996; Liefner et al., 2000; Shamash et al., 2002). It can act as a chemoattractant for macrophages but may also act to recruit macrophages indirectly by upregulating expression of chemokines such as MCP-1 and other factors such as MMP-9 (Wang et al., 1990; Subang and Richardson, 2001; Shubayev et al., 2006). MMP-9 is upregulated by Schwann cells and macrophages after nerve injury and *MMP-9* knockout mouse nerves show reduced macrophage infiltration after injury, though it is currently unknown how MMP-9 contributes to macrophage recruitment (Shubayev et al., 2006). Another molecule, pancreatitis-associated protein-III (PAP-III), has recently been shown to be a chemoattractant signal for macrophages (Namikawa et al., 2006). PAP-III is mainly released from Schwann cells after nerve injury and overexpression or knockdown of PAP-III *in vivo*, using adenoviruses, can increase or retard macrophage recruitment into crushed sciatic nerves (Namikawa et al., 2005; Namikawa et al., 2006).

Although most studies analyse Schwann cell inflammatory gene expression from a mixed nerve, like the sciatic, a recent investigation has highlighted the possibility that myelinating Schwann cells and non-myelinating Schwann cells may react differently to nerve injury, in terms of cytokine and chemokine expression. Non-

myelinating Schwann cells show upregulation of *MCP-1* but not *IL-1β* or *LIF* mRNA after selective capsaicin induced destruction of unmyelinated C-fibres, unlike myelinating Schwann cells after sciatic nerve transection (Cheepudomwit et al., 2008).

In addition to macrophage chemoattractant signals produced by Schwann cells during Wallerian degeneration, complement components from the bloodstream also help to recruit macrophages. Blocking complement activation *in vitro* and *in vivo*, using complement protein 3 (C3) deficient serum, blocking antibodies to complement receptor 3 (CR3) or cobra venom can impair both the recruitment of macrophages and their phagocytic ability and thus delay myelin clearance (Lunn et al., 1989; Brück and Friede, 1990; Brück and Friede, 1991; Dailey et al., 1998). The use of complement protein 6 (C6) deficient rats demonstrated a requirement for C6 and formation of the membrane attack complex (MAC, a complex of complement proteins C5b-9) in macrophage recruitment and phagocytic activation after nerve injury, since in these rats demyelination was delayed (Ramaglia et al., 2007). The classical pathway of the complement system is activated after nerve injury and inhibiting its activation prevents activation of downstream complement proteins and retards myelin clearance during nerve injury (Vargas and Barres, 2007). The classical pathway can be activated by the binding of C1q to non-self epitopes, either directly or via antibodies. Interestingly, production of autoantibodies to degenerating myelin may be involved in macrophage recruitment and activation as both are delayed in B-cell deficient mice (Vargas and Barres, 2007).

1.6.6 Schwann cell activation versus dedifferentiation?

Some researchers refer to Schwann cells dedifferentiating after nerve injury, due to the loss of expression of myelin specific genes and the upregulation of a number of immature genes. Other researchers prefer to describe Schwann cells as becoming activated after nerve injury due to their expression of cytokines and growth factors. However, in this thesis, the term 'Schwann cell activation' refers to the general phenotype of the Schwann cell after nerve injury, whereas 'Schwann cell dedifferentiation' will only be used in reference to the upregulation of genes expressed by Schwann cells after nerve injury that were previously expressed during embryonic development (see Fig.1.1, 1.2 and Chapter 4).

1.6.7 How do Schwann cells become activated during Wallerian degeneration?

As previously described, Schwann cells react during Wallerian degeneration with a large number of changes, this argues for a molecular mechanism of Schwann cell activation, rather than a passive response to nerve injury due to loss of axonal myelin inducing signals (Decker et al., 2006). Furthermore, the fact that a number of toxins and pathogens can actively induce Schwann cells to demyelinate prior to axon degeneration points to a potential pre-existing molecular pathway for demyelination that may be 'hijacked' by pathogens, in the case of PNS diseases such as, Guillain-Barré syndrome and leprosy (Hall and Gregson, 1971; Tapinos et al., 2006; Lee et al., 2007).

1.6.7.1 Does the loss of the axon trigger activation of Schwann cells?

Upon nerve transection in the Wld^s mouse, Schwann cells fail to respond to the injury. However, when Wld^s Schwann cells ensheath a wild-type axon they react

normally upon transection of the axon (Lunn et al., 1989; Glass et al., 1993). This suggests that Schwann cells only become activated upon loss of axonal contact. As mentioned earlier, Krox-20 is an axonally induced Schwann cell transcription factor that controls myelination (Topilko et al., 1994; Jessen and Mirsky, 2005). After nerve injury, expression of Krox-20 disappears from the majority of myelinating Schwann cells within 3 days of the insult (Topilko et al., 1997). Simultaneously, Schwann cells down-regulate synthesis of myelin lipids and proteins (White et al., 1989; Trapp et al., 1988). A recent study, using a tamoxifen inducible Cre recombinase, ablated Krox-20 from adult myelinating Schwann cells. This demonstrated that the loss of Krox-20 from myelinating Schwann cells was sufficient to induce rapid demyelination in the absence of axonal degeneration (Decker et al., 2006). As the authors of this study suggested, the rapidity of the induction of the demyelination argues for an active programme of Schwann cell demyelination and one that is normally repressed by the presence of Krox-20 (Decker et al., 2006). An example of how Krox-20 may suppress a 'demyelination programme' is demonstrated by the fact that enforced Krox-20 expression in cultured Schwann cells can downregulate the expression of factors potentially involved in regulating the phenotype of denervated Schwann cells, such as c-Jun, Sox-2 and components of the Notch pathway (De Felipe et al., 1994; Stewart, 1995; Shy et al., 1996; Parkinson et al., 2004; Le et al., 2005; Parkinson et al., 2008; A. Woodhoo, unpublished observations). Furthermore, there are greatly increased levels of c-Jun, Sox-2 and the activated Notch intracellular domain (NICD) in Krox-20 null nerves (Parkinson et al., 2004; Le et al., 2005a; A. Woodhoo, unpublished observations). These results, together, imply that the down-regulation of Krox-20 in myelinating Schwann cells after loss of axonal contact could lead to the upregulation

of a 'normally suppressed' demyelination program, involving factors such as c-Jun, Sox-2 and the Notch pathway.

1.6.7.2 The role of ligand receptor signalling systems.

Another way that Schwann cells might sense nerve injury is through activation of extracellular receptors. This might occur through release of a ligand from the degenerating axon or potentially through autocrine loops induced within the Schwann cell by loss of axonal contact. One ligand-receptor signalling system that has been studied in some depth in the context of Wallerian degeneration is the NRG1/erbB system (see section 1.5.2). Upon sciatic nerve injury, expression of erbB2 and erbB3 are upregulated by Schwann cells (Cohen et al., 1992; Carroll et al., 1997), erbB2 is tyrosine phosphorylated and the downstream kinase, Src is activated (Kwon et al., 1997; Zhao et al., 2003; Guertin et al., 2005). Furthermore, the mRNA for *NRG1 type II* (*glial growth factor, GGF*) is induced as early as 3 days after injury and immunohistochemistry using a pan-neuregulin antibody showed that neuregulin protein colocalised with S100β, suggesting Schwann cells as a possible source of GGF during Wallerian degeneration (Carroll et al., 1997). A more recent study has shown that erbB2 is actually phosphorylated within minutes of nerve injury at nodal and paranodal regions (Guertin et al., 2005).

These observations indicate that the NRG1/erbB signalling system may be involved in the initiation of some of the events of Wallerian degeneration such as demyelination. In support of this, addition of high concentrations of GGF to myelinating Schwann cell/DRG cocultures can induce demyelination (Zanazzi et al., 2001). Also, blocking erbB2 activation in a coculture model of Wallerian degeneration or after nerve transection can delay demyelination and reduce injury

induced Schwann cell proliferation (Guertin et al., 2005). Furthermore, *mycobacterium leprae* can induce demyelination by binding to and activating erbB2 and chemically blocking erbB2 activation can reduce *m.Leprae*-induced demyelination *in vitro* and *in vivo* (Tapinos et al., 2006). Furthermore, constitutive erbB2 activation in terminal Schwann cells at neuromuscular junctions induces a phenotypic response characteristic of denervation, including process extension and proliferation (Hayworth et al., 2006). However, conditional ablation of *erbB2* in Schwann cells using a tamoxifen inducible *PLP-CreERT2* allele demonstrated that erbB2 was dispensable for most of the events during Wallerian degeneration, especially proliferation (Atanasoski et al., 2006). At present, it is difficult to reconcile these results with all the above findings unless other receptor signalling pathways are involved in the Schwann cell reaction to nerve injury.

Other ligand/receptor signalling pathways that have been implicated in the Schwann cell reaction to injury are the transforming growth factor β (TGFβ) signalling pathway, the Notch signalling pathway, fibroblast growth factors (FGFs), the toll-like receptors 2 and 3 (TLR2 and 3), platelet derived growth factor-BB (PDGF-BB) and parathyroid hormone related peptide (PTHrP) (Oya et al., 2002; Lee et al., 2006; Jungnickel et al., 2006; D'Antonio et al., 2006b; Macica et al., 2006; A. Woodhoo, unpublished observations). The TGFβ signalling pathway has been strongly linked with the Schwann cell response to Wallerian degeneration, since *TGFβ1* mRNA is upregulated after injury (Scherer and Salzer, 2001). Nevertheless, mice with a Schwann cell conditional mutation within the TGFβ receptor II (TGFβRII), which is considered to impair all TGFβ signalling, showed normal myelin clearance and Schwann cell proliferation after injury, suggesting that TGFβ1

signalling does not have a major involvement in these events (D'Antonio et al., 2006b).

Denervated Schwann cells upregulate expression of FGF-2 and FGF-5 after nerve injury and both isoforms can activate FGF receptors 1 and 2, which are also expressed by Schwann cells (Liu et al, 1995; Meisinger and Grothe, 1997; Scarlato et al., 2001). Although FGF-2 addition can inhibit the differentiation of cultured Schwann cells, unlike NRG1, it does not induce demyelination when added to Schwann cell/DRG myelinating cocultures (Morgan et al., 1994; Zanazzi et al., 2001). Transgenic overexpression of FGF-2 in mice increases Schwann cell proliferation after nerve injury whereas *FGF-2* knockout animals show faster rates of Wallerian degeneration close to the injury site (Jungnickel et al., 2004; Jungnickel et al., 2006). The results suggest that FGF signalling can modulate the early Schwann cell response to injury, though further experimentation is needed to identify its exact role.

The Notch signalling pathway is activated during Wallerian degeneration, as seen by the increased presence of the cleaved intracellular domain of the Notch receptor (NICD) in sciatic nerve extracts from transected nerves. Furthermore transgenic mice overexpressing NICD specifically in Schwann cells demonstrate faster myelin clearance after nerve injury. In addition, mice, where *RBP-J/Su(H)*(a transcription factor which is necessary for Notch signalling) or the *Notch 1* receptor have been conditionally ablated specifically in Schwann cells, show slower myelin clearance after injury. These results together implicate the Notch signalling pathway in modulating the Schwann cell response after injury (A. Woodhoo, unpublished observations).

TLRs bind necrotic cell-derived material thereby activating innate immune cells (for review see Akira and Takeda, 2004). In the case of Schwann cells, TLR2 and 3

were shown to mediate inflammatory gene expression, such as *MCP-1* and *inducible nitric oxide synthase (iNOS)*, by Schwann cells, in response to treatment with necrotic neuronal cell extracts (Lee et al., 2006). Furthermore, mice deficient in either TLR2 or TLR4 show reduced macrophage infiltration and delayed myelin clearance after nerve injury (Boivin et al., 2007). Although the identity of the ligand binding to Toll receptors after nerve injury is unknown, these studies offer an interesting prospect in understanding how Schwann cells may directly sense nerve damage, particularly at the site of injury.

1.6.7.3 Do Schwann cells become hypoxic after nerve injury?

Peripheral nerve ischemia can result in myelin degradation and axonal loss (Schmelzer et al., 1989; Myers et al., 1991; Myers et al., 1993; Schratzberger et al., 2000). During ischemia cells become hypoxic and react by trying to restore oxygen homeostasis by upregulation of specific genes, such as *iNOS* (Rocha, 2007). In the case of iNOS expression, the relative contribution by Schwann cells and macrophages in the degenerating peripheral nerve is still uncertain (Gonzalez-Hernandez et al., 1999; Levy et al., 2001; Conti et al., 2004). Nevertheless, sciatic nerve injury in *iNOS* knockout mice demonstrated a robust delay in myelin sheath degradation, suggesting iNOS has an important role to play during Wallerian degeneration (Levy et al., 2001).

Most of the genes regulated during hypoxia are under the control of members from the hypoxia inducible transcription factor (HIF) family (Rocha, 2007). Interestingly, a number of these genes are upregulated by Schwann cells after peripheral nerve injury, such as, heme oxygenase (H0-1), the transferrin receptor, vascular endothelial growth factor (VEGF) and erythropoietin (Epo) (Raivich et al., 1991a; Hirata et al., 2000; Levy et al., 2001; Scarlato et al., 2003; Keswani et al.,

2004; Li et al., 2005). The hypoxia regulated subunit of HIF, HIF-1α, is upregulated in the Sciatic nerves of diabetic rats and is expressed along with Epo and the Epo receptor (EpoR) in vestibular schwannomas (Chavez et al., 2005; Diensthuber et al., 2007). It will be of great interest for future studies to investigate whether expression of HIF-1α is induced in Schwann cells after nerve injury and to elucidate the roles of the many hypoxia responsive genes that are regulated during Wallerian degeneration.

1.6.7.4 Downstream intracellular signalling cascades.

Whatever the signals are that are responsible for the activation of Schwann cells after peripheral nerve injury it is becoming clear that they are, at least partially, transduced via intracellular signalling cascades. The mitogen-activated protein kinase pathway (MAPK) has recently been implicated in controlling Schwann cell dedifferentiation. The MAPK pathway consists of the Ras-Raf-MEK-ERK (Extracellular signal regulated kinase) signalling cascade. ERK1/2 is rapidly phosphorylated and activated after nerve injury and immunostaining shows that the majority of phosphorylated ERK1/2 is contained within Schwann cells (Harrisingh et al., 2004; Guertin et al., 2005). Strong activation of the MAPK pathway can block Schwann cell differentiation in culture (Harrisingh et al., 2004; Ogata et al., 2004). Furthermore, induction of sustained MAPK activation in Schwann cells in a Schwann cell/DRG coculture system induces demyelination (Harrisingh et al., 2004). Recent evidence has also shown that phosphatidic acid (PA) induced demyelination in Schwann cell/DRG cocultures required activation of the MAPK pathway (Nadra et al., 2008).

In addition to the MAPK pathway, the c-Jun N-terminal kinase (JNK) and p38-mitogen activated protein kinase (p38MAPK) are also rapidly phosphorylated and

activated after peripheral nerve injury (Myers et al., 2003; Parkinson et al., 2008; A. Bhaskaran, unpublished observations). The JNK and p38MAPK pathways have been implicated in the control of inflammatory gene expression, including TNFα and iNOS, in Schwann cells (Myers et al., 2003; Lee et al., 2006; Lee et al., 2007). Moreover, in the presence of either a JNK or a p38MAPK inhibitor, Schwann cells show significantly less myelin degeneration in a dissociated Schwann cell demyelination assay or in whole sciatic nerve segments allowed to degenerate in culture in the absence of haematogenous macrophages (A. Bhaskaran, unpublished observations). In summary, the MAPK, JNK and p38MAPK pathways may all be important regulators of Schwann cell demyelination and activation after nerve injury.

1.6.7.5 Is there evidence for a transcriptional program of Schwann cell activation after nerve injury?

After nerve injury, Schwann cells upregulate a number of transcription factors, many of which are also expressed by, albeit at lower levels, immature Schwann cells and non-myelinating Schwann cells (Scherer and Salzer, 2001). Schwann cells have been shown to upregulate Egr-1 (Krox-24), Oct-6 (SCIP/Pou3f1/Tst-1), Sox-2 and three members of the AP-1 family of transcription factors, c-Jun, c-fos and Activating transcription factor 3 (ATF3) after nerve injury (De Felipe and Hunt, 1994; Scherer et al., 1994a; Liu et al., 1995; Stewart et al., 1995; Shy et al., 1996; Topilko et al., 1997; Soares et al., 2001; Hunt et al., 2004; Le et al., 2005a). The up-regulation of Oct-6 after nerve transection is not thought to have a major role in the events during Wallerian degeneration as its exact expression does not correlate with the fall in P_0 mRNA or the induction of Schwann cell proliferation (Scherer et al., 1994). Egr-1 expression after nerve injury may be responsible for the upregulation of the low

affinity neurotrophin receptor ($p75^{NTR}$) by denervated Schwann cells since it was recently shown that Egr1 and Egr3 could upregulate expression of $p75^{NTR}$ in Schwann cells (Gao et al., 2007). The role of Sox-2 in Schwann cells after nerve injury is unknown, although it could potentially have a role in proliferation because a Sox-2 expressing lentivirus augmented NRG-1 induced Schwann cell DNA synthesis in culture (Le et al., 2005a).

1.6.8 How do Schwann cells promote axonal regeneration?

Studies of peripheral nerve regeneration in the Wld^S mouse have shown that in the absence of Wallerian degeneration, both sensory and motor fibre regeneration is severely compromised (Lunn et al., 1989; Brown et al., 1992; Chen and Bisby, 1993a; Chen and Bisby, 1993b; Brown et al., 1994). This suggests that the cellular and molecular changes that the distal stump undergoes after nerve injury are vital for adequate nerve regeneration. In support of this, normal uninjured adult peripheral nerves are not able to promote the growth of either motor or sensory axons (Langley and Anderson, 1904; Brown et al., 1991; Bedi et al., 1992).

The fast removal of myelin debris in the PNS is likely to be an important factor leading to successful peripheral nerve regeneration (Vargas and Barres, 2007). In the CNS, constitutive inhibitors of axonal regeneration such as Nogo, MAG and oligodendrocyte myelin glycoprotein (Omgp) are expressed in myelin (Filbin, 2003). Some of these proteins are also present in PNS myelin and over-expression of Nogo-A (which is not normally expressed in PNS myelin) in Schwann cells significantly impairs PNS axon regeneration (Pot et al., 2002). This suggests that PNS axons can respond to the same growth inhibitory signals as CNS axons, leading weight to the

argument that fast removal of myelin debris is needed in order to promote successful axonal regeneration.

After nerve injury, the Schwann cells and their basal lamina remain in the distal stump forming the bands of Büngner (Scherer and Salzer, 2001). The importance of these Schwann cell tubes was highlighted by an elegant study where the authors traced individual axons over time as they grew through the distal stump and into the neuromuscular junction of the sternocleidomastoid muscle. When the Schwann cell tubes remained intact after nerve crush, 96% of axons retraced their original paths and innervated their original endplate. However, when the Schwann cell tubes were disrupted through nerve transection, only about 10% of axons innervated the correct endplate (Nguyen et al., 2002). It was suggested that the main reason for this disparity was due to axons choosing the wrong basal lamina tube at the site of transection, as Cajal observed, but also because axon growth was delayed after nerve cut so that axons made branching mistakes in the distal stump of the nerve (Cajal, 1928; Nguyen et al, 2002).

A number of peripheral nerve regeneration studies have reported axons regrowing along the inner aspect of the basal lamina tubes (Barton, 1962; Nathaniel and Pearse, 1963; Ide et al., 1983; Scherer and Easter, 1984; Schwab and Thoenen, 1985, Martini and Schachner, 1988). This raised the question of whether the basal lamina in the absence of Schwann cells was sufficient to promote axonal regeneration. Indeed, axons do extend neurites into sections of sciatic nerve in which Schwann cells have been eradicated by repeated cycles of freeze-thawing (Ide et al., 1983; Schwab and Thoenen, 1985). However, growth of neurites is markedly reduced into acellular peripheral nerve grafts when compared with cellular grafts (Hall, 1986), and re-growing axons are always seen in contact with living cells, such as Schwann cells or

other axons but never exclusively with the basal lamina (Martini and Schachner, 1988). Furthermore, Schwann cells are among some of the best substrates for neurite growth in culture (Fallon, 1985; Tomaselli et al., 1986). Other research has shown that axons extend in tandem with Schwann cells processes projected from the cut end of a nerve. Furthermore, the axon regrowth is faster when Schwann cells are allowed to extend their processes before the axons start to regrow (Son and Thompson, 1995; Son et al., 1996). These findings suggest that Schwann cell processes may actually guide regenerating axons. Thus it appears likely that the presence of Schwann cells, their processes and an intact basal lamina are all required for successful peripheral nerve regeneration.

Little is known about the intracellular signalling that is required by Schwann cells to promote axonal regeneration, although mice deficient in glial fibrillary acidic protein (GFAP) show a regenerative deficit after nerve crush (Triolo et al., 2006). Most of the recent research has focused on the extracellular molecular signals that target axons, many of which are derived from Schwann cells, and are required for adequate nerve regeneration. These factors fall into two main categories, ECM and CAMs and neurotrophic factors. These two topics are briefly reviewed here but for a more detailed account see Scherer and Salzer, (2001); Boyd and Gordon, (2003a); Pizzi and Crowe, (2007); Raivich and Makwana, (2007).

1.6.8.1 Candidate ECM components and CAMs that promote regeneration.

To date the most important ECM component secreted by Schwann cells that is known to contribute to axonal regeneration is laminin; potentially laminin 2 and 8 (Cornbrooks et al., 1983; Tomaselli et al., 1986; Chen and Strickland, 2003). In vitro, antibodies to a laminin-heparan sulphate proteoglycan complex strongly inhibit the

growth of ciliary ganglion neurons on Schwann cell derived ECM substrates (Tomaselli et al., 1986). In vivo, conditional ablation of the *laminin γ1 chain* using cre recombinase under the control of the CAM kinase II promoter reduced the number of regenerating motorneurons, 21 days after sciatic nerve crush (Chen and Strickland, 2003). However, since this promoter is active in neurons in addition to Schwann cells it is difficult to interpret the findings in this study. Potentially, the integrin receptor $\alpha_7\beta_1$ could be involved in Schwann cell signalling during nerve regeneration as it is expressed by Schwann cells as well as by regrowing axons (Werner et al., 2000; Previtali et al., 2003c). Furthermore, mice lacking α_7-integrin demonstrate delayed peripheral nerve regeneration after injury (Werner et al., 2000). Another ECM component, produced by Schwann cells, Reelin, also plays some role in nerve regeneration. *Reeler* mice, which are deficient in Reelin, have a 30% reduction in axonal growth rates at 2 and 4 days after crush but show normal numbers of motorneurons regenerating at 21 days after crush (Panteri et al., 2006; Lorenzetto et al., 2008). Other ECM molecules associated with the Schwann cell basal lamina that may be involved in peripheral nerve regeneration are, fibronectin, tenascin C, hyaluronic acid, F-spondin and heparan sulpfate and chondroitin sulfate proteoglycans (HSPGs and CSPGs) (Martini et al., 1990; Wang et al., 1992; Tona et al., 1993; Braunewell et al., 1995; Burstyn-Cohen 1998).

In addition to promoting peripheral nerve regeneration, some ECM components such as CSPGs have been suggested to act as inhibitory signals (Muir et al., 1989; Zuo et al., 1998). Degradation of CSPGs in various models of peripheral nerve injury promotes axonal elongation (Krekosi et al., 2002; Zuo et al., 2002; Groves et al., 2005). Furthermore it has been proposed that MMPs, expressed by Schwann cells and macrophages after nerve injury, may be involved in the degradation of these

inhibitory CSPGs and thus contribute to efficient axonal regeneration (Ferguson and Muir, 2000; Krekosi et al., 2002).

There are a number of CAMs that have been implicated in promoting peripheral nerve regeneration. The Ca^{2+}-independent CAMs, neural-cell adhesion molecule (NCAM), L1 and close homolgue of L1 (CHL1) and the Ca^{2+}-dependent CAM, N-cadherin are all upregulated by Schwann cells in the distal stump of injured nerves (Daniloff et al., 1986; Martini and Schachner, 1988; Padilla et al., 1999; Zhang et al., 2000a). Furthermore, L1 and N-cadherin, but not NCAM, have been shown to mediate a large proportion of the neurite growth promoting effects of Schwann cells in culture, through use of blocking antibodies (Bixby et al., 1988; Seilheimer and Schachner, 1988). In addition, two novel CAMs, ninjurin1 and 2, which are capable of homophilic adhesion and are upregulated by Schwann cells and DRG neurons after nerve injury both promote neurite elongation of DRG neurons in vitro (Araki and Milbrandt, 1996; Araki and Milbrandt, 2000).

Interactions between cell adhesion molecules expressed on regrowing neurons and Schwann cells are certain to be involved in successful peripheral nerve regeneration. However, another level of complexity can be added to these interactions, as it appears that carbohydrate modifications on these proteins can alter the regenerative properties of axons. The carbohydrate epitope that is recognised by the HNK1/L2 antibody and is expressed on CAMs such as, NCAM and L1, regulates the outgrowth of chick motor axons on cryosections of rodent ventral root (Martini et al., 1992). Furthermore, the polysialic acid moiety on NCAM (PSA-NCAM) expressed by motor neurons has been shown to be required for generation of adequate collateral sprouts and ultimately for selective targeting of motor neurons to their original targets in the periphery (Franz et al., 2005).

1.6.8.2 Schwann cells produce neurotrophic factors for regenerating sensory and motor neurons.

After peripheral nerve injury Schwann cells upregulate production of a number of potential trophic factors for regenerating peripheral neurons. Many of these factors such as nerve growth factor (NGF), brain-derived growth factor (BDNF), glial-derived growth factor (GDNF), neurotrophin-3 (NT-3) and NT-4/5 have well established roles in survival of specific populations of neurons during development (Huang and Reichardt, 2001). However, because null mutations in many of these genes lead to embryonic lethality it has been difficult to investigate their specific roles in adult peripheral nerve regeneration (Huang and Reichardt, 2001).

1.6.8.2.1 The neurotrophins.

NGF, a member of the neurotrophin family, promotes the survival and differentiation of neural crest-derived sensory and sympathetic neurons during development (Levi-Montalcini and Angeletti, 1968). After nerve injury, Schwann cells massively upregulate their production of NGF and DRG neurons continue to express the NGF receptors trkA and $p75^{NTR}$, however the amount of NGF retrogradely transported by regenerating neurons is actually reduced compared to uninjured neurons (Heumann et al., 1987; Raivich et al., 1991b; Sebert and Shooter, 1993). Furthermore, the role of NGF during peripheral nerve regeneration is unclear. Although exogenous NGF can prevent permanent axotomy-induced death of some sensory neurons other reports suggest endogenous NGF is not required for sensory neuron regeneration, though it may be required for collateral sprouting (Diamond et al., 1987; Diamond et al., 1992a; Diamond et al., 1992b; Rush et al., 1995; Ljungberg et al., 1999).

Other members of the neurotrophin family are BDNF, NT-3 and NT-4/5. After nerve injury, Schwann cells slowly upregulate the expression of *BDNF* and *NT-4/5* mRNA, with *BDNF* levels peaking at 4 weeks after injury, but *NT-3* mRNA is initially downregulated before returning to control levels (Meyer et al., 1992; Funakoshi et al., 1993; Zhang et al., 2000b). After nerve injury, the BDNF and NT4/5 high affinity receptor, trkB, is expressed in the spinal cord and the DRG whereas the NT-3 receptor, trkC, is downregulated in the spinal cord (Funakoshi et al., 1993; Sebert and Shooter, 1993; Foster et al., 1994; Fernandes et al., 1998). The regeneration of motor axons is reduced in *trkB* (the high affinity receptor for BDNF) heterozygous null mouse sciatic nerves (Boyd and Gordon, 2001). Also, use of a blocking antibody to BDNF reduced the axon growth rate and strongly reduced the number of myelinated axons in the distal nerve after crush injury (Zhang et al., 2000b). Treatment of injured sciatic nerves with NT-4/5 enhanced axonal regeneration and, in addition, growth of axons through grafts of sciatic nerve from *NT-4/5* null mice is reduced in comparison to wild-type grafts (Yin et al., 2001; Simon et al., 2003; English et al., 2005). Furthermore, creation of transgenic mice that express pan-neurotrophin-1, which can activate all neurotrophin receptors, demonstrated considerably faster motor and sensory function recovery, measured by compound action potentials and reinnervation of target tissues (Funakoshi et al., 1998). All of these studies show that either reduction in or overactivation of neurotrophin signalling can modulate the rate of axonal regrowth during peripheral nerve regeneration.

1.6.8.2.2 The neuropoietic cytokines.

Another family of neurotrophic factors, expressed by Schwann cells that play a role in peripheral nerve regeneration are the neuropoietic cytokines, which include

factors such as ciliary neurotrophic factor (CNTF), LIF and IL-6 (Bauer et al., 2007). CNTF mRNA is expressed in myelinating Schwann cells but is downregulated after nerve injury (Friedman et al., 1992; Sendtner et al., 1992; Ito et al., 1998). Exogenously applied CNTF can rescue motor neurons from degeneration after facial nerve axotomy in neonatal mice and disruption of the *CNTF* gene in mice causes a progressive loss of motor neurons and weakening of peripheral muscles (Sendtner et al., 1990; Masu et al., 1993). After nerve injury, even though *CNTF* mRNA decreases, it is thought to be released by damaged myelinating Schwann cells as a lesion factor and contribute to motor neuron survival (Sendtner et al., 1997).

IL-6 mRNA and protein is rapidly expressed by Schwann cells but is also detected in the CNS, after peripheral nerve injury (Kiefer et al., 1993; Bolin et al., 1995; Kurek et al., 1996; Hirota et al., 1996; Ito et al., 1998). Early studies showed that a blocking antibody to IL-6 reduced motor axon regeneration whereas a transgenic mouse over-expressing IL-6 and the IL-6 receptor enhanced motor axon regeneration (Hirota et al., 1996). *IL-6* knockout mice show a modest decrease in speed of motor axon regrowth in the lesioned facial nerve and reduced functional recovery after sciatic nerve injury (Zhong et al., 1999; Inserra et al., 2000; Galiano et al., 2001). In addition, sensory axon regeneration also appears to be impaired in *IL-6* knockout mice, judged by reduced sensory compound action potential (Zhong et al., 1999). However, in all of these studies it is uncertain whether the consequences of *IL-6* removal are due to its role in CNS inflammation or due to local effects on axon growth within the PNS and thus further investigation is required (Klein et al., 1997; Galiano et al., 2001; Raivich and Makwana, 2007).

LIF, as already discussed, can mediate inflammatory responses after nerve injury. However, LIF also has significant effects on sensory axon regeneration as it is

taken up and retrogradely transported by sensory neurons after nerve injury (Thompson et al., 1997). Investigation of *LIF* null mice demonstrates that LIF is capable of promoting axonal elongation of regenerating small diameter sensory axons and preventing axotomy induced neurochemical changes, such as the loss of calcitonin gene-related peptide (CGRP) immunoreactivity, in this neuronal population (Cafferty et al., 2001).

1.6.8.2.3 Other neurotrophic factors: GDNF, IGFs and pleiotropin.

GDNF is a member of a sub-family of the TGFβ superfamily (Lin et al., 1993). After nerve injury, Schwann cells in the distal stump upregulate *GDNF* mRNA (Trupp et al., 1995; Naveilhan et al., 1997). Exogenously applied GDNF can enhance sensory axon regeneration and can reverse the axotomy-induced changes in small diameter IB4 positive C-fibres (Naveilhan et al., 1997; Bennet et al., 1998). In addition, GDNF enhances motor axon regeneration after acute and chronic axotomy (Chen et al., 2001; Boyd and Gordon, 2003b). A role for GDNF in motor and sensory nerve regeneration is supported by the fact that motor neurons upregulate the GDNF receptors, GFRα1 and RET and sensory neurons upregulate GFRα1 and GFRα3 after nerve injury (Naveilhan et al., 1997; Burazin and Gundlack, 1998; Tsujino et al., 1999; Bennet et al., 2000). Interestingly, the majority of large diameter sensory neurons appear to express GFRα1 whereas many small diameter sensory neurons express GFRα3 after injury, suggesting that the GFRα3 ligand, artemin, may play a role in nerve regeneration too (Bennett et al., 2000).

The insulin like growth factors, IGF-I and II are upregulated by Schwann cells after nerve injury, although macrophages also express IGF-I (Pu et al., 1995; Cheng et al., 1996; Meier et al., 1999). Addition of exogenous IGF-II or use of IGF blocking

antibodies can modulate the distance of motor axon regrowth and both IGF-I and II can improve sensory axon regeneration in a diabetic rat model (Near et al., 1992; Ishii and Lupien, 1995). However, since IGFs promote the survival and differentiation of Schwann cells (Gavrilovic et al., 1995; Stewart et al., 1996; Meier et al., 1999), it is uncertain whether IGFs are acting predominately on neurons, Schwann cells or both cell types during peripheral nerve regeneration.

Recently, a novel neurotrophic factor, pleiotrophin (PTN) has been shown to play a role in peripheral nerve regeneration. *PTN* mRNA is upregulated in the distal stump of the injured sciatic nerve, most likely in Schwann cells, with expression peaking at 7 days. In vitro PTN promotes the extension of spinal motor neurons and in vivo, exogenous PTN enhances regeneration after sciatic nerve cut. Additionally, PTN can rescue neonatal motorneurons from death after facial nerve transection (Mi et al., 2007).

1.6.8.3 Do Schwann cells from motor and sensory nerve fibres express different phenotypes during regeneration?

The first evidence that Schwann cells in motor and sensory nerves might possess distinct phenotypes came from the discovery that only Schwann cells in contact with motor axons express the L2/HNK-1 carbohydrate epitope (Martini et al., 1988). Furthermore, expression of L2/HNK-1 is lost after denervation and only induced again when motor but not sensory, axons reinnervate their original motor Schwann cells (Martini et al., 1994). Furthermore, Schwann cells that were previously innervated by sensory axons do not have the ability to express L2/HNK-1 when motor neurons are forced to innervate them (Martini et al., 1994). Thus Schwann cells

appear to retain some 'memory' of what type of axon they were originally innervated by.

More recent investigation has demonstrated that Schwann cells of the dorsal (sensory) and ventral (motor) roots upregulate different combinations of growth factors after nerve injury. Whereas Schwann cells in the dorsal roots upregulate NGF, BDNF, GDNF and IGF-I and II, Schwann cells in the ventral roots upregulate PTN and GDNF (Höke et al., 2006). Thus, these results suggest that Schwann cells adopt distinct sensory and motor phenotypes during regeneration.

1.6.8.4 Do Schwann cells control reformation of the blood nerve barrier (BNB) during remyelination?

1.6.8.4.1 BNB breakdown after injury.

During peripheral nerve injury the blood-nerve barrier (BNB) breaks down, possibly through induction of MMPs by endothelial cells and Schwann cells (George et al., 1995; Hughes et al., 2002). This allows components from the bloodstream such as fibrinogen, complement and haematogenous macrophages to enter the degenerating peripheral nerve. Fibrinogen is converted to fibrin via the clotting cascade and clearance of fibrin from the nerve is correlated with remyelination and nerve repair (Akassoglou et al., 2002). Fibrin is degraded by the serine protease plasmin, which is in turn activated by plasminogen activators (Akassoglou and Strickland, 2002). In the absence of tissue plasminogen activator (tPA) there is increased deposition of fibrin and increased nerve damage and demyelination and slower functional recovery after nerve injury (Akassoglou et al., 2000; Siconolfi and Seeds, 2001). Additionally, fibrin inhibits Schwann cell myelin differentiation in culture and fibrin knockout mice remyelinate faster after nerve crush (Akassoglou et al., 2002). Thus it appears that

blood-borne components, as well as promoting nerve repair, can sometimes have deleterious effects.

1.6.8.4.2 Schwann cell remyelination and BNB reformation.

Schwann cell remyelination occurs in very much the same way as the process of myelination during development (Scherer and Salzer, 2001; Jessen and Mirsky, 2005). Interestingly, BNB reformation appears to correlate better with remyelination than with axonal regeneration, per se, suggesting that the process of remyelination might be important for BNB restoration (Bouldin et al., 1991). One potential myelin regulated Schwann cell signal that could instruct the reformation of the BNB is Desert Hedgehog (DHH) (Bajestan et al., 2006; Sharghi-Namini et al., 2006). DHH is normally expressed by myelinating Schwann cells and is downregulated after nerve injury (Bajestan et al., 2006). After nerve crush, DHH is re-expressed by myelinating Schwann cells between 14-28 days after nerve injury, a time-point that correlates well with remyelination and the beginning of BNB restoration (Bouldin et al., 1991; Scherer and Salzer, 2001; Bajestan et al., 2006). In addition, it has recently been shown that DHH is a direct target for the myelin-related transcription factor Krox-20, which would explain DHH's re-expression around the time of remyelination (Le et al., 2005b; Jang et al., 2006). Further evidence to suggest that DHH mediates BNB restoration comes from analysis of *DHH* null nerves, which have a permeable BNB and show macrophage and neutrophil infiltration (Sharghi-Namini et al., 2006). Upon, sciatic nerve transection, *DHH* null nerves demonstrate faster myelin clearance, potentially due to an already permeable BNB (Bajestan et al., 2006; Sharghi-Namini et al., 2006). Thus, it is possible that myelinating Schwann cells could instruct BNB reformation through DHH during peripheral nerve remyelination.

1.7 Non-syndromic inherited motor and sensory neuropathies.

Non-syndromic inherited peripheral neuropathies are traditionally known as Charcot-Marie-Tooth disease (CMT) or hereditary motor and sensory neuropathy (HMSN). They are classified in groups depending on forearm nerve conductance velocities (NCVs), nerve pathology, age of onset and severity and pattern of inheritance. Briefly, patients presenting with CMT1 (HMSNI) generally have NCVs <38m/s, with age of onset in the first or second decade of life. CMT1 is referred to as a demyelinating neuropathy since nerve biopsies from patients often show segmental demyelination and remyelination, in addition to onion bulbs (supernumerary Schwann cells arranged concentrically around an improperly remyelinated axon) and axonal loss. CMT2 (HMSNII) is characterised by NCVs >38m/s, has a later onset than CMT1 and is associated predominantly with alteration and loss of axons. CMT3 (HMSNIII) includes more severe demylinating or dysmyelinating neuropathies with an early childhood onset. These include Déjérine-Sottas syndrome (DSS) and congenital hypomyelinating neuropathy (CHN). CMT4 is a collection of genetically heterogeneous autosomal recessive neuropathies, the majority of which are caused by defects in axonally expressed genes although some are due to Schwann cell defects. In addition, there is also a relatively mild condition called hereditary neuropathy with liability to pressure palsy (HNPP), which is classified as a recurrent focal neuropathy (Wrabetz et al., 2001; Suter and Scherer, 2003; Berger et al., 2006).

There is remarkable allelic heterogeneity underlying the CMT diseases. CMT is caused by mutations in genes in Schwann cells or peripheral neurons. Mutations in different genes often cause a similar form of the disease and moreover, different mutations in the same gene can lead to different forms of CMT (Suter and Scherer, 2003). To add further complexity, some forms of CMT2, that present with axonal

pathology, have actually been shown to be caused by a Schwann cell mutation demonstrating the intricacy of the axo-glial relationship in the PNS and the difficulty facing researchers and clinicians in understanding the pathology of CMT diseases (Wrabetz et al., 2001). I will briefly summarise the mutations and potential mechanisms of the main genes involved in causing CMT neuropathies in Schwann cells.

1.7.1 Mutations in the *PMP22* gene.

The majority of mutations causing CMT and HNPP are found in the *PMP22* gene. A deletion on chromosome 17 that includes the *PMP22* gene leads to HNPP. Whereas the most common form of inherited neuropathy, CMT1A, is usually caused by the heterozygous inheritance of a duplication that includes *PMP22*. The molecular basis of these diseases is due to two highly homologous sequences flanking the *PMP22* gene, which can lead to unequal crossing over during meiosis and the inheritance of a duplicated or a deleted allele (Lupski and Chance, 2005). How these mutations lead to neuropathies is not completely understood although it is believed that gene dosage is important since rodents with increasing *PMP22* gene dosages develop more severe CMT1-like neuropathies (Huxley et al., 1996, 1998; Sereda et al., 1996; Magyar et al., 1996). In addition to duplications and deletions, there are more than 40 different point mutations described in the *PMP22* gene, which often lead to more severe phenotypes in patients (Suter and Scherer, 2003). Many of these point mutations are thought to produce a toxic gain of function or dominant-negative effect. This notion is supported by evidence that mice that are heterozygous for the naturally occurring PMP22 point mutations Trembler (Tr) and Trembler-J (Tr-J) produce a more severe neuropathy than $PMP22^{+/-}$ mice (Adlkofer et al., 1997).

Mechanisms that may play a role in the development of these phenotypes include retention of mutant PMP22 proteins within the cell and increased association with the molecular chaperone calnexin (Tobler et al., 1999; Dickson et al., 2002). In addition mutant PMP22 may accumulate in aggresomes within cells leading to dysfunction (Notterpek et al., 1999; Ryan et al., 2002). Furthermore the ability of wild-type PMP22 to associate with $\alpha_4\beta_6$ integrin, P_0 or influence proliferation may in part underlie some of the defects in Schwann cells caused by mutant forms of PMP22 (Berger et al., 2006; See section 1.4).

1.7.2 Mutations in the *P_0* gene.

There are around 100 different mutations in the *P_0* gene that lead to inherited peripheral neuropathies. The majority of these mutations are inherited in an autosomal dominant pattern and cause diseases of radically variable phenotypes, ranging from CMT1 to DSS and CHN and even CMT2, with predominantly axonal pathology (Wrabetz et al., 2001). The majority of these mutations produce more severe phenotypes than haploinsufficiency for *P_0*, which causes a relatively mild CMT1B phenotype in both man and mice (Wrabetz et al., 2001; Martini et al., 1995a). Thus, many believe that most mutations in the *P_0* gene must produce dominant negative or gain of function effects. In support of this, recent mouse models of two *P_0* mutations, S63C, which causes DSS and S63del which causes CMT1B where shown to have separate gain of function effects on Schwann cells. Whereas the P_0 S63del caused a packaging defect in the myelin sheath, P_0 S63C was retained within the endoplasmic reticulum and caused an unfolded protein response (UPR)(Wrabetz et al., 2006). Further work then actually demonstrated that ablation of the transcription factor

CHOP that mediates part of the UPR could ameliorate the phenotype in the P_0 S63C mouse (Pennuto et al., 2008).

1.7.3 Mutations in *GJB1* (Connexin32).

More than 240 different mutations in *GJB1*, which encodes connexin 32, lead to CMT1X. Mutations have been reported in every domain of Cx32, in addition to the promoter and the 3' untranslated region. There are also mutations that lead to deletion of the entire gene. The clinical phenotypes of the many CMT1X mutations are more homogenous, though point mutations sometimes lead to a more severe phenotype (some including CNS involvement) than gene deletion suggesting potential dominant negative or gain of function effects (Suter and Scherer, 2003). Mice lacking Cx32 develop a peripheral neuropathy although this appeared not to be correlated with disruption of the radial pathway for diffusion through the SLIs, to which Cx32 is thought to contribute (Balice-Gordon et al., 1998; Anzini et al., 1997; Scherer et al., 1998). Furthermore, evidence suggests that some of the more severe point mutations lead to disruption in trafficking of Cx32 within the cell, which may lead to dominant negative effects on other connexins (Kleopa et al., 2002; Yum et al., 2002; Suter and Scherer, 2003).

1.7.4 Mutations in *periaxin* gene.

Recessive mutations in the *periaxin* gene lead to CMT4F, which is characterised by a DSS like phenotype. Unlike other inherited demyelinating neuropathies sensory loss and ataxia are more common features of CMT4F. CMT4F is thought to be caused by loss of periaxin function (Boerkoel et al., 2001; Guilbot et al., 2001). Mice lacking the periaxin gene are initially relatively normal but develop a severe demyelinating

neuropathy around 6 weeks after birth characterised by tomacula (hypermyelination) and infoldings of internodal myelin. Mice have reduced motor and sensory mechanoreceptor NCVs and develop reflex behaviours associated with allodynia and hyperalgesia (Gillespie et al., 2000). How loss of function of periaxin leads to demyelinating neuropathies is not completely understood although it may be due to disruption of the dystroglycan-DRP2 complex (Sherman et al., 2001). Disruption of this complex leads to defects in Schwann cell internodal extension during nerve elongation postnataly and reduced NCVs (Court et al., 2004).

1.7.5 Mutations in *EGR2* gene.

Mutations in *EGR2* lead to development of peripheral neuropathies of varying severity including CMT1, DSS and CHN. The majority of mutations are found in the DNA binding domain and are inherited autosomal dominantly. These mutations are believed to act by a dominant negative or gain of function mechanism (Warner et al., 1998; Nagarajan et al., 2001; LeBlanc et al., 2007; Szigeti et al., 2007; see Chapter 5). Additionally, recessive mutations in the NAB binding domain of EGR2 cause severe peripheral neuropathies in humans and mice potentially due to the fact that these mutations lead to loss of Egr2:Nab1/2 interactions and the dysregulation of Egr2 target genes (Warner et al., 1998; Le et al., 2005b; Szigeti et al., 2007; Demazières et al., 2008; see section 1.5.4.1).

1.7.6 Mutations in *Myotubularin-related* genes (MTMR).

Recessive mutations in MTMR2 and MTMR13/SBF2 lead to CMT4B1 and CMT4B2 respectively (Bolino et al., 2000; Azzedine et al., 2003; Senderek et al., 2003). These diseases are characterised by a demyelinating neuropathy with myelin

outfoldings, which have been replicated in mice lacking *MTMR2* suggesting the disease is caused by a loss of function (Bolino et al., 2004; Bonneick et al., 2005). MTMRs are present in neurons and Schwann cells and are phosphoinositide lipid 3-phosphatases that are thought to regulate endocytosis (Previtali et al., 2003b; Berger et al., 2006), although development of CMT4B like phenotypes in mice is due to loss of MTMR2 in Schwann cells and not axons (Bolis et al., 2005).

1.7.7 Other mutations associated with Schwann cells causing CMT.

Autosomal recessive mutations in frabin cause CMT4H, a demyelinating neuropathy also characterized by myelin outfoldings (Delague et al., 2007; Stendel et al., 2007). Frabin is a Rho GDP/GTP exchange factor, specific for cdc42. Since cdc42 is important for Schwann cell proliferation, axonal sorting and myelination (Benninger et al., 2007), it is believed that frabin mutations would lead to impairment of cdc42 activity in Schwann cells (Stendel et al., 2007). Mutations in a small integral membrane protein of the lysosome/late endosome (SIMPLE) lead to the dominant demyelinating neuropathy CMT1C. Since myelinating Schwann cells express high levels of SIMPLE the disease is believed to be caused by a Schwann cell defect although the exact mechanism is very unclear. Additionally mutations in N-myc downstream-regulated gene 1 (NDRG1) lead to recessive CMT4D, dynamin 2 mutations are associated with dominant-intermediate CMT1B and recessive mutations in ganglioside-induced differentiation associated protein 1 (GDAP1) cause various demyelinating, intermediate and axonal forms of CMT (for review see, Suter and Scherer, 2003; Berger et al., 2006).

AIMS

The aim of this thesis was first to investigate the role of cyclic AMP, NRG1 and the CREB family of transcription factors in mouse Schwann cell myelin differentiation (Chapter 3). I then wanted to investigate the role of the transcription factor, c-Jun in Schwann cells, *in vivo*, particularly during peripheral nerve injury and regeneration (Chapter 4). Finally, I wanted to characterise the functional properties in Schwann cells of a mutant transcription factor, mutant Egr2 (S382R/D383Y) that is known to cause congenital hypomyelinating neuropathy in humans (Chapter 5).

CHAPTER 2: Materials and Methods

2.1 List of reagents

2.1.1 Reagents for tissue culture

Transferrin, selenium, putrescine, triiodothyronine (T3), thyroxine (T4), progesterone, dexamethasone, bovine serum albumin (BSA), insulin, cytosine arabinoside (Ara C), poly-D-lysine (PDL), poly-L-lysine (PLL), laminin, dimethyl sulphoxide (DMSO), bromodeoxyuridine (BrdU) and 2'-*O*-dibutyryladenosine 3':5'-cyclicAMP (dbcAMP) were obtained from Sigma (Poole, UK). 8-pCPT-2-O-Me-cAMP and 6-Bnz-cAMP were purchased from BIOLOG (Bremen, Germany). Collagenase was obtained from Worthington (Lorne Laboratories, Reading, UK). Dulbecco's modified Eagles medium (DMEM), Minimum Essential Medium (MEM), Ham's F-12 medium, L-15 medium, horse serum (HS) and glutamine were from Invitrogen Ltd (Paisley, UK). Trypsin and penicillin/streptomycin was obtained from PAA (UK). Foetal calf serum (FCS) was purchased from Perbio (UK). Tissue culture Petri dishes, 24 well plates and centrifuge tubes were obtained from VWR (UK) and forskolin was from Calbiochem (CA, USA). Round 13 mm coverslips were from BDH (Lutterworth, UK). TGFβ-1 and NRGβ-1 were obtained from R & D Systems (Minneapolis, MN, USA).

2.1.2 Reagents for molecular biology

Taq DNA-polymerase, dNTPs, 1KB plus DNA ladder and Agarose were from Invitrogen Ltd (Paisley, UK). EDTA disodium salt, ethidium bromide, Sodium Citrate, phenylmethylsulphonylfluoride (PMSF) and bromophenol blue were from Sigma (Poole, UK). Hybond-N nitrocellulose membrane was from Amersham

Pharmacia Biotech (UK). Absolute ethanol, isopropanol, methanol, sodium dodecyl sulphate (SDS), sodium chloride (NaCl) and glycerol were from BDH Lab. Supplies (Poole, UK). Kaleidoscope pre-stained standards were from Biorad (CA, USA). TUNEL label and enzyme were from Roche Diagnostics (Germany). Phenol-chloroform was from Fluka Chemicals Ltd. (Buchs, Switzerland).

2.1.3 Reagents for immunolabelling

Paraformaldehyde was obtained from Fluka Chemicals Ltd. (Buchs, Switzerland). Triton X-100, lysine and Hoechst dye H33258 were from Sigma (Poole, UK). Citifluor was from Citifluor Ltd. (London, UK). HCl and glycerol were purchased from BDH (Lutterworth, UK).

2.1.4 Reagents for histology and Electron Microscopy

Glutaraldehyde, Agar 100 Resin, methyl nadic anhydride (MNA), dodecenyl succinic anhydride (DDSA), N-benzyldimethylamine (BDMA), Tissue Tek OCT compound and rubber coffin moulds were from Agar Scientific (UK). DPX mountant and 13mm coverslips were from Merck Biosciences (Germany), frosted and Superfrost Plus microscope slides were from BDH (Lutterworth, UK).

2.2 List of Antibodies

2.2.1 List of Primary antibodies

β-galactosidase: Mouse monoclonal antibody was purchased from Sigma (UK) and used at a concentration of 1:500 for immunocytochemistry (ICC).

β-tubulin: Mouse monoclonal antibody was purchased from Sigma (UK) and used at a concentration of 1:1000 for western blotting (WB).

Bromodeoxyuridine: Mouse monoclonal antibody was purchased from Roche Diagnostics (UK) and used at a concentration of 1:200 for ICC.

Bromodeoxyuridine: biotinylated mouse monoclonal antibody was purchased from Zymed (CA, USA) and used at a concentration of 1:50 for immunohistochemistry (IHC).

c-Jun: Mouse monoclonal antibody was purchased from BD Transduction Laboratories (UK) and used at a concentration of 1:500 for ICC and 1:2500 for WB.

c-Jun: Rabbit polyclonal antibody was purchased from Santa Cruz Biotechnology (USA) and used at a concentration of 1:500 for IHC and 1:2500 for WB.

Cre recombinase: Rabbit polyclonal antibody was purchased from Novagen (Merck Biosciences, Germany) and used at a concentration of 1:10000 for ICC.

Cdk2: Rabbit polyclonal antibody was purchased from Santa Cruz Biotechnology (USA) and used at a concentration of 1:100 for ICC.

Cyclin D1: Mouse monoclonal antibody was purchased from Santa Cruz Biotechnology (USA) and used at a concentration of 1:100 for ICC and 1:500 for WB.

ERK1/2 (native): Mouse monoclonal antibody was purchased from Sigma (UK) and used at a concentration of 1:2500 for WB.

F4/80: Rat polycloncal antibody was purchased from AbD Serotec (UK) and used at a concentration of 1:50 for ICC.

Gal-C: The Gal-C hybridoma cell line was a generous gift from Dr B. Ranscht (Max-Plank Institute, Germany) (Ranscht *et al*, 1982), and the mouse monoclonal supernatant was used at a 1:5 dilution for ICC.

GAPDH: Mouse monoclonal antibody was purchased from Abcam Ltd. (Cambridge, UK) and used at a concentration of 1:1000 for WB.

GFP: Rabbit polyclonal antibody was purchased from Invitrogen and used at a concentration of 1:1000 for ICC and 1:5000 for WB.

Krox-20: Rabbit polyclonal antibody purchased from Covance (USA) and used at a concentration of 1:250 for ICC and 1:2500 for WB.

L1 (324): Rat monoclonal antibody (clone 324) was a gift from Dr R. Martini (Martini et al., 1994) and was used in hybridoma form for ICC and IHC.

L1 (ASCS4): Mouse monoclonal antibody (clone ASCS4) was a gift from Dr. P. Patterson (Caltech, USA). This antibody was used in the form of a hybridoma supernatant and diluted 1:1 with MEM-H 10% FCS for ICC.

L-periaxin: Rabbit polyclonal antibody was a gift from Prof. P.J. Brophy (University of Edinburgh, Scotland, UK) (Gillespie et al., 1994) and was used at a concentration of 1:8000 for ICC and 1:15000 for WB.

Myelin basic protein: Mouse monoclonal antibody was purchased from Sternberger Monoclonals Inc. (Covance, USA) and used at a concentration of 1:1000 for ICC.

NAB2: Polyclonal antibody (IC4) was a gift from Dr. Judith Johnson (Kirsch et al., 1996). This antibody was used in the form of a hybridoma supernatant (neat).

N-cadherin: Rabbit polyclonal antibody was purchased from Abcam Ltd. (Cambridge, UK) and was used at a concentration of 1:500 for IHC and ICC.

NCAM: Rabbit polyclonal antibody was a gift from Dr G. Rougon (Rougon and Marshak, 1986) and used at a concentration of 1:500 for IHC and ICC.

O4: The O4 hybridoma cell line was a generous gift from Dr. I. Sommer (Sommer and Schachner, 1981), and the mouse monoclonal supernatant was used at a 1:5 dilution for ICC.

OX7: OX7 hybridoma cell line secreting IgM recognizing rat Thy1.1 was from the European Collection of Animal Cell Cultures (DERA, Wiltshire, UK) and was used for negative immunopanning in order to purify rat Schwann cell cultures.

p27: Rabbit polyclonal antibody was purchased from Santa Cruz Biotechnology (USA) and used at a concentration of 1:100 for ICC and 1:500 for WB.

$p75^{NTR}$: Rabbit polyclonal antibody was purchased from Upstate (Virginia, USA) and used at a concentration of 1:200 for IHC and ICC.

p-AKT: Rabbit polyclonal antibody specific to the phosphorylated form (Thr308) of Akt was from Cell Signalling Tech (Hertfordshire, UK) and used at a concentration of 1:500 for WB.

p-ERK 1/2: Mouse monoclonal antibody was purchased from Sigma (UK) and used at a concentration of 1:5000 for WB.

Protein zero (P_0): Mouse monoclonal antibody obtained from Austexx (Austria), used at a concentration of 1:500 for ICC and IHC and 1:2500 for WB.

Protein zero (P_0): Rabbit polyclonal antibody against rat P_0 was generated and characterized in the laboratory by Louise Morgan (Morgan et al., 1994). The antibody was used at a dilution of 1:1000 for ICC.

S100β: Rabbit polyclonal antibody against cow S100β was purchased from Dako Immunoglobulins (Dakopatts, Copenhagen, Denmark) and used at a final dilution of 1:1000 for IHC.

Sox2: Rabbit polyclonal antibody was purchased from Chemicon (CA, USA) and used at a concentration of 1:500 for ICC and IHC and 1:2500 for WB.

T24: T24 hybridoma cell line secreting antibodies recognizing mouse Thy1 (pan-Thy1) was a gift from Dr L. Lopez and was used for negative immunopanning in order to purify mouse Schwann cell cultures.

TuJ1: Rabbit polyclonal antibody against β-tubulin III was purchased from Covance (USA) and used at a final concentration of 1:5000 for IHC.

2.2.2 List of Secondary antibodies

Biotinylated anti-mouse Ig, streptavidin-Cy3 and streptavidin-FITC were purchased from Amersham International plc. Rhodamine-conjugated goat anti-mouse Ig was purchased from MP Biomedicals (Cappel). Cy3-conjugated donkey anti-rabbit Ig and Cy3-conjugated donkey anti-mouse IG were purchased from Jackson Immunoresearch Laboratories, Inc (USA). Goat anti-rabbit and mouse horse radish peroxidase-conjugated antibodies were obtained from Promega Inc. Anti-mouse and anti-rabbit Cy5-conjugated secondary antibodies were purchased them from Biological Detection Systems, Inc. Goat anti-mouse IgG (Fab specific) was purchased from Sigma.

2.3 Tissue culture techniques

2.3.1 Substratum coating of coverslips and dishes

Poly-D-lysine (PDL) or poly-L-lysine (PLL): Round 13mm glass coverslips were baked in an oven for 4 hours at 140°C and were coated with 20μg/ml PDL in ultra pure water (UPH_20) or 20μg/ml PLL in UPH_20 for 4 hours at room temperature (RT). Coverslips were then washed 3 times, for 15 minutes each time, in sterilised water and dried overnight in a class I tissue culture hood before being stored sterile and desiccated (in presence of silica gel) at RT.

Tissue culture dishes (35mm and 60mm) were coated with PDL (20μg/ml) or PLL (20μg/ml) for 4 hours at RT. The solution was removed and the dishes were air-dried without washing.

Laminin: A 15µl drop of laminin, diluted in DMEM (20µg/ml) was placed centrally on each coverslip and incubated at 37°C for at least 30 minutes. Excess laminin solution was removed after incubation and cells were immediately plated Alternatively, laminin in DMEM (10µg/ml) was added to dishes and left for 30 minutes to 1hour prior to plating of cells.

2.3.2 Medium components

Defined supplemented medium (DM): This medium is a modification of the medium of Bottenstein and Sato (1979). A 1:1 mixture of DMEM (containing 1000mg/l glucose) and Ham's F12 medium was enhanced with bovine serum albumin (0.3mg/ml), putrescine (16µg/ml), transferrin (100µg/ml), thyroxine (400ng/ml), progesterone (60ng/ml), dexamethasone (38ng/ml), glutamine (1mM), penicillin (100 U/ml) and streptomycin (100 U/ml), triiodothyronine (10.1ng/ml) and selenium (160ng/ml) and insulin (10^{-6}M). This medium is referred to as DM in the text.

DMEM: DMEM containing 1000mg/l glucose, pyridoxine and sodium pyruvate was used for Schwann cell cultures, whereas DMEM containing 4500mg/l glucose, pyridoxine and sodium pyruvate was used for HEK293 cell cultures. Both forms of DMEM were supplemented with penicillin (100 U/ml) and streptomycin (100 U/ml) before use.

2.3.3 Cell cultures

2.3.3.1 Serum purified rat and mouse Schwann cells

Methods for purifying neonatal rat and mouse Schwann cells were based on methods by Brockes et al., (1979) and Stevens et al., (1998) respectively. Using aseptic techniques, the sciatic nerves and brachial plexuses of postnatal day 3 Sprague-Dawley rats or post-natal day 2 (P2) ICR or C57BL/6 mice, killed by decapitation, were dissected out and placed in sterile L-15 medium on ice. The epineurial sheaths and any superfluous connective tissue were removed and the de-sheathed nerves were transferred to a sterile 35mm tissue culture dish containing of 0.25% trypsin and of 0.4% collagenase. They were incubated at 37°C, 5% CO_2 and 95% air for 35minutes, after which the nerves were triturated gently until fully dissociated (using first a blue 1ml and then a yellow 200µl Gilson pipette tip). Then the enzyme reaction was halted with the addition of 2-3ml of DMEM containing 10% FCS for rat cultures or 5% HS for mouse cultures. The cell suspension was transferred into a 15ml centrifuge tube and spun for 10 minutes at 1000rpm and 4°C. Maintaining sterile conditions, the supernatant was removed using a suction pump and the pellet was resuspended in 2ml DMEM containing 10% FCS (rat) or 5% HS (mouse) and Ara C (10^{-5}M). Ara C is an anti-mitotic and will kill contaminating fibroblasts that have been stimulated to divide by addition of the serum. For rat cultures the cell suspension was transferred onto a PDL and laminin coated tissue culture dish whereas a PLL/ laminin coated dish was used for mouse cultures. The cells were then incubated for at least 3 days at 37°C and 5%CO_2 until the majority of fibroblasts have been eliminated leaving highly pure cultures of Schwann cells.

2.3.3.2 Immunopanning of Schwann cells

Purification of rat or mouse Schwann cells was also performed by reverse immunopanning using an antibody that recognises Thy 1.1, which is expressed on fibroblasts but not Schwann cells (Dong et al., 1999). Freshly isolated or serum-purified Schwann cells from Sprague-Dawley rats were placed in DM on a 90 mm Petri dish, coated with anti-mouse IgG and mouse anti-rat Thy1.1 and incubated at 37°C, 5% CO_2 for 30 min. Every 10 min the cells were removed from the incubator and agitated by gentle shaking. The cell suspension obtained was devoid of almost all fibroblasts as they had bound to the Thy1.1 specific antibodies coating the dish. The cells were then centrifuged at 1000rpm for 10 min at 4°C and the resulting pellet was resuspended in the appropriate medium. For mouse Schwann cells, a 90 mm Petri dish was coated with anti-rat IgG and rat anti-mouse Thy1.1.

2.3.3.3 Expanding Schwann cells

For western blot analysis it was necessary to expand rat or mouse Schwann cell cultures in order to extract sufficient quantities of protein. Schwann cells were previously serum-purified and immunopanned before being replated on several PDL/laminin or PLL/laminin coated dishes in medium containing DM, 0.5% FCS or HS, NRG-1 (10ng/ml) and 2μM forskolin. NRG-1 in the presence of low concentrations of forskolin is highly mitogenic for rat and mouse Schwann cells and induced them to proliferate until confluent. Cells were then placed in DM without mitogenic factors for 12 hours until experimental reagents were added.

2.3.4 Adenoviral constructs and preparation

Adenoviruses expressing either full length Egr2, mutant Egr2 (S382R, D383Y) or the appropriate empty vector were obtained as a gift from Dr J. Milbrandt (Nagarajan et al., 2001) and these were made in the laboratory of Dr M. Ehrengruber (Ehregruber et al., 2000). Wild-type *Egr2* (Chavrier et al., 1988) or mutant *Egr2 (S382R, D383Y)* was inserted into the E1 regions of Ad5PacIsGFP to yield AdGFP Egr2 or AdGFP mutant Egr2. Ad5PacIsGFP was prepared by ligating an expression cassette, CMV-sGFP-SV40pA, into the *Pac*I site (in the E3 deletion) of Ad5PacI as described (Ehrengruber et al., 1998). The adenovirus expressing full length Egr2 is referred to as wild-type Egr2 in the text and its matched control adenovirus expressing the empty vector plasmid, is referred to as GFP control. Both viruses also express GFP after infection of cells.

The adenovirus expressing VP16-CREB, a fusion protein between Herpes Simplex Virus *VP16* (aa 363-490) and CREB (aa 88-341) (Barco et al., 2002) and GFP control adenovirus were a gift from Dr M.T. Filbin (Gao et al., 2004). The adenovirus was constructed using the Tet-Off system from Clontech and inserted by homologous recombination into pAdeasy-1 (He et al., 1998). The VP16-CREB adenovirus and its corresponding empty vector control both express GFP after infection.

The adenovirus expressing A-CREB (a dominant negative inhibitor of CREB formed by fusing an acidic amphiphatic extension onto the CREB leucine zipper domain) (Ahn et al., 1998) and control adenovirus were a gift from Dr J. Uney (Warburton et al., 2005). The adenoviruses were generated by cloning cDNAs for *A-CREB* and *EGFP,* individually, into the multiple cloning site of the plasmid pXCXCMV (Harding et al., 1998). Recombinant E1 deleted adenoviral constructs were then

generated by homologous recombination in HEK 293 cells. The A-CREB adenovirus and its corresponding empty vector control both express GFP after infection.

The adenovirus expressing Cre recombinase was obtained as a gift from Dr A. Behrens and was made in the laboratory of Dr A. Berns (Akagi et al., 1997). The HindIII fragment of PBS185 containing the Cre recombinase open reading frame, under the control of the human CMV immediate early promoter and the metallothionein I polyadenylation signal was inserted into the HindIII site of pdE1spIA. This was then co-transfected with pJM17 into 293 cells and adenovirus was obtained via plaque purification (Akagi et al., 1997).

Adenoviral supernatants were prepared and titred as described previously (Parkinson et al., 2001). Briefly, confluent HEK 293 cells were infected with adenovirus and once cells began to show cytopathic effects (rounding up and detachment from the culture dish, usually after 2 days) the cell supernatant was collected and purified with the vivapure AdenoPACK 500 (Sartorius AG, UK) according to manufacturer's protocol. The viruses were then titred by infection of serum-purified Schwann cells with different volumes of virus. The volume which resulted in an infection rate of >95% (as seen by expression of GFP) and no cytopathic death was chosen. For western blotting, extracts were probed with an antibody to GFP, to ensure equal levels of infection between conditions. Please note that after each viral preparation, the amount of virus used was always titred.

2.3.4.1 Adenoviral infections

Expanded rat or mouse Schwann cells grown on PDL/laminin or PLL/laminin dishes and serum purified rat or mouse Schwann cells plated onto PDL/laminin or PLL/laminin coated coverslips (5000 cells/coverslip) were infected by adenoviral

preparations in medium containing DM, 0.5% FCS or HS and 2μM forskolin. After 24 hours the medium was changed to DM and 0.5% FCS or HS. Infected cultures were treated in various ways and fixed at different times for ICC or proteins were extracted for analysis by western blot.

2.3.5 Retroviral constructs and preparation

Using PCR, the cDNA for wild-type *Krox-20* was engineered with a myc tag (Evan et al., 1985) at the 5' end. This was cloned into the retroviral vector pBABEpuro (Morgenstern and Land, 1990) and the GP + E ecotropic packaging cell line (Morgenstern and Land, 1990), grown in DMEM/10%FCS, was then transfected with 10ug of pBABEpuro empty vector or pBABEpuro wild-type *Krox-20*. Stably transfected clones were selected using puromycin (2.5μg/ml), pooled and expanded.

2.3.5.1 Retroviral infections

For retroviral infections, GP + E cells were then transferred to puromycin free medium and after 48 hours the supernatant containing the virus was collected, filtered and polybrene polycation was added (8μg/ml). Rat Schwann cell cultures that were 70% confluent and thus actively proliferating were treated with the retroviral supernatant, since the retrovirus will only infect proliferating cells. After 4 hours, three quarters of the viral supernatant was removed and replaced with the same volume of DMEM, 10% FCS and 4μM Forskolin (expansion medium). The following day the expansion medium was changed and after a further 24 hours cells were spilt and selected in expansion medium containing puromycin (1μg/ml). Pools of Schwann cells with strong expression of the retrovirus were used for experiments.

2.3.6 Myelin differentiation Assays

cAMP/NRG1 induction experiments in mouse Schwann cells: Serum-purified mouse Schwann cells were plated on PLL/laminin coated coverslips (5000 cells/coverslip) in medium containing DM treated with NRG1 (20ng/ml), dbcAMP (1mM), dbcAMP (1mM) and NRG1 (20ng/ml) or left unstimulated (Control) for between 48 and 120 hours before fixation and analysis by ICC.

2.3.7 Demyelination Assay

Nerve segment demyelination assay: I removed equal 6mm length segments from the tibial nerve measured from the sciatic notch from adult male mice (2-4 months old) and placed them floating in a 35mm tissue culture dish containing DMEM and 5%HS at 37°C for 6 days. Nerves were then fixed and processed for EM analysis (see section 2.12.1). Only the middle 2mm of each nerve segment was analysed in order to standardise the observations between conditions. For details on quantification of this experiment see section 2.14.

Dissociated cell demyelination assay: Sciatic nerves were dissected from P8 animals, dissociated in trypsin and collagense and then plated on laminin coated coverslips, at a concentration of a 1000 cells per coverslip, in DM, 0.5% HS and AraC (10^{-5}M). Cells were cultured for a maximum of 10 days with half the medium replaced every 3 days. At 3 hours, 3, 5, 7 and 10 days after plating cells were then fixed and analysed by ICC. Experiments were quantified by sampling 15 fields across each coverslip and counting the total number of P_0 or MBP positive cells, in each field, for each time point. Counts were then expressed as a percentage of the counts at the 3 hour time point. For upregulation of non-myelin genes, like L1, N-cadherin and $p75^{NTR}$,

percentages of positive Schwann cells, recognised by S100β immunolabelling, were recorded over 15 fields per coverslip for each time point. Two coverslips were included for each time point and experiments were repeated a minimum of three times.

2.3.8 *In vitro* BrdU proliferation assay

Bromodeoxyuridine (BrdU), is a uridine derivative that can be incorporated specifically into DNA in the place of thymidine when cells undergo DNA synthesis (during the S-phase of the cell cycle). Anti-BrdU immunolabelling can then be used to identify cells that undergo DNA synthesis.

Mutant Egr2 proliferation assay: Serum-purified rat Schwann cells were infected as previously described (Parkinson et al., 2001) with GFP control, Egr2 wild type or mutant Egr2 adenoviruses, in DM and 0.5% FCS. Cells were, again, placed in fresh medium 24 hours after infection and NRG-1 (20ng/ml) was added after a further 22 hours. BrdU (10^{-5}M) was added for the last 20 hours of the experiment and cells were fixed at 72 hours after infection for analysis by ICC.

NRG-1 proliferation assays: c-jun$^{f/f}$ or *c-jun*-null mouse Schwann cells (see section 4.2.6) were plated on PLL/laminin coated coverslips (5000 cells/coverslip) in medium containing DM treated with NRG-1 (20ng/ml). BrdU (10^{-5}M) was added for the last 20 hours of the experiment and cells were fixed after 72 hours of growth factor addition for analysis by ICC.

Cyclic AMP/ NRG-1 proliferation assays: Serum-purified mouse Schwann cells were plated on PLL/laminin coated coverslips (5000 cells/coverslip) in medium containing DM and treated with NRG-1 (20ng/ml) and varying concentrations of dbcAMP (1μM-2mM). BrdU (10^{-5}M) was added for the last 20 hours of the experiment and cells were fixed after 72 hours of growth factor addition for analysis by ICC. Results shown are pooled from at least three individual experiments.

In order to quantify Schwann cell proliferation, counts were performed, recording the number of GFP expressing or hoechst labelled cells that incorporated BrdU and then converting this to a percentage. All Schwann cell cultures were greater than 95% pure (Schwann cells were identified by a combination of S100β immunolabelling, the presence of cigar-shaped nuclei and a bi- or tri-polar shape, see Jessen et al., 1994) and the few fibroblasts in each culture were easily identifiable due to their much larger overall size, larger nucleus and flattened shape.

2.3.9 *In vitro* Cell Death Assay

Immunopanned Schwann cells from a newborn rat were infected as previously described (Parkinson et al., 2001) with GFP control, GFP/wild-type Egr2 or GFP/mutant Egr2 (S382R, D383Y) adenoviruses, in DM. Cells were placed into fresh medium after 24 hours. After 48 hours, cells were then either fixed (time zero control), or treated with or without TGFβ (5ng/ml) for a further 24 hours and then fixed for immunocytochemistry. Results shown are pooled from three individual experiments. Cell survival in this assay was measured by recording the number of GFP positive Schwann cells at the end of the experiment as a percentage of the number of GFP positive Schwann cells that had been plated successfully at the

beginning of the experiment. Dying cells were identified by Hoechst nuclear labelling, as described previously (Parkinson et al., 2001).

2.3.10 Inhibitor experiments

Different inhibitors were used to block specific pathways in our culture system as mentioned in the text:

U0126: MEK1/2 blocker (prevents phosphorylation and activation of the MEK1/2 downstream targets ERK 1/2), obtained from Calbiochem (Nottingham, UK) and used at 20μM (Maurel and Salzer, 2000; Harrisingh et al., 2004).

SP600125: a JNK1/2 blocker, obtained from Affiniti Research Products, Ltd and used at 30μM (Parkinson et al., 2004).

DJNK1 peptide: a JNK1/2 phosphorylation blocker, obtained as a gift from Dr. H. Mehmet (Imperial College London, UK) (Borsello et al., 2003) and used at 10μM (Parkinson et al., 2004).

H89: a PKA blocker, obtained from Sigma (UK) and used at 1μM (Kim et al., 1997).

LY294002: a blocker of the catalytic activity of phosphatidylinositol 3-kinase (PI3-K) obtained from Calbiochem (Nottingham, UK) and used at 10μM (Maurel and Salzer, 2000).

2.4 Molecular Biology Techniques

2.4.1 Western Blotting

Frozen nerve samples or cell lysates were transferred into either a triton based lysis buffer (25mM Hepes pH 7.5, 0.1M NaCl, 1% Triton X-100 and proteinase and phosphatase inhibitors) or a SDS lysis buffer (25mM Tris-HCL pH 7.4, 95mM NaCl, 10mM EDTA, 2% SDS and proteinase and phosphatase inhibitors) and homogenized

with micropestle homogenizers (Fisher Scientific UK). Proteinase inhibitor cocktail: leupeptin (10μg/ml) and soya bean trypsin inhibitor (10μg/ml) from Sigma (UK), α2-macroglobulin (0.1U/ml) from Roche Diagnostics (Germany) and 1mM phenylmethanesulphonyylfluoride (PMSF). Phosphatase inhibitor cocktail: okadaic acid (1μM) from Sigma (UK), sodium fluoride (50mM), sodium orthovanadate (1mM), EDTA (5mM), β-glycerophosphate (10.8mg/ml) and para-nitrophenylphosphate (7.4mg/ml). Before protein estimation, SDS extracted samples were boiled and centrifuged. Protein concentration was measured by colorimetry, using the Biorad protein assay kit (Biorad, USA), according to the manufacturer's instructions. Samples were then treated with 1/5 volume of 5X Laemmli loading buffer and stored at -80°C before being separated by SDS-PAGE. Between 5μg and 50μg of protein samples were loaded and separated by SDS-PAGE, under denaturing conditions, with a mini Protean II gel electrophoresis apparatus (Biorad, USA) containing running buffer. Kaleidoscope pre-stained standards molecular weight (Biorad, USA) was run alongside samples to enable identification of band sizes. Separated proteins were then transferred to a nitrocellulose membrane, Hybond-N, in a mini gel tank (Biorad, USA) containing transfer buffer at 4°C. The composition of all the reagents used is found in appendix I.

The membrane was incubated in 5% fat free milk powder in tris-buffered saline (TBS) for 2hours, in order to block non-specific binding sites. Then, primary antibodies were incubated in 5% fat free milk powder in TBS overnight at 4°C on a slow rotator (Gallenkamp, UK). Membranes were washed 3X 5 minutes at RT and subsequently incubated with horse radish peroxidase (HRP) -conjugated secondary antibody diluted in TBS for 1 hour at RT and again washed in TBS 3X 5 minutes. Membranes were then treated with a mix of homemade ECL 1 and 2

chemiluminescent reagents. ECL1 solution was made from 2.5mM luminol, 0.4mM coumaric acid, 0.1M Tris (pH 8.5) in distilled water. ECL2 solution was made using 0.1M Tris (pH 8.5), 0.02% hydrogen peroxide in distilled water. Both solutions were kept at 4°C in dark conditions and mixed 1:1 just prior to use. Specific protein complexes were then revealed by placing membranes in autoradiography cassettes (Appligene, USA) and developed by brief exposure (5 seconds to 10 minutes) to Kodak BioMax Mr-1 film in an X-Ograph Compact X2 automatic developer (UK).

2.4.2 Genotyping

DNA extraction: 5mm of tail samples were digested at 55°C overnight in lysis buffer (0.01M Tris pH 8.0, 0.05M EDTA pH 8.0, 0.04M NaCl and 1% SDS in UP H_20) containing 20ng/ml Proteinase K (Sigma, UK). DNA was obtained from this mix using a phenol-choloform (Fluka, UK) extraction. The DNA was then precipitated using 100% ethanol, washed in 70% ethanol, air dried and then dissolved in UP H_20 in order to use for PCR.

Genotyping by semi-quantitative PCR: PCR reactions were set up for each sample using 100-200ng of DNA and run at specific conditions for each primer set and performed in a MWG Biothec Primus96 Thermal Cycler or in a Perkin Elmer Gene Amp 2400 thermocycler. Typically 50µl reaction volumes containing 20mM Tris-HCl, pH 8.4, 50mM KCl, 1.5mM $MgCl_2$, 0.2mM dNTPs, 50pmol of each primer and 2.5 units of Taq DNA-polymerase were used. The reaction conditions, sequence of the primers and band sizes generated can be found in the appendix II. Upon completion of PCR, one tenth volume of 10x loading buffer (0.5M EDTA, pH 7.5, 10% SDS, 50% glycerol and 0.25% bromophenol blue) was added to each PCR

sample and 10μl of each reaction was electrophoresed on 2% agarose gels including ethidium bromide in 1x Tris Acetate EDTA (TAE) buffer in a Horizon 58 gel apparatus (BRL-Life Technologies, Gaithersburg, MD). In order to determine band sizes, samples were run alongside 10μl of 1kb DNA ladder diluted in DNA loading buffer.

2.4.3 *In situ* Hybridisation

A digoxigenin-labelled cDNA probe was used to detect P_0 mRNA induced by cyclic AMP and NRG1 in mouse Schwann cell cultures. These cells were fixed in 4% paraformaldehyde and washed 3X in RNAse-free PBS (1X). They were then incubated with hybridisation buffer containing 2.5ng/ml of the P_0 probe (Lee et al., 1997) and left overnight at 65°C in a humidified box containing 2X SSC. The next day, the coverslips were rinsed with 1X SSC at RT, after which they were washed with 1X SSC at 65°C for 1hour. They were then washed again with 1X SSC for 5 min at RT, after which they were incubated with buffer B1 containing 10% normal goat serum (Sigma, UK) for at least 1 hour. They were incubated overnight with anti-DIG antibody (roche diagnostics, USA) overnight at 4°C. The next day, the coverslips were washed with buffer B1 3X for 5 min each, after which they were treated with buffer B3 for 5 min. Then buffer B4 was added to the coverslips and the plates wrapped in aluminium foil and developed according to manufacturer's protocol. The cells were then mounted in aquamount (VWR, UK) and allowed to dry. The composition of all reagents used can be found in appendix III.

2.5 Animals used

c-Jun 'floxed' mice: Transgenic mice in which loxP sites are present in the 5' untranslated region (UTR) of *c-jun* and in the 3' flanking sequence 2.5 kb downstream of the translation stop codon. Breeding with a Cre transgenic mouse leads to excision of the entire *c-jun* gene (Behrens et al., 2002). A schematic representation of the floxed *c-jun* allele and deleted *c-jun* allele, after Cre mediated excision, is shown in Figure 4.2, A (Chapter 4). These animals were kindly provided by Dr A. Behrens (Cancer Research UK).

P0-Cre mice: Transgenic mice expressing Cre-recombinase under a transgene driven by the P_0 promoter. Strong *P0-Cre* activity was only detected in the peripheral nerve, starting from around E13.5, with slight activity in the occipital lobe of the cerebral cortex, Purkinje cell layer of the cerebellum and in the heart (Feltri et al., 1999a, 1999b, 2002). These mice were kindly provided by Dr L. Wrabetz and Dr M.L. Feltri (San Raffaelle Institute, Italy).

Krox-20 mice: Knockout mice in which a null allele is created in the *Krox-20* gene by an in-frame insertion of the E. coli *lacZ* gene (Schneider-Maunoury et al., 1993). Heterozygous animals were kindly provided by Dr P. Charnay (Ecole Normale Superieur, France).

WLD^S mice: C57BL/6OlaHsd-*Wld^S* mice carry a spontaneous mutation resulting in a 85Kb tandem triplication on chromosome 4 (Lyon et al., 1993; Coleman et al., 1998). Male animals (2 months old) were purchased from Harlan (UK).

C57BL/6 mice: Male mice (2 months old) were purchased from Harlan (UK). These mice were used as controls for C57BL/6OlaHsd-*Wld*^{S} mice.

ICR mice: Breeding pairs were purchased from Charles River (UK) to generate post-natal pups.

Sprague-Dawley rats: Post-natal pups were obtained from the Biological services Unit at University College London.

2.6 Peripheral nerve injury experiments

All the experiments in which animals were involved were performed following the UK Home Office guidelines.

Short-term sciatic nerve transections: Adult transgenic mice (2-4 months old) were anaesthetised with either 2% halothane or 2% isofluorane, and the right sciatic nerve was exposed and cut at the level of the sciatic notch. A piece of the proximal stump was removed and the remaining proximal stump was diverted to limit the possibility of axonal regeneration into the degenerating distal stump. Wounds were sutured with 3/0 black polyamide monofilament, mersilk (Johnson&Johnson, USA) and skin was sealed using vetinerary autoclips (VET-TECH, UK). Three, five or seven days following transection, the animals were culled and both the distal stump of the right, transected sciatic nerve and the contralateral control nerve were excised. Tissue was then processed for WB, IHC and EM (see sections 2.4.1, 2.10 and 2.13.1 respectively). After IHC and EM processing, the distal stump was cut into 3 segments

before analysis (0-2mm distal to the cut site, known as the injury region; 2-4mm distal to the cut site and 4-6mm distal to the cut site).

Long-term sciatic nerve transections: Adult transgenic mice (2-4 months old) were anaesthetised with either 2% halothane or 2% isofluorane, and the right sciatic nerve was exposed and cut at mid thigh level. The proximal stump was then ligated and sutured into the gluteal muscle using 8/0 black polyamide monofilament, mersilk (Johnson&Johnson, USA) to prevent axonal regeneration into the degenerating distal stump. Wounds were sutured with 3/0 black polyamide monofilament, mersilk (Johnson&Johnson, USA) and skin was sealed using vetinerary autoclips (VET-TECH, UK). Seven days after the surgery, skin autoclips were removed. Four weeks following transection, the animals were culled and both the distal stump of the right, transected sciatic nerve and the contralateral control nerve were excised. Tissue was then processed for osmium staining or EM (see sections 2.9 and 2.13.1 respectively).

Sciatic nerve crushes: Adult transgenic mice (2-4 months old) were anaesthetised with either 2% halothane or 2% isofluorane, and the right sciatic nerve was exposed and crushed using watchmaker's forceps three times for 10 seconds at the level of the sciatic notch. Wounds were sutured with 3/0 black polyamide monofilament, mersilk (Johnson & Johnson, USA) and skin was sealed using vetinerary autoclips (VET-TECH, UK). Seven days after the surgery, skin autoclips were removed. Ten weeks following nerve crush, some animals were anaesthetised and perfused (see section 2.7). Following this, both right and left dorsal and ventral roots from spinal level L5 and a 2 centimeters length of the right sciatic and tibial nerve distal to the sciatic

notch (including crush site) and of the contralateral control nerve were excised. Tissue was then processed for EM (see section 2.13.1).

2.7 Mouse perfusion

For 10 week cut and crush experiments, transgenic mice were terminally anaesthetised with a 0.2ml intraperitoneal injection of sodium pentobarbital (conc.5μg/ml) and intracardially perfused with 75-100ml of ice cold 4% PF over a 5 minute period using a peristaltic pump at 4rpm. On completion, sciatic nerves and L5 dorsal and ventral roots were removed for histology (see section 2.13.1).

2.8 *In vivo* BrdU proliferation assay

Schwann cell proliferation after nerve cut: 2-4month old mice that had their right sciatic nerve transected at the sciatic notch. Wounds were sutured and the mice were allowed to recover. Five days after the surgery, these mice were injected intraperitoneally with 100μg BrdU solution per g of body weight and allowed to rest without disturbance for two hours. Both the injured and the contralateral uninjured sciatic nerves were dissected out and fixed in -20°C methanol for 2 hours and then placed in 4% PF overnight. Nerves were then washed in 1X PBS for 3X 15 minutes before being placed in 20% sucrose overnight. The next day the tissues were embedded in OCT compound and stored at -70°C. Frozen sections (10μm thickness) were cut using a cryostat (Reichert-Jung, Germany) and double IHC was performed on sections for BrdU and S100β (Schwann cell specific marker) (see section 2.10).

To quantify the number of BrdU positive Schwann cells in uninjured and injured nerves, 5 sample areas (40,000μm^2) on at least 3 sections, 50μm apart were counted using average confocal projections (see section 2.13.2). The total area

counted was then calculated and the total number of BrdU positive cells was expressed per 1mm^2 of nerve. At least 4 separate nerves were counted per condition.

2.9 Osmium staining of sciatic nerves

Sciatic nerves were embedded in OCT compound in rubber coffin moulds and stored at -80°C. Sections of 10μm thickness were cut using a cryostat (Reichert-Jung, Germany) and collected on Superfrost Plus microscope slides. Before staining, sections were air-dried for 30 minutes and then fixed in 4% PF for 10 minutes, washed twice with 1X PBS and then incubated with 2% osmium solution in the dark overnight at RT. The next day the sections were drained and washed 3 times in PBS and mounted using Citifluor antifade mountant and sealed with nail varnish.

2.10 Immunohistochemistry (IHC)

Sciatic nerves were embedded in OCT compound in rubber coffin moulds and stored at -80°C. Sections of 10μm thickness were cut using a cryostat (Reichert-Jung, Germany) and collected on Superfrost Plus microscope slides. Before immunolabelling, sections were air-dried for 30 minutes and then treated with different fixatives and blocking solutions depending on the primary antibody used. For *N-cadherin IHC*, sections were fixed in 4% PF for 10 minutes, blocked in 0.1% triton X-100, 1% BSA in PBS for 1 hour at RT, then primary antibody, diluted in blocking solution, was applied o/n at 4°C.

For *L1 (324) IHC*, sections were fixed in 4% PF for 10 minutes, then primary antibody was applied o/n at 4°C. For p75^{NTR} and NCAM IHC, sections were fixed in 2% PF for 5 minutes, then primary antibodies, diluted in MEM-Hepes 10% calf serum, were applied o/n at 4°C.

For *Krox-20 IHC*, sections were fixed in 4% PF for 10 minutes, blocked in 0.5% triton X-100 in antibody diluting solution (ADS, PBS containing 10% calf serum, 0.1% lysine and 0.02% sodium azide) for 30 minutes at RT and then primary antibodies, diluted in blocking solution, were applied o/n at 4°C.

For *polyclonal P_0 IHC*, sections were fixed in 2M HCl for 10 minutes, neutralized with 0.1M sodium borate for 7 minutes, blocked with ADS for 2 hours at RT and then primary antibody, diluted in ADS, was applied o/n at 4°C.

For *polyclonal c-Jun IHC*, sections were fixed in 4% PF for 10 minutes, blocked in 0.2% triton X-100 in ADS for 30 minutes at RT and then primary antibodies, diluted in blocking solution, were applied o/n at 4°C.

For *TuJ1 IHC*, sections were fixed in 4% PF for 10 minutes and then primary antibody, diluted in ADS was applied o/n at 4°C.

For *BrdU IHC*, sections were fixed in 2M HCl for 20 minutes at 50°C, neutralized with 0.1M sodium borate for 7 minutes and primary antibody, diluted in 0.1% triton X-100 in PBS, was applied o/n at 4°C.

For *S100β/BrdU IHC*, sections were treated with -20°C methanol for 10 minutes, permeabilised with 0.2% triton X-100 in PBS for 30 minutes at RT, blocked in 3% bovine gelatin (Sigma, UK) in PBS for 30 minutes at 37°C and then incubated with primary polyclonal antibody to S100β, diluted in ADS was applied o/n at 4°C. The next day sections were incubated with secondary antibody for 30 minutes at RT, treated with -20°C methanol for 10 minutes, treated with 2M HCl for 20 minutes at 50°C, neutralized with 0.1M sodium borate for 7 minutes and primary antibody, diluted in 0.1% triton X-100 in PBS, was applied o/n at 4°C.

For the dilutions of different primary and secondary antibodies, please see section 2.2. All secondary antibodies were diluted in ADS and applied for 30 minutes at RT. Between each step, slides were washed 3 times with PBS for 5 minutes each and slides were mounted using Citifluor antifade mountant and sealed with nail varnish. In order to ensure that secondary antibodies did not cause any non-specific background staining, primary antibodies were excluded from a single sample in each experiment.

2.11 Immunocytochemistry (ICC)

For ICC, cells were fixed in different fixatives and blocked in different solutions depending on the primary antibody used.

For *monoclonal c-Jun, Sox-2, Krox-20, p27, cdk2, β-galactosidase, Cyclin D1 and Cre-recombinase ICC*, cells were fixed in 4% PF for 10 minutes, blocked in 0.2% triton X-100 in ADS for 30 minutes at RT and then primary antibodies, diluted in blocking solution, were applied o/n at 4°C.

For *L-periaxin ICC*, cells were were fixed in 4% PF for 10 minutes, blocked in 0.2% triton X-100 in ADS for 30 minutes at RT and then primary antibody, diluted in ADS, was applied o/n at 4°C.

For *MBP ICC*, cells were fixed in 2% PF for 10 minutes, permeabilised in ice cold methanol for 10 minutes, treated with 0.2% triton X-100 in ADS for 30 mins at RT and then primary antibody, diluted in ADS, was applied for 2 hours at RT.

For *monoclonal P_0 ICC*, cells were fixed in 4% PF for 10 minutes, permeabilised in ice cold methanol for 10 minutes, blocked in ADS for 30 minutes and then primary antibody, diluted in ADS, was applied o/n at 4°C.

For *polyclonal P_0 ICC*, cells were fixed in 2M HCl for 10 minutes, neutralized in 0.1M sodium borate for 7 minutes, blocked in ADS for 2 hours and then primary antibody, diluted in ADS, was applied o/n at 4°C.

For *BrdU ICC*, cells were fixed in 2M HCl for 10 minutes, neutralized in 0.1M sodium borate for 7 minutes and then primary antibody, diluted in 0.1% triton X-100 in PBS, was applied for 1 hour at RT.

For *N-cadherin ICC*, cells were fixed in 4% PF for 10 minutes, blocked in 0.1% triton X-100, 1% BSA in PBS for 1 hour at RT, then primary antibody, diluted in blocking solution, was applied o/n at 4°C.

For *L1 (324) ICC*, cells were fixed in 4% PF for 10 minutes, then primary antibody was applied o/n at 4°C.

For *L1 (ASCS4)*, cells were fixed in 2% PF for 5 minutes, then primary antibody, diluted in MEM-Hepes 10% calf serum, was applied for 1 hour at RT.

For *NCAM and $p75^{NTR}$ ICC*, cells were fixed in 2% PF for 5 minutes, then primary antibody, diluted in MEM-Hepes 10% calf serum, was applied o/n at 4°C.

For *O4 and Gal-C*, primary antibodies were added to unfixed cells for 1 hr and then incubated with relevant secondary antibodies, after which they were post-fixed with 4% PF for 10 minutes.

S100βICC was done in conjunction with *MBP, N-cadherin, L1 (324) and $p75^{NTR}$ ICC*. In the case of *MBP ICC*, primary antibodies were added at the same time, in ADS o/n at 4°C. For all other labelling, *S100βICC* was carried out after *N-cadherin, L1 (324) and $p75^{NTR}$ ICC*. The cells were post fixed in 4% PF for 10 minutes, permeabilised with ice cold methanol for 10 minutes, blocked with 0.2% triton X-100 for 30 minutes and primary antibodies, diluted in the blocking solution, were applied o/n at 4°C.

All secondary antibodies were diluted in ADS and applied for 30 minutes at RT. For *L1 (ASCS4)* a three layer system was employed, using a biotinylated secondary antibody, applied for 30 minutes at RT and a tertiary antibody to strepavidin, applied for 15 minutes at RT. Both antibodies were diluted in ADS. Between each step, cells were washed 6 times with PBS and coverslips were mounted using Citifluor antifade mountant and sealed with nail varnish. In order to ensure that secondary antibodies did not cause any non-specific background staining, primary antibodies were excluded from a single sample in each experiment.

2.12 *In vivo* cell death assay

Apoptotic cells were identified by *in situ* labeling of DNA fragmentation, using terminal deoxynucleotidyl transferase-mediated dUTP-biotin nick end labeling (TUNEL). For TUNEL labelling, sections were fixed in 4% PF for 10 minutes, treated with permeabilisation solution (0.1% triton X-100, 0.1% Na citrate in PBS) for 2 minutes at 4°C, incubated with 50μl reaction mix (5μl TUNEL enzyme and 45μl TUNEL mix) for 1 hour at 37°C in dark and then stained with hoechst in ADS for 5 minutes at RT. For positive controls sections were incubated with DNase I (Sigma, UK) (30U/ml in 50mM Tris-HCL, pH 7.5, 1mg/ml BSA) for 10 minutes at RT prior to incubation with TUNEL mix. A negative control was also included which involved incubating sections with TUNEL mix without enzyme.

To quantify the number of TUNEL positive cells in uninjured and injured nerves, 5 sample areas (40,000μm^2) on at least 3 sections, 50μm apart were counted (see section 2.12.2). The total area counted was then calculated and the total number of TUNEL positive cells was expressed per 1mm^2 of nerve. At least 4 separate nerves were counted per condition.

2.13 Microscopy

2.13.1 Electron Microscopy

The injured sciatic nerve, contralateral control nerve and L5 dorsal and ventral roots from mutant mice were fixed *in situ* for 15 minutes, using freshly prepared 2% glutaraldehyde in 0.1M sodium phosphate buffer, pH 7.4. Nerves were then dissected out from the animals and placed in fixative overnight at 4°C. The next day, the tissue was washed three times for 15 minutes in 0.1M phosphate buffer, pH 7.4 and then stained with 1% osmium tetroxide in 0.2M phosphate buffer for 1.5 hours. The samples were then washed twice, for 15 minutes, in UPH_2O before being dehydrated as follows; 25% ethanol for 5 minutes; 50% ethanol for 5 minutes; 70% ethanol for 5 minutes; 90% ethanol for 10 minutes; 100% ethanol, 4X 10 minutes; propylene oxide, 3X 10 minutes. The nerves were then incubated in a 1:1 mixture of propylene oxide and resin (12g agar resin, 8g DDSA, 5g MNA and 16 drops of BDMA) for 1 hour, after which, nerves were placed in resin alone overnight at RT. The following morning, the resin was replaced with fresh resin and 8 hours after this tissue samples were placed in rubber coffin moulds containing resin and thermo-cured at 65°C overnight. Semi-thin and ultra-thin sections were both cut using an Ultracut E ultramicrotome (Leica, Germany). Handmade glass knives were used to cut semi-thin sections, which were collected on microscope slides and then stained with 0.1% toluidine blue in ethanol. Ultra-thin sections were cut by Mr M. Turmaine (Department of cell and developmental biology, Universty College London) using a diamond knife (Diatome, USA) and collected on copper grids (Agar scientific) or films (made by M. Turmaine). Sections were stained for 15 minutes in lead citrate solution, washed in UPH_20, dried and viewed using a Jeol 10p0 electron microscope (Japan).

2.13.2 Fluorescent microscopy

Immunofluorescent cells or sections were visualised using either a Nikon Optiphot-2 or a Nikon Eclipse E800 fluorescent microscope. Images were captured using a digital camera (model: DXM1200, Nikon) and ACT-1 acquisition software (Nikon). Confocal microscopy was performed using a Leica DMRE fluorescence microscope with a SP1 confocal head and Leica confocal software. The average confocal projection of 15 sections over a distance of 10μm was used in all experiments. All images were imported into Adobe Photoshop version 8.0.

2.14 Quantification of observations in semithin and ultrathin sections

Thickness of myelin sheath (G-ratio): Between 15 and 20 photographs were taken of tranverse ultrathin sections of the tibial nerve at the mid-thigh level (5mm from sciatic notch) in control and experimental conditions at x2500 magnification. Images were imported into Image J (NIH, USA) in order to measure the axon diameter and diameter of the axon plus myelin sheath. Using Microsoft Excel, from these measurements the g-ratio for each myelinated fibre (axon diameter divided by diameter of the axon and myelin sheath) was calculated.

Numbers of myelinated axons in the uninjured adult mouse and after nerve crush: Photographs of semithin sections of the tibial nerve stained with toluidine blue were taken at x100 magnification. Images were imported into Photoshop, a montage of the whole nerve was made and the total number of myelinated axons in the tibial nerve (5mm distal to the sciatic notch) was made.

Numbers of intact myelin sheaths after nerve cut: Ultrathin sections of samples were cut and placed on copper grids and viewed by EM. Counts of intact compact myelin sheaths with either a collapsed or swollen axon were made for every complete grid square ($64\mu m^2$) for the entire tibial nerve at x2500 magnification for 3 (1mm from sciatic notch), 5 and 7 (5mm from sciatic notch) days after sciatic nerve transection. The total number of sheaths counted and the total area sampled were then calculated. The area of the nerve was then measured by importing a x150 magnification photo of the tibial nerve into Image J (NIH, USA). Using this information the total number of intact myelin sheaths could be calculated for the entire tibial nerve.

Numbers of Remak fibres and unmyelinated axons in the adult mouse sciatic nerve and after nerve crush: Ultrathin sections of samples were cut and placed on copper grids and viewed by EM. Counts of Remak fibres and number of axons per Remak fibre were made for every complete grid square ($64\mu m^2$) for the entire tibial nerve (5mm distal to the sciatic notch) at x2500 magnification. The total number of Remak fibres and unmyelinated axons counted and the total area sampled was then calculated. The area of the nerve was then measured by importing a x150 magnification photo of the tibial nerve into Image J (NIH, USA). Using this information the total number of Remak fibres and unmyelinated axons could be calculated for the entire tibial nerve.

Numbers of Schwann cell nuclei: Ultrathin sections of samples were cut and placed on copper grids and viewed by EM. Counts of Schwann cell nuclei (identified by nuclei containing peripheral heterochromatin within a cell containing a basal lamina, macrophages, fibroblasts, mast cells and endothelial cells were all identifiable and

discounted) were made for every complete grid square ($64\mu m^2$) for the entire tibial nerve (5mm distal to sciatic notch) at x2500 magnification, 4 and 10 weeks after sciatic nerve transection. The total number of Schwann cell nuclei counted and the total area sampled were then calculated. The area of the nerve was then measured by importing a x150 magnification photo of the tibial nerve into Image J (NIH, USA). Using this information the total number of Schwann cell nuclei could be calculated for the entire tibial nerve.

Numbers of myelinated axons in the dorsal and ventral roots: Photographs of semithin sections of the right and left L5 dorsal and ventral roots stained with Toluidine Blue were taken at x100 magnification. Images were imported into Photoshop, a montage of the each whole root was made and the total number of myelinated axons was counted.

2.15 Functional testing for animal regeneration experiments

All the experiments in which animals were involved were performed following the UK Home Office guidelines.

The presence of a toe-spreading reflex was recorded after mice were lifted gently by the tail (Gutmann et al., 1942; Siconolfi and Seeds, 2001). Mice demonstrating full extension of the hind limb and full extension and abduction of all five toes so that clear space can be seen between each toe were given a toe-spreading reflex score of 2. Whereas, mice showing a partial toe spreading reflex, such as improper hind limb extension or only abduction and extension of some but not all five toes were given a toe-spreading reflex score of 1. Mice showing no abduction of all 5 toes, in response to being lifted by their tail, were given a score of 0.

Recovery of pressure and pain sensitivity was tested on mice, by pinching the most distal part of the lateral three toes, which derive sensation from the sciatic nerve, on both uninjured and injured limbs, with a number 5 forceps. Hind limb withdrawal and/or vocalization were recorded as positive responses, demonstrating functional sensory regeneration after injury (Siconolfi and Seeds, 2001).

2.16 Statistical analysis

All data are presented as arithmetic mean ± standard deviation (SD). Unless otherwise stated (either in the main text or figure legends) statistical significance was estimated by the Student's *t* test using Microsoft Excel program (Microsoft UK, UK). Other statistical tests, including one-way and two-way analysis of variance (ANOVA) and the non-parametric Mann-Whitney U test were performed using the software package Prism version 5 (GraphPad).

CHAPTER 3: β-neuregulin-1 and cyclic-AMP synergise to induce myelin differentiation in mouse Schwann cells.

3.1 INTRODUCTION

The generation of myelinating Schwann cells from immature Schwann cells appears to be controlled from signals from the axon (Jessen and Mirsky, 2005; see Chapter 1). One axonally derived molecule that has shown to be important in regulating the process of myelination in Schwann cells is NRG1 (Nave and Salzer, 2006; see Chapter 1). However, cultured Schwann cells are not induced to express myelin genes by exogenously applied NRG1, in either a soluble or a membrane bound form, and instead proliferate, suggesting that other signals are likely to play a role in myelin differentiation, potentially modulating NRG1 signalling (Taveggia et al., 2005).

Once such signal that is known to modulate NRG1 signalling in Schwann cells is cyclic AMP. Addition of cyclic AMP analogues or the adenylate cyclase activator, forskolin, to Schwann cell cultures can boost proliferation stimulated by NRG1 and prolongs activation of the MAPK and PI3K pathways (Raff et al., 1978; Levi et al., 1995; Kim et al., 1997; Rahmatullah et al., 1998; Monje et al., 2006). In addition intracellular cyclic AMP elevation is a prerequisite for most growth factors, such as PDGF and FGFs, to induce rat Schwann cell proliferation (Chen et al., 1991; Stewart et al., 1991; Kim et al., 2001). Cyclic AMP elevation has also been shown to act as a differentiation factor for cultured rat Schwann cells, upregulating genes such as galactocerebroside (galC), 04 antigen, E-cadherin, periaxin, Krox-20, P_0 and MBP (Sobue and Pleasure, 1984; Lemke and Chao, 1988; Mirsky et al., 1990; Morgan et al., 1991; Parkinson et al., 2003; Crawford et al., 2008) and downregulating genes expressed on immature Schwann cells, like, $p75^{NTR}$, NCAM, N-cadherin, GFAP,

growth-associated protein-43 (GAP-43), c-Jun and Sox-2 (Jessen et al., 1987b; Mokuno et al., 1988; Morgan et al., 1991; Scherer et al., 1994b; Parkinson et al., 2004, 2008; Crawford et al., 2008). Importantly, the capacity to induce Schwann cell differentiation by cyclic AMP elevation is independent from its role in assisting growth factor or serum induced proliferation (Morgan et al., 1991).

Cyclic AMP effectors include protein kinase A (PKA), cyclic nucleotide-gated cation channels and a family of guanine nucleotide exchange factors (GEFs) (Fig. 3.1). In cultured rat Schwann cells, myelin differentiation induced by contact with neurons or by cyclic AMP elevation requires PKA activity (Howe and McCarthy, 2000; Yoon et al., 2008). Furthermore, the peak of PKA activity in the sciatic nerve occurs around the time when myelination begins (Yoon et al., 2008).

In this study, I wanted to investigate possible interactions between NRG1 and cyclic AMP signalling pathways in Schwann cell differentiation. However, one caveat with this proposal is that all the evidence showing the importance of the NRG1/erbB signalling pathway in myelin differentiation has come from experiments in mice whereas the majority of cyclic AMP studies have been carried out using rat Schwann cells. For this reason, I opted to establish a technique for readily culturing mouse Schwann cells (Stevens et al., 1998; see Chapter 2), in order to investigate whether the two factors played a role in myelin differentiation in Schwann cells from the same species.

Figure 3.1: Overview of cyclic AMP signalling.

Ligand binding to G-protein coupled receptors activates adenylyl cyclases and generates a pool of cyclic AMP, the concentration and distribution of which is regulated by phosphodiesterases. Cyclic AMP binds to and activates dissociation of the PKA heterotetramer, the catalytic domains (C) migrate to the nuclear compartment and phosphorylate the transcription factor CREB on Ser133, which promotes CREB dependent transcription. In addition to numerous other targets, PKA activation can also positively and negatively regulate the Raf/MEK/ERK pathway depending on the context (Stork and Schmitt, 2002). Cyclic AMP can also bind and active the guanine exchange factors, epac1 and 2, which carry out their downstream effects through Rap1, a small GTPase (Bos, 2003). Adapted from Tasken and Aandahl, (2004).

3.2 RESULTS

3.2.1 Cyclic AMP has concentration dependent effects in the presence of NRG1 in mouse Schwann cells.

Previous studies have demonstrated a concentration dependent action of cyclic-AMP analogues on Schwann cell proliferation and differentiation. In these investigations, it was found that relatively low concentrations of cyclic AMP analogues were sufficient to induce Schwann cell proliferation whereas concentrations 10-fold higher induce maximal expression of the early differentiation marker, gal-C (Sobue et al., 1986; Yamada et al., 1995). However, both of these studies used calf serum in their experiments and cyclic AMP is unable to promote proliferation in the absence of serum or growth factors (Stewart et al., 1991; Morgan et al., 1991). Therefore, I decided to investigate the effects of cyclic AMP and NRG1 signalling on mouse Schwann cell proliferation and differentiation, in serum free conditions. Briefly, mouse Schwann cells were plated a density of 5000 cells per coverslip in DM. Cells were then treated with a constant concentration of NRG1 (20ng/ml) and a varying concentration of the cyclic AMP analogue, dbcAMP, ranging from 1μM to 2mM for a 72 hour period. Some cells were pulsed with BrdU for the last 24 hours of the experiment and then fixed and labelled with an antibody against BrdU, whereas other cells were fixed and labelled with an antibody detecting Krox-20.

I found that a concentration of 100μM dbcAMP achieved the maximal elevation of NRG1 induced Schwann cell BrdU incorporation, from 41.6 +/-4.4% BrdU positive cells in NRG1 alone to 77.2 +/-1% in the presence of 100μM dbcAMP and NRG1 ($n=6$)($p<0.001$). However concentrations of dbcAMP above 100μM began to reduce Schwann cell BrDU incorporation with the result that, 1mM dbcAMP had

no effect on NRG1 induced Schwann cell DNA synthesis and a concentration of 2mM dbcAMP actually inhibited proliferation induced by NRG1 ($n=4$)($p<0.001$)(Fig. 3.2, A). In contrast, under these conditions in the presence of NRG1, only high concentrations of dbcAMP (<500μM) were able to induce significant levels of Krox-20 protein expression in mouse Schwann cells, with maximal induction occurring at 1mM dbcAMP where 49.3 +/-5.8% of Schwann cells expressed Krox-20 ($n=5$)($p<0.001$)(Fig.3.2, B). Thus, these experiments confirm that the cyclic AMP analogue, dbcAMP, demonstrates similar concentration dependent effects on mouse Schwann cell proliferation and differentiation, in the presence of NRG1 as previous reports showed with cyclic AMP analogues in the presence of serum in rat Schwann cells (Sobue et al., 1986).

3.2.2 Only a combination of cyclic AMP and NRG1 is sufficient to induce Krox-20 expression in mouse Schwann cells.

Cyclic AMP elevation alone, in the absence of serum or growth factors, is sufficient to induce myelin gene expression in cultured rat Schwann cells (Morgan et al., 1991; Parkinson et al., 2003). Thus, it was important to discern whether cyclic AMP was able to induce myelin gene expression in mouse Schwann cells. To test this, expanded mouse Schwann cells were treated with either NRG1 (20ng/ml) alone, dbcAMP (1mM) alone, a combination of NRG1 (20ng/ml) and dbcAMP (1mM) or left in just DM for 72 hours. After this, protein was extracted from the cells and analysed by Western blotting. Surprisingly, I found that 1mM dbcAMP treatment was insufficient to induce Krox-20 expression in mouse Schwann cells, as was NRG1 treatment. However, a combination of both 1mM dbcAMP and NRG1 demonstrated a

robust induction of Krox-20 protein, confirming results from the previous experiments (Fig.3.2, C).

In order to substantiate this finding, I used Schwann cells from mice that were heterozygous for a *Krox-20/lacZ* chimaeric gene (referred to as *Krox-20*$^{+/-}$) (Schneider-Maunoury et al., 1993). In these mice, expression of the *lacZ* gene reflects the normal expression pattern of the *Krox-20* gene (Topilko et al., 1994; Murphy et al., 1996). *Krox-20*$^{+/-}$ Schwann cells were serum purified, plated in DM and HI and treated with the same conditions as in the above experiment for 72 hours. Cells were then fixed and stained with an antibody to β-galactosidase (β-gal), the *lac-Z* gene product. Schwann cells maintained in DM or NRG1 expressed virtually no β-gal and only 2.2 +/-1.3% of Schwann cells expressed β-gal in response to 1mM dbcAMP treatment. However, 43.5 +/-3.2% of Schwann cells treated with a combination of both 1mM dbcAMP and NRG1 displayed strong β-gal expression ($n=4$)($p<0.001$)(Fig.3.2, D-H). Thus it appears that either dbcAMP or NRG1 treatment alone are incapable of inducing significant levels of Krox-20 and that both are required in combination in order to induce strong Krox-20 expression in cultured mouse Schwann cells.

Figure 3.2: A combination of cyclic AMP and NRG1 induces Krox-20 in mouse Schwann cells.

(A) Effects of varying concentrations of dbcAMP (0-2mM) on NRG1 induced Schwann cell BrdU incorporation. For these experiments mouse Schwann cells were kept in a constant concentration of NRG1 (20ng/ml) for 72 hours. The concentration of dbcAMP (x-axis) is plotted on a log scale. Error bars show the standard deviation of the mean. Statistical analysis was measured by one-way ANOVA with Tukey's Multiple Comparison test.

(B) Effects of varying concentrations of dbcAMP (0-2mM) in the presence of NRG1 (20ng/ml) on Schwann cell Krox-20 expression after 72 hours treatment. The concentration of dbcAMP (x-axis) is plotted on a log scale. Error bars show the standard deviation of the mean. Statistical analysis was measured by one-way ANOVA with Tukey's Multiple Comparison test. Note how the optimal concentrations for dbcAMP for the enhancement of NRG1 induced proliferation (A) were an order of magnitude lower than the optimal concentrations for Krox-20 induction (B).

(C) Western blot showing Krox-20 expression by expanded mouse Schwann cells after 72 hour treatment with NRG1 (20ng/ml) alone, dbcAMP (1mM) alone, dbcAMP (1mM) and NRG1 (20ng/ml) or cells were left unstimulated (Control). β-tubulin was used as a loading control. Molecular weight (MW) of proteins is illustrated in kDs.

(D-G) Schwann cells from mice that were heterozygous for a *Krox-20/lacZ* chimaeric gene were cultured and treated with NRG1 (20ng/ml) alone, dbcAMP (1mM) alone, dbcAMP (1mM) and NRG1 (20ng/ml) or left unstimulated (Control) for 72 hours. Arrowheads demonstrate β–gal positive Schwann cells. Cells are co-labelled with hoescht nuclear dye (Ho). Scale bar, 50μm.

(H) The percentage of Schwann cells that express β–gal in response to NRG1 (20ng/ml) alone, dbcAMP (1mM) alone, dbcAMP (1mM) and NRG1 (20ng/ml) treatment or after left unstimulated (Control) for 72 hours. Error bars show the standard deviation of the mean.

Figure 3.2

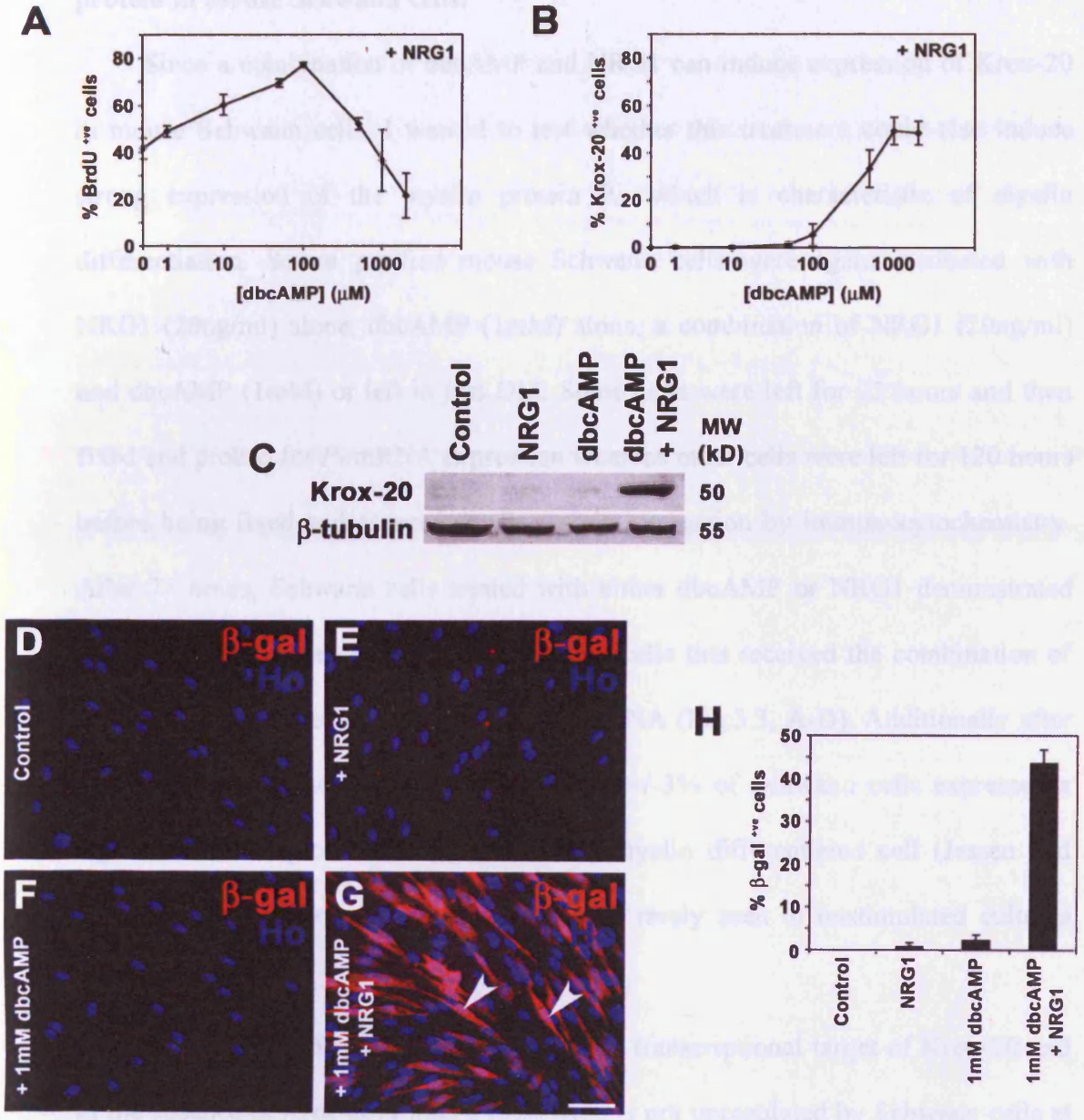
A
+ NRG1
% BrdU +ve cells
[dbcAMP] (μM)
B
+ NRG1
% Krox-20 +ve cells
[dbcAMP] (μM)
C
Control
NRG1
dbcAMP
dbcAMP + NRG1
MW (kD)
Krox-20
β-tubulin
50
55
D
β-gal
Ho
Control
E
+ NRG1
F
+ 1mM dbcAMP
G
+ 1mM dbcAMP + NRG1
H
% β-gal +ve cells
Control
NRG1
1mM dbcAMP
1mM dbcAMP + NRG1

3.2.3 Cyclic AMP and NRG1 synergistically induce high levels of P_0 mRNA and protein in mouse Schwann cells.

Since a combination of dbcAMP and NRG1 can induce expression of Krox-20 in mouse Schwann cells, I wanted to test whether this treatment could also induce strong expression of the myelin protein P_0, which is characteristic of myelin differentiation. Serum purified mouse Schwann cells were again incubated with NRG1 (20ng/ml) alone, dbcAMP (1mM) alone, a combination of NRG1 (20ng/ml) and dbcAMP (1mM) or left in just DM. Some cells were left for 72 hours and then fixed and probed for *P_0* mRNA expression whereas other cells were left for 120 hours before being fixed and assayed for P_0 protein expression by immunocytochemistry. After 72 hours, Schwann cells treated with either dbcAMP or NRG1 demonstrated slightly elevated levels of *P_0* mRNA but only cells that received the combination of the two factors expressed high levels of *P_0* mRNA (Fig.3.3, A-D). Additionally after 120 hours of dbcAMP/NRG1 treatment, 18.2 +/-3% of Schwann cells expressed a high level of P_0 protein, characteristic of a myelin differentiated cell (Jessen and Mirsky, 2005), whereas these cells were very rarely seen in unstimulated cultures ($n=4$)($p<0.01$)(Fig.3.3, E and F).

As mentioned in Chapter 1, P_0 is a direct transcriptional target of Krox-20 and in the absence of *Krox-20*, *P_0* gene expression is not upregulated by Schwann cells at the beginning of myelination (Topilko et al., 1994; LeBlanc et al., 2006). Therefore, I wanted to test whether the P_0 induction by dbcAMP/NRG1 treatment relied on the expression of Krox-20. To investigate this I stimulated Schwann cells from control or *Krox-20*$^{-/-}$ mice (Schneider-Maunoury et al., 1993), with dbcAMP (1mM) and NRG1 (20ng/ml) for 96 hours and then fixed and stained the cells with antibodies to P_0 and Krox-20. No *Krox-20*$^{-/-}$ Schwann cells expressed significant levels of P_0 or Krox-20

protein in response to dbcAMP/NRG1 (Fig.3.3, G-K), demonstrating that dbcAMP/NRG1 P_0 upregulation requires prior induction of Krox-20.

Interestingly, 22.1 +/-0.4% of control Schwann cells expressed high levels of P_0 after 96 hours, suggesting that no more Schwann cells are recruited to express P_0 protein between 96 and 120 hours after dbcAMP/NRG1 stimulation (Fig.3.3, F and K). However, Schwann cells treated for 120 hours with dbcAMP/NRG1 do appear much flatter and appear to express a greater amount of P_0 (Fig.3.3, E) than cells stimulated for only 96 hours (Fig.3.3, G). In summary, these experiments show that prolonged treatment of mouse Schwann cells with a combination of 1mM dbcAMP and NRG1 leads to strong induction of P_0 mRNA and protein and that this induction is dependent on the upregulation of the transcription factor Krox-20.

Figure 3.3: A combined cyclic AMP and NRG1 signal induce P0 mRNA and protein expression in mouse Schwann cells.

(A-D) Expression of P_0 mRNA in serum purified mouse Schwann cells either after treatment with NRG1 (20ng/ml), dbcAMP (1mM), dbcAMP (1mM) and NRG1 (20ng/ml) or left unstimulated (Control) for 72 hours. Arrowheads show Schwann cells expressing high levels of P_0 mRNA after the combined treatment of dbcAMP and NRG1. Scale bar, 50μm.

(E) Immunocytochemistry for P_0 in serum purified mouse Schwann cells treated with dbcAMP (1mM) and NRG1 (20ng/ml) for 120 hours. Notice the significant flattening of the P_0 positive cells (denoted by arrowheads) compared to the normal spindle shaped morphology seen in panel (G). Cells are co-labelled with hoescht nuclear dye (Ho). Scale bar, 50μm.

(F) The percentage of Schwann cells that express high levels of P_0 protein after dbcAMP (1mM) and NRG1 (20ng/ml) treatment or left unstimulated for 120 hours. Error bars show the standard deviation of the mean.

(G-J) Serum purified Schwann cells from control (G and I) and *Krox-20*$^{-/-}$ mice (H and J) were treated with dbcAMP (1mM) and NRG1 (20ng/ml) for 72 hours and assayed for P_0 (G and H) and Krox-20 protein expression (I and J). Arrowheads mark P_0 positive Schwann cells from control mice. Cells are co-labelled with hoescht nuclear dye (Ho). Scale bar, 50μm.

(K) The percentage of P_0 positive Schwann cells in control and *Krox-20*$^{-/-}$ cultures after 96 hours of dbcAMP (1mM) and NRG1 (20ng/ml) treatment. Error bars show the standard deviation of the mean.

Figure 3.3

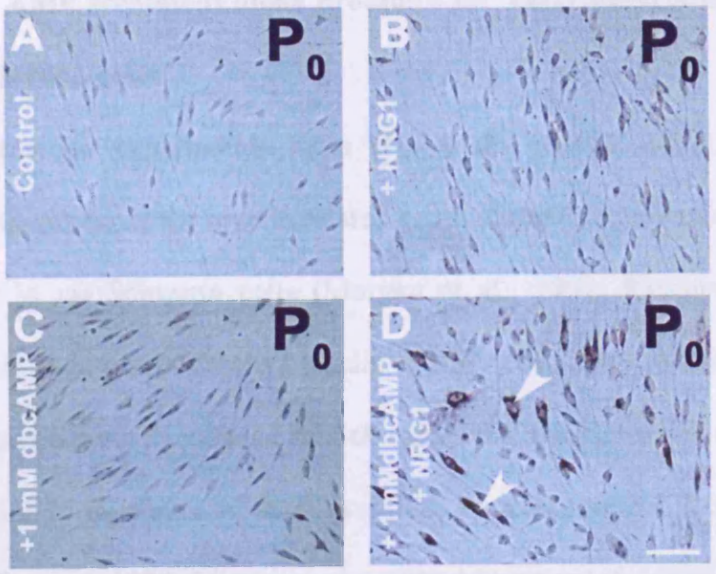
A
P0
Control
B
P0
+ NRG1
C
P0
+1 mM dbcAMP
D
P0
+1 mM dbcAMP
+ NRG1

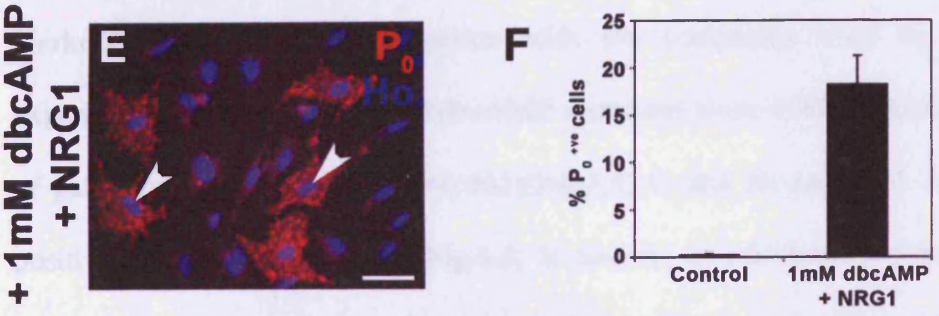
+ 1mM dbcAMP
+ NRG1
E
P0
Ho
F
% P0 +ve cells
25
20
15
10
5
0
Control
1mM dbcAMP
+ NRG1

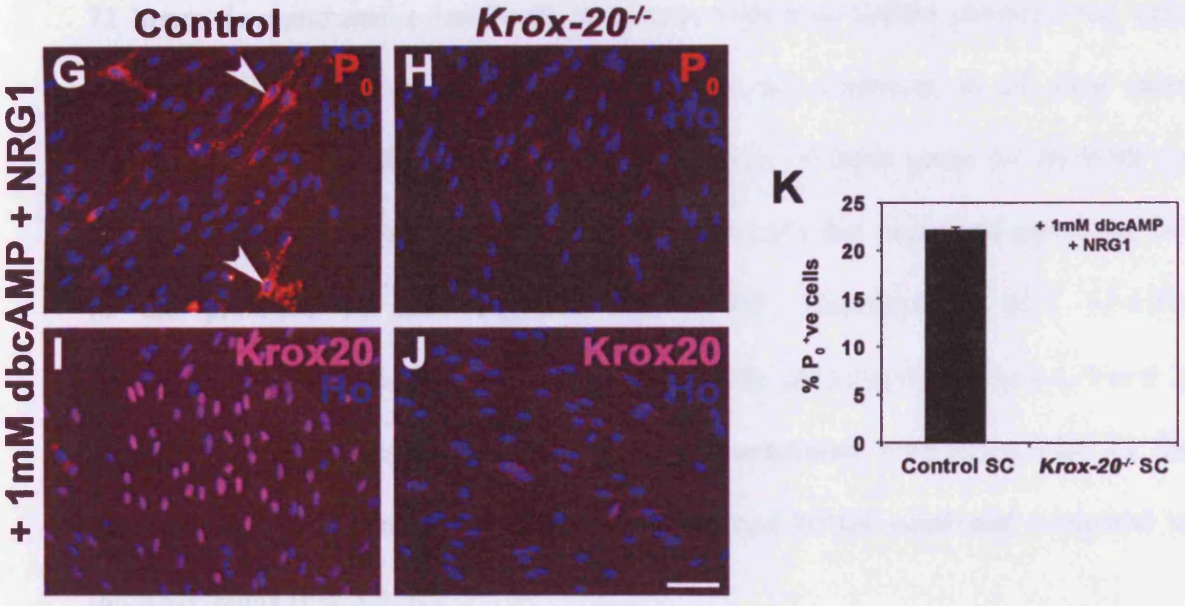
Control
Krox-20-/-
+ 1mM dbcAMP + NRG1
G
P0
Ho
H
P0
Ho
I
Krox20
Ho
J
Krox20
Ho
K
% P0 +ve cells
25
20
15
10
5
0
+ 1mM dbcAMP
+ NRG1
Control SC
Krox-20-/- SC

3.2.4 Cyclic AMP treatment alone promotes an 'early differentiated' phenotype in mouse Schwann cells.

The previous experiments have shown that cyclic AMP alone does not upregulate expression of the myelin related genes, Krox-20 and P_0, in mouse Schwann cells, unlike in rat Schwann cells (Morgan et al., 1991; Parkinson et al., 2003). However, as mentioned earlier, cyclic AMP can also induce expression of differentiation markers in cultured rat Schwann cells that appear on Schwann cells, *in vivo*, just prior to myelination, such as gal-C, 04 and periaxin (Jessen et al., 1985; Sobue and Pleasure, 1984; Mirsky et al., 1990; Morgan et al., 1991; Parkinson et al., 2003). Therefore, I tested mouse Schwann cells for the expression of these three markers after a 72 hour induction with the conditions used in the previous experiments. Interestingly, 1mM dbcAMP treatment alone could induce 24.2 +/-3.7% of gal-C positive cells (n=5)($p<0.001$)(Fig.3.4, C and E) and 54.5 +/-6.6% of 04 positive cells (n=5)($p<0.0001$)(Fig.3.4, H and J). In addition, Western blotting of protein extracts from expanded mouse Schwann cells treated with 1mM dbcAMP for 72 hours demonstrated a low level of peraxin induction unlike unstimulated cells which did not show periaxin expression (Fig.3.4, K). However, in all three cases addition of NRG1 could further boost the induction of these genes by dbcAMP in mouse Schwann cells. The percentage of Schwann cells that expressed gal-C and 04, in the presence of both dbcAMP and NRG1, increased to 65.5 +/-8.7% (n=5)($p<0.001$)(Fig.3.4, D and E) and 76.2 +/-7.9% (n=5)($p<0.01$)(Fig.3.4, I and J) respectively. Furthermore, Western blotting demonstrated a large increase in the amount of periaxin protein induced by dbcAMP and NRG1 combined compared to dbcAMP alone (Fig.3.4, K).

In addition, to investigating genes that could potentially be induced by cyclic AMP, I also tested whether cyclic AMP was sufficient to downregulate inhibitors of Schwann cell myelin differentiation, such as c-Jun and Sox-2, in mouse Schwann cells as it can in rat Schwann cells (Le et al., 2005a; Parkinson et al., 2008; see Chapter 4). Western blotting demonstrated that treatment of mouse Schwann cells with 1mM dbcAMP for 72hours was sufficient to strongly inhibit protein expression of both c-Jun and Sox-2 by cultured mouse Schwann cells (Fig.3.4, K). Furthermore, although NRG1 on its own appeared to enhance Sox-2 expression, Schwann cells maintained little c-Jun or Sox-2 expression after treatment with the combination of both dbcAMP and NRG1 (Fig.3.4, K).

Thus, cyclic AMP alone can induce expression of the early markers of Schwann cell differentiation, gal-C, 04 and periaxin on cultured mouse Schwann cells. Furthermore, cyclic AMP is sufficient to downregulate the inhibitors of myelin differentiation, c-Jun and Sox-2. However, although cyclic AMP treatment can induce early differentiation of mouse Schwann cells, it must be noted that, only when cyclic AMP is used in combination with NRG1 can high levels of gal-C, 04 and periaxin be induced on mouse Schwann cells.

Figure 3.4: Cyclic AMP can induce partial differentiation of mouse Schwann cells.

(A-D) Immunocytochemistry for gal-C on serum purified mouse Schwann cells treated with NRG1 (20ng/ml) alone, dbcAMP (1mM) alone, dbcAMP (1mM) and NRG1 (20ng/ml) or left unstimulated (Control) for 72 hours. Arrowheads demonstrate gal-C positive Schwann cells in both dbcAMP alone (C) and dbcAMP and NRG1 (D) conditions. Notice that generally Schwann cells treated with dbcAMP and NRG1 express a higher level of gal-C compared with Schwann cells treated with dbcAMP alone. Cells are co-labelled with hoescht nuclear dye (Ho). Scale bar, 50μm.

(E) Percentage of Schwann cells that express gal-C after treatment with NRG1 (20ng/ml) alone, dbcAMP (1mM) alone, dbcAMP (1mM) and NRG1 (20ng/ml) or left unstimulated (Control) for 72 hours. Error bars show the standard deviation of the mean.

(F-I) Immunocytochemistry for 04 on serum purified mouse Schwann cells treated with NRG1 (20ng/ml) alone, dbcAMP (1mM) alone, dbcAMP (1mM) and NRG1 (20ng/ml) or left unstimulated (Control) for 72 hours. Arrowheads demonstrate 04 positive Schwann cells in both dbcAMP alone (C) and dbcAMP and NRG1 (D) conditions. Cells are co-labelled with hoescht nuclear dye (Ho). Scale bar, 50μm.

(J) Percentage of Schwann cells that express 04 after treatment with NRG1 (20ng/ml) alone, dbcAMP (1mM) alone, dbcAMP (1mM) and NRG1 (20ng/ml) or left unstimulated (Control) for 72 hours. Error bars show the standard deviation of the mean.

(K) Western blot of expanded mouse Schwann cells treated with NRG1 (20ng/ml) alone, dbcAMP (1mM) alone, dbcAMP (1mM) and NRG1 (20ng/ml) or left unstimulated (Control) for 72 hours. Blots were probed with antibodies to periaxin, c-Jun and Sox-2. β-tubulin was used as a loading control. Molecular weight (MW) of proteins is illustrated in kDs.

Figure 3.4

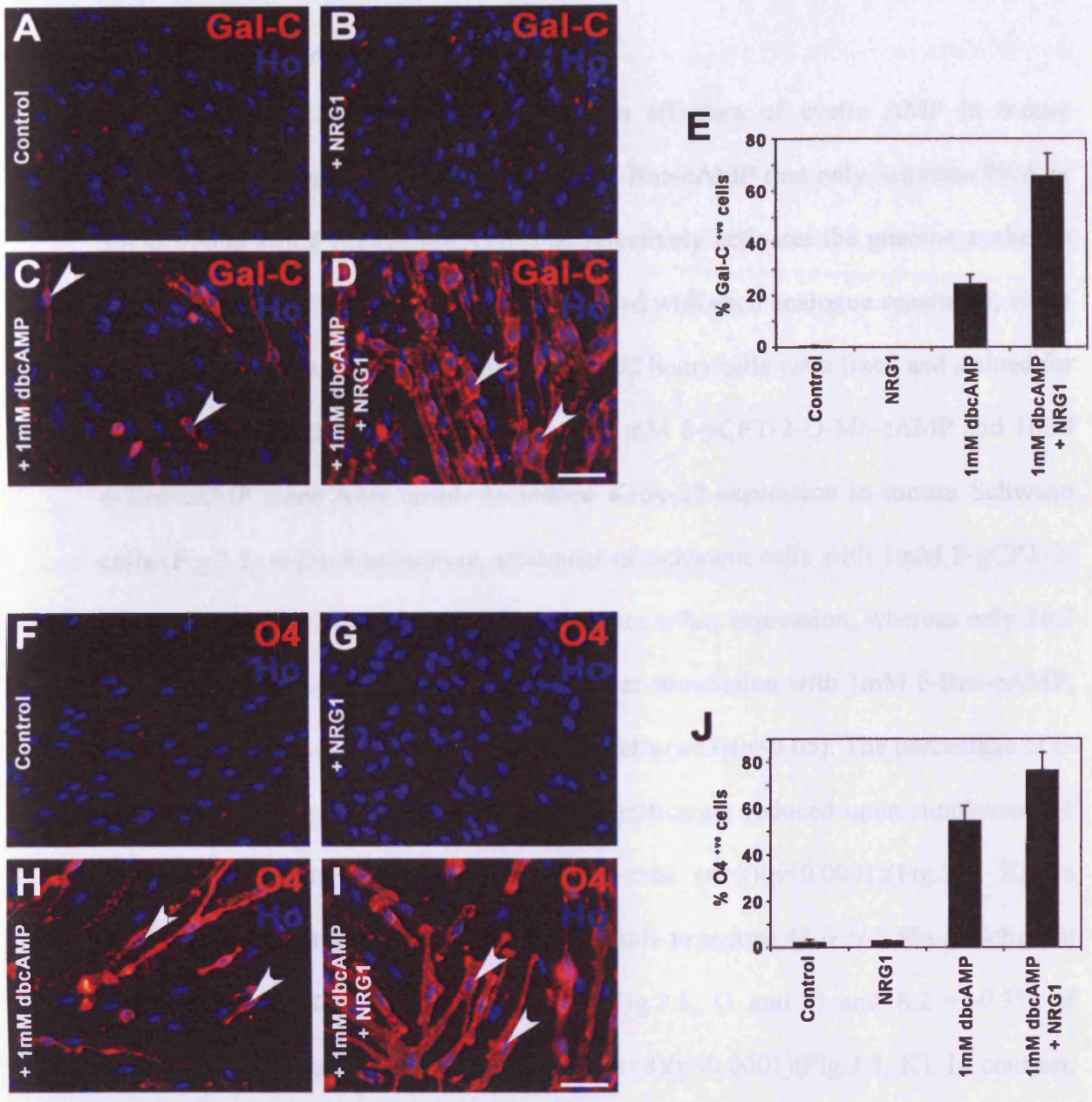
A
Gal-C
Ho
Control
B
Gal-C
Ho
+ NRG1
C
Gal-C
Ho
+ 1mM dbcAMP
D
Gal-C
Ho
+ 1mM dbcAMP
+ NRG1
E
% Gal-C +ve cells
80
60
40
20
0
Control
NRG1
1mM dbcAMP
1mM dbcAMP
+ NRG1
F
O4
Ho
Control
G
O4
Ho
+ NRG1
H
O4
Ho
+ 1mM dbcAMP
I
O4
Ho
+ 1mM dbcAMP
+ NRG1
J
% O4 +ve cells
80
60
40
20
0
Control
NRG1
1mM dbcAMP
1mM dbcAMP
+ NRG1

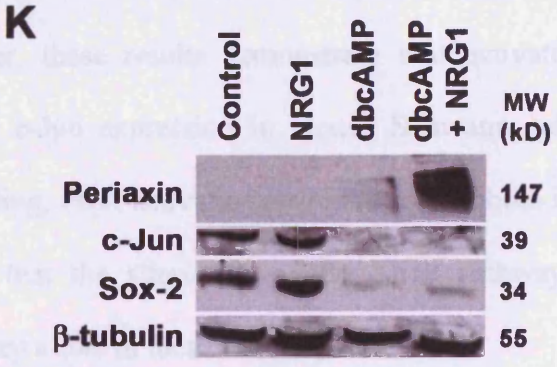
K
Control
NRG1
dbcAMP
dbcAMP
+ NRG1
MW
(kD)
Periaxin
147
c-Jun
39
Sox-2
34
β-tubulin
55

3.2.5 Activation of PKA is sufficient to replicate the effects of cyclic AMP on mouse Schwann cells.

In order to determine the downstream effectors of cyclic AMP in mouse Schwann cells I used cyclic AMP analogue 6-Bnz-cAMP that only activates PKA or the analogue 8-pCPT-2-O-Me-cAMP that selectively activates the guanine exchange factors, epac1 and 2. Schwann cells were treated with each analogue separately, either on its own or in the presence of NRG1. After 72 hours cells were fixed and stained for c-Jun, Krox-20 and P_0. Like dbcAMP, both 1mM 8-pCPT-2-O-Me-cAMP and 1mM 6-Bnz-cAMP alone were unable to induce Krox-20 expression in mouse Schwann cells (Fig.3.5, A-D). Furthermore, treatment of Schwann cells with 1mM 8-pCPT-2-O-Me-cAMP for 72 hours was unable to reduce c-Jun expression, whereas only 26.7 +/-2.7% of Schwann cells expressed c-Jun after stimulation with 1mM 6-Bnz-cAMP, compared to 97 +/-0.7% of control Schwann cells ($n=3$)($p<0.05$). The percentage of c-Jun positive Schwann cells also remained significantly reduced upon supplement of 1mM 6-Bnz-cAMP and NRG1 in combination ($n=3$)($p<0.0001$)(Fig.3.5, E). In addition, 1mM 6-Bnz-cAMP and NRG1 was able to induce 41.6 +/-2.8% of Schwann cells to express Krox-20 ($n=4$)($p<0.0001$)(Fig.3.5, G and J) and 8.2 +/-0.3% of Schwann cells to express high levels of P_0 ($n=4$)($p<0.0001$)(Fig.3.5, K). In contrast, the combination of 1mM 8-pCPT-2-O-Me-cAMP and NRG1 was unable to induce significant levels of either Krox-20 or P_0 protein (Fig.3.5, F and J).

Together, these results demonstrate that activation of PKA is sufficient to downregulate c-Jun expression in mouse Schwann cells and in combination with NRG1 signalling, PKA activation is able to induce both Krox-20 and P_0. These results also suggest that the alternative cyclic AMP pathway, utilising epac 1 and 2 is unlikely to play a role in these events.

Figure 3.5: The PKA activator, 6-Bnz-cAMP, mimics the effects of dbcAMP on cultured mouse Schwann cells.

(A-D) Immunocytochemistry for c-Jun and Krox-20 on cultured mouse Schwann cells after treatment with 1mM 8-pCPT-2-O-Me-cAMP (A and C) or 1mM 6-Bnz-cAMP (B and D) for 72 hours. Arrowheads demonstrate Schwann cells that are negative for c-Jun after treatment with 6-Bnz-cAMP. Cells are co-labelled with hoescht nuclear dye (Ho). Scale bar, 50μm.

(E) The percentage of mouse Schwann cells that express c-Jun after treatment with 1mM 8-pCPT-2-O-Me-cAMP alone, 1mM 6-Bnz-cAMP alone, 1mM 6-Bnz-cAMP and 20ng/ml NRG1 or left unstimulated (Control) for 72 hours. Error bars show the standard deviation of the mean.

(F-I) Immunocytochemistry for Krox-20 on cultured mouse Schwann cells after treatment with 1mM 8-pCPT-2-O-Me-cAMP and 20ng/ml NRG1 (F and H) or 1mM 6-Bnz-cAMP and 20ng/ml NRG1 (G and I) fro 72 hours. Arrowheads demonstrate Schwann cells that are positive for Krox-20 after treatment with 6-Bnz-cAMP and NRG1. Cells are co-labelled with hoescht nuclear dye (Ho). Scale bar, 50μm.

(J) The percentage of mouse Schwann cells that express Krox-20 after treatment with either 1mM 8-pCPT-2-O-Me-cAMP and 20ng/ml NRG1 or 1mM 6-Bnz-cAMP and 20ng/ml NRG1 for 72 hours. Error bars show the standard deviation of the mean.

(K) Immunocytochemistry for P_0 on cultured mouse Schwann cells after treatment with 1mM 6-Bnz-cAMP and 20ng/ml NRG1 for 72 hours. Arrowheads show P_0 positive Schwann cells. Cells are co-labelled with hoescht nuclear dye (Ho). Scale bar, 50μm.

Figure 3.5

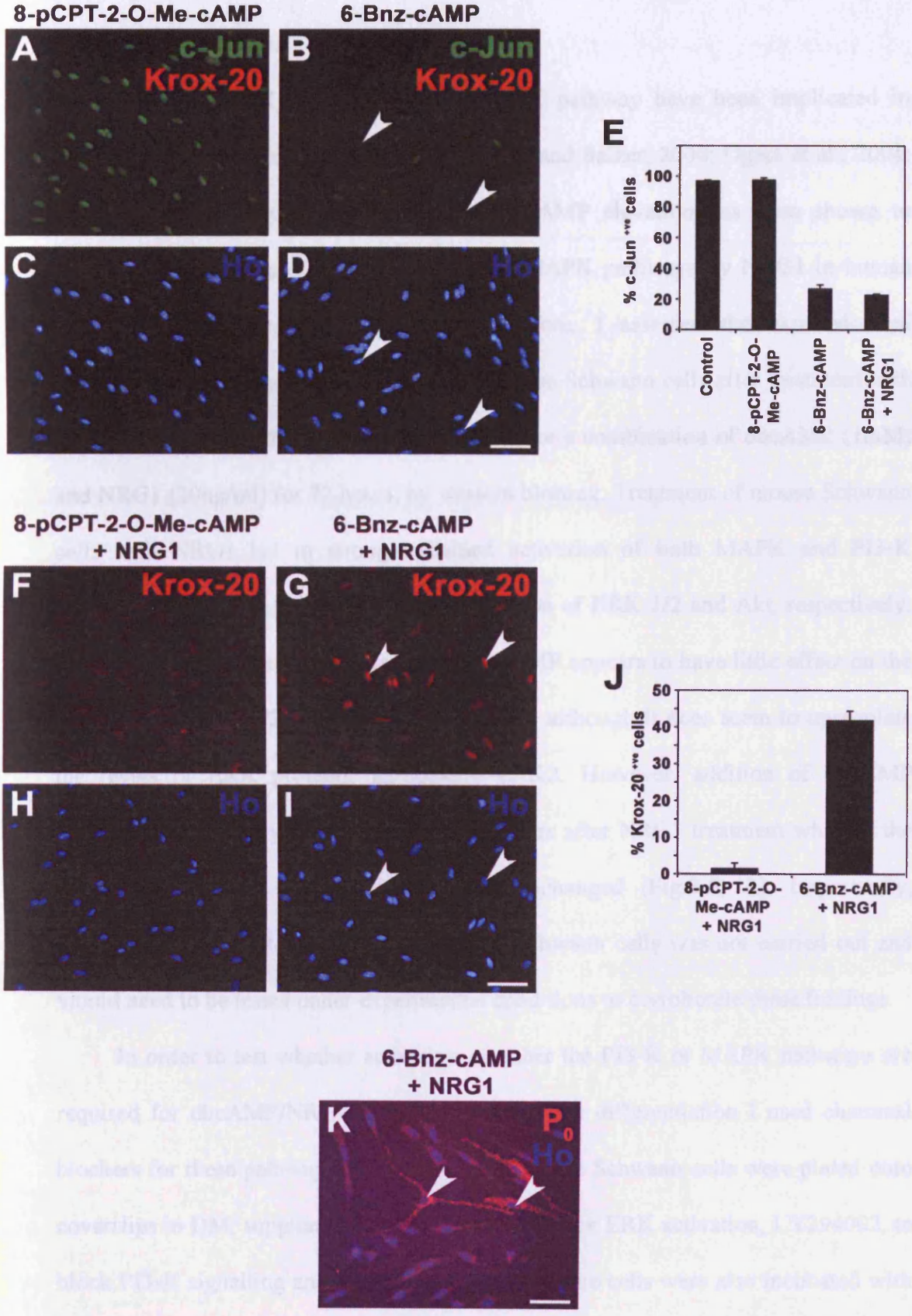
8-pCPT-2-O-Me-cAMP
6-Bnz-cAMP
A
c-Jun
Krox-20
B
c-Jun
Krox-20
C
Ho
D
Ho
E
% c-Jun +ve cells
100
80
60
40
20
0
Control
8-pCPT-2-O-Me-cAMP
6-Bnz-cAMP
6-Bnz-cAMP + NRG1
8-pCPT-2-O-Me-cAMP + NRG1
6-Bnz-cAMP + NRG1
F
Krox-20
G
Krox-20
H
Ho
I
Ho
J
% Krox-20 +ve cells
50
40
30
20
10
0
8-pCPT-2-O-Me-cAMP + NRG1
6-Bnz-cAMP + NRG1
6-Bnz-cAMP + NRG1
K
P0
Ho

3.2.6 Cyclic AMP treatment alters NRG1 activation of the MAPK pathways in mouse Schwann cells.

Both the PI3-K pathway and the MAPK pathway have been implicated in regulating Schwann cell differentiation (Maurel and Salzer, 2000; Ogata et al., 2004; Harrisingh et al., 2004). Furthermore, cyclic AMP elevation has been shown to prolong the activation of both the PI3-K and MAPK pathways by NRG1 in human Schwann cells (Monje et al., 2006). Therefore, I assessed the expression of components of these pathways in expanded mouse Schwann cells after treatment with NRG1 (20ng/ml) alone, dbcAMP (1mM) alone or a combination of dbcAMP (1mM) and NRG1 (20ng/ml) for 72 hours, by western blotting. Treatment of mouse Schwann cells with NRG1 led to strong sustained activation of both MAPK and PI3-K pathways at 72 hours, judged by phosphorylation of ERK 1/2 and Akt, respectively. In addition, at the same time point, 1mM dbcAMP appears to have little effect on the basal level of ERK1/2 and Akt phosphorylation although it does seem to upregulate the levels of ERK proteins, particularly ERK2. However, addition of dbcAMP reduces the phosphorylation of ERK1/2, 72 hours after NRG1 treatment whereas the phosphorylation of Akt seems to remain unchanged (Fig.3.6, A). Importantly, measurement of the levels of Akt protein in Schwann cells was not carried out and would need to be tested under experimental conditions to corroborate these findings.

In order to test whether activation of either the PI3-K or MAPK pathways are required for dbcAMP/NRG1 induced Schwann cell differentiation I used chemical blockers for these pathways. Briefly, cultured mouse Schwann cells were plated onto coverslips in DM, supplemented with U0126, to block ERK activation, LY294002, to block PI3-K signalling and DMSO as a control. Some cells were also incubated with the PKA inhibtor, H89 as well. After 1hour incubation with their respective inhibitors,

cells were pulsed with a combination of dbcAMP (1mM) and NRG1 (20ng/ml) for 48 hours before being fixed and assayed for Krox-20 expression by immunocytochemistry. Blocking ERK1/2 phosphorylation, using the U0126 inhibitor completely abolished Krox-20 induction by dbcAMP/NRG1 ($n=3$)($p<0.001$). Surprisingly, blocking the PI3-kinase pathway, using the LY294002 blocker, led to a 2.3 fold increase in the percentage of Krox-20 positive Schwann cells induced by dbcAMP/NRG1 compared to the DMSO control ($n=3$)($p<0.05$). Predictably, blocking PKA activation, using the H89 inhibitor, led to a 7.1 fold reduction in Krox-20 expression by mouse Schwann cells in response to dbcAMP/NRG1 compared to the DMSO control ($n=3$)($p<0.01$)(Fig.3.6, B).

Together, these results demonstrate that cyclic AMP can reduce NRG1 activation of the MAP kinase pathway but not the P13-kinase pathway, yet this reduced MAP kinase activation is still necessary for Krox-20 induction. Furthermore, PI3-kinase signalling appears to antagonize Krox-20 induction in cultured mouse Schwann cells.

Figure 3.6: MAPK signalling by cyclic AMP and NRG1 in mouse Schwann cells.

(A) Western blot of expanded mouse Schwann cells treated with NRG1 (20ng/ml), dbcAMP (1mM), dbcAMP (1mM) and NRG1 (20ng/ml) or left unstimulated (Control) for 72 hours. Blots were probed with antibodies to phosphorylated ERK1/2 (ERK1, 44kD and ERK2, 42kD), native ERK1/2 and phosphorylated Akt (Thr308). GAPDH was used as a loading control. Molecular weight (MW) of proteins is illustrated in kDs.

(B) Percentage of Krox-20 positive Schwann induced by a 48 hour treatment of dbcAMP (1mM) and NRG1 (20ng/ml) in the presence of U0126 (20μM), LY294002 (10μM) and H89 (1μM). Supplement of DM with DMSO was used as a control. Error bars show the standard deviation of the mean.

Figure 3.6

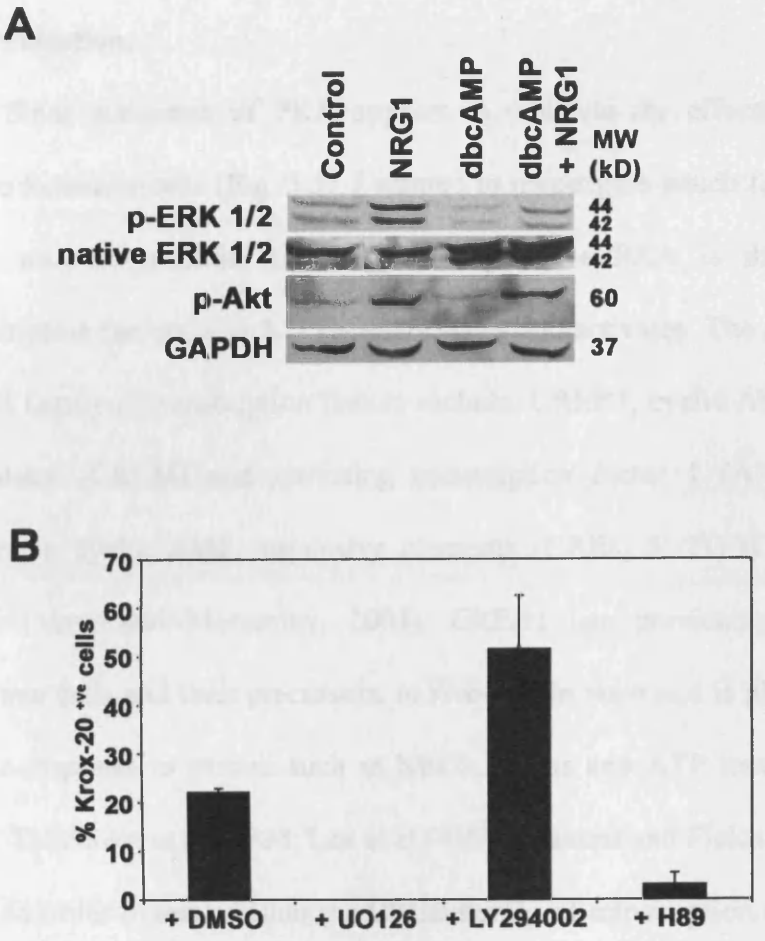
A
Control
NRG1
dbcAMP
dbcAMP + NRG1
MW (kD)
p-ERK 1/2
native ERK 1/2
p-Akt
GAPDH
44
42
44
42
60
37
B
% Krox-20 +ve cells
70
60
50
40
30
20
10
0
+ DMSO
+ UO126
+ LY294002
+ H89

3.2.7 The cyclic AMP response element binding protein (CREB) family of transcription factors are required for cyclic AMP/NRG1 induced Schwann cell differentiation.

Since activation of PKA appears to replicate the effects of cyclic AMP on mouse Schwann cells (Fig. 3.5), I wanted to investigate which factors downstream of PKA were responsible. One set of targets for PKA is the CREB family of transcription factors, which it phosphorylates and activates. The main members of the CREB family of transcription factors include, CREB1, cyclic AMP response element modulator (CREM) and activating transcription factor 1 (ATF1), which bind as dimers to cyclic AMP responsive elements (CREs, 5'-TGACGTCA-3') in target genes (Mayr and Montminy, 2001). CREB1 has previously been identified in Schwann cells and their precursors, *in vivo* and *in vitro* and is phosphorylated at Ser-133 in response to stimuli such as NRG1, axons and ATP treament (Stewart et al., 1995; Tabernero et al., 1998; Lee et al., 1999; Stevens and Fields, 2000).

In order to test whether the CREB family of transcription factors were required for cyclic AMP/NRG1 induced Schwann cell differentiation I used adenoviruses expressing a dominant negative form of CREB, A-CREB and GFP (Ahn et al., 1998)(see section 2.3.4 for method of inhibition), and a control virus expressing only GFP (CMV control)(Warburton et al., 2005). Serum purified mouse Schwann cells were plated and infected with either A-CREB or CMV control viruses in DM, 0.5% HS and 2μM forskolin for 48 hours (see legend to Fig. 3.7, A). During this time the medium was replaced with the same medium after 24 hours. Schwann cells were then pulsed with a combination of dbcAMP (1mM) and NRG1 (20ng/ml) for a further 48 hours before cells were fixed and stained for a number of differentiation markers by immunocytochemistry. Expression of A-CREB in mouse Schwann cells significantly

inhibited dbAMP/NRG1 induced P_0, with 3.2 +/-2.3% P_0 positive cells compared to 19.5 +/-1.3% P_0 positive for CMV control infected cells (n=3)($p<0.05$)(Fig.3.7, A). In addition, A-CREB strongly reduced periaxin induction by dbAMP/NRG1, with only 34.1 +/-8.8% of periaxin positive cells compared to 81.9 +/-7.6% of positive cells infected with the CMV control virus (n=4)($p<0.001$)(Fig.3.7, B-F). Thus, the CREB family of transcription factors are required for dbcAMP/NRG1 induced myelin-related gene expression.

To test whether CREB is required for the initiation of the myelin differentiation program, I assayed cultured mouse Schwann cells for the expression of Krox-20 after dbcAMP/NRG1 treatment in the presence of A-CREB or CMV control adenoviruses. Krox-20 expression was strongly inhibited by the presence of A-CREB compared to CMV control infected cells, with 3.6 +/-0.6% compared to 55.7 +/-5.3% of Krox-20 positive cells in their respective conditions (n=4)($p<0.001$)(Fig.3.8, A-E). Similarly, the A-CREB adenovirus strongly inhibited β-gal expression by 9.3 fold in *Krox-20*$^{-/-}$ Schwann cells induced by dbcAMP/NRG1, 4.1 +/-1.4% versus 38 +/-7.1% for A-CREB and CMV control infected cells respectively (n=4)($P<0.01$)(Fig.3.8, F-J). Thus, the CREB family of transcription factors is required, at least at the level of Krox-20 induction, during dbcAMP/NRG1 induced myelin differentiation.

Figure 3.7: The CREB family of transcription factors is required for P_0 and periaxin induction by cyclic AMP/NRG1.

(A) The percentage of CMV control and A-CREB adenovirally infected Schwann cells expressing P_0 after a 48 hour induction by dbcAMP (1mM) and NRG1 (20ng/ml), preceded by a 48 hour pre-treatment by 2μM forskolin. Modest pre-treatment with a cyclic AMP elevating agent prior to cyclic AMP/NRG1 treatment was found to increase the number of myelin differentiating Schwann cells compared to induction by cyclic AMP/NRG1 without any pre-treatment (see section 3.3.3). Error bars show the standard deviation of the mean.

(B-E) Cultured mouse Schwann cells immunolabelled for periaxin after infection with CMV control (B and D) and A-CREB (C and E) adenoviruses and treatment with 2μM forskolin for 48 hours and then dbcAMP (1mM) and NRG1 (20ng/ml) for a further 48hours. Arrows show CMV control infected Schwann cells that are positive for GFP and periaxin. Arrowheads demonstrate A-CREB infected Schwann cells that are GFP positive but periaxin negative. Cells are co-labelled with hoescht nuclear dye (Ho). Scale bar, 50μm.

(F) The percentage of CMV control and A-CREB adenovirally infected Schwann cells expressing P_0 after treatment with 2μM forskolin for 48 hours and then dbcAMP (1mM) and NRG1 (20ng/ml) for a further 48hours. Error bars show the standard deviation of the mean.

Figure 3.7

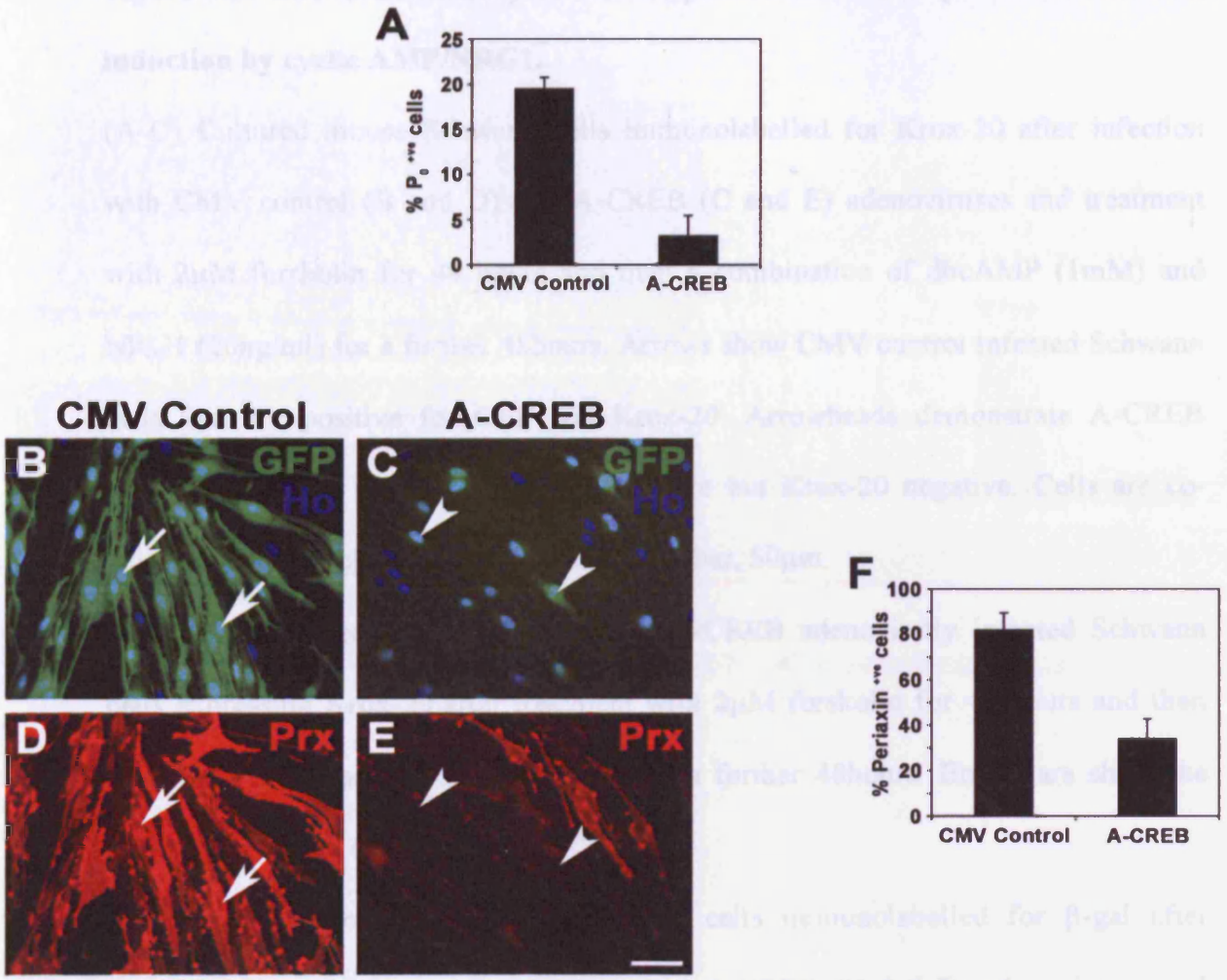
A
% P0 +ve cells
25
20
15
10
5
0
CMV Control
A-CREB
CMV Control
A-CREB
B
GFP
Ho
C
GFP
Ho
D
Prx
E
Prx
F
% Periaxin +ve cells
100
80
60
40
20
0
CMV Control
A-CREB

Figure 3.8: The CREB family of transcription factors is required for Krox-20 induction by cyclic AMP/NRG1.

(A-D) Cultured mouse Schwann cells immunolabelled for Krox-20 after infection with CMV control (B and D) and A-CREB (C and E) adenoviruses and treatment with 2μM forskolin for 48 hours and then a combination of dbcAMP (1mM) and NRG1 (20ng/ml) for a further 48hours. Arrows show CMV control infected Schwann cells that are positive for GFP and Krox-20. Arrowheads demonstrate A-CREB infected Schwann cells that are GFP positive but Krox-20 negative. Cells are co-labelled with hoescht nuclear dye (Ho). Scale bar, 50μm.

(E) The percentage of CMV control and A-CREB adenovirally infected Schwann cells expressing Krox-20 after treatment with 2μM forskolin for 48 hours and then dbcAMP (1mM) and NRG1 (20ng/ml) for a further 48hours. Error bars show the standard deviation of the mean.

(F-I) Cultured mouse *Krox-20*$^{-/-}$ Schwann cells immunolabelled for β-gal after infection with CMV control (B and D) and A-CREB (C and E) adenoviruses and treatment with 2μM forskolin for 48 hours and then dbcAMP (1mM) and NRG1 (20ng/ml) for a further 48hours. Arrows show CMV control infected Schwann cells that are positive for GFP and β-gal. Arrowheads demonstrate A-CREB infected Schwann cells that are GFP positive but β-gal negative. Cells are co-labelled with hoescht nuclear dye (Ho). Scale bar, 50μm.

(J) The percentage of CMV control and A-CREB adenovirally infected *Krox-20*$^{-/-}$ Schwann cells expressing β-gal after treatment with 2μM forskolin for 48 hours and then dbcAMP (1mM) and NRG1 (20ng/ml) for a further 48hours. Error bars show the standard deviation of the mean.

Figure 3.8

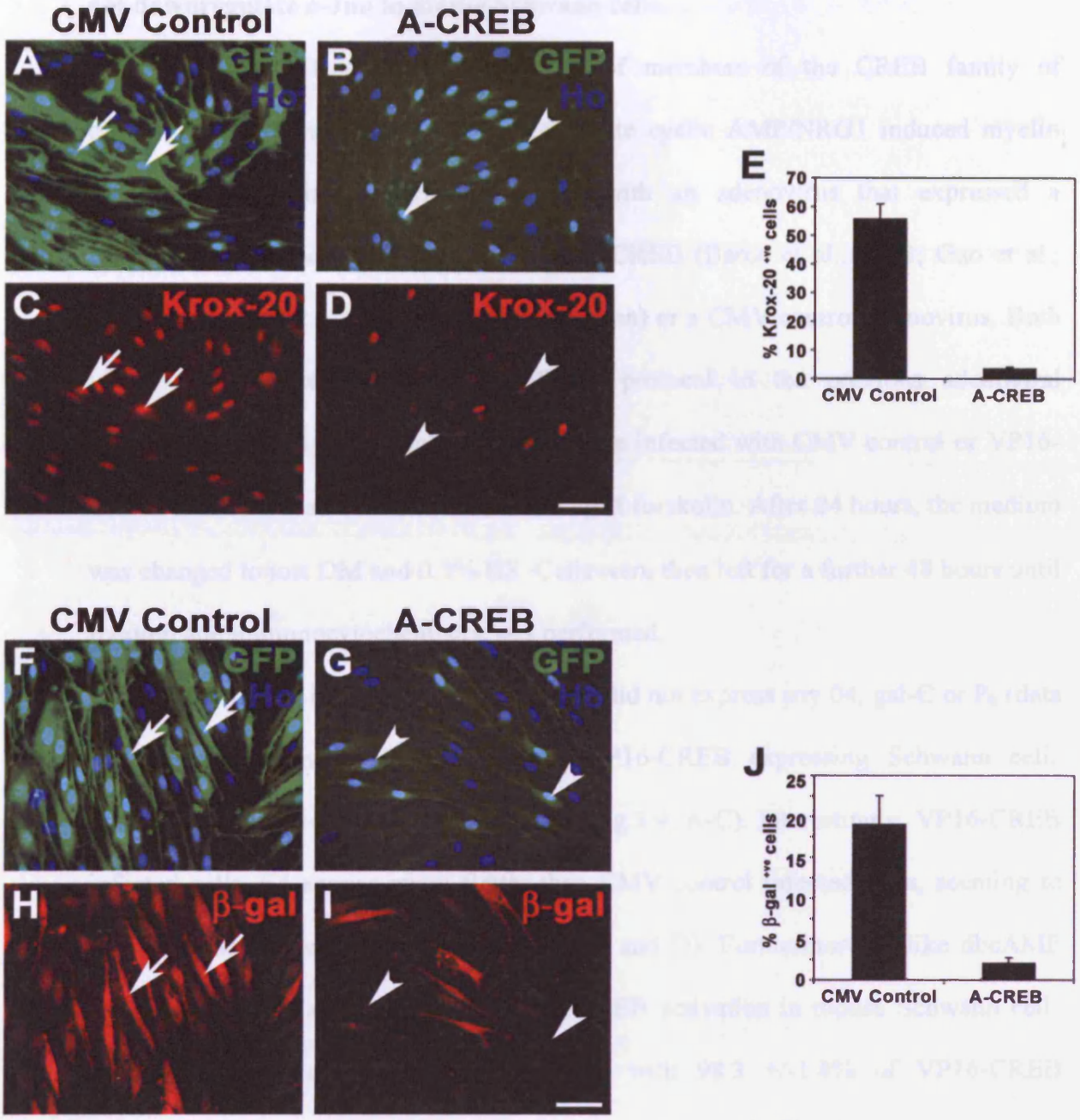
CMV Control
A-CREB
A
GFP
B
GFP
C
Krox-20
D
Krox-20
E
% Krox-20 +ve cells
70
60
50
40
30
20
10
0
CMV Control
A-CREB
CMV Control
A-CREB
F
GFP
G
GFP
H
β-gal
I
β-gal
J
% β-gal +ve cells
25
20
15
10
5
0
CMV Control
A-CREB

3.2.8 Constitutive activation of a CREB-like molecule induces periaxin but does not downregulate c-Jun in mouse Schwann cells.

In order to test whether activation of members of the CREB family of transcription factors was sufficient to replicate cyclic AMP/NRG1 induced myelin differentiation, I infected Schwann cells with an adenovirus that expressed a constitutively active CREB molecule, VP16-CREB (Barco et al., 2002; Gao et al., 2004)(see section 2.3.4 for mechanism of action) or a CMV control adenovirus. Both viruses co-expressed GFP. In a different protocol to the previous adenoviral infections, cultured mouse Schwann cells were infected with CMV control or VP16-CREB adenoviruses in DM, 0.5% HS and 2μM forskolin. After 24 hours, the medium was changed to just DM and 0.5% HS. Cells were then left for a further 48 hours until fixation and immunocytochemistry was performed.

VP16-CREB expressing Schwann cells did not express any 04, gal-C or P_0 (data not shown) however, 30.9 +/-4.5% of VP16-CREB expressing Schwann cells upregulated periaxin protein (n=4)($p<0.01$)(Fig.3.9, A-C). Interestingly, VP16-CREB infected cells did appear much flatter than CMV control infected cells, seeming to possess many more lamellipodia (Fig.3.9, A and D). Furthermore, unlike dbcAMP treatment or PKA activation, constitutive CREB activation in mouse Schwann cells failed to reduce c-Jun protein expression, with 98.3 +/-1.4% of VP16-CREB expressing Schwann cells also positive for c-Jun (Fig.3.9, D-G).

I postulated that the reason VP16-CREB expressing Schwann cells did not express the majority of myelin differentiation markers was due to the inability to downregulate inhibitors of myelin gene activation, such as c-Jun (Parkinson et al., 2008; Chapter 4). To test this, I used *c-Jun* null Schwann cells in which *c-Jun* was deleted by infecting $c\text{-}Jun^{f/f}$ Schwann cells with an adenovirus expressing cre

recombinase (see Chapter 4). I then infected control (*c-Jun*$^{f/f}$) or *c-Jun* null Schwann cells with adenoviral VP16-CREB, using the same protocol as described above. Deletion of *c-Jun* lead to a 1.9 fold increase in the percentage of periaxin positive VP16-CREB expressing Schwann cells, to 53.7 +/-8.6% compared to 28 +/-8.2% of CMV control infected Schwann cells (n=4)($p<0.05$)(Fig.3.9, H-J). However, even in the absence of *c-Jun*, VP16-CREB was still unable to induce P_0 expression in mouse Schwann cells.

Thus, these results demonstrate that CREB activation is sufficient to induce periaxin expression in mouse Schwann cells and that the transcription factor, c-Jun antagonizes VP16-CREB induced periaxin expression. However VP16-CREB expression is not sufficient to induce expression of other myelin differentiation markers, like P_0.

Figure 3.9: Constitutively active CREB can induce periaxin expression in mouse Schwann cells.

(A and B) Cultured mouse Schwann cells immunolabelled for periaxin after infection with VP16-CREB adenovirus for 72 hours in DM and 0.5% HS (Cells were incubated with 2μM forskolin for only the first 24 hours). Arrows show VP16-CREB infected Schwann cells positive for both GFP and periaxin. Cells are co-labelled with hoescht nuclear dye (Ho). Scale bar, 50μm.

(C) The percentage of CMV control and VP16-CREB adenovirally infected Schwann cells expressing periaxin after 72 hour infection. Error bars show the standard deviation of the mean.

(D-G) Cultured mouse Schwann cells immunolabelled for c-Jun after infection with either CMV control or VP16-CREB adenovirus, for 72 hours in DM and 0.5% HS (Cells were incubated with 2μM forskolin for only the first 24 hours). Arrowheads show CMV control or VP16-CREB infected Schwann cells that are positive for GFP and c-Jun. Cells are co-labelled with hoescht nuclear dye (Ho). Scale bar, 50μm.

(H-I) *c-Jun* null Schwann cells immunolabelled for periaxin after infection with VP16-CREB adenovirus for 72 hours in DM and 0.5%HS (Cells were incubated with 2μM forskolin for only the first 24 hours). Arrows show VP16-CREB infected *c-Jun* null Schwann cells that are positive for GFP and periaxin. Cells are co-labelled with hoescht nuclear dye (Ho). Scale bar, 50μm.

(J) The percentage of control Schwan cells (Control SC, $c\text{-}Jun^{f/f}$) or *c-Jun* null Schwann cells (*c-Jun* null SC) infected with VP16-CREB adenovirus that express periaixn after 72 hour infection. Error bars show the standard deviation of the mean.

Figure 3.9

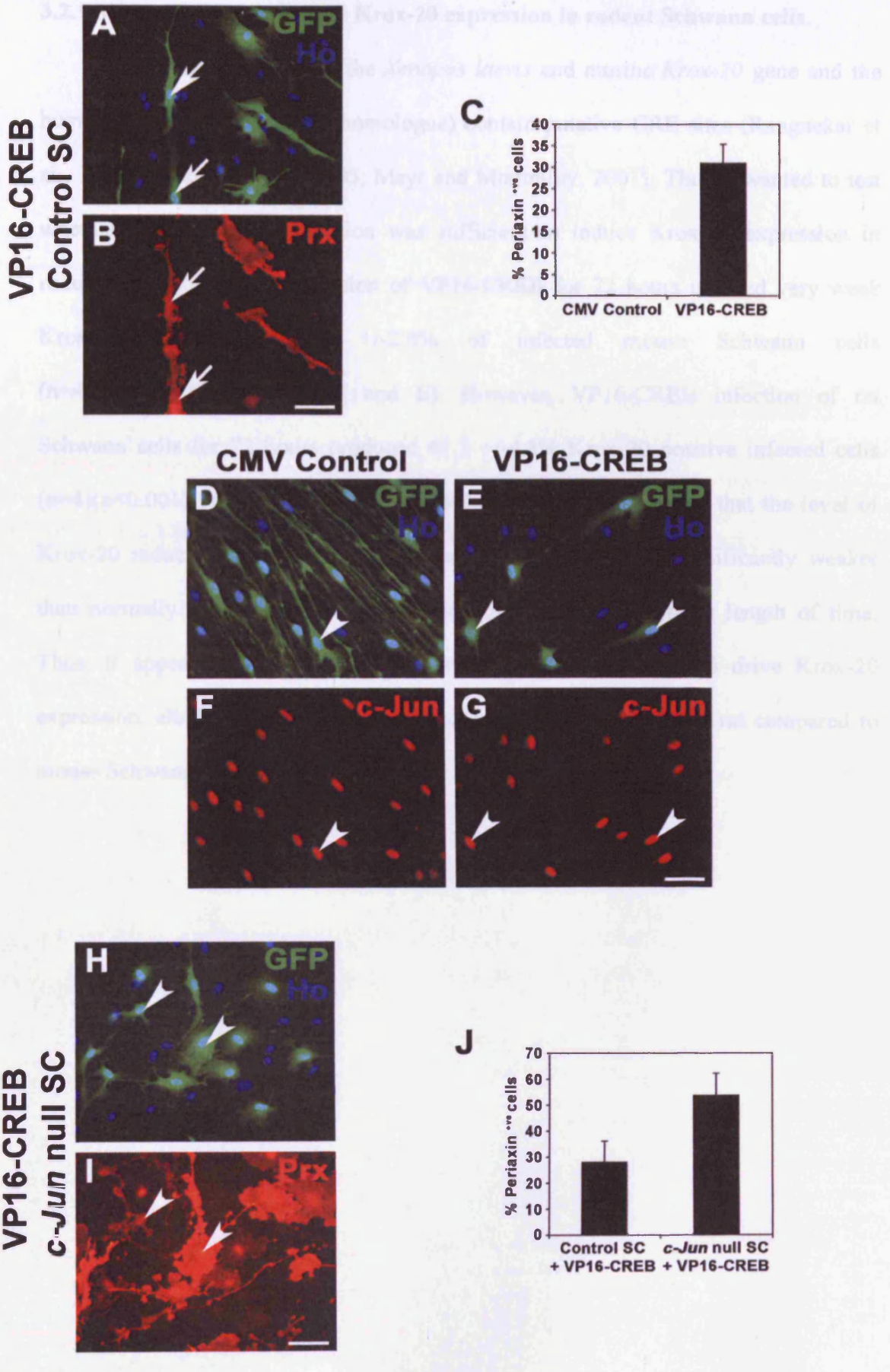
VP16-CREB
Control SC
A
GFP
Ho
B
Prx
C
% Periaxin +ve cells
CMV Control
VP16-CREB
D
E
F
c-Jun
G
VP16-CREB
c-Jun null SC
H
I
J
Control SC
+ VP16-CREB
c-Jun null SC
+ VP16-CREB

3.2.9 VP16-CREB can induce Krox-20 expression in rodent Schwann cells.

The promoter region of the *Xenopus laevis* and murine *Krox-20* gene and the human *EGR2* gene (*Krox-20* homologue) contain putative CRE sites (Rangnekar et al., 1990; Watanabe et al., 2005; Mayr and Montminy, 2001). Thus, I wanted to test whether VP16-CREB expression was sufficient to induce Krox-20 expression in rodent Schwann cells. Expression of VP16-CREB for 72 hours induced very weak Krox-20 protein in 7.1 +/-2.4% of infected mouse Schwann cells ($n=4$)($p<0.05$)(Fig.3.10, A, C and E). However, VP16-CREB infection of rat Schwann cells for 72 hours produced 61.3 +/-4.8% Krox-20 positive infected cells ($n=4$)($p<0.001$)(Fig.3.10, B, D and E). Although, it must be noted that the level of Krox-20 induction by VP16-CREB in rat Schwann cells was significantly weaker than normally achieved by 1mM dbcAMP treatment for the same length of time. Thus, it appears that constitutively active CREB is sufficient to drive Krox-20 expression, albeit at a low level and significantly more strongly in rat compared to mouse Schwann cells.

Figure 3.10: Constitutively active CREB can induce expression of Krox-20 in rodent Schwann cells.

(A-D) Cultured mouse (mouse SC, A and C) and rat (rat SC, B and D) Schwann cells immunolabelled for Krox-20 after infection with VP16-CREB for 72 hours. Arrows demonstrate Schwann cells infected with VP16-CREB that are positive for GFP and Krox-20. Importantly, photos for Krox-20 immunostaining in mouse and rat Schwann cells were taken at the same exposure. Notice the much stronger expression of Krox-20 in rat Schwann cells compared to mouse. Cells are co-labelled with hoescht nuclear dye (Ho). Scale bar, 50μm.

(E) Percentage of mouse (mouse SC) and rat Schwann cells (rat SC) infected with either CMV control or VP16-CREB adenoviruses that express Krox-20 protein. Error bars show the standard deviation of the mean.

Figure 3.10

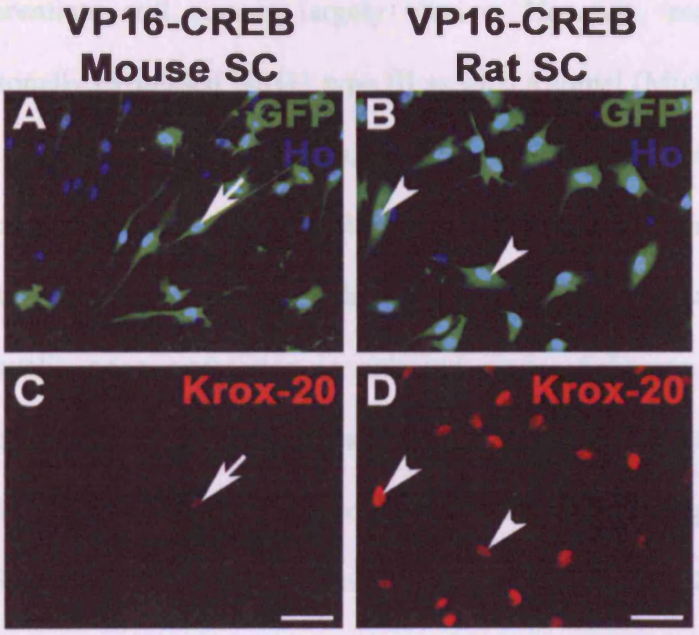
VP16-CREB
Mouse SC
VP16-CREB
Rat SC
A
GFP
B
GFP
C
Krox-20
D
Krox-20

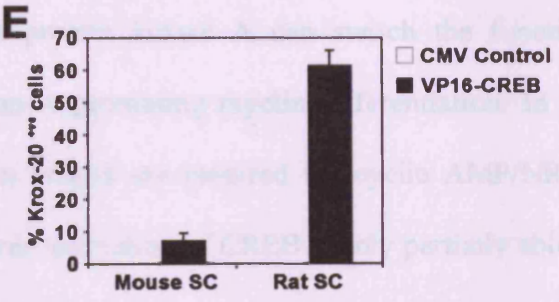
E
% Krox-20 +ve cells
70
60
50
40
30
20
10
0
Mouse SC
Rat SC
CMV Control
VP16-CREB

3.3 DISCUSSION

The identities of the signals from the axon that potentially instruct a Schwann cell to differentiate still remain largely elusive. However, recent studies have implicated axonally expressed NRG1 type III as such a signal (Michailov et al., 2004; Taveggia et al., 2005). Nevertheless, the mechanism by which NRG1 might potentially activate myelin gene expression in Schwann cells is unknown.

In this study, I have shown that NRG1 alone is incapable of activating significant myelin gene expression in cultured mouse Schwann cells, confirming previous reports using rat Schwann cells (Taveggia et al., 2005). Furthermore, I have demonstrated that cyclic AMP, long known to promote myelin gene expression in cultured rat Schwann cells (Morgan et al., 1991; Parkinson et al., 2003), is incapable of performing this function in cultured mouse Schwann cells. Thus, using cultured mouse Schwann cells as an experimental model, my experiments identify that cyclic AMP, acting through protein kinase A can switch the function of NRG1 from promoting proliferation to promoting myelin differentiation. In addition, the CREB family of transcription factors are required for cyclic AMP/NRG1 induced myelin differentiation. However, activation of CREB is only partially able to induce Schwann cell differentiation, suggesting cooperation with other factors.

3.3.1 Cyclic AMP signalling and Schwann cell proliferation.

My findings clearly show that a relatively low concentration of dbcAMP (100μM) can augment NRG1 induced Schwann cell proliferation in cultured mouse Schwann cells. This confirms similar findings in human and rat Schwann cells (Levi et al., 1995; Rahmatullah et al., 1998; Monje et al., 2006; Iacovelli et al., 2007). Furthermore, as mentioned earlier, in rat Schwann cells most growth factors, such as

PDGF, actually require cyclic AMP elevating agents to promote proliferation (Chen et al., 1991; Stewart et al., 1991), however this may not necessarily be the same for mouse Schwann cells (Stevens et al., 2004). Further work on rat Schwann cells demonstrated that cyclic AMP elevation induced cyclin D1 expression which was required for growth factor induced cell cycle progression past G_1 (Kim et al., 2001). In addition, modest cyclic AMP elevation was shown to prolong NRG1 activation of MAPK and PI3-K pathways and blocking both pathways inhibited proliferation (Monje et al., 2006). Interestingly, a target of active ERK1/2, S6-Kinase, was shown to be strongly phosphorylated in response to low but not high concentrations of cyclic AMP analogues in rat Schwann cells (Mutoh et al., 1998).

The direct downstream effector of cyclic AMP effects on Schwann cell proliferation is likely to be PKA, however, there are conflicting reports of whether PKA is involved in Schwann cell axon induced proliferation (Kim et al., 1997; Howe and McCarthy, 2000). Indirect evidence for a role for PKA in Schwann cell proliferation comes from the study of an autosomal dominant neoplasia syndrome called Carney complex. Here, loss-of-function mutations in the *PRKAR1A* gene (PKA type 1A regulatory subunit) lead to excessive PKA signalling and development of schwannomas in both humans and mice (Kirschner et al., 2000; Stratakis et al., 2001; Kirschner et al., 2005).

3.3.2 Cyclic AMP signalling and Schwann cell differentiation.

The fact that cyclic AMP signalling can promote myelin differentiation in both cultured rat and mouse Schwann cells, suggests that cyclic AMP or components of the cyclic AMP pathway could be important for Schwann cell myelination, *in vivo*. However, studies have shown that cyclic AMP levels from whole nerve extracts do

not correlate well with remyelination after sciatic nerve crush (Poduslo et al., 1995). However this does not preclude localised subcellular elevations in cyclic AMP being important for Schwann cell differentiation (Tasken and Aandahl, 2004). There is stronger evidence for a role for PKA in Schwann cell differentiation, since activation of PKA is highest in the sciatic nerve just after birth, when myelination begins and blocking PKA inhibits myelination in Schwann cell/DRG cocultures (Howe and McCarthy, 2000; Yoon et al., 2008). PKA phosphorylation of the p65 subunit of the transcription factor Nuclear Factor-κB (NF-κB) is required for cyclic AMP induced rat Schwann cell differentiation and also myelination in Schwann cell/DRG cocultures (Yoon et al., 2008). In both experimental models NF-κB activation was necessary for induction of the transcription factor Oct-6 (Nickols et al., 2003; Yoon et al., 2008).

In my experiments, activation of PKA, using a PKA specific cyclic AMP analogue, appeared to replicate the effects of cyclic AMP, with and without the presence of NRG1, on mouse Schwann cells. However, downstream of PKA, activation of the CREB family of transcription factors was required but not sufficient to induce mouse Schwann cell differentiation. In other experiments, I also found VP16-CREB unable to induce Oct-6 expression in mouse Schwann cells (P.Arthur-Farraj, data not shown), despite putative CRE sites being present in the Oct-6 Schwann cell specific enhancer (Mandemakers et al., 2000). In contrast, constitutively active p65 can actually induce Oct-6 in rat Schwann cells. Thus, NF-κB activation is likely to be another component of PKA induced Schwann cell differentiation, in addition to CREB.

3.3.3 NRG1 and Schwann cell differentiation.

The fact that NRG1 alone cannot promote differentiation in cultured Schwann cells has prompted many researchers to look for mechanisms by which NRG1 signalling may be modulated (Nave and Salzer, 2006). One possibility is that the different isoforms of NRG1 may have different functions in Schwann cells. To support this, overexpression of NRG1 type III on axons leads to PNS hypermyelination whereas overexpression of NRG1 type I does not (Michailov et al., 2004). There is also evidence that NRG1 may be developmentally processed or cleaved by enzymes such as the endopeptidase, Bace1, which could alter its signalling (Michailov et al., 2004; Willem et al., 2006; Hu et al., 2008). However, results in this study suggest that alteration in the levels of cyclic AMP signalling is sufficient to switch NRG1 into driving myelin differentiation in mouse Schwann cells. Furthermore, in all the experiments in this study, the EGF domain from NRG1, which is common between all 3 NRG1 isoforms, was used to induce mouse Schwann cells. This suggests that the particular type of NRG1 isoform expressed may not be the most important factor in determining the outcome of NRG1 signalling. In other experiments in mouse Schwann cells, it was shown that constant cyclic AMP signalling was required at the same time as NRG1 signalling in order to induce myelin differentiation. In addition, pre-treatment of Schwann cells with as little as 2μM forskolin or 100μM dbcAMP for 48 hours prior to high dbcAMP (1mM) and NRG1 treatment boosts the number of differentiating cells compared to cells that were not primed with cyclic AMP or cells that were primed with NRG1 (K. Wanek and P. Arthur-Farraj, data not shown). Thus cyclic AMP appears to be able to modulate the cellular environment in mouse Schwann cells in order to allow NRG1 to promote differentiation. An example of this is the fact cyclic AMP alone can downregulate the

expression of two known inhibitors of myelin differentiation, c-Jun and Sox-2 (Le et al., 2005a; Parkinson et al., 2008; Chapter 4).

Whether and potentially how cyclic AMP signalling is activated in Schwann cells in development remains to be tested, though it could possibly be through signals derived from either the axon or the extracellular matrix. Signals other than NRG1 that have been identified to play a role in Schwann cell differentiation include BDNF signalling through the $p75^{NTR}$ receptor, Lgi4, laminin and integrin signalling, the Rho GTPases, Rac1 and cdc42 and action potential activity dependent signals such as ATP and adenosine (Stevens and Fields, 2000; Chan et al., 2001; Cosgaya et al., 2002; Feltri et al., 2002; Chen and Strickland, 2003; Yu et al., 2005; Bermingham et al., 2006; Stevens, 2006; Nodari et al., 2007; Benninger et al., 2007; see section 1.5). Of the list above, adenosine is particularly interesting since it has been shown to activate cyclic AMP linked $A2_A$ receptors on Schwann cells and increase intracellular cyclic AMP to a similar level as 20μM forskolin treatment (which has similar effects as 1mM dbcAMP) in cultured mouse Schwann cells (Stevens et al., 2004). It will be interesting to test whether adenosine can cooperate with NRG1 signalling in mouse Schwann cells to regulate differentiation.

3.3.4 Cyclic AMP modulation of NRG1 signalling in Schwann cells.

Cyclic AMP demonstrates concentration dependent effects in response to serum or NRG1 in both rat and mouse Schwann cells. Low cyclic AMP concentrations promote proliferation whereas higher concentrations promote differentiation (Sobue et al., 1986; Mutoh et al., 1998; Fig. 3.1 A and B; P. Arthur-Farraj, K.Wanek and D.B. Parkinson, data not shown). One study demonstrated that low concentrations of cyclic AMP promoted strong but transient phosphorylation of ERK1/2 pathway whereas

concentrations 10 fold higher produced a lower but sustained activation of ERK1/2 in rat Schwann cells (Mutoh et al., 1998). This idea of transient versus sustained ERK1/2 activation is known to regulate proliferation and differentiation, respectively in other cell types (Marshall et al., 1995). Certainly, my finding that high concentrations of dbcAMP actually reduce NRG1 induced phosphorylation of ERK1/2 after 72 hours are consistent with this view. Another report demonstrated that forskolin addition also reduced MAP kinase activation by GGF (NRG1)(Kim et al., 1997). In the presence of high concentrations of U0126 that presumably cause complete inhibition of ERK1/2 activation, cAMP/NRG1 is unable to induce myelin differentiation in mouse Schwann cells. This suggests that this low ERK1/2 activation is required for differentiation. Similarly, blocking ERK1/2 activation in dbcAMP treated rat Schwann cells abrogates myelin differentiation (Harrisingh et al., 2004; P.Arthur-Farraj, data not shown). It must be noted that blocking the MEK/ERK1/2 pathway in Schwann cell/DRG cocultures did not affect myelination, although the data was not shown (Maurel and Salzer, 2000). Cyclic AMP has also been shown to prolong activation of the PI3-K pathway in human Schwann cells (Monje et al., 2006), although in my experiments blocking this pathway did not inhibit cyclic AMP/NRG induced differentiation and actually increased Krox-20 expression. Interestingly, a recent study demonstrated that constitutive over-activation of Akt in mouse Schwann cells does not affect myelination (Flores et al., 2008), however it is unknown whether Akt phosphorylation is actually required for PNS myelination.

Both cyclic AMP induced proliferation and differentiation appear to require PKA activation (Kim et al., 1997; Howe and McCarthy, 2000; Fig.3.5 and Fig.3.6, C), suggesting that cyclic AMP modulation of NRG1 signalling also requires PKA activation. In support of this activation of the epac pathway, a PKA independent

cyclic AMP pathway did not appear to cooperate with NRG1 to induce Schwann cell myelin differentiation (Fig.3.5) or increase proliferation (data not shown, unpublished observations). It is not known how PKA activation could lead to two alternative cell fates. One simple explanation is that low levels of activation might promote proliferation whereas strong activation might be sufficient for differentiative changes. Also, the PKA holoenzymes, I and II have different affinities for cyclic AMP (PKA type I having roughly 4 times lower activation thresholds by cyclic AMP than PKA type II) and generally PKA type II is often confined to subcellular structures by A-Kinase anchoring proteins (AKAPs) whereas PKA type I is though to be located mainly in the cytoplasm. Futhermore, PKA and AKAPs can be specifically localised in lipid rafts with certain cellular receptors. Thus expression of different PKA holoenzymes, AKAPs and both of their subcellular localizations can all lead to the generation of cell and signal specific responses to cyclic AMP (Tasken and Aandahl, 2004). Clearly, further investigation is required to understand the mechanisms by which PKA can interact with growth factor pathways and regulate Schwann cell biology.

3.3.5. The role of CREB in Schwann cell biology.

The findings in this study suggest that the CREB family of transcription factors may have a role in regulating Schwann cell differentiation. Active CREB can induce periaxin expression in mouse Schwann cells and this is potentially due to the presence of a CRE -360bp from the transcriptional initiation site (Dytrych et al., 1998). However, the requirement for CREB in Schwann cell myelin differentiation appears to be at the level of Krox-20 induction, although a potential role in Oct-6 induction cannot be ruled out (section 3.3.2). Yet CREB activation was not sufficient for robust

Krox-20 expression in mouse Schwann cells, even in combination with NRG1 (data not shown). Thus, CREB is likely to cooperate with other transcription factors such as, Oct-6, NF-κB and Sox-10 in inducing Krox-20 in response to cyclic AMP/NRG1 in mouse Schwann cells. Significantly, constitutively active CREB was a much more potent activator of Krox-20 expression in rat Schwann cells, which may underlie part of the reason why cyclic AMP elevation alone can induce Krox-20 in rat Schwann cells but not in mouse Schwann cells.

CREB has previously been shown to be phosphorylated at Ser-133 in response to NRG1 treatment of rat Schwann cells, although addition of 2μM forskolin and NRG1 induces a more sustained phosphorylation of CREB (Tabernero et al., 1998; Rahmatullah et al., 1998). It has been postulated that CREB activation may have a role in Schwann cell proliferation (Rahmatullah et al., 1998), although A-CREB expression does not block NRG-1 or low cyclic AMP/NRG1 induced rat Schwann cell proliferation (K.Wanek, unpublished observations). Interestingly, CREB was shown to be phosphorylated in cultured Schwann cells after prolonged contact with neurite membranes (Lee et al., 1999), however it is not known whether CREB phosphorylation in Schwann cells is regulated by axonal contact *in vivo*.

The use of the A-CREB inhibitor or the VP16 fused constitutively active CREB molecule does not discriminate between CREB family members such as CREB1, ATF1 and CREM, thus it would be necessary to check the expression of the various family members in Schwann cells. A CREB null mutation causes lethality in mice, late in embryogenesis (Rudolph et al., 1998), thus conditional inactivation of CREB and potentially other family members would be a useful approach in the future to determine its role in Schwann cells.

In summary this study has demonstrated that high concentrations of cyclic AMP analogues in combination with NRG1 signalling induce myelin differentiation in cultured mouse Schwann cells, including expression of Krox-20 and P_0 protein. Furthermore, PKA activation is sufficient to combine with NRG1 signalling to induce Schwann cell differentiation and there is also a requirement for the CREB family of transcription factors in cyclic AMP/NRG1 induced Schwann cell differentiation.

CHAPTER 4: The role of c-Jun in the Schwann cell response to peripheral nerve injury.

4.1 INTRODUCTION

The success of nerve regeneration after PNS injury is discussed in more detail in Chapter 1. However, the Schwann cell is thought to play a central role in the capacity of the PNS to regenerate. In particular, the fact that adult myelinating and non-myelinating Schwann cells retain the ability to dedifferentiate after injury and re-differentiate during axonal regrowth is thought to be a key step that is required for the regeneration process (Jessen and Mirsky, 2005).

The basic-leucine zipper transcription factor, c-Jun, is a member of the AP-1 transcription factor family forming dimers with itself or other members, including JunB, JunD, fos proteins (c-fos, FosB, Fra-1 and Fra-2) and some ATF/CREB family members. Whereas Jun:Jun and Jun:fos dimers bind AP-1 DNA elements or TREs (12-0-Tetradecanoylphorbol-13-acetate (TPA) responsive elements; 5'-TGAC/CTCA-3'), Jun:ATF dimers preferentially bind cyclic-AMP responsive elements (CRE, 5'-TGACGTCA-3') (Shaulian and Karin, 2001). c-Jun and AP-1 transcriptional activity is activated by many signals but in particular by extracellular stress (Shaulian and Karin, 2001). Interestingly, in both hepatocytes and peripheral neurons, c-Jun is activated by tissue damage and is required for the *in vivo* regenerative ability of these cell types (Behrens et al., 2002; Raivich et al., 2004). In the peripheral nerve, c-Jun is expressed in immature Schwann cells before birth (Stewart, 1995; Parkinson et al., 2008). After birth, c-Jun is downregulated in Schwann cells that begin to myelinate and is therefore not expressed in myelinating Schwann cells in the adult and is only expressed at low levels in non-myelinating Schwann cells (Shy et al., 1996; Parkinson et al., 2008). However, Schwann cells re-express c-Jun protein during peripheral

nerve injury or during culture (DeFelipe and Hunt, 1994; Stewart, 1995; Shy et al., 1996; Soares et al., 2001; Parkinson et al., 2008). Thus c-Jun expression in Schwann cells appears to be correlated with the immature or denervated phenotype. To further investigate this, I wanted to discern whether c-Jun is in fact an axonally regulated factor or is simply activated by injury or cellular stress during peripheral nerve transection. Second, I wanted to test whether the dedifferentiation of Schwann cells during nerve injury might actually require a transcriptional program to actively drive Schwann cells back to an immature-like state. Thus I sought to investigate the role of c-Jun as a potential regulator of the cellular processes that occur in Schwann cells during peripheral nerve injury and regeneration (discussed in more detail in Chapter 1).

Since mice lacking c-Jun die between E12.5 and E13.5 with defects in cardiac morphogenesis and increased apoptosis of hepatoblasts and haematopoietic cells analysis of the peripheral nervous system is not feasible (Hilberg et al., 1993; Johnson et al., 1993; Eferl et al., 1999). Therefore, I opted to generate a conditional knockout mouse in which c-Jun is specifically deleted in Schwann cells. To achieve this, I crossed a mouse carrying a floxed c-Jun gene (Behrens et al., 2002) with a transgenic *P0 CRE* mouse, where CRE recombinase is expressed under the Schwann cell specific P_0 promoter (Feltri et al., 1999a, 1999b). Both of these transgenic mice have been used previously: the c-Jun floxed mouse has been used to specifically delete c-Jun in hepatocytes and neurons (Behrens et al., 2002; Raivich et al., 2004) and the *P0 CRE* mouse has been used to ablate many genes, including β1-integrin, dystroglycan and TGFβRII (Feltri et al., 2002; Saito et al., 2003; D'Antonio et al., 2006b). In addition, c-Jun is located on chromosome 1 whereas the *P0 CRE* allele has been mapped to chromosome 13 (M. D'Antonio, personal communication) suggesting that

the combination of the c-Jun floxed and P0 CRE mice should successfully ablate c-Jun in Schwann cells.

4.2 RESULTS

4.2.1 The timing of axonal degeneration during nerve injury, regulates the expression of both c-Jun and Krox-20 in Schwann cells.

Strong c-Jun protein expression in Schwann cells is not only inversely correlated with the presence of axons but also with the expression of the transcription factor Krox-20, that controls myelination both *in vitro* and *in vivo* (Shy et al., 1996; Parkinson et al., 2004; Parkinson et al., 2008). Thus, *in vivo* strong c-Jun expression can be used as a marker for denervated Schwann cells whereas Krox-20 expression denotes axon associated myelinating Schwann cells. To confirm whether this reciprocal relationship between Krox-20 and c-Jun is maintained during nerve injury in a situation where axons remain intact for prolonged periods of time, we performed sciatic nerve transections on control and Wld^s transgenic mice. In Wld^s mice axons remain intact for at least 14 days after nerve injury compared to 24-48 hours in control mice (Coleman et al., 2005; see section 1.6.1). Either 7 or 28 days after the initial surgery (see section 2.6 for protocol), the distal stumps of control and Wld^s mice were collected and processed for sectioning. 10μm thick cryosections of each nerve were then immunolabelled with antibodies for c-Jun or Krox-20.

Confirming previous studies, in control mice, 7 days after sciatic nerve transection, axons have degenerated and Schwann cells in the distal stump are strongly immunoreactive for c-Jun protein and do not express Krox-20 (Fig. 4.1, A-E). Interestingly, Schwann cells in control mice appear to express a lower level of c-Jun 28 days after nerve cut compared to 7 days after nerve injury (Fig. 4.1, K-O). However, in Wld^s mice 7 days after nerve transection, when axons in the distal stump remain intact, Schwann cells do not express c-Jun and, remarkably, still express Krox-20 protein (Fig. 4.1, F-J). Only after 28 days post injury in Wld^s mice, when the

majority of axons have degenerated, do Schwann cells in the distal stump upregulate c-Jun protein and lose Krox-20 expression (Fig. 4.1, P-T). These results suggest that the loss of Krox-20 and the upregulation of c-Jun expression in Schwann cells along the distal stump of the nerve during injury are dependent on the eventual degeneration of the axon rather than the initial insult.

Figure 4.1: Interruption of axon-Schwann cell interactions in both control and Wld^s mice determines c-Jun and Krox-20 expression after sciatic nerve injury.

(A-E) Schwann cells in the distal stump of control sciatic nerve 7 days after transection express high levels of c-Jun (arrowheads) and do not express Krox-20.

(F-J) Schwann cells in the distal stump of the Wld^s sciatic nerve 7 days after transection do not express c-Jun and still express Krox-20 protein (arrows).

(K-O) Schwann cells in the distal stump of control sciatic nerve 28 days after transection still express c-Jun (arrowheads), albeit at a lower level, and do not express Krox-20.

(P-T) Schwann cells in the distal stump of the Wld^s sciatic nerve 28 days after transection now express high levels of c-Jun (arrowheads) and have lost expression of Krox-20 protein.

(Panels A, F, K and P) Axonal degeneration in each condition was determined by morphology in 1μm thick transverse semi-thin sections of the distal stump of nerves stained with toluidine blue. Note the preservation of intact axons and myelin sheaths in Wld^s sciatic nerve 7 days after transection (F), whereas axons and myelin sheaths have degenerated in all other conditions (A,K and P). Scale bars, 20μm.

(Panels, B-E, G-J, L-O and Q-T). 10μm thick longitudinal cryosections of nerves from each condition were immunolabelled with polyclonal antibodies for either c-Jun or Krox-20 and co-stained with hoescht nuclear dye (Ho). Scale bars, 20μm.

Figure 4.1

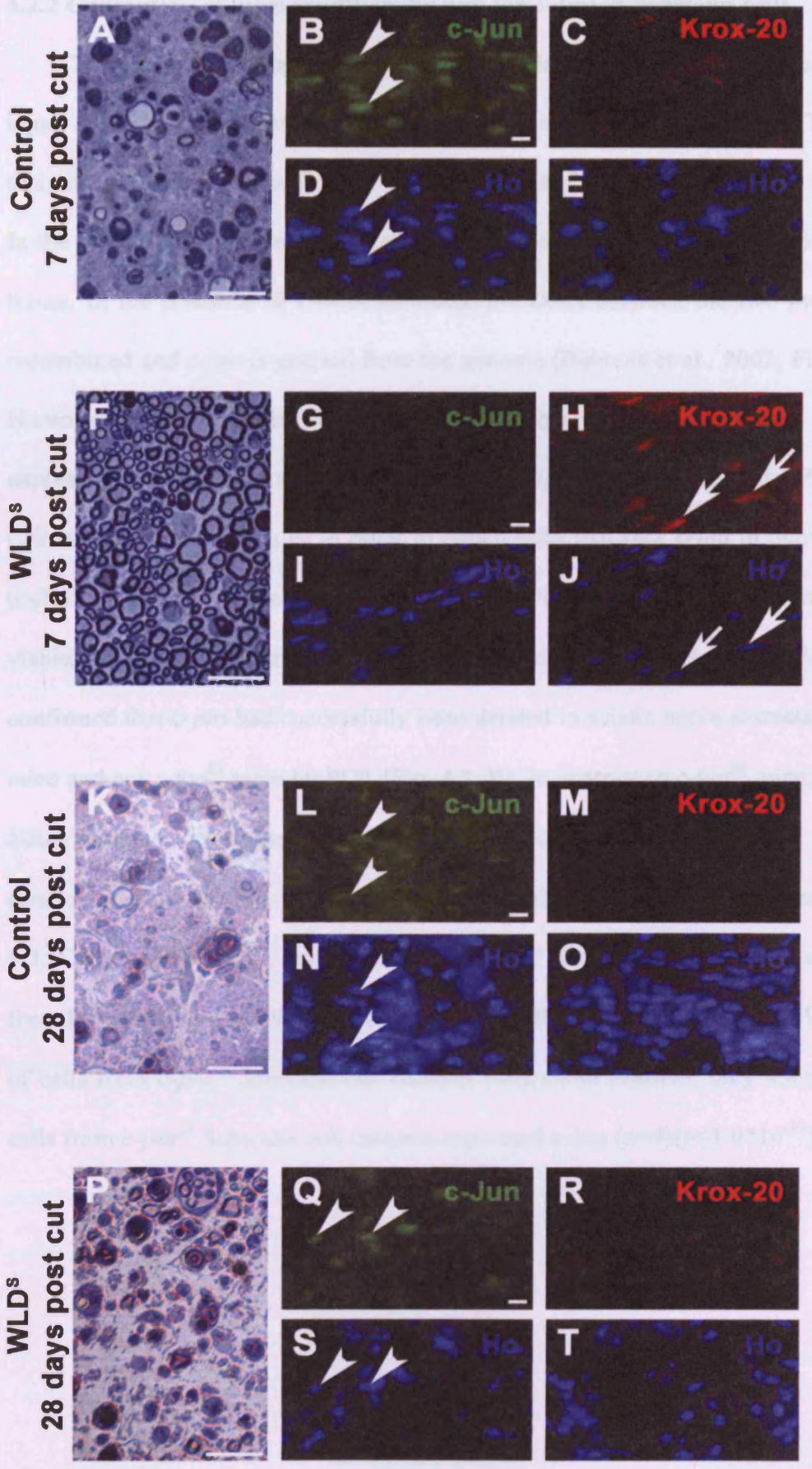
Control
7 days post cut
A
B
c-Jun
C
Krox-20
D
Ho
E
Ho
WLD^s
7 days post cut
F
G
c-Jun
H
Krox-20
I
Ho
J
Ho
Control
28 days post cut
K
L
c-Jun
M
Krox-20
N
Ho
O
Ho
WLD^s
28 days post cut
P
Q
c-Jun
R
Krox-20
S
Ho
T
Ho

4.2.2 Generation of mice conditionally null for c-Jun in Schwann cells.

To further investigate the role that c-Jun plays in Schwann cells during nerve injury I decided to conditionally inactivate *c-jun* in Schwann cells *in vivo*. To achieve this, mice that carried two floxed *c-jun* alleles (*c-jun*$^{f/f}$; *c-jun* floxed mice) were used. In the c-Jun floxed mouse, loxP sites are inserted either side of the *c-jun* open reading frame. In the presence of cre-recombinase, the DNA between the two loxP sites is recombined and *c-jun* is excised from the genome (Behrens et al., 2002; Fig. 4.2, A). Homozygous *c-jun*$^{f/f}$ mice were crossed with heterozygous transgenic mice that express cre-recombinase under the Schwann cell specific promoter of the P_0 gene (*P0 CRE*; Feltri et al., 1999a, b) in order to obtain mice that lack *c-jun* in Schwann cells (*c-jun*$^{\Delta S}$). *c-jun*$^{\Delta S}$ mice were born approximately with Mendelian frequencies and were viable, fertile and indistinguishable from control littermates (*c-jun*$^{f/f}$; P_0 *CRE*$^{-}$). I confirmed that *c-jun* had successfully been deleted in sciatic nerve extracts of *c-jun*$^{\Delta S}$ mice and not *c-jun*$^{f/f}$ mice by PCR (Fig. 4.2, B). In contrast to *c-jun*$^{f/f}$ mice, very little c-Jun protein is expressed in the sciatic nerve of adult *c-jun*$^{\Delta S}$ mice, 7 days after sciatic nerve transection, judged by Western blotting and immunocytochemistry (Fig. 4.2, C-G). Additionally, purified dedifferentiated Schwann cell cultures were made from P5 *c-jun*$^{\Delta S}$ and *c-jun*$^{f/f}$ mice and immunolabelled for c-Jun. Whereas, 94 +/-1.2% of cells from *c-jun*$^{f/f}$ Schwann cell cultures were c-Jun positive, only 4.8 +/-1.3% of cells from *c-jun*$^{\Delta S}$ Schwann cell cultures expressed c-Jun ($n=4$)($p<1.0*10^{-10}$).

Figure 4.2: Conditional ablation of *c-jun* from Schwann cells.

(A) Schematic representation of the *c-jun* targeting locus, the *c-jun* floxed allele (*c-jun*^{f}) and the *c-jun* deleted allele (*c-jun*$^{\Delta}$). The *c-jun* open reading frame is characterized by a rectangle and the thin lines represent the untranslated region of the c-jun locus. The neomycin resistance gene (NeoR) and the thymidine kinase gene (tk) are also shown. Adapted from Behrens et al., (2002).

(B) PCR analyis for the deleted *c-jun* allele (*c-jun*$^{\Delta}$) from genomic DNA from either tail (T) or sciatic nerve (N) of mice from the indicated genotypes. Note that the *c-jun*$^{\Delta}$ allele is only seen in the nerve from *c-jun*$^{f/f}$; P_0 *CRE*$^{+}$ and *c-jun*$^{f/+}$; P_0 *CRE*$^{+}$ animals and not the tail where P_0 *CRE* is not expressed (M. D'Antonio personal communication). No PCR product is seen in either the tail or the nerve of *c-jun*$^{f/f}$; P_0 *CRE*$^{-}$ animals. Equal amounts of DNA were amplified in each reaction. PCR for Interleukin-2 (IL-2) ensured DNA integrity.

(C) Western blot of uninjured (U) and 7 day transected (C) sciatic nerve extracts from *c-jun*$^{f/f}$ (*c-jun*$^{f/f}$; P_0 *CRE*$^{-}$) and *c-jun*$^{\Delta s}$ (*c-jun*$^{f/f}$; P_0 *CRE*$^{+}$). GAPDH is used as a loading control.

(D-G) Immunohistochemistry for c-Jun shows c-Jun is barely expressed in Schwann cells of the distal stump 7 days after sciatic nerve cut in *c-jun*$^{\Delta s}$ animals (E and G) in comparison to *c-jun*$^{f/f}$ animals (D and F). Sections are co-labelled with hoescht nuclear dye (Ho). Scale bar, 50μm.

Figure 4.2

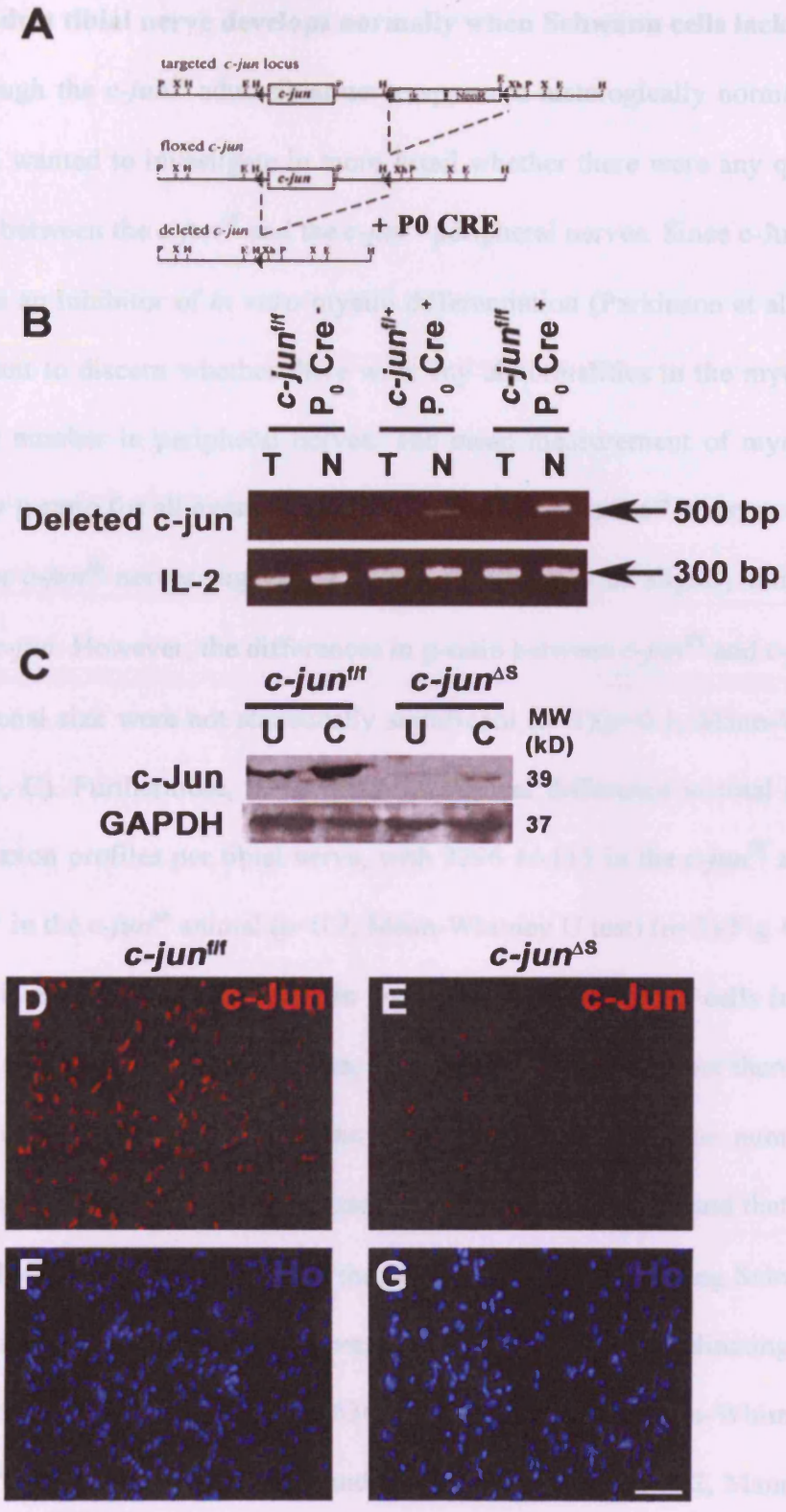
A
targeted c-jun locus
c-jun
floxed c-jun
deleted c-jun
+ P0 CRE
B
c-jun f/f P0 Cre -
c-jun f/+ P0 Cre +
c-jun f/f P0 Cre +
T N T N T N
Deleted c-jun
500 bp
IL-2
300 bp
C
c-jun f/f
c-jun ΔS
U C U C
MW (kD)
c-Jun
39
GAPDH
37
c-jun f/f
c-jun ΔS
D
c-Jun
E
c-Jun
7 days post cut
F
Ho
G
Ho

4.2.3 The adult tibial nerve develops normally when Schwann cells lack *c-jun*.

Although the *c-jun*$^{\Delta s}$ adult tibial nerve appeared histologically normal (Fig.4.3, A and B), I wanted to investigate in more detail whether there were any quantifiable differences between the *c-jun*$^{f/f}$ and the *c-jun*$^{\Delta s}$ peripheral nerves. Since c-Jun has been identified as an inhibitor of *in vitro* myelin differentiation (Parkinson et al., 2008), it was important to discern whether there were any abnormalities in the myelin sheath structure or number in peripheral nerves. The mean measurement of myelin sheath thickness by g-ratio for all axonal sizes in *c-jun*$^{f/f}$ nerves was 0.67 whereas the g-ratio was 0.70 for *c-jun*$^{\Delta s}$ nerves suggesting myelin sheaths may be slightly thinner in the absence of *c-jun*. However, the differences in g-ratio between *c-jun*$^{f/f}$ and *c-jun*$^{\Delta s}$ mice for each axonal size were not statistically significant (n=3)(p=0.1, Mann-Whitney U test)(Fig.4.3, C). Furthermore, there was no statistical difference in total number of myelinated axon profiles per tibial nerve, with 2296 +/-115 in the *c-jun*$^{f/f}$ animal and 2156 +/-221 in the *c-jun*$^{\Delta s}$ animal (p=0.7, Mann-Whitney U test) (n=3)(Fig.4.3, D).

c-Jun is expressed at low levels in non-myelinating Schwann cells in the adult rodent PNS (Shy et al., 1996). Therefore, I wanted to examine whether there were any differences in non-myelinating Schwann cells or unmyelinated axon number in the tibial nerve of the *c-jun*$^{\Delta s}$ mouse compared to the *c-jun*$^{f/f}$ mouse. I found that there was no statistically significant alteration in the number of non-myelinating Schwann cells or unmyelinated axons in the tibial nerve, with 614 +/-124 non-myelinating Schwann cells in the *c-jun*$^{f/f}$ mouse compared to 538 +/-49 (n=4) (p=0.6, Mann-Whitney U test) in the *c-jun*$^{\Delta s}$ mouse and 5486 +/-871 and 4614 +/-577 (n=4))(p=0.2, Mann-Whitney U test) for the unmyelinated axons, respectively (Fig.4.3, E and F). Thus the adult peripheral develops relatively normally in the absence of *c-jun* in Schwann cells.

Figure 4.3: Normal tibial nerve morphology and axon number in *c-jun*$^{\Delta s}$ mice.

(A and B) Electron micrographs showing no obvious differences in tibial nerve morphology between *c-jun*$^{f/f}$ and *c-jun*$^{\Delta s}$ mice. Scale bar, 10μm.

(C) Myelin sheath thickness measured by g-ratio (diameter of axon/ diameter of axon +sheath) for different sizes of axon in the tibial nerve of *c-jun*$^{f/f}$ and *c-jun*$^{\Delta s}$ mice. The mean g-ratio for each axonal size category is shown along with linear regression lines for nerves of *c-jun*$^{f/f}$ and *c-jun*$^{\Delta s}$ mice. Error bars show the standard deviation of the mean. Notice that the g-ratios for *c-jun*$^{\Delta s}$ mice appear slightly higher than for *c-jun*$^{f/f}$ animals although the differences in g-ratio for every axonal category were not statistically significant using the Mann-Whitney U test.

(D) Total number of myelin sheaths in the tibial nerve at mid thigh level in *c-jun*$^{f/f}$ and *c-jun*$^{\Delta s}$ mice. Error bars show the standard deviation of the mean.

(E) Total number of non-myelinating Schwann cell profiles (Remak fibres) in transverse profile at mid-thigh level in the tibial nerve in *c-jun*$^{f/f}$ and *c-jun*$^{\Delta s}$ mice. Error bars show the standard deviation of the mean.

(F) Total number of unmyelinated axons in the tibial nerve at mid thigh level in *c-jun*$^{f/f}$ and *c-jun*$^{\Delta s}$ mice. Error bars show the standard deviation of the mean.

Figure 4.3

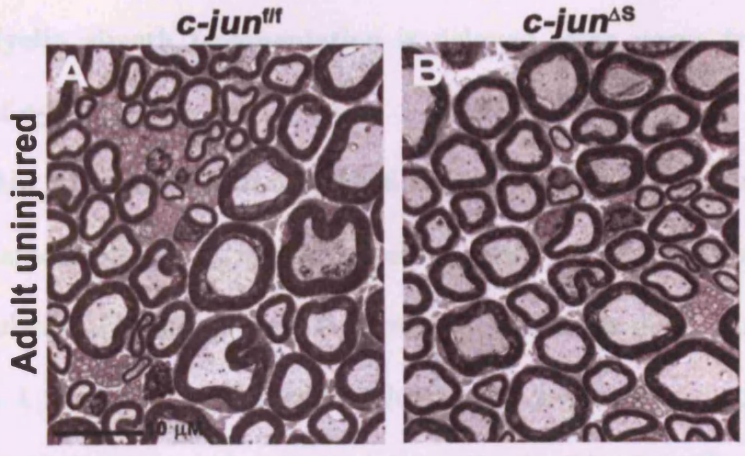
c-jun^f/f
c-jun^ΔS
A
B
Adult uninjured

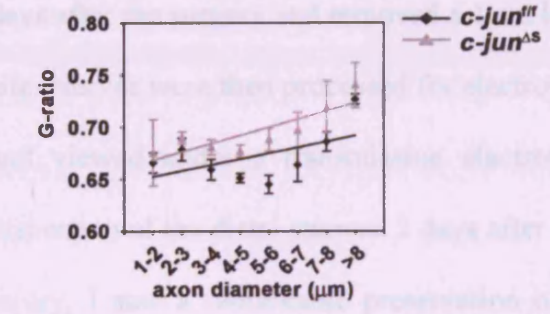
C
c-jun^f/f
c-jun^ΔS
G-ratio
0.80
0.75
0.70
0.65
0.60
1-2
2-3
3-4
4-5
5-6
6-7
7-8
>8
axon diameter (μm)

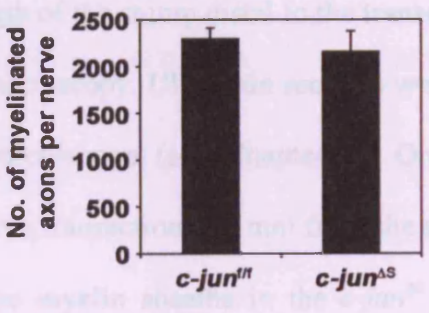
D
No. of myelinated axons per nerve
2500
2000
1500
1000
500
0
c-jun^f/f
c-jun^ΔS

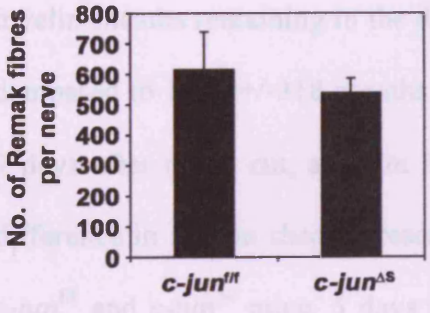
E
No. of Remak fibres per nerve
800
700
600
500
400
300
200
100
0
c-jun^f/f
c-jun^ΔS

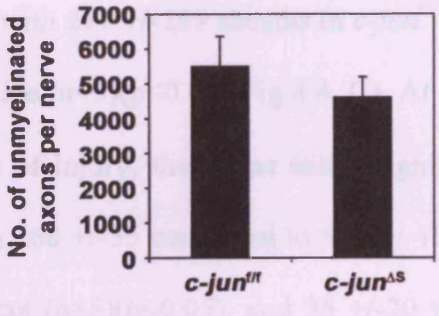
F
No. of unmyelinated axons per nerve
7000
6000
5000
4000
3000
2000
1000
0
c-jun^f/f
c-jun^ΔS

4.2.4 The role of *c-jun* in Schwann cell demyelination

4.2.4.1 Myelin sheath fragmentation is delayed after nerve transection in the absence of *c-jun*.

Within 2 to 3 days after peripheral nerve injury, myelin sheaths begin to break up into characteristic ovoid structures (see Chapter 1). This occurs at a similar time to the upregulation of c-Jun protein in Schwann cells of the distal stump (Parkinson et al., 2008). I wanted to test whether c-Jun played any role in regulating the rate of myelin sheath break up after nerve injury. To do this, I performed sciatic nerve transections on *c-jun*$^{f/f}$ and *c-jun*$^{\Delta s}$ mice. I then sacrificed the mice at either 3, 5 or 7 days after the surgery and removed a 1 cm length of the stump distal to the transection site. Nerves were then processed for electron microscopy. Ultra-thin sections were cut and viewed under a transmission electron microscope (see Chapter 2). On first inspection of the distal stumps, 3 days after nerve transection, at 1mm from the site of injury, I saw a remarkable preservation of the myelin sheaths in the *c-jun*$^{\Delta s}$ mice compared to the *c-jun*$^{f/f}$ mice (Fig.4.4, A and B). I counted the total number of intact myelin sheaths remaining in the distal stump, with 217 +/-289 sheaths in *c-jun*$^{f/f}$ mice compared to 1064 +/-318 sheaths in *c-jun*$^{\Delta s}$ mice ($n=5$)($p<0.05$)(Fig.4.4, C). At 5 and 7 days after nerve cut, at 5mm from the site of injury, there was still a significant difference in myelin sheath preservation, with 268 +/-55 compared to 504 +/-101 for *c-jun*$^{f/f}$ and *c-jun*$^{\Delta s}$ mice, 5 days after nerve cut ($n=5$)($p<0.05$), and 75 +/-20 versus 124 +/-25, 7 days after nerve cut, respectively ($n=5$)($p<0.05$)(Fig.4.4, D). Importantly, there is a noticeable drop in the number of intact sheaths in *c-jun*$^{\Delta s}$ mice between 5 and 7 days ($p<0.01$) suggesting that the lack of *c-jun* in Schwann cells only causes a delay in myelin sheath fragmentation after nerve cut rather than a complete block (Fig.4.4, D).

In addition I examined whether there was a difference in the rate of myelin protein clearance after sciatic nerve transection, in the absence of *c-jun* in Schwann cells. To test this, I labelled 10μm thick cryosections of 7 day cut sciatic nerves with a polyclonal antibody to the myelin protein, P_0. Confocal microscopy revealed that there was a visibly greater area of the nerve labelled with P_0 antibodies in *c-jun*$^{\Delta s}$ compared to *c-jun*$^{f/f}$ mice (n=3)(Fig.4.4, E and F).

Interestingly, the onset of axonal degeneration remains unaffected in *c-jun*$^{\Delta s}$ mice, since electron micrographs demonstrate that even though the myelin sheath may remain intact the space in between contains only axonal debris (Fig. 4.5, A-D). Furthermore, immunostaining for β-tubulin, 3 days after nerve cut, demonstrates that axonal microtubules have fragmented to a similar degree in the *c-jun*$^{f/f}$ and *c-jun*$^{\Delta s}$ animals (Fig. 4.5, E-H). In summary, these results suggest that, while Schwann cell *c-jun* may not be necessary for axonal degeneration, it is required for rapid demyelination after peripheral nerve injury.

Figure 4.4: Demyelination after nerve injury is delayed in the absence of *c-jun* in Schwann cells.

(A and B) Electron micrographs of the distal stump, 1mm from the site of injury of *c-jun*$^{f/f}$ and *c-jun*$^{\Delta s}$ animals, 3 days after sciatic nerve transection. Scale bar, 20μm.

(B) Number of remaining intact sheaths per tibial nerve, 3 days after cut at 1mm from the site of injury in *c-jun*$^{f/f}$ and *c-jun*$^{\Delta s}$ animals. Error bars show the standard deviation of the mean. Statistical analysis was performed using the Mann-Whitney U test.

(D) Number of remaining intact sheaths per tibial nerve, at 5 and 7 days after cut at 5mm from the site of injury, in *c-jun*$^{f/f}$ and *c-jun*$^{\Delta s}$ animals. Error bars show the standard deviation of the mean. Statistical analysis was performed using the Mann-Whitney U test.

(E and F) Confocal images of immunohistochemistry for P_0 in *c-jun*$^{f/f}$ and *c-jun*$^{\Delta s}$ nerves, 7 days after nerve cut, 5mm from the site of injury. Note that P_0 staining is brighter and covers a greater proportion of the *c-jun*$^{\Delta s}$ nerve in comparison to the *c-jun*$^{f/f}$ nerve.

Figure 4.4

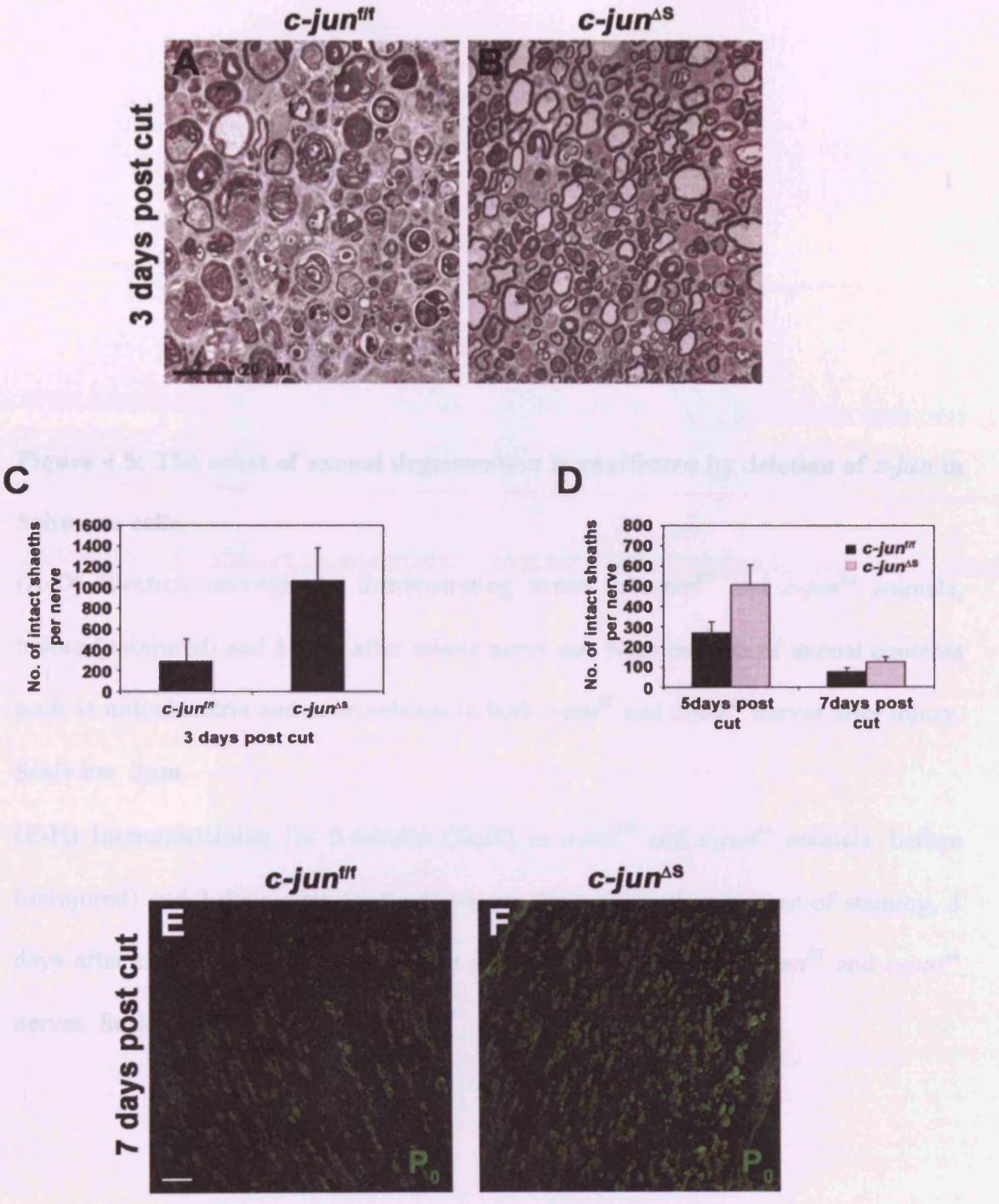
c-jun^f/f
c-jun^ΔS
A
B
3 days post cut
20 μM
C
No. of intact sheaths per nerve
1600
1400
1200
1000
800
600
400
200
0
c-jun^f/f
c-jun^ΔS
3 days post cut
D
No. of intact sheaths per nerve
800
700
600
500
400
300
200
100
0
c-jun^f/f
c-jun^ΔS
5days post cut
7days post cut
c-jun^f/f
c-jun^ΔS
E
F
7 days post cut
P0
P0

Figure 4.5: The onset of axonal degeneration is unaffected by deletion of *c-jun* in Schwann cells.

(A-D) Electron micrographs demonstrating axons in *c-jun*$^{f/f}$ and *c-jun*$^{\Delta s}$ animals, before (uninjured) and 3 days after sciatic nerve cut. Note the loss of axonal contents such as mitochondria and microtubules in both *c-jun*$^{f/f}$ and *c-jun*$^{\Delta s}$ nerves after injury. Scale bar, 2μm.

(E-H) Immunostaining for β-tubulin (TuJ1) in *c-jun*$^{f/f}$ and *c-jun*$^{\Delta s}$ animals, before (uninjured) and 3 days after sciatic nerve cut. Note the broken pattern of staining, 3 days after cut, suggesting microtubules are fragmenting in both *c-jun*$^{f/f}$ and *c-jun*$^{\Delta s}$ nerves. Scale bar, 50μm.

Figure 4.5

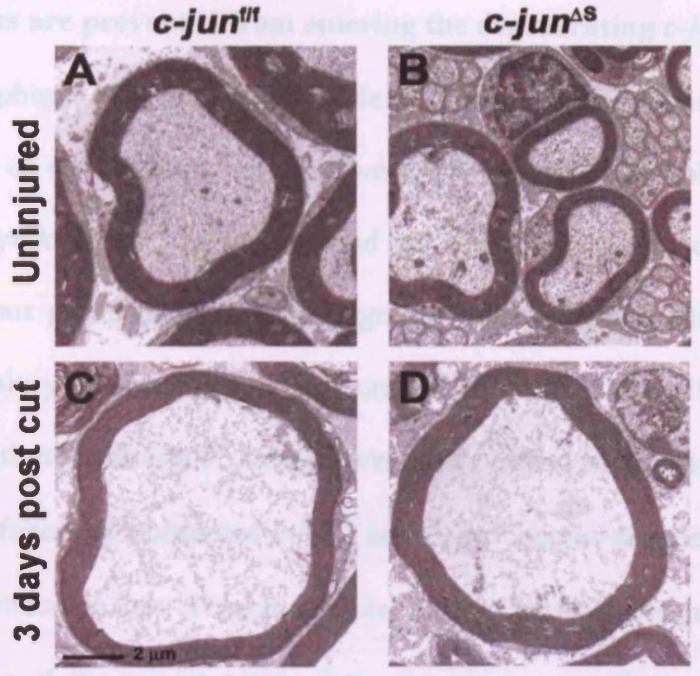
c-jun^f/f
c-jun^ΔS
A
B
C
D
Uninjured
3 days post cut
2 µm

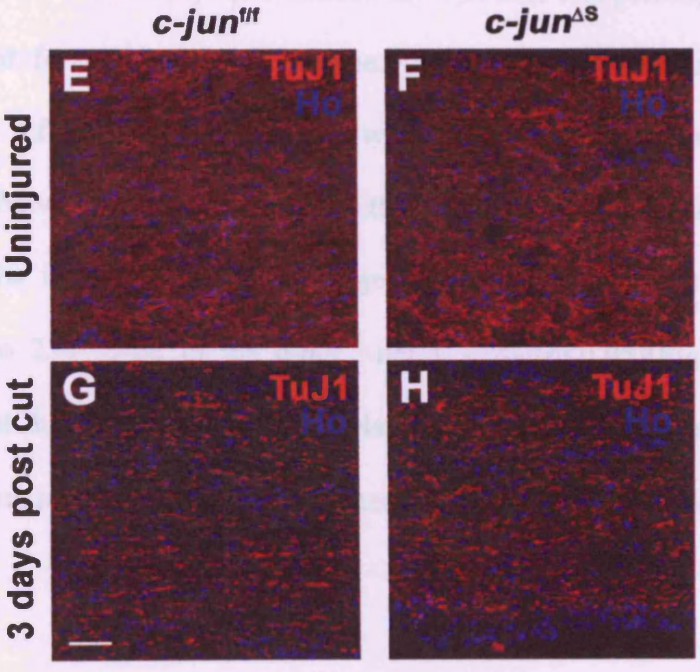
c-jun^f/f
c-jun^ΔS
E
F
G
H
TuJ1
Ho
Uninjured
3 days post cut

4.2.4.2. Myelin sheath fragmentation is delayed even when haematogenous macrophages are prevented from entering the degenerating *c-jun*$^{\Delta s}$ nerve.

Macrophages play a significant role in removing degenerating myelin from the distal stump of degenerating nerves. Two populations of macrophages contribute to removing myelin debris, the resident and the haematogenous macrophages, with the haematogenous group removing the large majority of myelin, starting from 3 days after nerve injury (see section 1.6.5). In order to discount the possibility that the delay in demyelination in the *c-jun*$^{\Delta s}$ animals was solely due to an effect on haematogenous macrophage function, I observed *c-jun*$^{f/f}$ and *c-jun*$^{\Delta s}$ nerves degenerate in the absence of invading macrophages. To achieve this, I removed equal length segments (about 6mm, starting at the sciatic notch) from the tibial nerve from *c-jun*$^{f/f}$ and *c-jun*$^{\Delta s}$ animals and placed them floating in a 35mm tissue culture dish containing DMEM and 5% HS at 37°C for 6 days (see section 2.3.7). After this period, nerves were fixed and processed for resin sections and analysed by electron microscopy. Only the middle 2mm of each nerve segment was analysed in order to standardise the observations between conditions. I found that there was still a striking preservation of myelin sheaths in the *c-jun*$^{\Delta s}$ nerve segement, with 604 +/-110 intact sheaths in comparison to 234 +/-62 in the *c-jun*$^{f/f}$ nerve ($n=4$)($p<0.05$)(Fig.4.6, A-C). These results suggest that at least part of the delay in demyelination observed in the *c-jun*$^{\Delta s}$ nerve is not due to a defect in the recruitment of haematogenous macrophages.

4.2.4.3. Demyelination is delayed in dissociated Schwann cell cultures deficient in *c-jun*.

In order to test whether there was an intrinsic deficit in the ability of Schwann cells to clear myelin debris in the absence of *c-jun*, I studied demyelination in dissociated Schwann cell cultures. Both sciatic nerves were dissected from P8 *c-jun*$^{f/f}$ and *c-jun*$^{\Delta s}$ animals, dissociated in trypsin and collagenase and then plated on laminin coated coverslips, at a concentration of a 1000 cells per 15μl drop, in DM supplemented with 0.5% HS and AraC (10^{-5}M). Cells were cultured for a maximum of 10 days with half the medium replaced every 3 days. Cells were then fixed and immunolabelled for the myelin proteins, P_0 and myelin basic protein (MBP) at 3 hours, 3, 5, 7 and 10 days after plating. Coverslips were also immunolabelled with an antibody against S100β, in order to identify Schwann cells (see section 2.3.7).

In the absence of *c-jun*, cultured Schwann cells were unable to rapidly clear myelin proteins, retaining myelin debris which was immunoreactive to P_0 and MBP, within their cytoplasm (Fig.4.6, D-G). When I quantified the rate of loss of either P_0 or MBP protein, it was significantly delayed in *c-jun*$^{\Delta s}$ Schwann cells compared to *c-jun*$^{f/f}$ cells, at all time points studied relative to the 3 hour time point ($n=5$)($p<0.0001$) (Fig.4.6, H-I). These cultures contained macrophages that were normally resident in uninjured nerves, judged by immunolabelling for the macrophage specific marker, F4/80. However there was no difference in macrophage number between genotypes, 3 days after culturing, with 5.6 +/-1.8% and 5.8 +/-1.7% in *jun*$^{f/f}$ and *c-jun*$^{\Delta s}$ cultures respectively. Importantly, no F4/80 positive cells contained any myelin debris at this time point, suggesting that these cells were not contributing significantly to the removal of myelin (data not shown). Together these results demonstrate that *c-jun* is

necessary for dissociated Schwann cells to quickly remove myelin debris from their cytoplasm using a mechanism that does not rely on the function of macrophages.

Figure 4.6: Cell autonomous delay in demyelination in *c-jun*$^{\Delta s}$ Schwann cells.

(A and B) Electron micrographs showing, *c-jun*$^{f/f}$ and *c-jun*$^{\Delta s}$ tibial nerve segments after 6 days *in vitro*. Scale bar, 5μm.

(C) Number of intact myelin sheaths remaining in *c-jun*$^{f/f}$ and *c-jun*$^{\Delta s}$ tibial nerve segments after 6 days in vitro. Error bars show the standard deviation of the mean. Statistical analysis was performed using the Mann-Whitney U test.

(D-G) Dissociated Schwann cells from *c-jun*$^{f/f}$ and *c-jun*$^{\Delta s}$ P8 nerves, after 5 days in culture. Cells are stained with antibodies to the Schwann cell marker, S100β and to MBP and also with hoescht nuclear stain (Ho). Arrowheads in E and G demonstrate *c-jun* null Schwann cells containing MBP positive myelin debris. Note that *c-jun* null Schwann cells develop a flattened morphology with multiple filopodia whereas *c-jun*$^{f/f}$ Schwann cells have a bipolar shape, characteristic of dedifferentiated Schwann cells in culture.

(H) Total number of MBP positive *c-jun*$^{f/f}$ and *c-jun*$^{\Delta s}$ Schwann cells over a 10day period of culturing, expressed as a percentage of the total number of MBP positive cells at the 3 hour time point. Error bars show the standard deviation of the mean. Statistical analysis was performed using two-way ANOVA and the unpaired students t-test.

(I) Total number of P_0 positive *c-jun*$^{f/f}$ and *c-jun*$^{\Delta s}$ Schwann cells over a 10 day period of culturing, expressed as a percentage of the total number of P_0 positive cells at the 3 hour time point. Error bars show the standard deviation of the mean. Statistical analysis was performed using two-way ANOVA and the unpaired students t-test.

Figure 4.6

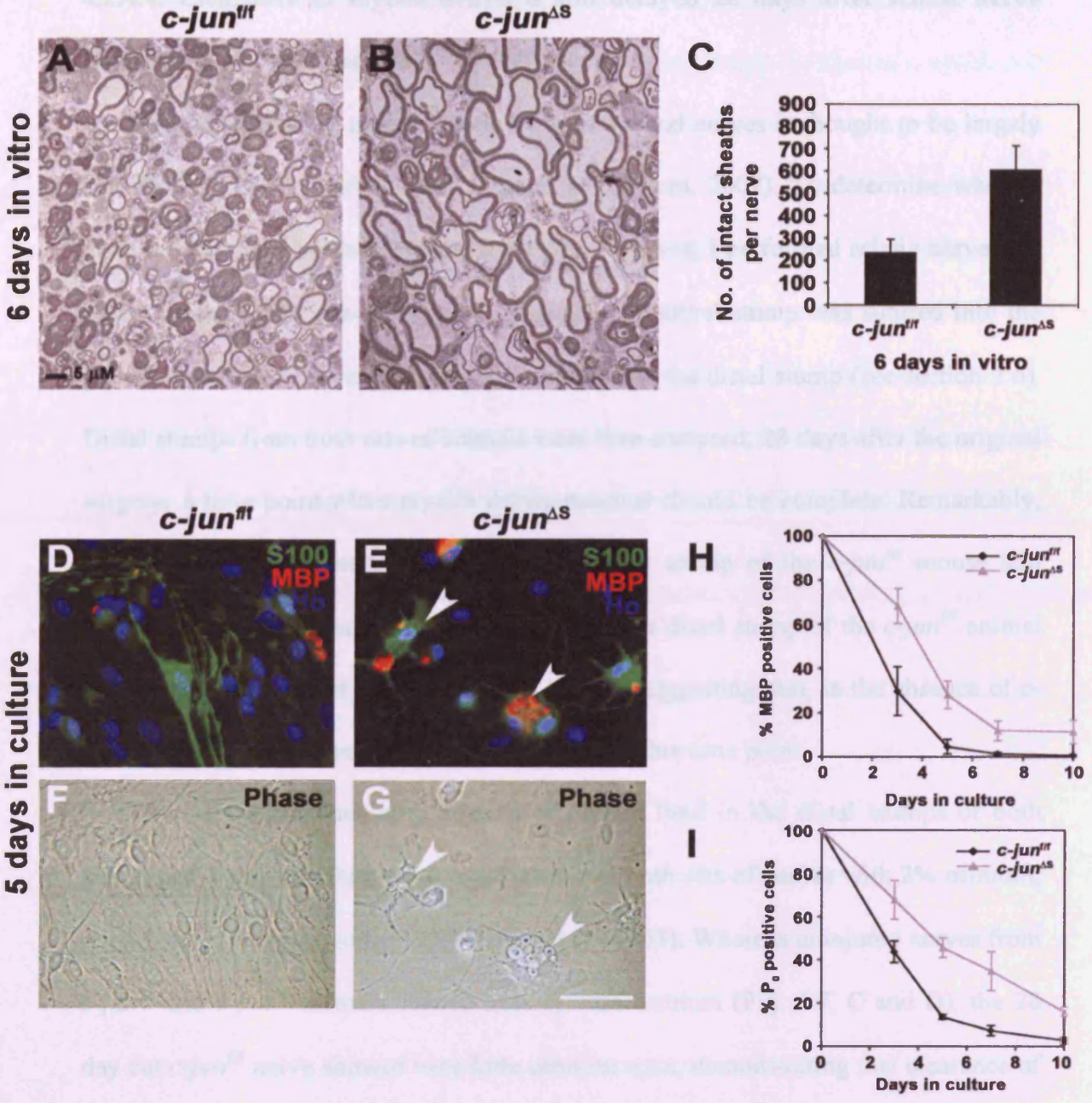
c-jun^fl/fl
c-jun^ΔS
A
B
C
6 days in vitro
5 μM
No. of intact sheaths per nerve
900
800
700
600
500
400
300
200
100
0
c-jun^fl/fl
c-jun^ΔS
6 days in vitro
c-jun^fl/fl
c-jun^ΔS
D
S100
MBP
Ho
E
S100
MBP
Ho
5 days in culture
F
Phase
G
Phase
H
% MBP positive cells
100
80
60
40
20
0
0
2
4
6
8
10
Days in culture
c-jun^fl/fl
c-jun^ΔS
I
% P0 positive cells
100
80
60
40
20
0
0
2
4
6
8
10
Days in culture
c-jun^fl/fl
c-jun^ΔS

4.2.4.4. Clearance of myelin debris is still delayed 28 days after sciatic nerve transection in *c-jun*$^{\Delta s}$ animals.

The clearance of myelin debris from peripheral nerves is thought to be largely complete by 14 days after injury (Vargas and Barres, 2007). To determine whether myelin debris is eventually cleared from *c-jun*$^{\Delta s}$ nerves, I performed sciatic nerve cuts on both *c-jun*$^{f/f}$ and *c-jun*$^{\Delta s}$ animals, where the proximal stump was sutured into the gluteal muscles to prevent axonal regeneration into the distal stump (see section 2.6). Distal stumps from both sets of animals were then analysed, 28 days after the original surgery, a time point when myelin debris removal should be complete. Remarkably, 28 days after sciatic nerve transection, the distal stump of the *c-jun*$^{\Delta s}$ mouse still maintained a white opaque appearance whereas the distal stump of the *c-jun*$^{f/f}$ animal had become translucent (n=5)(Fig.4.7, A and B), suggesting that, in the absence of *c-jun*, myelin lipid clearance may still be delayed at this time point.

To assess the remaining amount of myelin lipid in the distal stumps of both genotypes, I stained 10μm thick cryosections of both sets of nerves with 2% osmium, a lipid stain (Wigglesworth, 1957; Hayes et al., 1963). Whereas uninjured nerves from *c-jun*$^{f/f}$ and *c-jun*$^{\Delta s}$ animals stained heavily with osmium (Fig. 4.7, C and D), the 28 day cut *c-jun*$^{f/f}$ nerve showed very little osmium stain, demonstrating that clearance of myelin lipids was complete (Fig.4.7, E). In contrast, the 28 day cut *c-jun*$^{\Delta s}$ nerve demonstrated considerable osmium stain (Fig.4.7, F). I then quantified the percentage of nerve area stained with osmium relative to the uninjured nerves. In the *c-jun*$^{f/f}$ distal stump only 1.1 +/-0.6% of the original nerve area contained myelin lipid compared to 17.4 +/-1.1% in the *jun*$^{\Delta s}$ nerve, 28 days after injury (n=3)($p<0.001$)(Fig.4.7, G). Thus myelin lipid clearance is still delayed at 28 days after nerve cut in the absence of *c-jun* in Schwann cells.

In addition, I analysed the nerve ultrastructure of the *c-jun*$^{f/f}$ and *c-jun*$^{\Delta s}$ distal stumps, at 28 days after transection, by electron microscopy, to ascertain which cell types contained remaining myelin debris. In the *c-jun*$^{f/f}$ mouse, the majority of the distal stump contained large deposits of collagen and little myelin debris confirming the previous results. Discreet myelin whorls were often seen in macrophages but Schwann cells were always completely devoid of any myelin debris (Fig.4.7, H and J). The histology of the *c-jun*$^{\Delta s}$ nerve, 28 days after transection, was radically different. First, the nerve contained a lot of myelin debris and lipid droplets, the majority of which appeared to be inside grossly enlarged macrophages. In addition, Schwann cells, identified by their basal lamina, also often contained lipid droplets, which was in complete contrast to Schwann cells in the *c-jun*$^{f/f}$ nerve. Furthermore, characteristic structures, known as the Bands of Bungner that contain multiple Schwann cell processes inside a single basal lamina tube are seen in the *c-jun*$^{f/f}$ distal stump, but do not develop normally in the *c-jun*$^{\Delta s}$ nerve. Instead, a single Schwann cell process is seen in continuous association with the basal lamina (Fig. 4.7, H-K). In summary, these observations demonstrate that Schwann cells without *c-jun* are still impaired in processing myelin debris 28 days after nerve transection. c-Jun also appears to be important for Schwann cell morphology and correct formation of the Bands of Bungner. Moreover, macrophages in the *c-jun*$^{\Delta s}$ nerve appear to be unable to properly clear degenerating myelin once they have phagocytosed it, suggesting possible altered signalling between Schwann cells and macrophages in the *c-jun*$^{\Delta s}$ mouse.

Figure 4.7: Delayed clearance of myelin debris by Schwann cells and macrophages, 28 days after transection in the *c-jun*$^{\Delta s}$ sciatic nerve.

(A and B) Photographs of the distal stumps (black arrows), 28 days after sciatic nerve transection (cut), of *c-jun*$^{f/f}$ and *c-jun*$^{\Delta s}$ animals. Note that the control nerve (arrow) is translucent whereas the *c-jun*$^{\Delta s}$ nerve (arrow) remains opaque.

(C-F) 10μm thick cryosections, stained with 2% osmium, of uninjured nerves in transverse section (C and D) and distal stumps, 28 days after nerve transection, in longitudinal section (E and F), from *c-jun*$^{f/f}$ and *c-jun*$^{\Delta s}$ animals respectively. Scale bar, 50μm. Note the increased osmium stain in the *c-jun*$^{\Delta s}$ cut nerve compared with the *c-jun*$^{f/f}$ nerve.

(G) Percentage of area stained by osmium in the *c-jun*$^{f/f}$ and *c-jun*$^{\Delta s}$ 28 day cut nerves, relative to *c-jun*$^{f/f}$ and *c-jun*$^{\Delta s}$ uninjured nerves. Error bars show the standard deviation of the mean. Statistical significance was determined using the Mann-Whitney U test.

(H and I) Electron micrographs demonstrating the overall histology of the *c-jun*$^{f/f}$ and *c-jun*$^{\Delta s}$ nerve 28 days after sciatic nerve transection. Black arrowheads identify macrophages in both conditions. Note the enlarged size of the macrophages in the *c-jun*$^{\Delta s}$ nerve. Macrophages in the *jun*$^{\Delta s}$ nerve also appear to contain a more heterogeneous array of degenerating myelin profiles as well as many lipid droplets, in comparison to macrophages in the *c-jun*$^{f/f}$ distal stump. Scale bar, 5μm.

(J and K) Electron micrographs showing the structure of Schwann cells in the distal stump of *c-jun*$^{f/f}$ and *c-jun*$^{\Delta s}$ nerves 28 days after sciatic nerve transection. The red arrow demonstrates a Schwann cell containing a large lipid droplet in the *c-jun*$^{\Delta s}$ nerve. The black arrow shows the morphology of Schwann cells, identified by their basal lamina, 28 days after nerve cut in the *c-jun*$^{f/f}$ and *c-jun*$^{\Delta s}$ distal stumps. Note how in the *c-jun*$^{f/f}$ nerve multiple cell processes are found with collagen within one basal lamina tube (Bands of Bungner; see also inset in J, small black arrowheads denote the basal lamina), whereas in the *c-jun*$^{\Delta s}$ nerve a single continuous cell process often with an asteroid morphology is seen adhering to the basal lamina (see also inset in K, small black arrowheads denote the basal lamina). Scale bar, 2μm (scale bar for inset figures, 0.5μm).

Figure 4.7

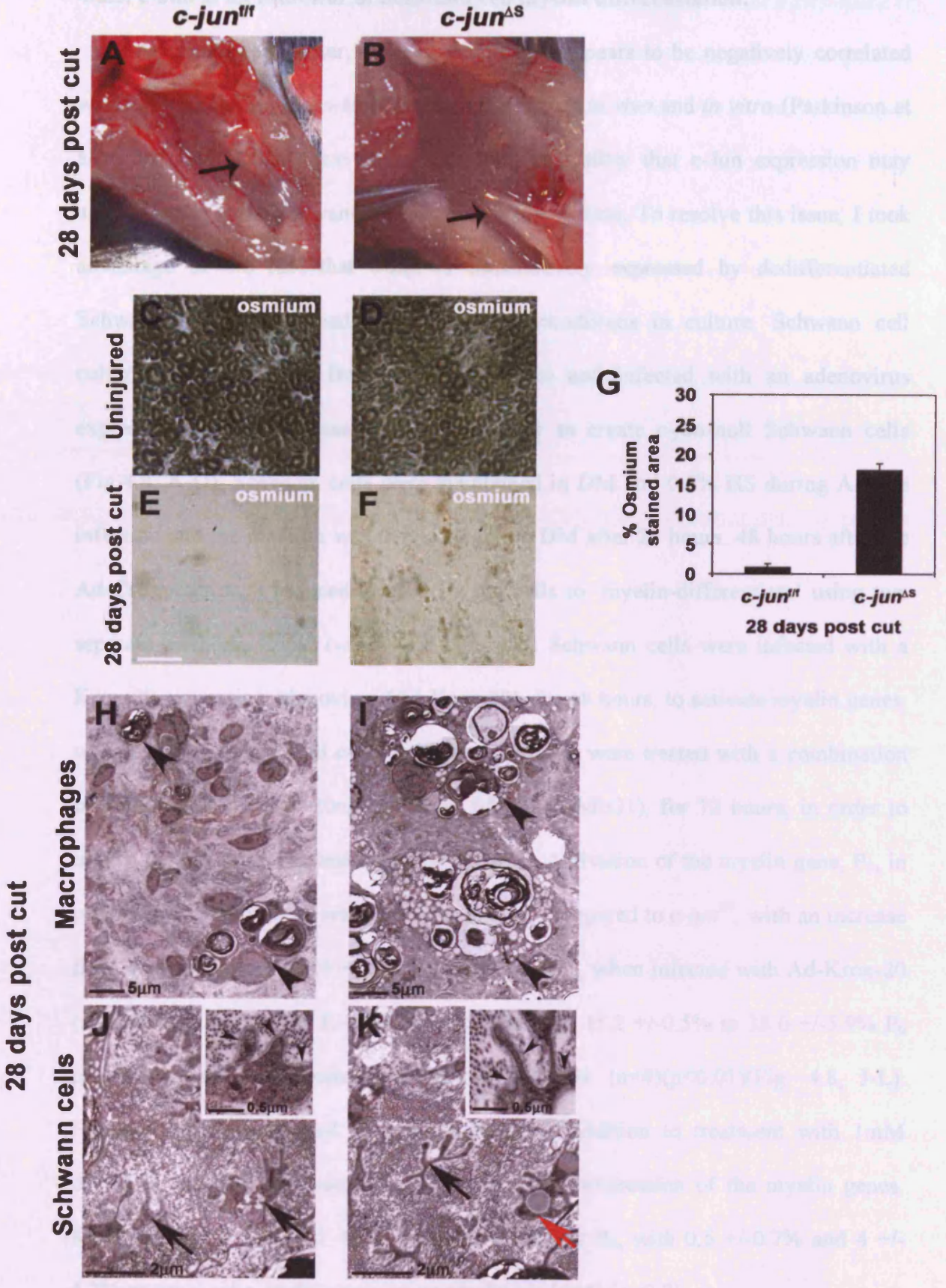
c-jun^f/f
c-jun^ΔS
28 days post cut
A
B
Uninjured
C
osmium
D
osmium
28 days post cut
E
osmium
F
osmium
G
% Osmium stained area
30
25
20
15
10
5
0
c-jun^f/f
c-jun^ΔS
28 days post cut
28 days post cut
Macrophages
H
5µm
I
5µm
Schwann cells
J
0.5µm
2µm
K
0.5µm
2µm

4.2.5. c-Jun is an inhibitor of Schwann cell myelin differentiation.

As mentioned earlier, expression of c-Jun appears to be negatively correlated with the myelinating Schwann cell phenotype, both *in vivo* and *in vitro* (Parkinson et al., 2004, 2008). This leaves the intriguing possibility that c-Jun expression may actually antagonize Schwann cell myelin differentiation. To resolve this issue, I took advantage of the fact that c-Jun is constitutively expressed by dedifferentiated Schwann cells, maintained under quiescent conditions in culture. Schwann cell cultures were prepared from *c-jun*$^{f/f}$ P5 mice and infected with an adenovirus expressing cre-recombinase (Ad-Cre) in order to create *c-jun*-null Schwann cells (Fig.4.8, A-D). Schwann cells were maintained in DM and 0.5% HS during Ad-Cre infection and the medium was then changed to DM after 24 hours. 48 hours after the Ad-Cre infection, I induced these Schwann cells to 'myelin-differentiate' using two separate methods. Some *c-jun*$^{f/f}$ and *c-jun*-null Schwann cells were infected with a Krox-20 expressing adenovirus (Ad-Krox-20), for 48 hours, to activate myelin genes, whereas other *c-jun*$^{f/f}$ and *c-jun*-null Schwann cells were treated with a combination of 1mM dbcAMP plus 20ng/ml NRG1 (dbcAMP/NRG1), for 72 hours, in order to induce myelin gene expression (see Chapter 3). Activation of the myelin gene, P_0, in *c-jun*-null Schwann cells was greatly enhanced, compared to *c-jun*$^{f/f}$, with an increase from 48.1 +/-3.0% to 79.4 +/-5.5% P_0 positive cells, when infected with Ad-Krox-20 ($n=4$)($p<0.001$)(Fig. 4.8, E-I) and an increase from 15.2 +/-0.5% to 38.6 +/-5.9% P_0 positive cells, when treated with dbcAMP/NRG1 ($n=4$)($p<0.01$)(Fig. 4.8, J-L). However, genetic removal of *c-jun* alone or in addition to treatment with 1mM dbcAMP was not sufficient to activate significant expression of the myelin genes, Krox-20, with 0 and 0.35 +/-0.1% positive cells, or P_0, with 0.5 +/-0.7% and 4 +/-4.2% positive cells, in their respective conditions ($n=4$) ($p=0.2$).

Collectively, these results demonstrate that although removal of *c-jun* alone is not sufficient to activate myelin gene expression, the constitutive endogenous expression of c-Jun in cultured mouse Schwann cells acts as a brake on myelin gene activation.

Figure 4.8: c-Jun acts as a negative regulator of myelin differentiation in cultured Schwann cells.

(A-D) Efficency of removal of *c-jun* from *c-jun*$^{f/f}$ Schwann cells (*c-jun*-null) using an adenovirus expressing cre-recombinase (Ad-Cre). (A and B) Immunocytochemistry for c-Jun in *c-jun*$^{f/f}$ and *c-jun*-null Schwann cell cultures, respectively. (C and D) Immuncytochemistry for cre-recombinase in *c-jun*$^{f/f}$ and *c-jun*-null Schwann cell cultures, respectively. Cells were co-stained with hoescht nuclear dye (Ho). In *c-jun*$^{f/f}$ cultures, 94.4 +/-4.1% of Schwann cells expressed c-Jun whereas in *c-jun*$^{f/f}$ cultures treated with Ad-Cre only 2.6 +/-0.2% of cells expressed c-Jun, 48 hours after infection (n=3). Scale bar, 50μm.

(E-H) Genetic removal of *c-jun* greatly increases expression of P_0 in Schwann cells (E and F) when infected with an adenovirus expressing Krox-20/GFP (Ad-Krox-20) (G and H). Cells were co-stained with hoescht nuclear dye (Ho). Scale bar, 50μm.

(I) The number of P_0 expressing Schwann cells in *c-jun*$^{f/f}$ and *c-jun*-null Schwann cells 48 hours after infection with Ad-Krox-20. Error bars show the standard deviation of the mean.

(J and K) Enhanced P_0 expression by *c-jun*-null Schwann cells, in comparison to *c-jun*$^{f/f}$ Schwann cells, when cultures were treated with 1mM dbcAMP and 20ng/ml of NRG-1 (dbcAMP/NRG1) for 72 hours. Cells were co-stained with hoescht nuclear dye (Ho). Scale bar, 50μm.

(L) The number of P_0 expressing Schwann cells in *c-jun*$^{f/f}$ and *c-jun*-null Schwann cells 72 hours after treatment with dbcAMP/NRG1. Error bars show the standard deviation of the mean.

Figure 4.8

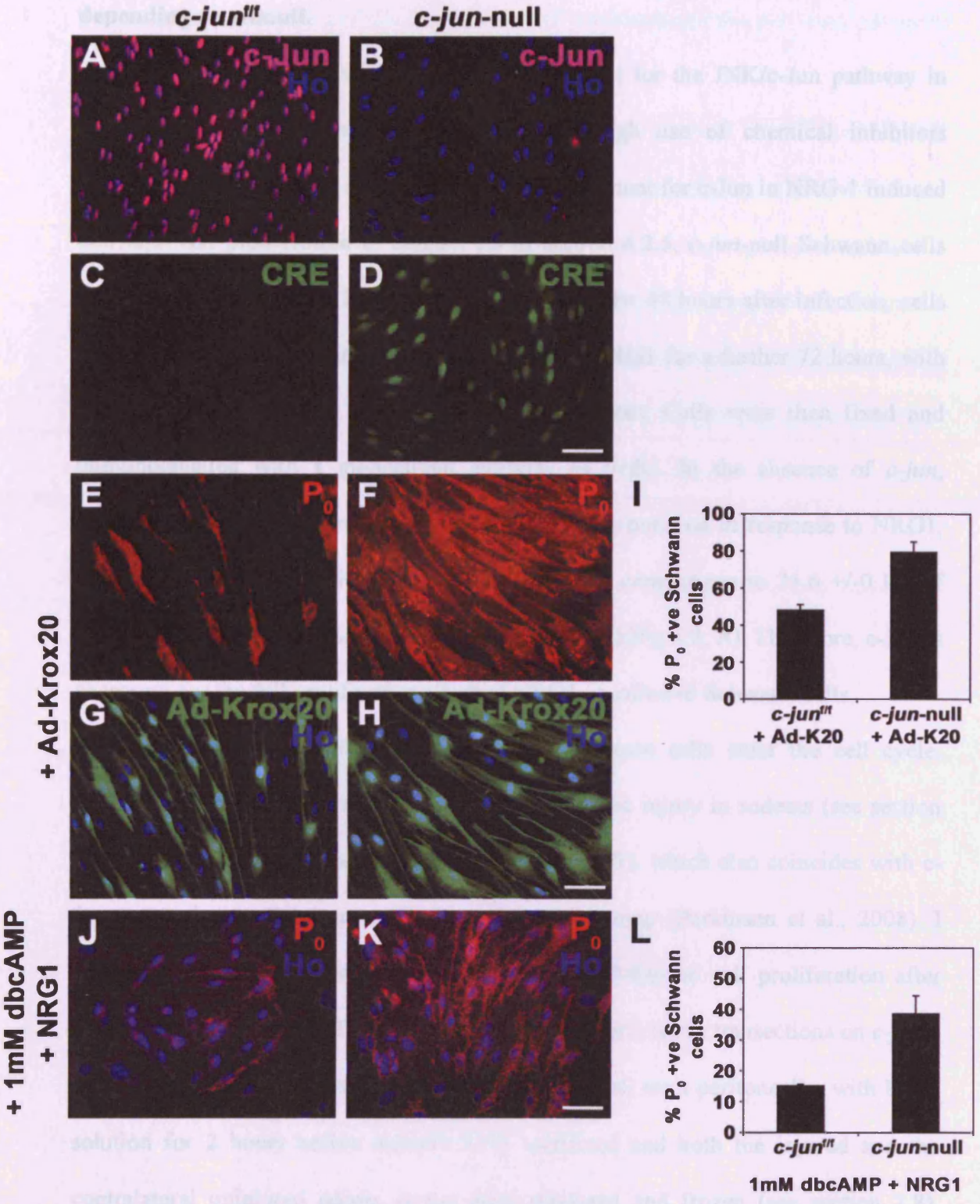
c-jun f/f
c-jun-null
A
c-Jun
Ho
B
c-Jun
Ho
C
CRE
D
CRE
E
P0
F
P0
+ Ad-Krox20
G
Ad-Krox20
Ho
H
Ad-Krox20
Ho
+ 1mM dbcAMP
+ NRG1
J
P0
Ho
K
P0
Ho
I
% P0 +ve Schwann cells
100
80
60
40
20
0
c-jun f/f
+ Ad-K20
c-jun-null
+ Ad-K20
L
% P0 +ve Schwann cells
60
50
40
30
20
10
0
c-jun f/f
c-jun-null
1mM dbcAMP + NRG1

4.2.6. Differential requirements for *c-jun* in Schwann cell proliferation, depending on stimuli.

Previous studies have identified a requirement for the JNK/c-Jun pathway in NRG1 induced Schwann cell proliferation, through use of chemical inhibitors (Parkinson et al., 2004). I decided to test the requirement for c-Jun in NRG-1 induced Schwann cell proliferation in culture. As in section 4.2.5, *c-jun*-null Schwann cells were created by infecting P5 *c-jun*$^{f/f}$ cells with Ad-Cre. 48 hours after infection, cells were maintained in DM and treated with 20ng/ml NRG1 for a further 72 hours, with BrdU added for the last 24 hours of the experiment. Cells were then fixed and immunolabelled with a monoclonal antibody to BrdU. In the absence of *c-jun*, Schwann cells showed a reduced level of BrdU incorporation in response to NRG1, with 51.3 +/-2.4% of BrdU positive *c-jun*$^{f/f}$ cells in comparison to 25.6 +/-0.1% of BrdU positive *c-jun*-null Schwann cells (n=3)($p<0.05$)(Fig.4.9, A). Therefore, c-Jun is necessary for the full proliferative effect of NRG1 on cultured Schwann cells.

After peripheral nerve injury, activated Schwann cells enter the cell cycle. Proliferation rates peak around 3 to 5 days after nerve injury in rodents (see section 1.6.4; Friede and Johnstone, 1967; Carroll et al., 1997), which also coincides with c-Jun expression in Schwann cells along the distal stump (Parkinson et al., 2008). I wanted to investigate whether *c-jun* had a role in Schwann cell proliferation after nerve transection *in vivo*. To test this, I performed sciatic nerve transections on *c-jun*$^{f/f}$ and *c-jun*$^{\Delta s}$. 5 days after the injury, mice were injected, intra-peritoneally, with BrdU solution for 2 hours before animals were sacrificed and both the injured and the contralateral uninjured sciatic nerves were dissected and frozen (see section 2.8). 10μm thick cryosections of nerves were cut and co-immunolabelled with a biotinylated-BrdU antibody and a S100β antibody, to recognise Schwann cells

undergoing DNA synthesis. A total of 15 separate areas over 3 different sections were analysed for each nerve and the total number of proliferating cells per $1mm^2$ of nerve was calculated.

As expected, uninjured contralateral sciaitc nerves from *c-jun*$^{f/f}$ and *c-jun*$^{\Delta s}$ showed no evidence of BrdU incorporation in endoneurial cells (n=4) (Fig.4.9, B and C). However, 5 days after sciatic nerve transection there was a large increase in BrdU incorporation in endoneurial cells yet, surprisingly, there was no significant difference in the number of BrdU positive cells between the two genotypes, with 202 +/-24 cells/mm^2 in *c-jun*$^{f/f}$ mice and 255 +/-47 cells/mm^2 in the *c-jun*$^{\Delta s}$ mice (n=4)(p=0.2, Mann-Whitney U test)(Fig.4.9, D-F). These experiments indicate that while *c-jun* is required for the full mitogenic effect of NRG1 on dedifferentiated Schwann cells in culture, *c-jun* appears to be dispensable for the induction of Schwann cell DNA synthesis after peripheral nerve injury.

Figure 4.9: *c-jun* is required for NRG1 induced Schwann cell DNA synthesis *in vitro* but is not necessary for Schwann cell proliferation after peripheral nerve injury.

(A) The percentage of Schwann cells that incorporate BrdU in *c-jun*$^{f/f}$ and *c-jun*-null (*c-jun*$^{f/f}$ + Ad-Cre) cultures, when treated with the mitogen NRG1 for 72 hours. Error bars show the standard deviation of the mean. Note lower rates of DNA synthesis in *c-jun*-null Schwann cells.

(B-E) Immunohistochemistry for BrdU and S100β on *c-jun*$^{f/f}$ and *c-jun*$^{\Delta s}$ uninjured nerves (B and C) and nerves 5 days after sciatic nerve transection at 5mm distal to the injury site (D and E). Scale bar, 50μm.

(F) The number of BrdU positive nuclei per 1mm^2 of nerve, 5 days after sciatic nerve transection, at 5mm distal to the injury site. Error bars show the standard deviation of the mean. Note that there is no significant difference in the rates of DNA synthesis between control and *c-jun*$^{\Delta s}$ Schwann cells within the distal stump.

Figure 4.9

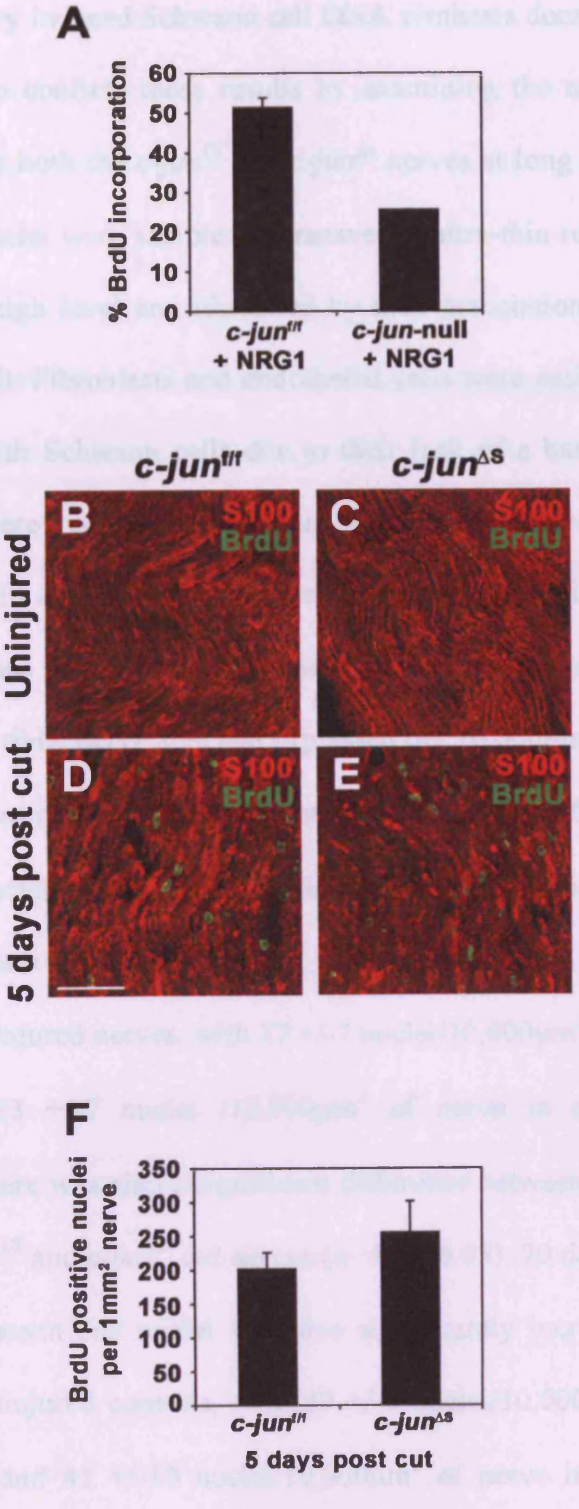
A
% BrdU incorporation
60
50
40
30
20
10
0
c-jun^f/f + NRG1
c-jun-null + NRG1
c-jun^f/f
c-jun^ΔS
Uninjured
5 days post cut
B
S100
BrdU
C
S100
BrdU
D
S100
BrdU
E
S100
BrdU
F
BrdU positive nuclei per 1mm² nerve
350
300
250
200
150
100
50
0
c-jun^f/f
c-jun^ΔS
5 days post cut

4.2.7. In the chronically injured peripheral nerve, Schwann cell number is reduced in the absence of *c-jun*.

Since injury induced Schwann cell DNA synthesis does not appear to require *c-jun*, I wanted to confirm these results by examining the number of Schwann cell nuclei present in both the *c-jun*$^{f/f}$ and *c-jun*$^{\Delta s}$ nerves at long time points after injury. Schwann cell nuclei were sampled in transverse, ultra-thin resin sections of the tibial nerve, at mid thigh level and identified by their association with basal lamina (see Fig.4.7, H and I). Fibroblasts and endothelial cells were easily identifiable and were not confused with Schwann cells due to their lack of a basal lamina. Furthermore, macrophages were recognized by their multiple processes, condensed peripheral nuclear chromatin and frequently they contained multiple digestion chambers full of myelin debris (see Fig.4.7, J and K). Schwann cell numbers were then standardised against the total tibial nerve area and expressed per 10,000μm^2 of nerve.

In uninjured *c-jun*$^{f/f}$ and *c-jun*$^{\Delta s}$ nerves there was no difference in the number of Schwann cell nuclei, with 11 +/-2 nuclei/10,000μm^2 of nerve in both genotypes (n=3). 28 days after nerve cut, there was a significant increase in Schwann cell nuclei compared to uninjured nerves, with 37 +/-7 nuclei/10,000μm^2 of nerve in *c-jun*$^{f/f}$ mice ($p<0.01$) and 23 +/-7 nuclei /10,000μm^2 of nerve in *c-jun*$^{\Delta s}$ mice ($p<0.05$). Interestingly, there was also a significant difference between the number of nuclei at 28 days in *c-jun*$^{f/f}$ and *c-jun*$^{\Delta s}$ cut nerves (n=4)($p<0.05$). 70 days after nerve crush, the number of Schwann cell nuclei was also significantly increased in both genotypes compared to uninjured controls, with 49 +/-8 nuclei/10,000μm^2 of nerve in *c-jun*$^{f/f}$ mice ($p<0.01$) and 41 +/-10 nuclei/10,000μm^2 of nerve in *c-jun*$^{\Delta s}$ mice ($p<0.01$). However, there was no significant difference between Schwann cell nuclei number between *c-jun*$^{f/f}$ and *c-jun*$^{\Delta s}$ nerves, 70 days after nerve crush (n=5)($p=0.2$)(Fig.4.10,

A). These results demonstrate that, although there is an increase in Schwann cell number in both *c-jun*$^{f/f}$ and *c-jun*$^{\Delta s}$ nerves after nerve cut and crush compared to uninjured nerves, there are relatively fewer Schwann cells in *c-jun*$^{\Delta s}$ cut nerves compared to *c-jun*$^{f/f}$ cut nerves, 28 days after transection. However, 70 days after nerve crush there are similar numbers of Schwann cells in the distal stump of *c-jun*$^{f/f}$ and *c-jun*$^{\Delta s}$ animals.

The above results were surprising, especially given that there was no difference in Schwann cell proliferation rates, 5 days after nerve cut, in the absence of *c-jun* (section 4.2.6). However, recent findings have shown that adult mouse Schwann cells are susceptible to apoptotic death after peripheral nerve injury, particularly after nerve cut (Yang et al., 2008). Thus, it was important to check whether there was increased apoptosis in the *c-jun*$^{\Delta s}$ nerve after transection, which might explain the reduction in Schwann cell nuclei at 28 days after cut. To investigate this possibility, *c-jun*$^{f/f}$ and *c-jun*$^{\Delta s}$ nerves were cut and 5 days after the operation, a time point reported to be the peak of Schwann cell apoptotic death (Yang et al., 2008), nerves were dissected and frozen. 10μm-thick cryosections were cut and immunolabelled using the TUNEL technique to detect nuclear fragmentation (see section 2.12). In *c-jun*$^{f/f}$ and *c-jun*$^{\Delta s}$ uninjured nerves, no TUNEL positive nuclei were detected (data not shown), whereas 5 days after nerve cut, 1 +/-0.6% of cells were TUNEL positive in *c-jun*$^{f/f}$ mice and 0.8 +/-0.1% of cells were TUNEL positive in *c-jun*$^{\Delta s}$ mice. However there was no statistical difference between the two genotypes (n=3)(Fig.4.10, B). Thus, without *c-jun* there is no significant change in immediate Schwann cell apoptosis, 5 days after sciatic nerve transection in adult mice.

Figure 4.10: Schwann cell number and rate of apoptosis after nerve injury, in *c-jun*$^{f/f}$ and *c-jun*$^{\Delta s}$ animals.

(A) The number of Schwann cell nuclei in uninjured sciatic nerves, sciatic nerves 28 days after nerve transection and 70 days after nerve crush, in *c-jun*$^{f/f}$ and *c-jun*$^{\Delta s}$ mice. Error bars show the standard deviation of the mean. Statistical significance was determined by the Mann-Whitney U test.

(B) The percentage of TUNEL positive cells in the sciatic nerve of *c-jun*$^{f/f}$ and *c-jun*$^{\Delta s}$ mice, 5 days after transection at 5mm from the site of injury. Error bars show the standard deviation of the mean. Statistical significance was determined by the Mann-Whitney U test.

Figure 4.10

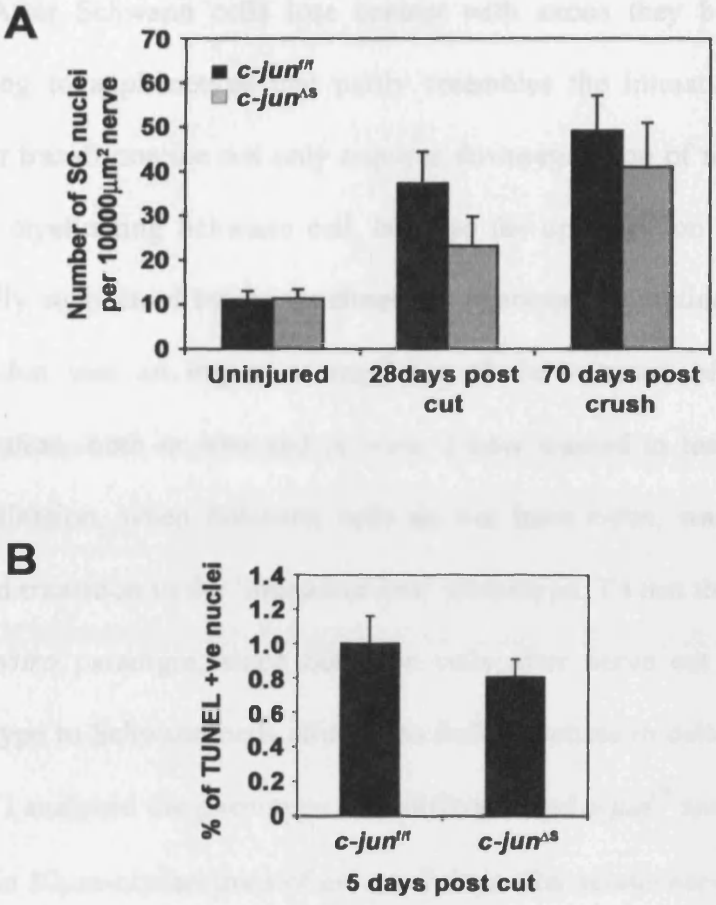
A
Number of SC nuclei per 10000μm² nerve
70
60
50
40
30
20
10
0
c-jun^fl
c-jun^ΔS
Uninjured
28days post cut
70 days post crush
B
% of TUNEL +ve nuclei
1.4
1.2
1.0
0.8
0.6
0.4
0.2
0
c-jun^fl
c-jun^ΔS
5 days post cut

4.2.8. Schwann cell dedifferentiation is retarded in the absence of *c-jun*.

After Schwann cells lose contact with axons they begin to dedifferentiate, returning to a phenotype that partly resembles the immature Schwann cell. This cellular transformation not only requires downregulation of myelin-associated genes, by the myelinating Schwann cell, but also the upregulation of many genes that are normally suppressed by the myelinating phenotype. In section, 4.2.4, I demonstrated that c-Jun was an important regulator of the removal of myelin proteins after denervation, both *in vivo* and *in vitro*. I now wanted to test whether this delay in demyelination, when Schwann cells do not have *c-jun*, was also accompanied by delayed transition to the 'immature-like' phenotype. To test this, I used an *in vivo* and an *in vitro* paradigm, since Schwann cells after nerve cut display a very similar phenotype to Schwann cells allowed to dedifferentiate in culture (Jessen and Mirsky, 2005). I analysed the phenotype of dedifferentiated *c-jun*$^{f/f}$ and *c-jun*$^{\Delta s}$ Schwann cells, either in 10μm-cryosections of nerves, 7 days after sciatic nerve transection, or during a 10 day demyelination assay in culture (see section 4.2.4.3). Both sections and cell cultures were immunolabelled with antibodies to L1, N-cadherin, p75^{NTR} and NCAM, all markers that are re-expressed during Schwann cell dedifferentiation (see Chapter 1).

In the *c-jun*$^{\Delta s}$ nerve, 7 days after nerve transection, Schwann cells in the distal stump expressed recognizably lower levels of the adhesion molecule L1, compared to *c-jun*$^{f/f}$ Schwann cells (Fig.4.11, A and B). Similarly, after 10 days in culture only 47.8 +/-2.3% of *c-jun*$^{\Delta s}$ Schwann cells managed to re-express L1 protein compared to 94.7 +/-3.9% of *c-jun*$^{f/f}$ Schwann cells ($n=5$)($p<0.0001$)(Fig.4.11, C-G). Furthermore, Schwann cells in the *c-jun*$^{\Delta s}$ nerve were unable to induce normal levels of expression of N-cadherin, 7 days after nerve transection (Fig.4.12, A and B).

Figure 4.11: *c-jun*$^{\Delta s}$ Schwann cells fail to properly re-express L1 after denervation.

(A and B) Confocal images of immunohistochemistry for the adhesion molecule, L1 in *c-jun*$^{f/f}$ and *c-jun*$^{\Delta s}$ nerves, 7 days after sciatic nerve transection, at a distance of 5mm from the site of injury. Sections are co-stained with hoescht nuclear dye (Ho). Scale bar, 50μm.

(C-F) Dissociated Schwann cells from *c-jun*$^{f/f}$ and *c-jun*$^{\Delta s}$ P8 nerves, after 10 days in culture. Cells are labelled with antibodies to the Schwann cell marker, S100β and to L1 and also with hoescht nuclear stain (Ho). (D and F) Arrowheads demonstrate *c-jun*$^{\Delta s}$ Schwann cells, positive for S100β, that do not express L1. Scale bar, 50μm.

(G) The percentage of L1 positive *c-jun*$^{f/f}$ and *c-jun*$^{\Delta s}$ Schwann cells over a 10day period of culturing. Error bars show the standard deviation of the mean. Statistical significance was determined using two-way ANOVA and the unpaired students t-test.

Figure 4.11

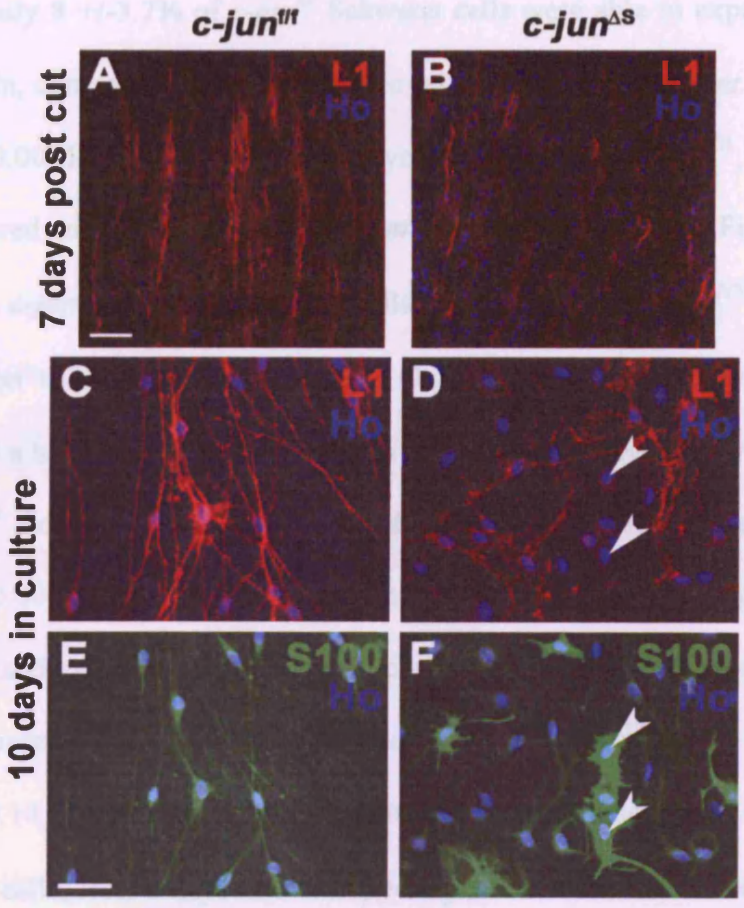
c-jun^f/f
c-jun^ΔS
7 days post cut
10 days in culture
A
B
C
D
E
F
L1
S100
Ho

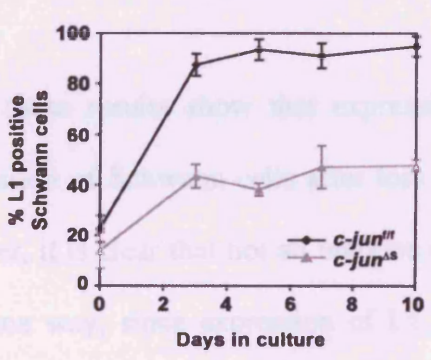
G
% L1 positive Schwann cells
Days in culture
c-jun^f/f
c-jun^ΔS
0
20
40
60
80
100
0
2
4
6
8
10

When I examined the expression of N-cadherin in Schwann cells in culture, I found that although all *c-jun*$^{\Delta s}$ Schwann cells managed to re-express some N-cadherin protein, only 8 +/-3.7% of *c-jun*$^{\Delta s}$ Schwann cells were able to express high levels of N-cadherin, compared to 84 +/-3.7% of *c-jun*$^{f/f}$ Schwann cells, after 10 days in culture (n=4)($p<0.0001$)(Fig.4.12, C-E). The level of expression of p75^{NTR}, 7 days after nerve cut appeared to be similar in both *c-jun*$^{f/f}$ and *c-jun*$^{\Delta s}$ animals (Fig.4.13, A and B). However, *c-jun*$^{\Delta s}$ cultured Schwann cells showed defects in p75^{NTR} upregulation, in comparison to *c-jun*$^{f/f}$ Schwann cells. Only 58.9 +/-5% of *c-jun*$^{\Delta s}$ Schwann cells expressed a high level of p75^{NTR} protein after 10 days in culture, whereas 99 +/-1.7% of *c-jun*$^{f/f}$ Schwann cells demonstrated strong p75^{NTR} staining at this time point (n=4)($p<0.0001$)(Fig.4.13, C-G). In contrast to the impaired upregulation of L1, N-cadherin and p75^{NTR}, in *c-jun*-null Schwann cells, NCAM appeared to be more strongly upregulated in the *c-jun*$^{\Delta s}$ nerve than in the *c-jun*$^{f/f}$ nerve, 5 days after nerve cut (Fig.4.14, A and B). Additionally, NCAM was expressed by all *c-jun*$^{f/f}$ and *c-jun*$^{\Delta s}$ Schwann cells, after 3 days in culture, yet *c-jun*$^{\Delta s}$ Schwann cells always demonstrated much stronger staining for NCAM than *c-jun*$^{f/f}$ cells at all time points investigated (Fig.4.14, C and D).

In summary, these results show that expression of c-Jun is critical for the normal dedifferentiation of Schwann cells after loss of axonal contact, both *in vitro* and *in vivo*. However, it is clear that not all markers of denervated Schwann cells are regulated in the same way, since expression of L1, N-cadherin and p75^{NTR} are all reduced in the absence of *c-jun* whereas NCAM appears to be upregulated.

Figure 4.12: Re-expression of N-cadherin in *c-jun*$^{\Delta s}$ Schwann cells is perturbed after denervation.

(A and B) Confocal images of immunohistochemistry for the adhesion molecule, N-cadherin in *c-jun*$^{f/f}$ and *c-jun*$^{\Delta s}$ nerves, 7 days after sciatic nerve transection, at a distance of 5mm from the site of injury. Sections are co-stained with hoescht nuclear dye (Ho). Scale bar, 50μm.

(C and D) Dissociated Schwann cells from *c-jun*$^{f/f}$ and *c-jun*$^{\Delta s}$ P8 nerves, after 10 days in culture. Cells are labelled with an antibody to N-cadherin and also with hoescht nuclear stain (Ho). (D) Arrowheads demonstrate *c-jun*$^{\Delta s}$ Schwann cells that only express a low level of N-cadherin compared to *c-jun*$^{f/f}$ cells in (C). Scale bar, 50μm.

(G) The percentage of N-cadherin positive *c-jun*$^{f/f}$ and *c-jun*$^{\Delta s}$ Schwann cells over a 10day period of culturing. Error bars show the standard deviation of the mean. Statistical significance was determined using two-way ANOVA and the unpaired students t-test.

Figure 4.12

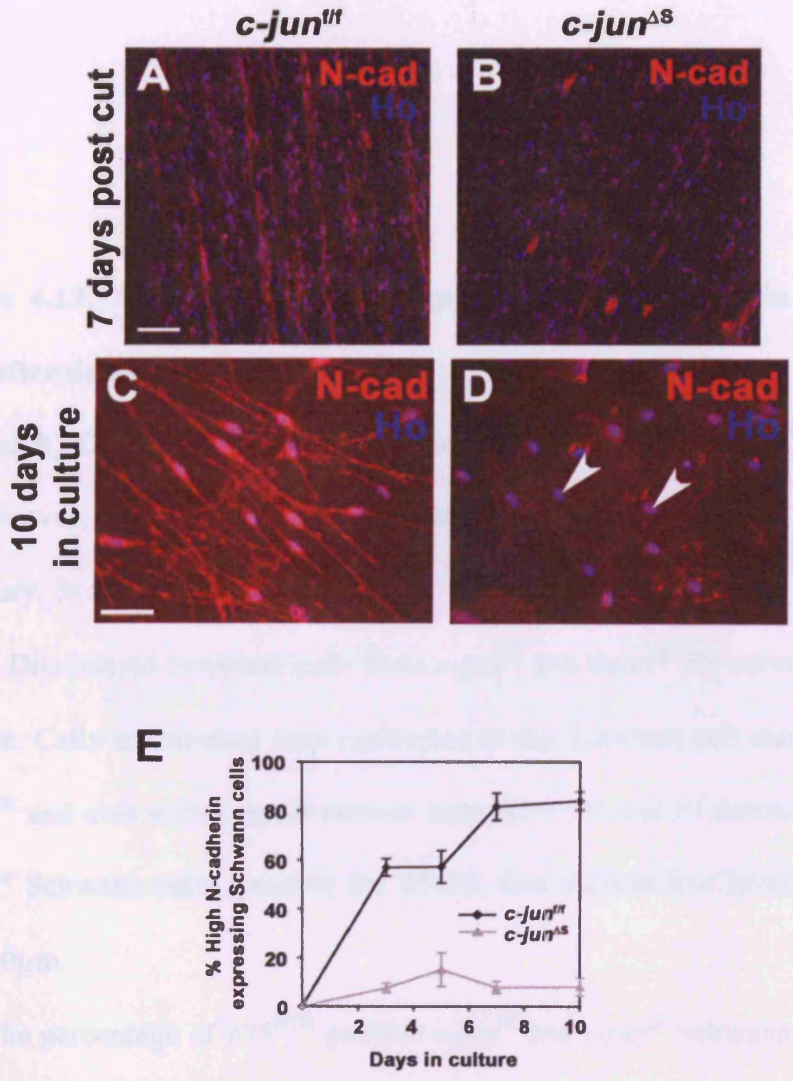
c-jun^f/f
c-jun^ΔS
7 days post cut
10 days in culture
A
B
C
D
N-cad
Ho
E
% High N-cadherin expressing Schwann cells
Days in culture
c-jun^f/f
c-jun^ΔS
0
20
40
60
80
100
2
4
6
8
10

Figure 4.13: Abnormalities in the up-regulation of $p75^{NTR}$ in *c-jun*$^{\Delta s}$ Schwann cells after denervation.

(A and B) Confocal images of immunohistochemistry for $p75^{NTR}$ in *c-jun*$^{f/f}$ and *c-jun*$^{\Delta s}$ nerves, 7 days after sciatic nerve transection, at a distance of 5mm from the site of injury. Scale bar, 50μm.

(C-F) Dissociated Schwann cells from *c-jun*$^{f/f}$ and *c-jun*$^{\Delta s}$ P8 nerves, after 10 days in culture. Cells are labelled with antibodies to the Schwann cell marker, S100β and to $p75^{NTR}$ and also with hoescht nuclear stain (Ho). (D and F) Arrowheads demonstrate *c-jun*$^{\Delta s}$ Schwann cells, positive for S100β, that express low levels of $p75^{NTR}$. Scale bar, 50μm.

(G) The percentage of $p75^{NTR}$ positive *c-jun*$^{f/f}$ and *c-jun*$^{\Delta s}$ Schwann cells over a 10day period of culturing. Error bars show the standard deviation of the mean. Statistical significance was determined using two-way ANOVA and the unpaired students t-test.

Figure 4.13

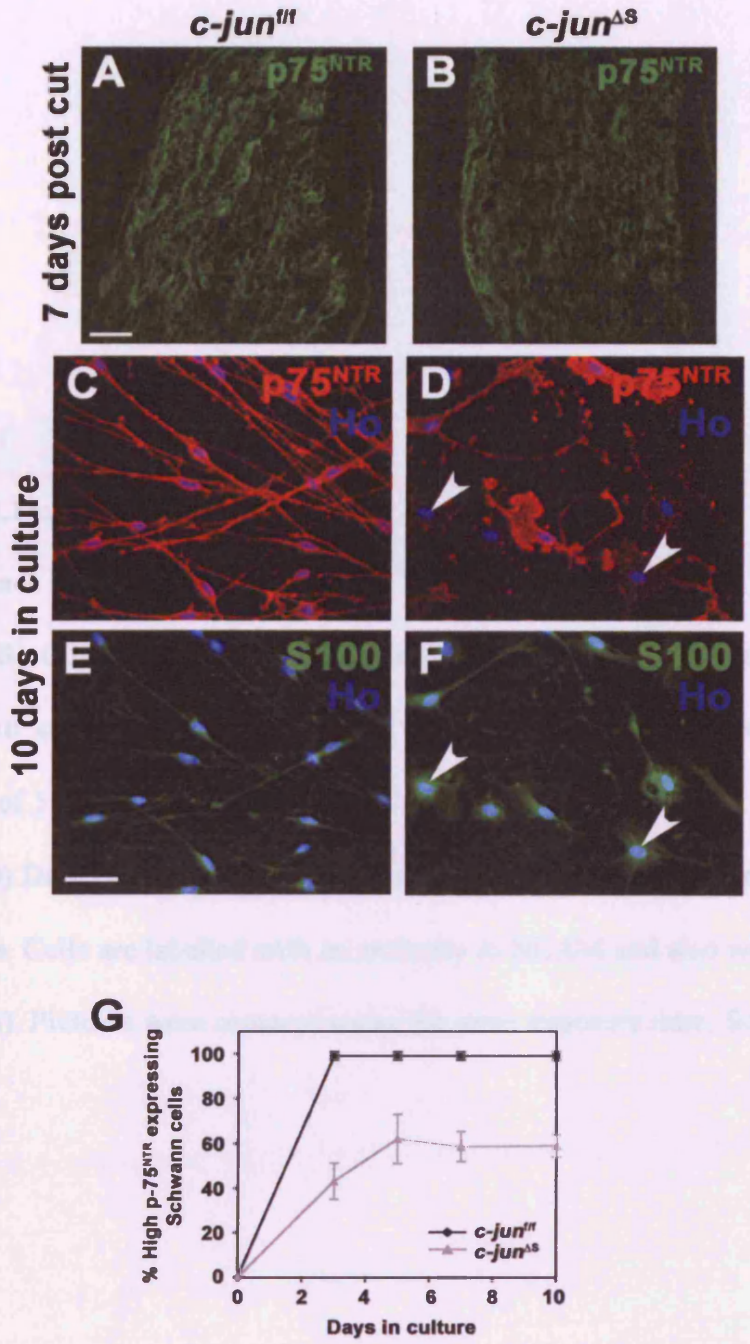
c-jun^fl/fl
c-jun^ΔS
7 days post cut
10 days in culture
A
p75NTR
B
p75NTR
C
p75NTR
Ho
D
p75NTR
Ho
E
S100
Ho
F
S100
Ho
G
% High p-75NTR expressing Schwann cells
100
80
60
40
20
0
0
2
4
6
8
10
Days in culture
c-jun^fl
c-jun^ΔS

Figure 4.14: NCAM is more strongly expressed by denervated Schwann cells, in the absence of *c-jun*.

(A and B) Confocal images of immunohistochemistry for the adhesion molecule, NCAM in *c-jun*$^{f/f}$ and *c-jun*$^{\Delta s}$ nerves, 5 days after sciatic nerve transection, at a distance of 5mm from the site of injury. Scale bar, 50μm.

(C and D) Dissociated Schwann cells from *c-jun*$^{f/f}$ and *c-jun*$^{\Delta s}$ P8 nerves, after 10 days in culture. Cells are labelled with an antibody to NCAM and also with hoescht nuclear stain (Ho). Pictures were captured using the same exposure time. Scale bar, 50μm.

Figure 4.14

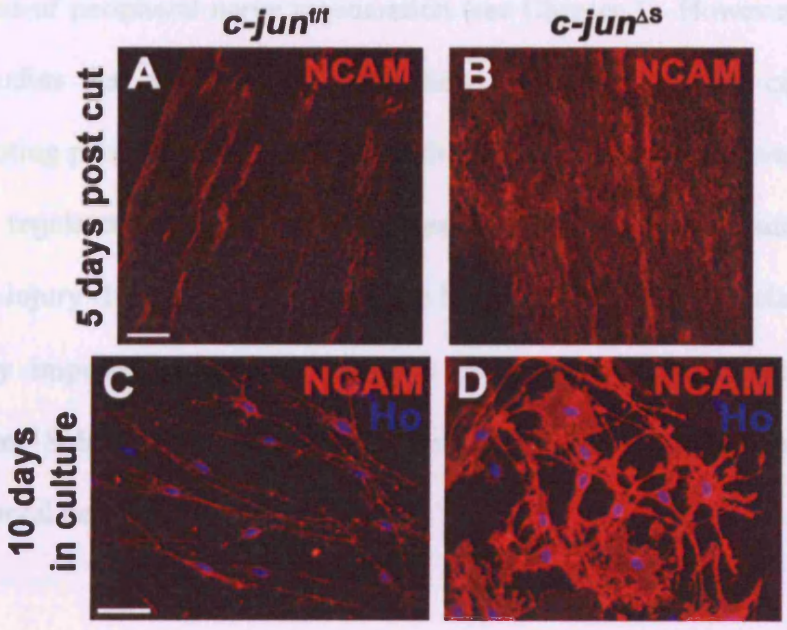
c-jun^fl/fl
c-jun^ΔS
A
NCAM
B
NCAM
5 days post cut
C
NCAM
Ho
D
NCAM
Ho
10 days
in culture

4.2.9. The role of Schwann cell derived *c-jun* in peripheral nerve regeneration

The reaction of the Schwann cell to injury is thought to underlie much of the success of peripheral nerve regeneration (see Chapter 1). However, to date, there are no studies that clearly demonstrate how important Schwann cell activation is in promoting peripheral nerve injury. In the previous sections, I have identified *c-jun* as a key regulator of Schwann cell demyelination and dedifferentiation after peripheral nerve injury. In the *c-jun*$^{\Delta s}$ mice, these key events during Wallerian degeneration are greatly impeded. Thus, this provided me with a unique situation to investigate whether Schwann cell activation after nerve injury was necessary for successful peripheral nerve regeneration.

4.2.9.1. Both motor and sensory functional recovery after sciatic nerve crush are severely impaired in *c-jun*$^{\Delta s}$ mice.

To analyse peripheral nerve regeneration in *c-jun*$^{f/f}$ and *c-jun*$^{\Delta s}$ mice, right sciatic nerve crushes were performed at the level of the sciatic notch. Nerve crush was used instead of nerve transection as the experimental paradigm in this situation since nerve crush, while effectively destroying all axons distally, maintains the structural connection between the proximal and distal stumps, including the Schwann cell basal lamina tubes. This allows for faster axonal regeneration and better functional recovery after injury, compared to nerve transection (Nguyen et al., 2002; Raivich and Makwana, 2007). Functional recovery after sciatic nerve crush was measured by two methods. Firstly, the presence of a toe-spreading reflex was recorded after, both *c-jun*$^{f/f}$ and *c-jun*$^{\Delta s}$ mice, were lifted gently by the tail (Gutmann et al., 1942; Siconolfi and Seeds, 2001). Mice demonstrating full extension of the hind limb and full extension and abduction of all five toes so that clear space can be seen between each

toe were given a toe-spreading reflex score of 2. Whereas, mice that showed a partial toe spreading reflex, such as improper hind limb extension or only abduction and extension of some but not all five toes were given a toe-spreading reflex score of 1. Mice that showed no abduction of all 5 toes, in response to being lifted by their tail, were given a score of 0. Secondly, recovery of pressure and pain sensitivity was tested on *c-jun*$^{f/f}$ and *c-jun*$^{\Delta s}$ mice, by pinching the most distal part of the lateral three toes, which derive sensation from the sciatic nerve, on both uninjured and injured limbs, with a number 5 forceps. Hind limb withdrawal and/or vocalization were recorded as positive responses, demonstrating functional sensory regeneration after injury (Siconolfi and Seeds, 2001). Both tests were performed before surgery to test that all mice responded normally in an uninjured situation and immediately after surgery, when mice were awake, to check that the operation had successfully removed all sciatic nerve function prior to regeneration. Mice were then tested every two to three days up until 30 days after surgery, at this point mice were then tested once a week up until 70 days after surgery.

For the toe-spreading reflex test, *c-jun*$^{\Delta s}$ mice showed a strong impairment in regaining a normal toe spread. Whereas, all *c-jun*$^{f/f}$ mice (n=11), obtained a score of 2 by day 23, even at day 70 only 1 out of 8 of the *c-jun*$^{\Delta s}$ mice achieved a score of 2, with the remaining *c-jun*$^{\Delta s}$ mice scoring 1 ($p<0.0001$, two-way ANOVA)(Fig.4.15, A). Most *c-jun*$^{\Delta s}$ mice always showed some impairment throughout the analysis, often abducting some but not all of their toes on the injured limb. At later stages of the experiment, *c-jun*$^{\Delta s}$ mice, unlike *c-jun*$^{f/f}$ mice, would initially withhold extension of their hind limb in response to being lifted by the tail. Furthermore, the hind paw on the injured side of *c-jun*$^{\Delta s}$ mice usually adopted a 'claw-paw' phenotype. (Fig.4.15, B and C). The data from the toe-reflex test can also be illustrated by time taken until the

first response, which is sustained thereafter in subsequent tests. In this case a score of 1 or 2 was counted as a response. Thus, *c-jun*$^{f/f}$ animals achieved a positive response by day 10 +/-2, whereas *c-jun*$^{\Delta s}$ mice showed a positive response by day 17 +/-2 (n=7)($p<0.01$, Mann-Whitney U test)(Fig.4.15, D). This demonstrates that the general reinnervation of the hind paw is delayed in *c-jun*$^{\Delta s}$ mice compared to *c-jun*$^{f/f}$ animals.

Recovery of toe pinch responses in the lateral three toes of *c-jun*$^{\Delta s}$ mice showed a greater functional impairment than in the toe reflex tests. *c-jun*$^{f/f}$ animals achieved a positive response in toe 3 by day 18 +/-5, toe 4 by day 20 +/-4 and toe 5 by day 23 +/-7. In contrast, 6 out of 8 *c-jun*$^{\Delta s}$ mice never showed a positive response when toes 3 and 4 were pinched and 8 out 8 *c-jun*$^{\Delta s}$ mice never showed a positive response when toe 5 was pinched, over the entire 70 day period of analysis ($p<0.01$, two-way ANOVA).

Together, this data demonstrates that in the absence of *c-jun* in Schwann cells, the peripheral nerve is no longer capable of promoting successful regeneration and functional recovery after sciatic nerve crush.

Figure 4.15: Recovery of both motor and sensory function is severely impeded after sciatic nerve crush, in *c-jun*$^{\Delta s}$ mice.

(A) The percentage of *c-jun*$^{f/f}$ (n=11) and *c-jun*$^{\Delta s}$ (n=8) mice analysed that achieved a toe spreading reflex score of 2 at various time points over a 70 day period. Comparison of toe reflex scores between *c-jun*$^{f/f}$ and *c-jun*$^{\Delta s}$ mice at each time point showed a statistical difference from day 12 through to day 70 ($p<0.05$). Statistical significance was determined by two-way ANOVA and unpaired student's t-test.

(B and C) Demonstration of the toe-spreading reflex in *c-jun*$^{f/f}$ and *c-jun*$^{\Delta s}$ mice, 70 days after right sciatic nerve crush. Arrows indicate toe spread on the operated limbs of both genotypes. Both uninjured and injured *c-jun*$^{f/f}$ limbs show a normal reflex. Note how the *c-jun*$^{\Delta s}$ mouse holds the injured limb in towards the body. There is also a noticeable claw paw phenotype on the paw of the injured limb whereas the uninjured limb shows a normal reflex in response to being lifted by the tail.

(D) Time taken for an initial toe spread response (a score of 1 or 2 was counted as a response) that is sustained in subsequent tests, in *c-jun*$^{f/f}$ and *c-jun*$^{\Delta s}$ mice. Error bars show the standard deviation of the mean. Statistical significance was determined by the Mann-Whitney U test.

(E-G) The percentage of *c-jun*$^{f/f}$ (n=11) and *c-jun*$^{\Delta s}$ (n=8) mice analysed that demonstrated a positive response (either foot withdrawal and/or vocalisation) to pinching of the most distal portion of toes 3, 4 and 5, at various time points over a 70 day period. Comparison of toe pinch responses between *c-jun*$^{f/f}$ and *c-jun*$^{\Delta s}$ mice, at each time point, showed a statistical difference from day 21 through to day 70 ($p<0.05$). Statistical significance was determined by two-way ANOVA and unpaired student's t-test.

Figure 4.15

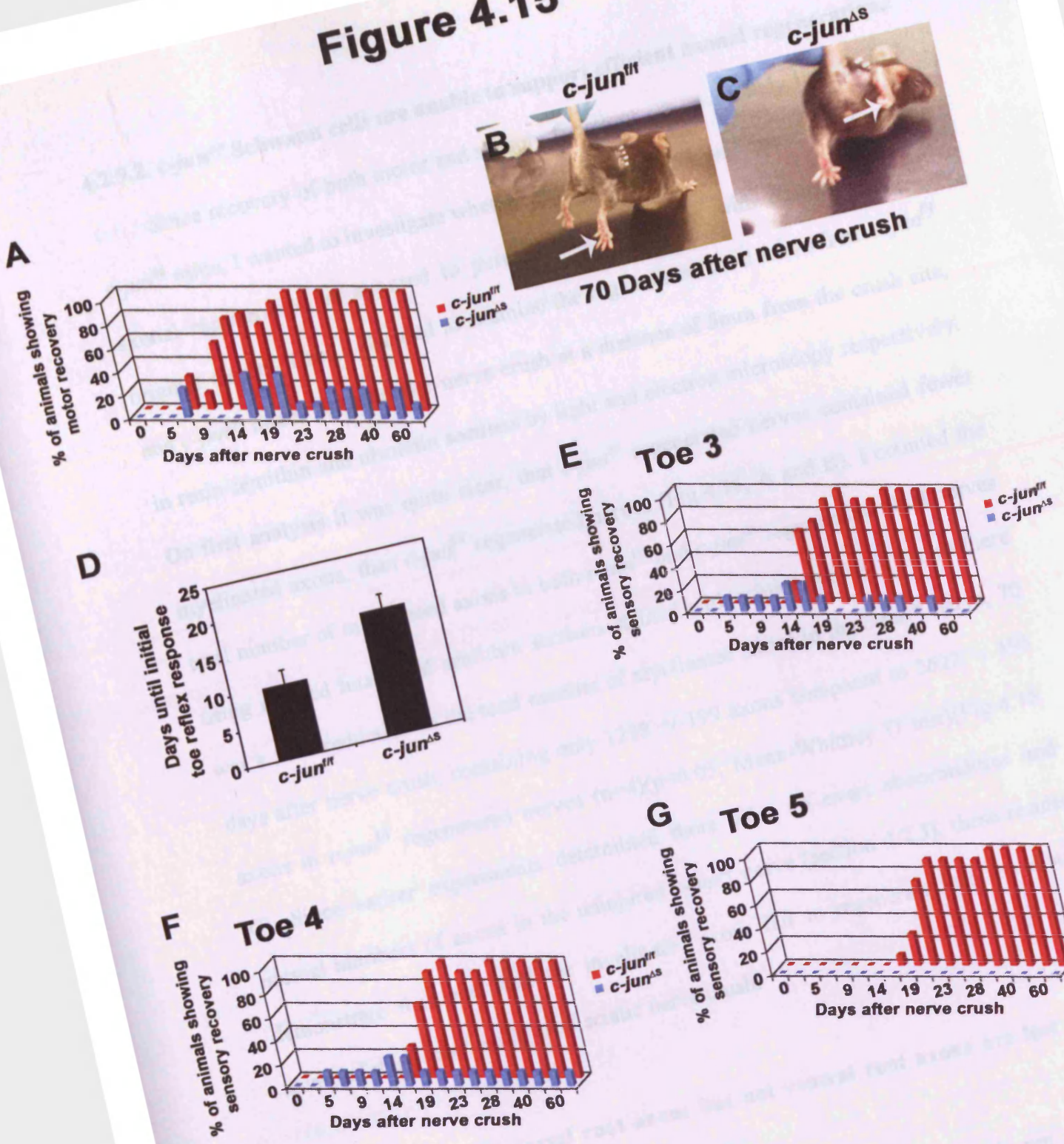
A
% of animals showing motor recovery
100
80
60
40
20
0
0 5 9 14 19 23 28 40 60
Days after nerve crush
c-jun^f/f
c-jun^ΔS
B
c-jun^f/f
C
c-jun^ΔS
70 Days after nerve crush
D
Days until initial toe reflex response
25
20
15
10
5
0
c-jun^f/f
c-jun^ΔS
E
Toe 3
% of animals showing sensory recovery
Days after nerve crush
F
Toe 4
% of animals showing sensory recovery
Days after nerve crush
G
Toe 5
% of animals showing sensory recovery
Days after nerve crush

4.2.9.2. *c-jun*$^{\Delta s}$ Schwann cells are unable to support efficient axonal regeneration.

Since recovery of both motor and sensory functions are so strongly impeded in *c-jun*$^{\Delta s}$ mice, I wanted to investigate whether an element of this was due to a failure in axonal regeneration as opposed to purely being a problem with reinnervation of original targets. Thus, I decided to examine the regenerated tibial nerve from *c-jun*$^{f/f}$ and *c-jun*$^{\Delta s}$ mice, 70 days after nerve crush at a distance of 5mm from the crush site, in resin semithin and ultrathin sections by light and electron microscopy respectively. On first analysis it was quite clear, that *c-jun*$^{\Delta s}$ regenerated nerves contained fewer myelinated axons, than *c-jun*$^{f/f}$ regenerated nerves (Fig.4.16, A and B). I counted the total number of myelinated axons in both *c-jun*$^{f/f}$ and *c-jun*$^{\Delta s}$ regenerated tibial nerves using merged images of semithin sections stained with toluidine blue. I found there was a 51% reduction in the total number of myelinated axons in the *c-jun*$^{\Delta s}$ nerve, 70 days after nerve crush, containing only 1298 +/-199 axons compared to 2622 +/-195 axons in *c-jun*$^{f/f}$ regenerated nerves (n=4)($p<0.05$, Mann-Whitney U test)(Fig.4.16, C). Since earlier experiments determined there were no overt abnormalities and normal numbers of axons in the uninjured *c-jun*$^{\Delta s}$ nerve (section 4.2.3), these results demonstrate that over half the myelinated axons fail to regenerate into the distal stump of the *c-jun*$^{\Delta s}$ nerve after sciatic nerve crush.

4.2.9.3. Myelinated dorsal root axons but not ventral root axons are lost in *c-jun*$^{\Delta s}$ mice, after sciatic nerve crush.

After adult sciatic nerve cut or crush, motor neuron survival is not affected whereas there are differing rates of sensory neuron survival, dependent on the neuronal subtype (Romanes, 1946; Lowrie et al., 1994; Coggeshall et al., 1997 Tandrup et al., 2000; Ma et al., 2001; Groves et al., 2003). In the dorsal root ganglion

(DRG), the large A-cells that give rise to myelinated axons in the dorsal root and in the nerve are not susceptible to sciatic nerve injury. However, up to 50% of the small B-cells, which give rise to unmyelinated axons, are lost from the DRG by 32 weeks after either sciatic nerve cut or crush (Coggeshall et al., 1997; Tandrup et al., 2000). I therefore wanted to assess the survival rates of both motor and sensory neurons in both *c-jun*$^{f/f}$ and *c-jun*$^{\Delta s}$ mice, 70 days after sciatic nerve crush.

Motorneurons project into the sciatic nerve from spinal levels L3-L6, with the majority coming from L4 and L5 (Swett et al., 1986), whereas 98-99% of sciatic sensory neurons originate solely from the L4 and L5 DRGs (Swett et al., 1991). Counting the total number of myelinated axons in the L5 dorsal root can be used as an indication of the sensory A-cell neuronal numbers in the corresponding DRG, since one DRG neuron will project one axon into the dorsal root (Coggeshall et al., 1997). In the uninjured L5 dorsal root there were 2432 +/-262 and 2215 +/-35 myelinated axons in *c-jun*$^{f/f}$ and *c-jun*$^{\Delta s}$ mice, respectively. After sciatic nerve crush there were 2379 +/-208 myelinated axons in the *c-jun*$^{f/f}$ L5 dorsal root, suggesting that there was no loss of myelinated sensory axons after injury. In contrast, there was a dramatic loss of 36% of the myelinated axons in the *c-jun*$^{\Delta s}$ L5 dorsal root, with only 1421 +/-156 axons remaining, 70 days after sciatic nerve crush ($n=4$)($p<0.05$, Mann-Whitney U test)(Fig.4.16, D).

Closer observation of the *c-jun*$^{\Delta s}$ L5 dorsal root, 70 days after sciatic nerve crush, demonstrated that there were still signs of ongoing axon loss, including many demyelinating profiles, shrunken axons and the presence of macrophages full of myelin debris. These phenomena were rarely seen in *c-jun*$^{f/f}$ dorsal roots after nerve crush (Fig.4.16, F-H). In addition, there appear to be many abnormal unmyelinated axon profiles in the *c-jun*$^{\Delta s}$ dorsal root after nerve crush, particularly axons that are

swollen or starting to fragment. Again, these observations are not seen in the *c-jun*$^{f/f}$ dorsal roots 70 days after nerve crush, suggesting that there may be a greater loss of unmyelinated axons in *c-jun*$^{\Delta s}$ mice than is normally expected after nerve injury (Fig.4.16, I and J).

I also analysed the L5 ventral root, in order to get an assessment of the potential numbers of surviving motorneurons after sciatic nerve crush. In the uninjured *c-jun*$^{f/f}$ and *c-jun*$^{\Delta s}$ mice, there are 981 +/-79 and 973 +/-106 myelinated axons in the L5 ventral root, respectively (n=3). These numbers do not significantly change, 70 days after nerve crush, with 956 +/-44 axons in the *c-jun*$^{f/f}$ (n=6) and 942 +/-31 axons in the *c-jun*$^{\Delta s}$ (n=4) L5 ventral root (p=0.6, Mann-Whitney U test)(Fig.4.16, E).

These experiments demonstrate that potentially a large population of A-cell sensory neurons, that are not normally susceptible after peripheral nerve injury, are dying when they try to regenerate into the *c-jun*$^{\Delta s}$ distal stump after sciatic nerve crush. In addition there may also be a greater loss of small B-cell sensory neurons in *c-jun*$^{\Delta s}$ mice after nerve injury. Interestingly, although there are large defects in the dorsal roots of *c-jun*$^{\Delta s}$ mice after sciatic nerve injury, the ventral roots appear normal, which suggests that motor neuron survival is likely to be unaffected.

Figure 4.16: Myelinated axon loss in the distal stump of the tibial nerve and in the L5 dorsal root, 70 days after sciatic nerve crush in *c-jun*$^{\Delta s}$ mice.

(A and B) Electron micrographs of the *c-jun*$^{f/f}$ and *c-jun*$^{\Delta s}$ tibial nerve, 70 days after sciatic nerve crush, at a distance of 5mm from the site of injury. Note that although there are fewer myelinated axons in the *c-jun*$^{\Delta s}$ nerve, the thickness of their myelin sheaths appears similar to axons in the *c-jun*$^{f/f}$ nerve. Scale bar, 10μm.

(C) The total number of myelinated axons in both the *c-jun*$^{f/f}$ and *c-jun*$^{\Delta s}$ tibial nerve, 70 days after sciatic nerve crush, at a distance of 5mm from the site of injury. Error bars show the standard deviation of the mean.

(D) The total number of myelinated axons in L5 dorsal roots of the *c-jun*$^{f/f}$ and *c-jun*$^{\Delta s}$ mice, 70 days after sciatic nerve crush. Error bars show the standard deviation of the mean.

(E) The total number of myelinated axons in L5 ventral roots of the *c-jun*$^{f/f}$ and *c-jun*$^{\Delta s}$ mice, 70 days after sciatic nerve crush. Error bars show the standard deviation of the mean.

(F and G) Electron micrographs showing a representative field from the L5 dorsal roots of the *c-jun*$^{f/f}$ and *c-jun*$^{\Delta s}$ mice, 70 days after sciatic nerve crush. (G) Arrows point to shrunken axons, detaching from their myelin sheath. Arrowheads mark demyelinating profiles in the *c-jun*$^{\Delta s}$ dorsal root that are devoid of an axon. Neither of these phenomena appeared to be fixation artefacts since they were commonly seen in dorsal roots from 3 separate *c-jun*$^{\Delta s}$ mice and rarely observed in *c-jun*$^{f/f}$ roots (n=3), after nerve crush. Scale bar, 5μm.

(H) Electron micrograph demonstrating a macrophage, full of myelin debris, present in the *c-jun*$^{\Delta s}$ dorsal root, 70 days after sciatic nerve crush. Arrowhead marks the nucleus of the macrophage. Scale bar, 2μm.

(I and J) Electron micrographs showing unmyelinated axons in the *c-jun*$^{f/f}$ and *c-jun*$^{\Delta s}$ mice, 70 days after sciatic nerve crush. Arrowheads in (I) demonstrate normal axon profiles in the *c-jun*$^{f/f}$ dorsal root whereas arrowheads in (J) show swollen and fragmenting axons in the *c-jun*$^{\Delta s}$ dorsal root. Scale bar, 500nm.

Figure 4.16

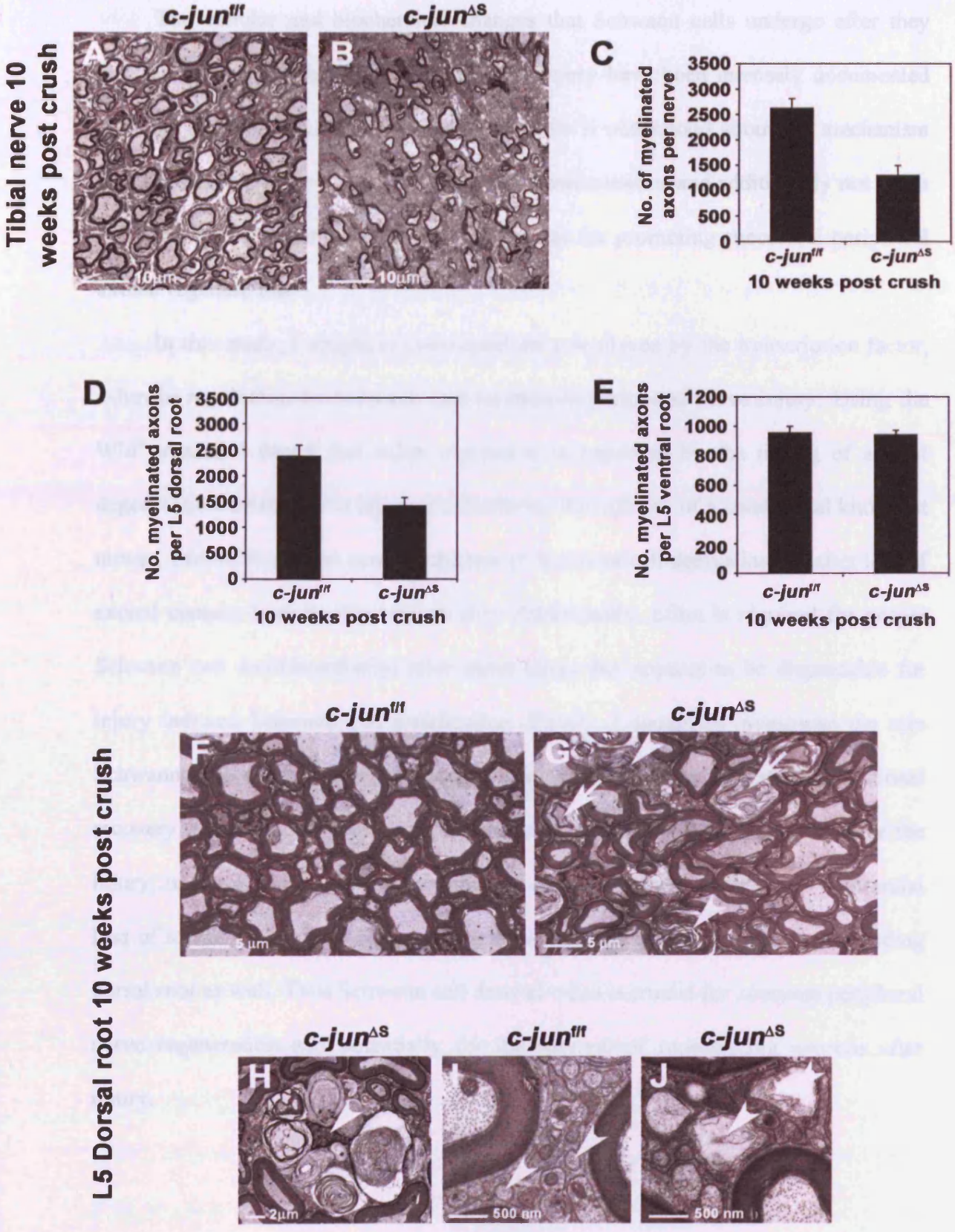
c-jun^f/f
c-jun^ΔS
Tibial nerve 10 weeks post crush
A
B
10µm
10µm
C
No. of myelinated axons per nerve
3500
3000
2500
2000
1500
1000
500
0
c-jun^f/f
c-jun^ΔS
10 weeks post crush
D
No. myelinated axons per L5 dorsal root
3500
3000
2500
2000
1500
1000
500
0
c-jun^f/f
c-jun^ΔS
10 weeks post crush
E
No. myelinated axons per L5 ventral root
1200
1000
800
600
400
200
0
c-jun^f/f
c-jun^ΔS
10 weeks post crush
L5 Dorsal root 10 weeks post crush
c-jun^f/f
c-jun^ΔS
F
G
5 µm
5 µm
c-jun^ΔS
c-jun^f/f
c-jun^ΔS
H
I
J
2µm
500 nm
500 nm

4.3 DISCUSSION

The cellular and biochemical changes that Schwann cells undergo after they lose axonal contact during peripheral nerve injury have been intensely documented over the last 50 years. However, relatively little is understood about the mechanism through which Schwann cells can make this transformation and additionally not much is known about how relevant these changes are for promoting successful peripheral axonal regeneration.

In this study, I sought to understand the role played by the transcription factor, c-Jun in regulating the Schwann cell reaction to peripheral nerve injury. Using the Wld^S mouse, I found that c-Jun expression is regulated by the timing of axonal degeneration during nerve injury. Furthermore, through use of a conditional knockout mouse, I found that c-Jun controls the rate of Schwann cell demyelination after loss of axonal contact, both *in vitro* and *in vivo*. Additionally, c-Jun is required for proper Schwann cell dedifferentiation after nerve injury but appears to be dispensable for injury induced Schwann cell proliferation. Finally, I sought to investigate the role Schwann cell derived c-Jun played in peripheral nerve regeneration. Functional recovery after sciatic nerve crush was severely inhibited, even 10 weeks after the injury, in the absence of *c-jun* in Schwann cells. Moreover, there was a substantial loss of axons in the distal stump of the nerve and surprisingly, in the corresponding dorsal root as well. Thus Schwann cell derived c-Jun is crucial for adequate peripheral nerve regeneration and potentially for the survival of regenerating neurons after injury.

4.3.1. The timing of axonal degeneration regulates activation of Schwann cells after nerve injury.

As mentioned in Chapter 1, in the absence of axonal degeneration, Schwann cells appear not to respond to nerve injury in Wld^s mice (Lunn et al., 1989; Glass et al., 1993). Furthermore, in normal situations, Schwann cells appear to start breaking up their myelin sheath into ovoids, only 20-32 hours after the initial injury (Lubinska, 1977), which corresponds well with the length of delay before axons begin to degenerate (Coleman, 2005).

This switch in Schwann cell phenotypes after injury can be marked by the downregulation of the axon dependent myelin transcription factor, Krox-20 and the upregulation of c-Jun (Parkinson et al., 2008). The fact that 7 days after sciatic nerve cut in Wld^s mice Schwann cells maintain Krox-20 expression and do not upregulate c-Jun confirms that Schwann cells do not react to the injury if axons remain intact. However, Schwann cells in Wld^s mice do eventually lose expression of Krox-20 and upregulate c-Jun expression, 28 days after injury, when the majority of axons have degenerated. This confirms original observations that Wld^s Schwann cells do have the capacity to become active after injury (Glass et al., 1993) but it seems likely that their activation depends on the timing of degeneration of the axon that they ensheath.

At a molecular level, it appears that the loss of Krox-20 expression is sufficient to activate Schwann cells in the absence of injury (Decker et al., 2006). Thus a possible mechanism through which Schwann cells could 'sense' injury may involve the upregulation of a demyelination programme, through derepression (Decker et al., 2006). Expression of factors that could potentially regulate denervated Schwann cells, such as c-Jun, Sox-2 and components of the Notch pathway, are normally suppressed in myelinating Schwann cells, most likely by a mechanism involving Krox-20

(Parkinson et al., 2004, 2008; Le et al., 2005a; Aswhin Woodhoo, unpublished observations). However, once myelinating Schwann cells lose contact with the axon after axonal degeneration, they lose expression of Krox-20 and these factors would become derepressed and, thus, potentially able to activate Schwann cells.

4.3.2. *c-jun* is dispensable in Schwann cells for normal peripheral nerve development.

In order to investigate the role of c-Jun in regulating the phenotype of denervated Schwann cells, I created a mouse that had a Schwann cell specific deletion of *c-jun*. The resulting *c-jun*$^{\Delta s}$ mouse showed successful deletion of the *c-jun* gene in the peripheral nerve by PCR and Schwann cells from these mice did not re-express c-Jun protein after nerve injury or during culture. The adult tibial nerve of *c-jun*$^{\Delta s}$ mice appears to contain a normal number of myelinated axons and there is no significant difference in the thickness of their myelin sheaths, in comparison to *c-jun*$^{f/f}$ mice. Thus, *c-jun* is not required for myelination or myelin sheath maintenance in Schwann cells, which is consistent with the absence of detectable c-Jun expression in myelinating Schwann cells (Parkinson et al., 2004). However, c-Jun is still expressed, albeit at low levels, in adult non-myelinating Schwann cells in the peripheral nerve (Shy et al., 1996). Yet, the number of non-myelinating Schwann cells and of unmyelinated axons in the tibial nerve was not significantly different in *c-jun*$^{\Delta s}$ mice. Since the *P0 CRE* allele is expressed from around E13.5 and has been shown to lead to recombination in non-myelinating Schwann cells in two previous studies (Feltri et al., 2002; D'Antonio et al., 2006b), one may assume that it would lead to recombination in non-myelinating Schwann in this situation. Furthermore, around 95% of Schwann cells purified from the P5 *c-jun*$^{\Delta s}$ sciatic nerve did not express c-Jun

in culture suggesting that recombination must have occurred in non-myelinating cells, since they make up around 20-30% of the Schwann cells in such cultures (data not shown). Thus, these findings suggest that *c-jun* may not be crucial for the development of non-myelinating Schwann cells either.

4.3.3. *c-jun* controls demyelination in Schwann cells.

Schwann cells normally upregulate c-Jun within 24 hours after nerve injury and within 6 hours after culturing (Parkinson et al., 2008). In the absence of *c-jun*, denervated Schwann cells are unable to rapidly demyelinate. This is observed after nerve injury in both neonatal and adult *c-jun*$^{\Delta s}$ mice (neonatal data not shown, see Parkinson et al., 2008), where myelin sheaths fragment more slowly than in *c-jun*$^{f/f}$ mice and in culture, where neonatal *c-jun*$^{\Delta s}$ Schwann cells are unable to rapidly remove myelin proteins from their cytoplasm. The mechanism by which Schwann cells can digest parts of their myelin sheath is almost completely unknown, though it may involve processes similar to phagocytosis (Bigbee et al., 1987) or autophagy (Holtzman and Novikoff, 1965). Various enzymes are certainly very likely to play a role in myelin sheath digestion in Schwann cells, especially since mice with null mutations in genes for PLA_2 and MMP-9 showed delayed demyelination after peripheral nerve injury (see Chapter 1; De et al., 2003; Shubayev et al., 2006). Interestingly, AP-1 sites are present in nearly all MMP genes with two consensus AP-1 sites present in the human MMP-9 gene and AP-1 can also regulate expression of human collagenase-1 in a monocyte-like cell line (Benbow and Brinckerhoff, 1997; Doyle et al., 1997). Additionally, as described in chapter 1, extracellular signalling also seems to be important in regulating the rate of demyelination, particularly as knockout mice for iNOS and Toll receptors show slower demyelination after nerve

injury (Levy et al., 2001; Boivin et al., 2007). Furthermore, a recent study has found that iNOS is directly regulated by c-Jun/AP-1 in hepatocytes (Hasselblatt et al., 2007).

In addition to the involvement of c-Jun in the early stages of demyelination, such as myelin sheath fragmentation and myelin protein clearance, it appears that c-Jun is also crucial for the removal of the majority of myelin lipid from the injured nerve. The fact that the majority of remaining myelin debris and lipid appears to reside in abnormally large macrophages in the *c-jun*$^{\Delta s}$ nerve, 28 days after sciatic nerve cut, suggests a more complex interaction between Schwann cells and macrophages. Since the Schwann cells appear to be unable to process the myelin debris properly in the absence of *c-jun*, macrophages may ingest too much myelin and subsequently be unable to digest it efficiently. The other possibility is that macrophages may be unable to properly digest myelin unless they receive adequate signalling from Schwann cells, which may be altered without c-Jun. Certainly, further investigation is required to resolve these issues, possibly by co-culturing Schwann cells and macrophages together and investigating the effects of Schwann cell conditioned medium from *c-jun*$^{f/f}$ and *c-jun*$^{\Delta s}$ mice on macrophage myelin phagocytosis. Hopefully, a greater understanding of the mechanisms by which Schwann cells break down myelin sheaths and cooperate with macrophages in clearance of myelin debris will lead to a better understanding of how Schwann cell c-Jun contributes to these processes.

4.3.4. c-Jun is a negative regulator of myelin gene activation.

Removal of *c-jun* in cultured Schwann cells can enhance myelin gene activation by either Krox-20 or a combined dbcAMP/NRG1 signal. Thus the constitutive expression of c-Jun in cultured Schwann cells acts as a brake to myelin

differentiation. Furthermore, enforced expression of c-Jun inhibits myelin gene expression in cultured Schwann cells and in myelinating Schwann cell-neuron co-cultures (Parkinson et al., 2008). Since, *c-jun* is an inhibitor of myelin differentiation, one might expect there to be enhanced myelination in *c-jun*$^{\Delta s}$ neonatal mice or during remyelination after nerve crush. Preliminary analysis of newborn and P5 *c-jun*$^{\Delta s}$ sciatic nerves shows no signs of precocious myelination or hypermyelination (data not shown; Parkinson et al., 2008). Furthermore there appear to be no overt differences in the thickness of the myelin sheath of the axons that do regenerate in *c-jun*$^{\Delta s}$ mice compared to *c-jun*$^{f/f}$ mice (see Fig.4.16, A and B). This suggests that removal of *c-jun* does not greatly affect the myelination process or the overall thickness of the myelin sheath after remyelination. This effect is not surprising, however, since c-Jun expression is downregulated in the sciatic nerve during myelination and remyelination (Shy et al., 1996; Parkinson et al., 2008). Thus, it appears that the ability to inhibit myelin differentiation, in the case of c-Jun, demonstrates part of a functionally opposing programme to myelination that seems to be more important for driving Schwann cell activation after nerve injury.

A number of factors have been identified that are inhibitory to myelin gene activation or the myelination process. In addition to c-Jun, these include, NRG1, FGF-2, ERK1/2, Sox-2, Oct-6 (Pou3f1), Id-2 (inhibitor of DNA binding-2), p57kip2 and components of the Notch and p38MAPK pathway (Zanazzi et al., 2001; Ogata et al., 2004; Harrisingh et al., 2004; Le et al., 2005a; Ryu et al., 2007; Mager et al., 2008; Heinen et al., 2008; A. Woodhoo and A. Bhaskaran, unpublished observations). Like c-Jun, the expression of a number of these factors is downregulated during myelination in the peripheral nerve and in the case of Oct-6 and the Notch pathway continuous constitutive expression actually antagonizes the myelination process *in*

vivo (Jessen and Mirsky, 2005; Ryu et al., 2007; A. Woodhoo, unpublished observations). Thus, it would be interesting to test, *in vivo*, whether downregulation of c-Jun in Schwann cells, during postnatal development, is actually necessary for myelination to proceed. This could be achieved by creating a transgenic mouse that constitutively expresses c-Jun in Schwann cells during postnatal development.

4.3.5. Differential requirements for *c-jun* in Schwann cell proliferation and survival.

In many different systems *c-jun* is required for cell cycle progression. In particular, *c-jun* null fibroblasts appear to be capable of only one or two divisions in culture before they undergo pseudo-senescence (Johnson et al., 1993; Shaulian and Karin, 2001). Many studies point to a requirement for *c-jun* for cells to progress beyond the G1-S phase of the cell cycle, though *c-jun* may also be involved at later stages as well (Shaulian and Karin, 2001). In Schwann cells, I find that *c-jun* is required for the full mitogenic effect of NRG1 on cultured Schwann cells. This corroborates previous findings that JNK/c-Jun pathway activity is required for NRG1 induced Schwann cell proliferation in culture (Parkinson et al., 2004). However, in contrast to *c-jun* null Schwann cells *in vitro*, *c-jun*$^{\Delta s}$ Schwann cells *in vivo* show normal levels of BrdU incorporation 5 days after sciatic nerve cut. At this time point after injury Schwann cell proliferation rates have peaked (Friede and Johnstone, 1967; Carroll et al., 1997), arguing against a potential delay in proliferation rates in *c-jun*$^{\Delta s}$ mice. In confirmation of this, I also assayed BrdU incorporation at 3 and 7 days after cut and saw no visible differences between *c-jun*$^{f/f}$ and *c-jun*$^{\Delta s}$ mice (data not shown). Thus, these findings would suggest that the mechanisms that regulate growth factor induced and injury induced proliferation in Schwann cells may be different. Certainly,

recent studies have shown mechanistic differences between embryonic, postnatal and injury induced Schwann cell proliferation (Kim et al., 2000; Antanasoski et al., 2001; Atanasoski et al., 2008), and while NRG1 is a potent mitogen for cultured Schwann cells, NRG1/erbB2 signalling appears not to be involved in injury induced Schwann cell proliferation (Atanasoski et al., 2006).

At long time points after nerve transection there is a reduction in the number of Schwann cell nuclei in transverse profile in *c-jun*$^{\Delta s}$ mice compared to *c-jun*$^{f/f}$ mice. However, as mentioned previously, there is no difference in Schwann cell DNA synthesis after nerve injury between the two genotypes. This disparity in these results may be reconciled in one of two ways. Firstly, BrdU incorporation only marks the S phase of the cell cycle and thus would not identify any block later in the cell cycle. Thus, it would be useful to look at the expression of a marker for the G2-M phase, such as phospho-histone H3 in order to substantiate these findings. Secondly, this difference may reflect increased loss of Schwann cells at long time points after nerve injury, in the absence of *c-jun*. Initially after nerve cut, Schwann cell numbers increase but at long time points after nerve transection Schwann cell numbers begin to decrease (Abercrombie, 1946; Weinberg and Spencer, 1978). Furthermore, a proportion of Schwann cells in the mouse sciatic nerve have been shown to undergo apoptosis at both short and long time points after nerve cut (Ferri and Bisby, 1999; Yang et al., 2008). However, at 5 days after nerve cut there was no difference in the number of apoptotic nuclei between the *c-jun*$^{f/f}$ and *c-jun*$^{\Delta s}$ sciatic nerves but this does not preclude increased apoptotic death at later time points after injury in *c-jun*$^{\Delta s}$ nerves or indeed death by necrosis. Interestingly, there is no significant difference in the number of Schwann cell nuclei in transverse section, between *c-jun*$^{f/f}$ and *c-jun*$^{\Delta s}$ mice, 70 days after nerve crush. A potential reason for this difference between cut

and crush might be that, at long time points after injury, the presence of axons confers greater survival ability to the Schwann cells of the distal stump (Weinberg and Spencer, 1978).

Naturally, *c-jun* is more commonly linked with induction of cell death rather than survival (Shaulian and Karin, 2001) and in Schwann cells, blocking the JNK/c-Jun pathway can protect cultured Schwann cells from apoptotic cell death (Parkinson et al., 2001, 2004). However, *c-jun* can potentially act as a prosurvival factor in other systems, since early in embryogenesis there is massive apoptotic cell death in the liver in the absence of *c-jun* (Eferl et al., 1999). Clearly, further investigation needs to be carried out to clarify the role of *c-jun* in Schwann cell survival, particularly during development, which has not been addressed in this study. Nevertheless, there remains the intriguing possibility that *c-jun* may demonstrate both pro-survival and pro-death abilities in Schwann cells depending on the cellular context and developmental stage.

4.3.6. *c-Jun* controls Schwann cell 'dedifferentiation'.

Dedifferentiation of myelinating Schwann cells is commonly thought of as combining the loss of expression of myelin associated genes and the upregulation of a large number of genes, many of which are also expressed by immature Schwann cells during development (Scherer and Salzer, 2001; Jessen and Mirsky, 2005). Results from this study demonstrate that, even when myelin and myelin proteins are eventually cleared from *c-jun*$^{\Delta s}$ Schwann cells, this event is not always accompanied by the appropriate gene expression of molecules characteristic of dedifferentiated Schwann cells, judged by the deficits in L1, N-cadherin, p75^{NTR} and NCAM expression both *in vitro* and *in vivo*. Thus there may be a more complex relationship than previously thought between Schwann cell demyelination and the upregulation of

molecules associated with the denervated phenotype. In addition, it may be more correct to describe the Schwann cell phenotype after nerve injury as Schwann cell activation rather than dedifferentiation, since many genes that are expressed by denervated Schwann cells are different to those expressed by immature Schwann cells (see Chapter 6; Bosse et al., 2006; Le et al., 2005a; D'Antonio et al., 2006a). Furthermore, non-myelinating Schwann cells are also seen to react after injury, downregulating expression of gal-C and 04 and upregulating MCP-1, IL-2 and IL-6 (Jessen et al., 1987; Mirsky et al., 1990; Cheepudomwit et al., 2008). Since this study analysed Schwann cells from a mixed nerve, it would be particularly interesting to discern whether activation of both myelinating and non-myelinating Schwann cells is perturbed after nerve injury in the absence of *c-jun*. Hopefully, *in vivo* and *in vitro* studies using nerves containing purely myelinated (facial) or unmyelinated (sympathetic trunk) fibres should resolve this issue.

4.3.7. Schwann cell derived *c-jun* is required for successful peripheral nerve regeneration.

Both motor and sensory functional recovery are severely impaired in *c-jun*$^{\Delta s}$ mice after sciatic nerve crush. Furthermore this impairment appears to be permanent as there is no evidence of any improvement in *c-jun*$^{\Delta s}$ mice after day 40, a time point when all *c-jun*$^{f/f}$ mice have regained full motor and sensory responses in toe reflex and toe pinch tests. Further evidence to support these findings has come from analysing the functional improvement after sciatic nerve crush in *c-jun*$^{f/f}$ and *c-jun*$^{\Delta s}$ mice using a walking tract test and evaluating the sciatic functional index (SFI)(Inserra et al., 1998). In this analysis, scores vary roughly between -100 (no function) to 0 (full function) (Inserra et al., 1998). By 28 days after sciatic nerve crush, *c-jun*$^{f/f}$ animals

had regained normal function, obtaining a mean score of 0.23 +/-4.6 whereas, even by day 70 after nerve crush, *c-jun*$^{\Delta s}$ mice only recorded a mean SFI of -62.4 +/-8.9 (D.Wilton and P. Arthur-Farraj, data not shown). In addition, analysis of the reinnervation of whisker pads after facial nerve cut demonstrated a strong impairment in the return of whisker movements in *c-jun*$^{\Delta s}$ mice in comparison to *c-jun*$^{f/f}$ mice (G.Raivich, unpublished observations).

The reason for such a strong inhibition of nerve regeneration in *c-jun*$^{\Delta s}$ mice appears to be due to the large reduction in myelinated fibres and potentially non-myelinated fibres in the *c-jun*$^{\Delta s}$ nerve after injury. These axon counts were performed 70 days after nerve crush and at a distance relatively close to the crush site (5mm distal), thus the axon counts are likely to reflect the total number of surviving regenerated axons in the nerve. This reduction in axon number in the distal stump of the *c-jun*$^{\Delta s}$ sciatic nerve is likely due to a loss of 36% of the myelinated axons in the L5 dorsal root of *c-jun*$^{\Delta s}$ mice, after nerve crush. These axons belong to sensory A-cells in the DRG and are not normally susceptible to death after sciatic nerve cut or crush (Coggeshall et al., 1997; Tandrup et al., 2000). In addition, the fact there appeared to be few remaining healthy unmyelinated axons in either the L5 dorsal root or the tibial nerve, in *c-jun*$^{\Delta s}$ mice, suggests that there is most likely to be an increased loss of B-cells in the *c-jun*$^{\Delta s}$ DRG as well. These findings, of course, need to be corroborated with counts of A and B cells within the DRG, but do propose a potential explanation to the reason why *c-jun*$^{\Delta s}$ mice score so badly in the mechanosensory and nocieceptive toe pinch tests. Moreover, these results demonstrate that *c-jun* in Schwann cells is actually required for regenerating sensory neuron survival in the crushed sciatic nerve. In light of this it would be particularly interesting to investigate

the growth factor expression of *c-jun*$^{\Delta s}$ Schwann cells in comparison to *c-jun*$^{f/f}$ Schwann cells.

Curiously, the L5 ventral root of *c-jun*$^{\Delta s}$ mice showed no difference to that of *c-jun*$^{f/f}$ mice after sciatic nerve crush, signifying that motor neuron survival is likely to be unchanged. Yet *c-jun*$^{\Delta s}$ mice show impairment in both the speed of the initial motor response and the quality of the eventual motor recovery after sciatic nerve crush. Studies from the facial nerve demonstrate that motor neurons have a moderately reduced growth rate in the *c-jun*$^{\Delta s}$ distal stump after nerve crush (G.Raivich, unpublished observations), which correlates with the increase in time taken to observe the initial toe reflex response in *c-jun*$^{\Delta s}$ mice. However, further investigation is required in order to discover why motor recovery does not eventually return to normal in *c-jun*$^{\Delta s}$ mice, after sciatic nerve crush. Potentially, experiments using retrograde tracing techniques to quantify the number of neurons that reconnect with a given muscle could identify whether there is a problem with motorneuron reinnervation of targets in *c-jun*$^{\Delta s}$ mice after sciatic nerve crush.

Since *c-jun*$^{\Delta s}$ mice show such a strong impairment in peripheral nerve regeneration, this study underlines the importance of the Schwann cell in this process. Importantly, the deficit in axon and potentially neuronal survival is unlikely to be due to a reduced number of Schwann cells in the *c-jun*$^{\Delta s}$ distal stump because, as mentioned earlier, there was no statistically significant difference between the number of Schwann cell nuclei in transverse section between *c-jun*$^{f/f}$ and *c-jun*$^{\Delta s}$ mice, 70 days after sciatic nerve crush. However, the deficit is more likely to be due to a combination of the delayed myelin clearance in the *c-jun*$^{\Delta s}$ nerve and the improper activation of *c-jun*$^{\Delta s}$ Schwann cells. The relative importance of each of these to peripheral nerve regeneration still remains to be determined although other transgenic

animals that demonstrate similar delays in myelin sheath removal after nerve injury mice do not appear to have such severe regeneration deficits as *c-jun*$^{\Delta s}$ mice (Levy et al., 2001; Ramaglia et al., 2007; A. Woodhoo and D. Wilton, unpublished observations)

Overall this study has demonstrated that Schwann cells actively respond to clear myelin debris, interact with macrophages and promote peripheral nerve regeneration after nerve injury, and that the transcription factor *c-jun* is crucial in regulating these processes.

CHAPTER 5: Investigation of the functional properties of a mutant form of Egr2 (S382R/D383Y) in Schwann cells.

5.1 INTRODUCTION

The early growth response gene 2 (Egr2; also named Krox-20) and the associated proteins Nab1 and 2 are essential transcriptional regulators of Schwann cell myelination (Topilko et al., 1994; Nagarajan et al., 2001; Le et al., 2005a, 2005b). Therefore, it is not surprising that mutations in *EGR2* can lead to myelin abnormalities and severe peripheral neuropathies in humans. These include congenital hypomyelinating neuropathy (CHN), Dejerine Sottas syndrome (DSS) and Charcot-Marie-Tooth 1 (CMT1). At present 11 different mutations have been identified in EGR2 (Bellone et al., 1998; Warner et al., 1998; Timmerman et al., 1999; Pareyson et al., 2000; Yoshihara et al., 2001; Vandenberghe et al., 2002; Numakura et al., 2003; Mikesova et al., 2005; Szigeti et al., 2007).

The majority of these mutations occur in the DNA binding domain and follow a dominant mode of inheritance in affected families. The autosomal dominant S382R, D383Y double point mutation is associated with the most serious clinical phenotype, identified in a seven year-old girl diagnosed with CHN. A sural nerve biopsy revealed absence or loss of myelin in virtually all axons and her nerve conduction velocities were severely slowed (under 10 m/s; Warner et al., 1998). The underlying mechanism by which this mutation leads to such severe disruption of the myelination process is of great interest. It is known that this mutant has minimal DNA binding activity but retains the ability to weakly transactivate an artificial luciferase promoter with Egr2 binding sites (Warner et al., 1999). Furthermore, experiments in mouse and rat Schwann cells in vitro demonstrated that in contrast to wild-type Egr2, this mutant

fails to activate transcription of myelin genes, and that it acts as a dominant-negative protein by inhibiting myelin gene expression driven by wild-type Egr2 (Nagarajan et al., 2001; Le Blanc et al., 2007). This mechanism would help to explain why the mutation is inherited in a dominant fashion since studies on mouse mutants reveal that one copy of Egr2 is sufficient to sustain normal myelination (Topilko et al., 1994; Zorick et al., 1999).

In the present work I have examined the functional properties of the S382R/D383Y Egr2 mutant using cultured rat Schwann cells. In agreement with previous work, I found that mutant Egr2 prevents wild-type Egr2 from inducing the expression of the major myelin protein, P_0. Furthermore, mutant Egr2 fails to induce P_0 expression. Nevertheless, I found that mutant Egr2 retains some functions of the wild-type protein. It induces endogenous expression of the myelin-related protein periaxin and Nab2, albeit at lower levels than wild-type Egr2. Moreover, mutant Egr2 is at least as effective as the wild-type protein in preventing Schwann cell death and in common with wild-type Egr2, it suppresses expression of c-Jun. Significantly, I found that mutant Egr2 induces aberrant effects when expressed in Schwann cells. Mutant Egr2, under normal culture conditions or in the presence of NRG1, induces Schwann cell proliferation, activates the ERK/MAPK pathway and suppresses expression of the cell cycle inhibitor p27. This stands in clear contrast to wild-type Egr2, which inhibits Schwann cell proliferation (Parkinson et al., 2004). These effects are less marked when mutant Egr2 is expressed at higher levels within Schwann cells, when it behaves more like a wild-type allele. These observations add significant new aspects to the functional repertoire of the S382R/D383Y EGR2 mutant protein and will contribute to a comprehensive understanding of why this protein has such devastating consequences when expressed in human Schwann cells.

5.2 RESULTS

5.2.1 Mutant Egr2 dominant-negatively inhibits P_0 protein expression induced by wild-type Egr2.

Previous experiments show that in mouse Schwann cells mutant Egr2 (S382R, D383Y) can dominant-negatively inhibit myelin gene mRNA expression using adenoviral co-infection with a wild-type Egr2 construct (Nagarajan et al., 2001). To confirm these findings at the protein level and in the rat model, I used rat Schwann cells that had been retrovirally infected with wild-type Egr2 and then drug selected. These cells were subsequently infected with either a GFP control adenovirus or an adenovirus expressing GFP and mutant Egr2 for 72 hours. In this way, I ensured that the population of Schwann cells examined expressed both wild-type Egr2 and the control or mutant Egr2 constructs. Myelin gene expression was monitored by immunocytochemical labelling for the myelin gene P_0. I found, as expected, that mutant Egr2 strongly inhibited the expression of P_0 protein ($p<0.001$), normally induced by wild-type Egr2 (Fig. 5.1, A-E).

Figure 5.1: Mutant Egr2 inhibits wild-type Egr2 induced P_0 protein expression.

Following retroviral infection of Schwann cells with wild-type Egr2 (Egr2 WT), cells were also infected with either GFP control (GFP cont, A and B) or GFP/mutant Egr2 adenoviruses (Egr2 Mut, C and D), to test whether mutant Egr2 could repress P0 induction by wild-type Egr2. Immunolabelling for P0 reveals strong P0 suppression in cells co-infected with mutant Egr2 (e.g. arrowheads in C and D) whereas cells co-infected with GFP control virus (e.g. arrows in A and B) still express P0. Schwann cell nuclei are labelled with Hoescht nuclear dye (Ho). Bar, 20μM. (E) The percentage of cells expressing P0 in Schwann cell cultures infected with wild-type Egr2 and GFP control (Egr2 WT + GFP cont) and wild-type Egr2 and GFP/mutant Egr2 (Egr2 WT + Egr2 Mut). Error bars represent one standard deviation of the mean.

Figure 5.1

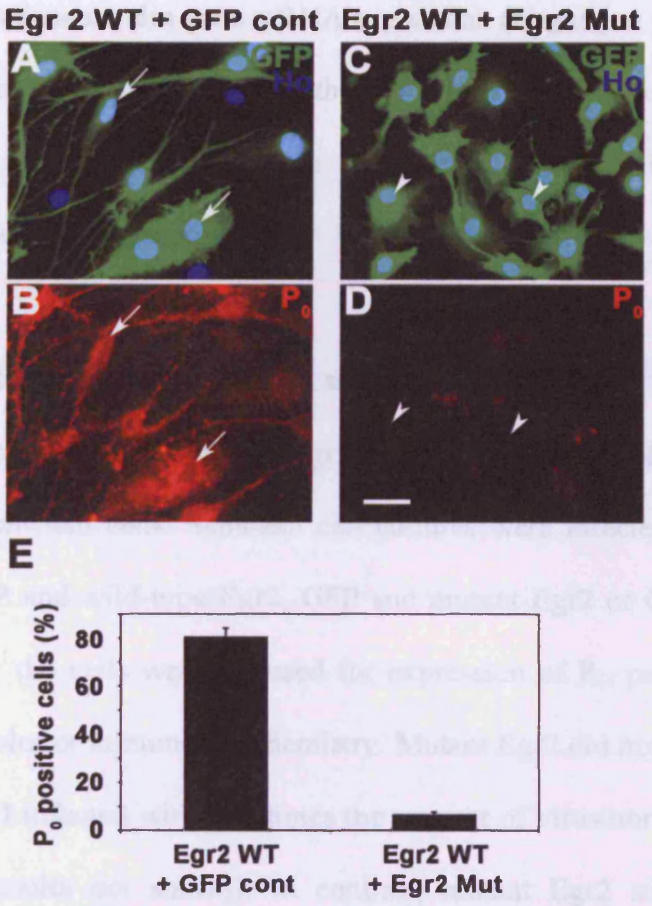
Egr 2 WT + GFP cont
Egr2 WT + Egr2 Mut
A
GFP
Ho
C
GFP
Ho
B
P0
D
P0
E
P0 positive cells (%)
80
60
40
20
0
Egr2 WT
+ GFP cont
Egr2 WT
+ Egr2 Mut

5.2.2 Mutant Egr2 retains several functions of the wild-type protein.

It has previously been shown by a transfection and electro-mobility shift assay, that the Egr2 (S382R, D383Y) mutant can weakly bind DNA and can activate weak expression of an artificial promoter when ectopically expressed in CV-1 cells (Warner et al., 1999). However, expression of mutant Egr2 for 24 hours in mouse Schwann cells failed to induce myelin gene mRNA expression (Nagarajan et al, 2001). I wished to determine more conclusively whether this Egr2 mutant retained properties in common with the wild-type allele in Schwann cells or whether it was, in fact, functionally equivalent to a null allele.

5.2.2.1 Mutant Egr2 induces periaxin and Nab2 expression.

First, I tested whether mutant Egr2 induced expression of any myelin related genes in rat Schwann cells. Schwann cell cultures were infected with adenoviruses expressing GFP and wild-type Egr2, GFP and mutant Egr2 or GFP alone. Seventy-two hours later the cells were assessed for expression of P_0, periaxin and Nab2 by either western blot or immunocytochemistry. Mutant Egr2 did not induce P_0 (Fig. 5.2, A), even when I infected with five times the amount of virus normally used for these experiments (results not shown). In contrast, mutant Egr2 still demonstrated an unambiguous ability to induce periaxin, although periaxin levels were significantly lower than those induced by wild-type Egr2 as shown by western blot (Fig. 2 B) and immunocytochemistry ($n=3$)($p<0.05$)(Fig. 5.2, C-G). Furthermore, I found that mutant Egr2 induced nuclear expression of Nab2 (25.8 +/- 3.7%), though, again, this effect was substantially reduced compared to that of wild-type Egr2 (99 +/-0.7%) ($n=3$)($p<0.05$)(Fig. 5.2, H-M).

Figure 5.2: Mutant Egr2 induces periaxin and Nab2 expression.

Schwann cell cultures were infected with GFP control (GFP cont), GFP/wild-type Egr2 (Egr2 WT) or GFP/mutant Egr2 (Egr2 Mut) adenoviruses and assessed for P_0 expression by immunolabelling (A), periaxin expression by western blot (B) and immunolabelling (C-G), and Nab2 by immunolabelling (H-M). Bar, 20μM. Note that mutant Egr2 does not induce P_0 but does induce periaxin and Nab2. However this induction is clearly less than that seen with wild-type Egr2. Arrowheads in L and M signify Schwann cells that express a low level of mutant Egr2 adenovirus and fail to upregulate Nab2. Schwann cell nuclei are labelled with Hoescht nuclear dye (Ho). β-Tubulin was used as a loading control for the western blot. Error bars on the graphs represent one standard deviation of the mean.

Figure 5.2

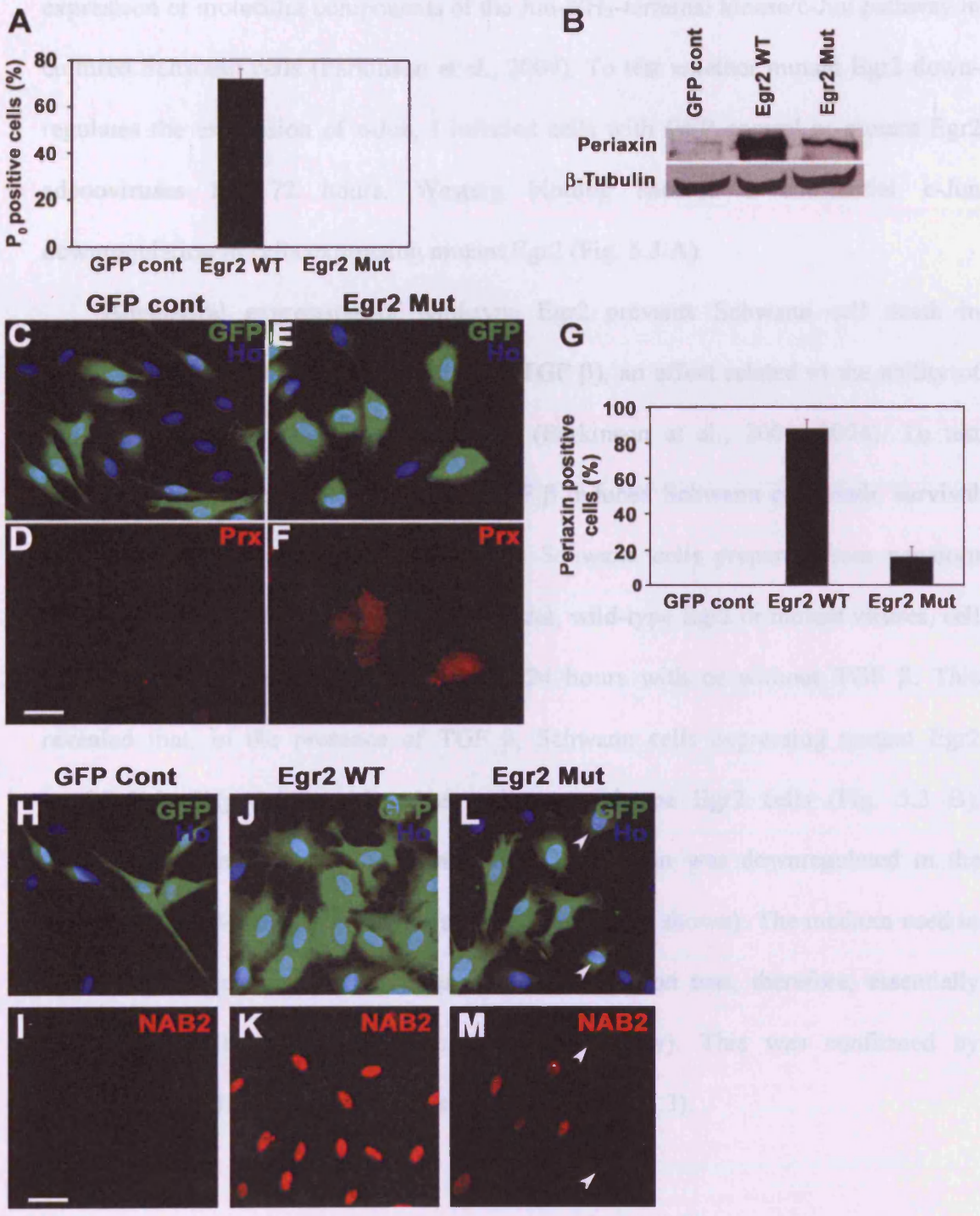
A
P0 positive cells (%)
80
60
40
20
0
GFP cont
Egr2 WT
Egr2 Mut
B
GFP cont
Egr2 WT
Egr2 Mut
Periaxin
β-Tubulin
GFP cont
Egr2 Mut
C
GFP
Ho
E
GFP
Ho
D
Prx
F
Prx
G
Periaxin positive cells (%)
100
80
60
40
20
0
GFP cont
Egr2 WT
Egr2 Mut
GFP Cont
Egr2 WT
Egr2 Mut
H
GFP
Ho
J
GFP
Ho
L
GFP
Ho
I
NAB2
K
NAB2
M
NAB2

5.2.2.2 Mutant Egr2 suppresses c-Jun and protects against TGFβ induced death.

Wild-type Egr2, in addition to inducing myelin genes, also downregulates the expression of molecular components of the Jun-NH_2-terminal kinase/c-Jun pathway in cultured Schwann cells (Parkinson et al., 2004). To test whether mutant Egr2 down-regulates the expression of c-Jun, I infected cells with GFP control or mutant Egr2 adenoviruses for 72 hours. Western blotting showed a substantial c-Jun downregulation in cells expressing mutant Egr2 (Fig. 5.3 A).

Adenoviral expression of wild-type Egr2 prevents Schwann cell death in response to transforming growth factor β (TGF β), an effect related to the ability of Egr2 to suppress the JNK/c-Jun pathway (Parkinson et al., 2001, 2004). To test whether mutant Egr2 could also block TGF β induced Schwann cell death, survival assays were performed on immunopanned Schwann cells prepared from newborn animals. Following infection with GFP control, wild-type Egr2 or mutant viruses, cell survival was measured over a period of 24 hours with or without TGF β. This revealed that, in the presence of TGF β, Schwann cells expressing mutant Egr2 survived ($n=3$)($p<0.01$) at least as well as wild-type Egr2 cells (Fig. 5.3 B). Additionally, immunolabelling demonstrated that c-Jun was downregulated in the mutant and wild-type Egr2-expressing cells (results not shown). The medium used in this series of experiments was serum-free. Proliferation was, therefore, essentially absent from all experimental conditions (see below). This was confirmed by measuring BrdU incorporation (not shown; see section 5.3).

Figure 5.3: Mutant Egr2 suppresses c-Jun and cell death.

(A) Western blot of c-Jun in Schwann cells infected with GFP control (GFP cont), GFP/wild-type Egr2 (Egr2 WT) or GFP/mutant Egr2 (Egr2 Mut) showing that mutant Egr2 reduces the expression of c-Jun, a protein associated with immature Schwann cells. β-Tubulin was used as a loading control.

(B) The graph demonstrates that mutant Egr2 functions similarly to wild-type Egr2 by inhibiting TGFβ induced Schwann cell death. Immunopanned Schwann cells were infected with GFP control (GFP cont), GFP/wild-type Egr2 (Egr2 WT) and GFP/mutant Egr2 (Egr2 Mut) adenoviruses for 48 hours in DM. Some cultures were then fixed (time zero control) or cultured with or without TGFβ (5ng/ml) for a further 24 hours. Values are given for the number of surviving GFP-positive cells as a percentage of the number of GFP-positive Schwann cells at time zero. The error bars represent one standard deviation of the mean.

Figure 5.3

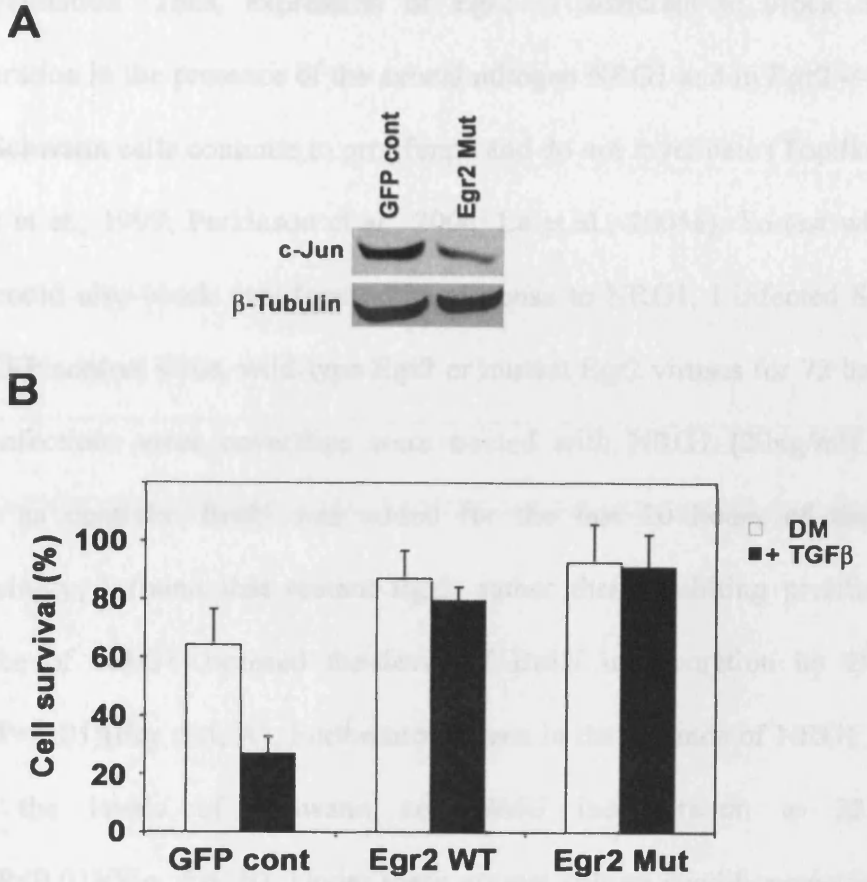
A
GFP cont
Egr2 Mut
c-Jun
β-Tubulin
B
Cell survival (%)
100
80
60
40
20
0
GFP cont
Egr2 WT
Egr2 Mut
DM
+ TGFβ

5.2.3 Mutant Egr2 shows gain-of-function effects that are the converse of those seen with the wild-type protein.

Egr2 has a key role in removing Schwann cells from the cell cycle at the onset of myelination. Thus, expression of Egr2 is sufficient to block Schwann cell proliferation in the presence of the axonal mitogen NRG1 and in Egr2 -/- and Egr2 $^{lo/lo}$ mice Schwann cells continue to proliferate and do not myelinate (Topilko et al., 1994; Zorick et al., 1999; Parkinson et al., 2004; Le et al., 2005a). To test whether mutant Egr2 could also block proliferation in response to NRG1, I infected Schwann cells with GFP control virus, wild-type Egr2 or mutant Egr2 viruses for 72 hours. 48 hours after infection, some coverslips were treated with NRG1 (20ng/ml) while others served as controls. BrdU was added for the last 20 hours of the experiment. Surprisingly, I found that mutant Egr2, rather than inhibiting proliferation in the presence of NRG1, boosted the level of BrdU incorporation by 29.2 +/-4.79% (n=3)($P<0.01$)(Fig. 5.4, A). Furthermore, even in the absence of NRG1, mutant Egr2 raised the levels of Schwann cell BrdU incorporation to 22.5 +/-2.99% (n=3)($P<0.01$)(Fig. 5.4, B). Under these normal culture conditions proliferation rates are minimal in control cells and, as expected, wild type Egr2 fails to promote Schwann cell proliferation (Fig. 5.4, B)(Parkinson et al., 2004). The routine culture medium in these experiments included 0.5% foetal calf serum (see Chapter 2). In the complete absence of serum mutant Egr2 was unable to induce DNA synthesis (data not shown).

Because the MEK/ERK pathway has been implicated in Schwann cell proliferation (Kim et al., 1997) I examined the levels of phosphorylated ERK1/2 in cells expressing mutant Egr2. This revealed that in contrast to wild-type Egr2, mutant Egr2 stimulated ERK1/2 phosphorylation (Fig. 5.4, C). In line with this observation,

an inhibitor of ERK1/2 phosphorylation, the MEK inhibitor, U0126, blocked BrdU incorporation stimulated by mutant Egr2 both in the absence and presence of NRG1 (n=5)($P<0.05$ and <0.000005 respectively, Fig. 5.4, D). The JNK inhibitor, SP600125 also inhibited mutant Egr2 induced BrdU incorporation in the absence and presence of NRG1 (n=5)($P<0.005$ and <0.0005 respectively, Fig. 5.4, D) a result confirmed by using the highly specific JNK blocking peptide, D-JNK1 (Borsello et al., 2003)(n=5) ($P<0.05$ and <0.0005 respectively)(Fig. 5.4, E). These results are consistent with the known involvement of the JNK/c-Jun pathway in Schwann cell proliferation *in vitro* (Parkinson et al., 2004; see Chapter 4).

In further contrast to the function of the wild-type protein, mutant Egr2 also markedly suppressed levels of the cell cycle inhibitor p27 (Fig. 5.4, F and G). P27 protein is present in quiescent Schwann cells but its expression is elevated by wild-type Egr2, presumably as part of the mechanism through which wild-type Egr2 inhibits cell division (Tikoo et al., 2000; Parkinson et al., 2004).

As expected, given the mitogenic effect of mutant Egr2, we found that mutant Egr2, even in the absence of NRG-1, induced nuclear expression of the early cell cycle marker, cyclin D1 (n=4)($P<0.001$)(Fig. 5.5, A-D). Furthermore, in cells expressing mutant Egr2, the G1-S phase cell cycle enzyme, cdk2 was shifted from the cytoplasm to the nucleus (Fig. 5.5, E and F, I and J). Wild-type Egr2, in contrast, caused a reduction in cdk2 levels (Fig. 5.5, G and H).

Figure 5.4: Mutant Egr2 induces DNA synthesis, ERK1/2 phosphorylation and the downregulation of p27.

(A) The proliferation of Schwann cells in DM and 0.5% FCS, measured by BrdU incorporation, infected with GFP control (GFP cont), GFP/wild-type Egr2 (Egr2 WT) and GFP/mutant Egr2 (Egr2 Mut) adenoviruses, in the presence of NRG1 (20ng/ml).
(B) BrdU incorporation in Schwann cells infected with GFP control (GFP cont), GFP/wild-type Egr2 (Egr2 WT) and GFP/mutant Egr2 (Egr2 Mut) and maintained in DM and 0.5% FCS without NRG1. Note that wild-type Egr2 inhibits proliferation in the presence of NRG1 and that mutant Egr2 stimulates DNA synthesis.
(C) Western blot of phosphorylated ERK1 (44kDa band) and ERK2 (42kDa band) in Schwann cells infected with GFP control (GFP), GFP/Egr2 wild type (Egr2 WT) and GFP/mutant Egr2 (Egr2 Mut) showing that mutant Egr2 induces phosphorylation of ERK1 and ERK2. β-Tubulin was used as a loading control.
(D) The graph shows the percentage of BrdU incorporation in Schwann cell cultures infected with mutant Egr2 adenovirus and treated with DMSO as a control, the JNK inhibitor, SP600125 (30μM); The MEK inhibitor, U0126 (20μM). The addition of NRG1 (20ng/ml) to the cultures is indicated by the black bars whereas white bars represent mutant Egr2 infected Schwann cells cultured in DM and 0.5% FCS (DM/FCS). Error bars represent one standard deviation of the mean.
(E) The inhibition of the JNK pathway, using a soluble JNK blocking peptide (DJNK1, 10μM), blocks mutant Egr2 mediated Schwann cell proliferation in DM and 0.5% FCS, with (black bars) and without (white bars) the addition of NRG1 (20ng/ml). Error bars represent one standard deviation of the mean.
(F) Western blot of the cell cycle inhibitor, p27, in GFP control (GFP cont) and GFP/mutant Egr2 (Egr2 Mut) infected Schwann cells showing that p27 is downregulated in mutant Egr2 expressing Schwann cells. β-Tubulin was used as a loading control.
(G) The graph shows the percentage of p27 positive Schwann cells showing nuclear staining from immunolabelling experiments, infected with GFP control (GFP cont), GFP/wild-type Egr2 (Egr2 WT) and GFP/mutant Egr2 (Egr2 Mut) adenoviruses for 72 hours. Error bars represent one standard deviation of the mean.

Figure 5.4

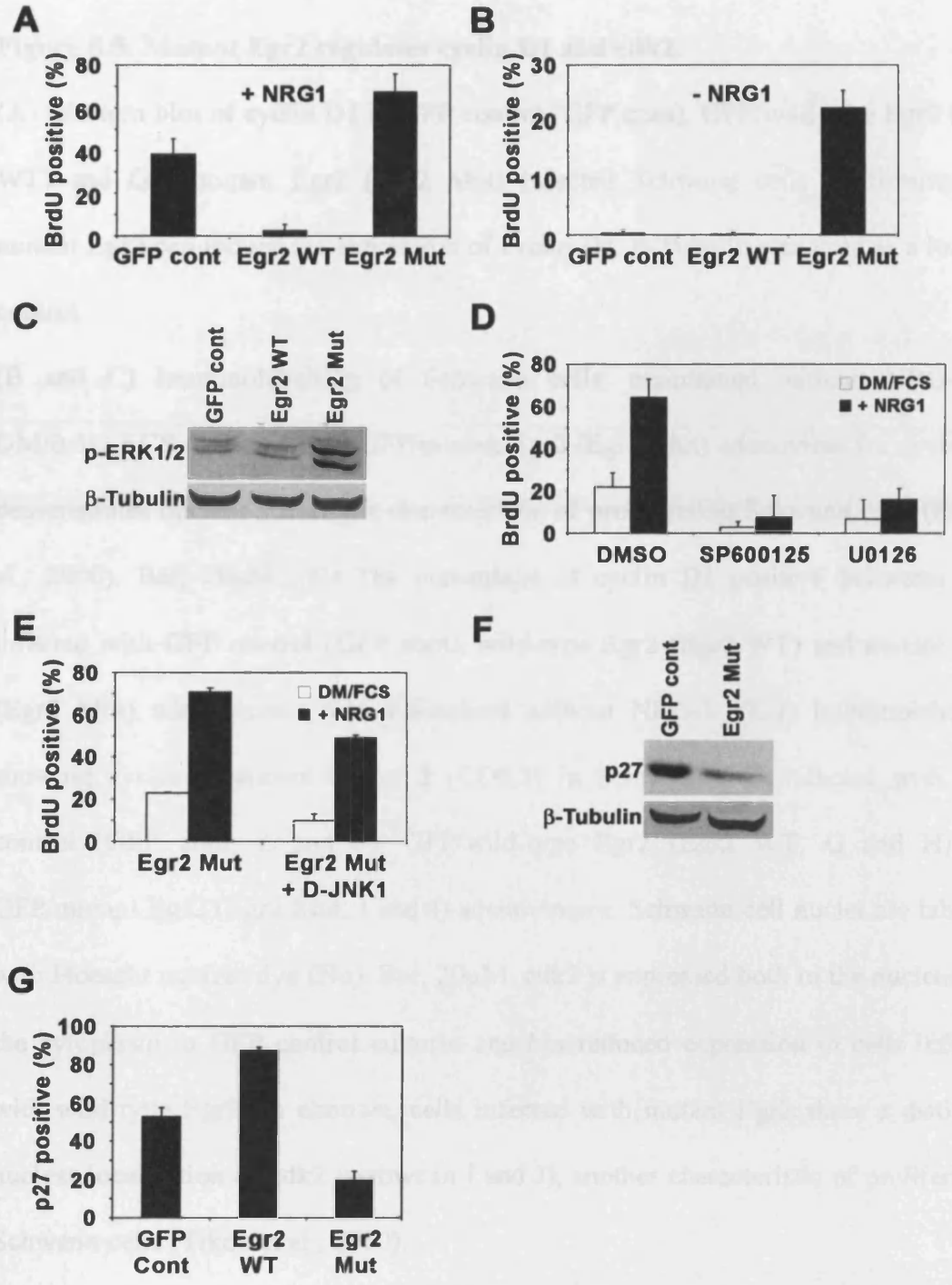
A
BrdU positive (%)
80
60
40
20
0
+ NRG1
GFP cont
Egr2 WT
Egr2 Mut
B
BrdU positive (%)
30
20
10
0
- NRG1
GFP cont
Egr2 WT
Egr2 Mut
C
GFP cont
Egr2 WT
Egr2 Mut
p-ERK1/2
β-Tubulin
D
BrdU positive (%)
80
60
40
20
0
DM/FCS
+ NRG1
DMSO
SP600125
U0126
E
BrdU positive (%)
80
60
40
20
0
DM/FCS
+ NRG1
Egr2 Mut
Egr2 Mut
+ D-JNK1
F
GFP cont
Egr2 Mut
p27
β-Tubulin
G
p27 positive (%)
100
80
60
40
20
0
GFP
Cont
Egr2
WT
Egr2
Mut

Figure 5.5: Mutant Egr2 regulates cyclin D1 and cdk2.

(A) Western blot of cyclin D1 in GFP control (GFP cont), GFP/wild-type Egr2 (Egr2 WT) and GFP/mutant Egr2 (Egr2 Mut) infected Schwann cells confirming that mutant Egr2 can induce the expression of cyclin D1. β-Tubulin was used as a loading control.

(B and C) Immunolabelling of Schwann cells, maintained without NRG-1 in DM/0.5% FCS, infected with GFP/mutant Egr2 (Egr2 Mut) adenovirus for cyclin D1 demonstrates nuclear staining, a characteristic of proliferating Schwann cells (Kim et al., 2000). Bar, 20μM. (D) The percentage of cyclin D1 positive Schwann cells infected with GFP control (GFP cont), wild-type Egr2 (Egr2 WT) and mutant Egr2 (Egr2 Mut) adenoviruses and maintained without NRG-1. (E-J) Immunolabelling showing cyclin-dependant kinase 2 (CDK2) in Schwann cells infected with GFP control (GFP cont; E and F), GFP/wild-type Egr2 (Egr2 WT; G and H) and GFP/mutant Egr2 (Egr2 Mut; I and J) adenoviruses. Schwann cell nuclei are labelled with Hoescht nuclear dye (Ho). Bar, 20μM. cdk2 is expressed both in the nucleus and the cytoplasm in GFP control cultures and has reduced expression in cells infected with wild-type Egr2. In contrast, cells infected with mutant Egr2 show a distinctly nuclear localisation of cdk2 (arrows in I and J), another characteristic of proliferating Schwann cells (Tikoo et al., 2000).

Figure 5.5

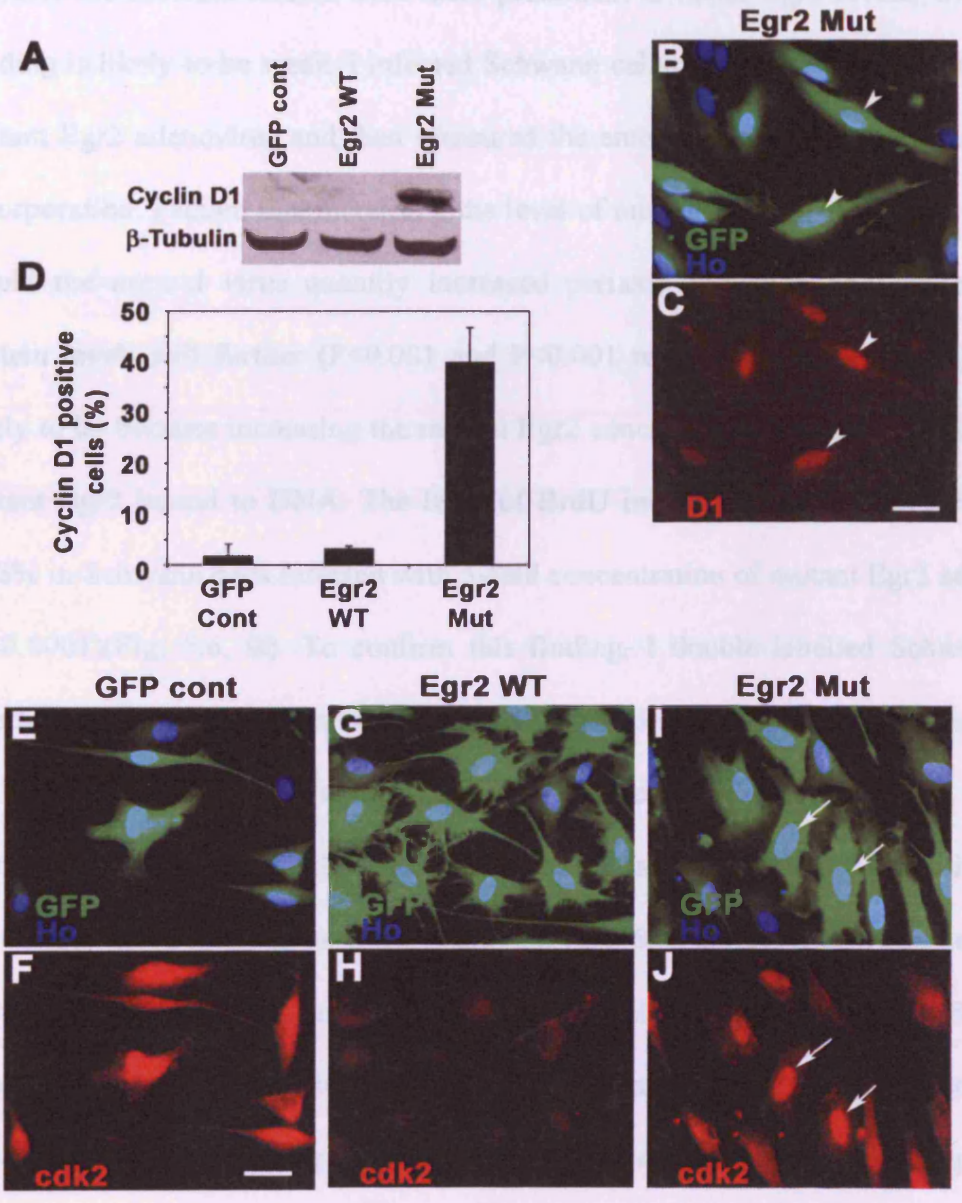
A
GFP cont
Egr2 WT
Egr2 Mut
Cyclin D1
β-Tubulin
B
Egr2 Mut
GFP
Ho
C
D1
D
Cyclin D1 positive cells (%)
50
40
30
20
10
0
GFP Cont
Egr2 WT
Egr2 Mut
GFP cont
Egr2 WT
Egr2 Mut
E
GFP
Ho
G
GFP
Ho
I
GFP
Ho
F
cdk2
H
cdk2
J
cdk2

5.2.4 At higher concentrations, mutant Egr2 behaves more like wild-type Egr2.

Mutant Egr2 binds DNA less strongly than wild-type Egr2. Intriguingly, it demonstrates some normal functions and some aberrant functions (see above). To test whether the aberrant effects were more prominent at lower Egr2 levels, when DNA binding is likely to be weak, I infected Schwann cells with varying concentrations of mutant Egr2 adenovirus and then measured the amount of periaxin, c-Jun and BrdU incorporation. I found that increasing the level of mutant Egr2 by infecting with up to 5-fold the normal virus quantity increased periaxin induction and reduced c-Jun protein levels still further ($P<0.001$ and $P<0.001$ respectively)(Fig. 5.6, A). This is likely to be because increasing the mutant Egr2 concentration increases the amount of mutant Egr2 bound to DNA. The level of BrdU incorporation also fell by 20.2 +/- 1.78% in Schwann cells infected with 5-fold concentration of mutant Egr2 adenovirus ($P<0.0001$)(Fig. 5.6, B). To confirm this finding, I double labelled Schwann cells infected with low concentrations of mutant Egr2 adenovirus with antibodies to Egr2 and BrdU. Schwann cells with intense GFP fluorescence, expressed high levels of mutant Egr2 and were BrdU negative, whereas the faintly Egr2 and GFP positive cells were much more likely to be BrdU positive (Fig. 5.6, C and D). I also double labelled Schwann cells under the same conditions with antibodies to periaxin and BrdU and found that the cell population that expressed periaxin and the one that incorporated BrdU were non-overlapping (Fig. 5.6, E and F) as expected from previous reports that myelin differentiation and proliferation are incompatible (Morgan et al., 1991).

Figure 5.6: Mutant Egr2 shows concentration-dependent effects.

(A) Increasing the amount of mutant Egr2 adenovirus used to infect Schwann cells up to 5 fold can induce a higher percentage of Schwann cells to express periaxin and fewer to express c-Jun, judged by immunocytochemistry and cell counting. Error bars represent one standard deviation of the mean. Statisical analysis was performed using one-way ANOVA and Tukey's Multiple Comparison test.

(B) Increasing the amount of mutant Egr2 adenovirus used to infect Schwann cell cultures, up to 5-fold, can reduce the level of BrdU incorporation. These cultures were maintained without NRG1 in DM/0.5%FCS. Error bars represent one standard deviation of the mean. Statisical analysis was performed using one-way ANOVA and Tukey's Multiple Comparison test.

(C and D) Double immunolabelling for Egr2 and BrdU in Schwann cell cultures infected with low concentrations of GFP/mutant Egr2 (Egr2 Mut) adenovirus. Arrows demonstrate Schwann cells expressing high levels of mutant Egr2 and GFP, which do not incorporate BrdU. Arrowheads show Schwann cells expressing low levels of mutant Egr2 and GFP, which have incorporated BrdU. Bar, 20μM.

(E and F) Double immunolabelling for periaxin and BrdU in Schwann cell cultures infected with low concentrations of GFP/mutant Egr2 (Egr2 Mut) adenovirus. Arrowheads show cells that express periaxin are strongly infected, judged by GFP expression, and do not incorporate BrdU. Arrows demonstrate Schwann cells weakly expressing GFP and mutant Egr2 (Egr2 Mut) that do not express periaxin but clearly incorporate BrdU. Bar, 20μM.

Figure 5.6

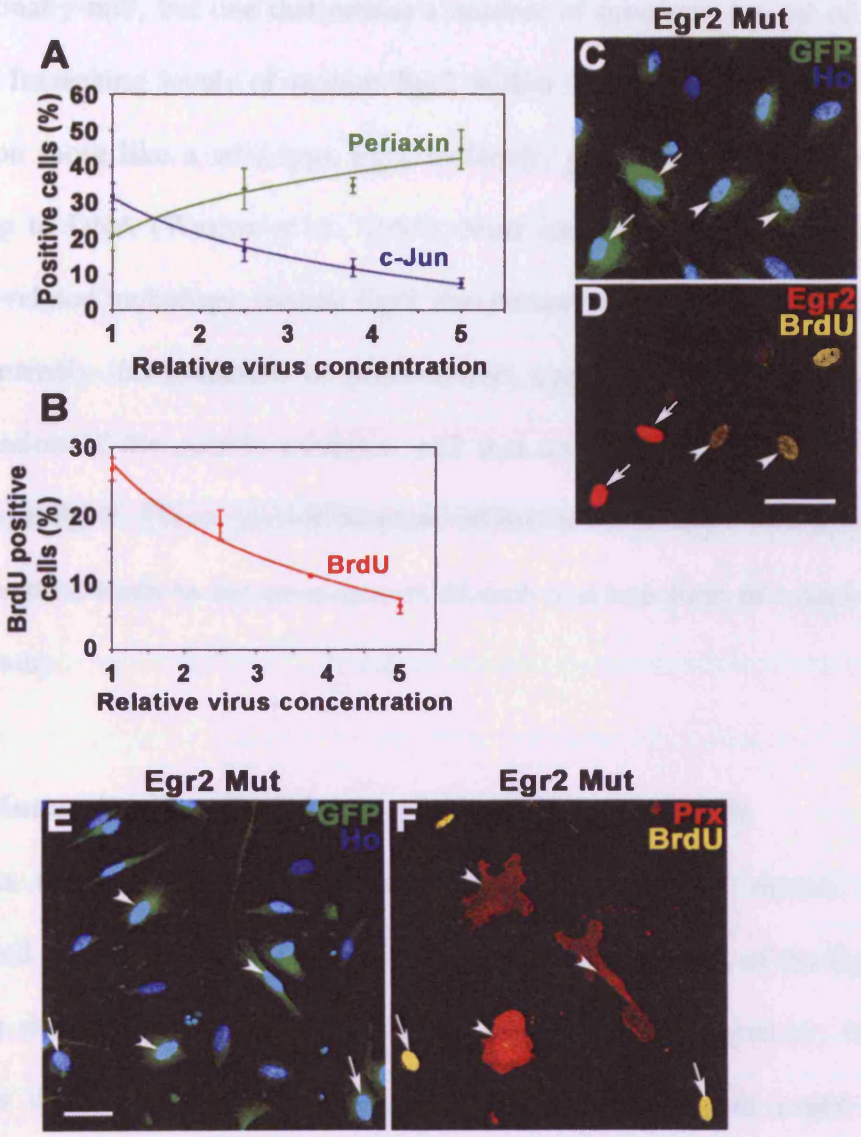
A
Positive cells (%)
60
50
40
30
20
10
0
Periaxin
c-Jun
1
2
3
4
5
Relative virus concentration
B
BrdU positive cells (%)
30
20
10
0
BrdU
1
2
3
4
5
Relative virus concentration
Egr2 Mut
C
GFP
Ho
D
Egr2
BrdU
Egr2 Mut
E
GFP
Ho
Egr2 Mut
F
Prx
BrdU

5.3 DISCUSSION

I have investigated the functional properties of the S382R/D383Y Egr2 mutant in rat Schwann cells. I found that this mutation does not create an allele that is functionally-null, but one that retains a number of functions typical of the wild-type allele. Increasing levels of mutant Egr2 within Schwann cells causes this allele to function more like a wild-type Egr2 molecule, presumably by increasing levels of binding to DNA (Warner et al., 1999). Most importantly for understanding mutant EGR2-related pathology, mutant Egr2 also demonstrates aberrant effects in Schwann cells, namely the induction of proliferation, cyclin D1 and nuclear cdk2 and the suppression of the mitotic inhibitor, p27 that are the converse of the properties of wild-type Egr2. These gain-of-function effects provide additional insight into how this mutation leads to the development of such a severe form of inherited peripheral neuropathy.

5.3.1 Mutant Egr2 can function as a wild-type Egr2 molecule.

As mentioned previously, the EGR2 S382R, D383Y mutant was initially identified as a molecule that showed a greatly reduced binding of the Egr2 consensus binding site in an electrophoretic mobility shift assay (Warner et al., 1999). Further analysis demonstrated that the Egr2 S382R, D383Y mutant could not activate transcription of the myelin-related genes periaxin, myelin associated glycoprotein (MAG), P_0 and PMP22, unlike wild-type Egr2 (Nagarajan et al., 2001). The initial aim was to identify whether the S382R, D383Y mutant retained any Egr2 wild-type functions because it weakly activates a luciferase reporter construct containing Egr2 binding sites (Warner et al., 1999). As expected, I found mutant Egr2 could not induce P_0 expression but could still induce low levels of periaxin protein. This finding

is in contrast to that of Nagarajan et al, (2001). One possibility for this disparity is that it may reflect a species difference because I used rat Schwann cells for these experiments whereas Nagarajan et al, (2001) used mouse Schwann cells. Furthermore, Nagarajan et al, (2001) also measured periaxin mRNA at 24 hours after infection of Schwann cells with mutant Egr2 whereas I assayed protein levels after both 48 and 72 hours. It is possible that, due to its weakened DNA binding ability, the induction of periaxin can only be observed at longer time points after adenoviral infection.

My findings also raise the possibility that there are differences in the Egr2-mediated induction of P_0 compared to that of periaxin. The fact that mutant Egr2 never induces P_0 expression suggests that a strong Egr2/DNA interaction is required whereas a weaker Egr2/DNA interaction is sufficient to induce periaxin. In a recent study, it was shown that Egr2 directly induces P_0 expression in Schwann cells through Egr2 binding sites found in a conserved element within the first intron of the P_0 gene (LeBlanc et al., 2006). It is still not known whether Egr2 directly induces periaxin expression in Schwann cells, as Egr2 was unable to activate a reporter construct containing an 8kb fragment of the periaxin promoter (Parkinson et al., 2003). It should be noted that, it is more correct to think of Egr2 as elevating pre-existing expression of periaxin and P_0 in Schwann cells, at the onset of myelination, as both proteins can be detected in Schwann cells before Egr2 is upregulated (Lee et al., 1997; Parkinson et al., 2003). Thus both genes can be regulated by Egr2-independent mechanisms (Peirano et al., 2000; Parkinson et al., 2003).

An important function of wild-type Egr2 is its ability to promote survival of Schwann cells, even in the presence of death signals such as TGF β (Parkinson et al., 2001, 2004). This is correlated with the observation that there is increased postnatal Schwann cell death in the Krox-20 null mouse (Zorick et al., 1999; see section

1.5.4.1). Furthermore, inhibition of the JNK/c-Jun pathway can block Schwann cell death, *in vitro* and thus the increased survival of Egr2 positive Schwann cells is related to its ability to downregulate c-Jun (Parkinson et al., 2001; 2004). If the S382R, D383Y Egr2 mutant had failed to promote Schwann cell survival, this might have suggested a further explanation for the severe hypomyelination observed in humans. Surprisingly, mutant Egr2 protects newborn Schwann cells from TGF β induced death at least as efficiently as wild-type Egr2 and was also able to downregulate expression of c-Jun. The survival experiments were carried out in serum free medium and therefore these results were unaffected by cell proliferation (see section 5.3.2). This finding argues against a mechanism involving increased Schwann cell death contributing to the CHN phenotype seen in the patient carrying the S382R, D383Y mutation. In addition, it is remarkable that even though mutant Egr2 has reduced DNA binding it still maintains fully the ability to promote Schwann cell survival. This suggests that the mechanisms that control Egr2 mediated myelin gene expression may differ from those that direct Egr2 mediated cell survival.

5.3.2 Mutant Egr2 also displays effects that are the converse of wild-type Egr2.

Schwann cells expressing mutant Egr2 demonstrate increased levels of DNA synthesis not only in the presence of the axonally-derived mitogen NRG1 but also when NRG1 is absent from the culture medium. Considering the established role of wild-type Egr2 in causing Schwann cell cycle exit, even in the presence of NRG1, this observation was very surprising (Zorick et al., 1999; Parkinson et al., 2004). Nevertheless, it has important consequences considering that a biopsy of the sural nerve of a patient carrying this mutation revealed numerous onion bulbs containing supernumerary Schwann cells, characterisic of increased proliferation of Schwann

cells (Warner et al., 1998). Furthermore, evidence from the rat model of CMT1A demonstrates that Schwann cells in demyelinated axonal segments, that presumably give rise to the supernumerary Schwann cells within onion bulbs, express nuclear cyclin D1 and proliferate (Atanasoski et al., 2002), as I observe with mutant Egr2 expressing Schwann cells.

The routine medium for these experiments contained 0.5% calf serum. When this was omitted from the culture medium I failed to observe significant Schwann cell DNA synthesis. This suggests that the mechanism by which mutant Egr2 stimulates Schwann cell proliferation involves changes in the response to potential mitogens in the cellular environment. Mutant Egr2 can induce nuclear expression of cyclin D1 and cdk2 and reduce levels of the cell cycle inhibitor, p27. Either or both of these responses may contribute to the increased proliferative response of mutant Egr2 expressing Schwann cells. Evidence from cyclin D1-null Schwann cells demonstrates that it is required for Schwann cells to proliferate in culture and after nerve transection (Kim et al., 2000; Atanasoski et al, 2001). Furthermore, overexpression of cyclin D1 in Schwann cells using a retrovirus caused DNA synthesis in a significant proportion of Schwann cells in the absence of growth factor treatment, such as PDGF (Kim et al., 2001). Although reduction in p27 levels is correlated with cell proliferation (Tikoo et al., 2000), it is unknown whether loss of p27 is sufficient to induce Schwann cells to proliferate in culture.

The findings that mutant Egr2 increases ERK1/2 phosphorylation and that the inhibition of the MEK/ERK1/2 and c-Jun/JNK pathways reduces DNA synthesis induced by mutant Egr2, may indicate that mutant Egr2 controls Schwann cell proliferation upstream of the cell cycle regulatory proteins. For instance, mutant Egr2 could increase the expression of growth factor receptors or their activity. I found,

however, that the levels of the erbB2 and erbB3 receptor proteins remained unchanged in mutant Egr2 infected cells (not shown). Furthermore, I found that proliferation induced by mutant Egr2 was not inhibited by the use of either of the erbB2 tyrosine-kinase inhibitors, AG1478 (Lyons et al., 2005) or GW2974 (not shown). This suggests that mutant Egr2 does not increase erbB2 receptor activity and that it exerts its influence on targets downstream of this receptor. It remains possible that mutant Egr2 alters the expression or phosphorylation state of other growth factor receptors, such as the PDGF receptor. Another possibility arises from the observation that mutant Egr2 induces a significant cell flattening (see Fig. 6.5, I) suggesting that adhesion between the cells and the substrate may be increased in Schwann cells expressing mutant Egr2. This may be important because Schwann cells were plated onto a laminin substrate and one set of adhesion molecules that may be altered by mutant Egr2 are the integrins, some of which are activated on binding to laminin (Previtali et al., 2001; Wrabetz and Feltri, 2005). This is particularly significant given that one of the functions of the integrin receptors is to modulate growth factor signalling (for review see Guo and Giancotti, 2004).

5.3.3 Mutant Egr2 demonstrates concentration-dependent effects.

Schwann cells tend to incorporate BrdU when they express lower levels of mutant Egr2 whereas Schwann cells expressing higher levels of mutant Egr2 are less likely to proliferate but instead tend to differentiate and express myelin related markers such as periaxin. The difference in functional consequence to the Schwann cell, depending on the level of mutant Egr2 expressed, may be linked with either the level of DNA binding of mutant Egr2 or with its ability to associate with other proteins. A recent publication showed that peripheral nerve myelination requires co-

operation between Egr2 and its co-factors Nab1 and Nab2 and that Egr2 induces Nab1 and Nab2 as well (Le et al., 2005b). Mutant Egr2 has reduced ability to induce Nab2 and this may contribute to the dysfunction of this protein. Interestingly, when Egr2 is expressed in the absence of both Nab1 and Nab2, it not only fails to induce significant levels of myelin genes, such as P_0, PMP22 and periaxin but also activates genes that are not activated when Nab1 and Nab2 are present (see section 1.5.4.1). In addition, the Egr2 I268N mutant, which does not bind Nab proteins and causes recessive CHN, also activates aberrant genes (Nagarajan et al., 2001; Le et al., 2005b; Desmazières et al., 2008).

5.3.4 Egr2 mutations in inherited peripheral neuropathies.

The fact that mutant Egr2 can induce proliferation may help explain the presence of supernumerary Schwann cells in nerves biopsies from patients carrying this mutation (Warner et al, 1998). Other studies have shown that the Egr2 S382R, D383Y mutant can dominantly-inhibit wild-type Egr2 function (Nagarajan et al., 2001; Le Blanc et al., 2007). We confirm that this mutant can act as a dominant-negative molecule, which is particularly important since this mutation follows an autosomal dominant pattern of inheritance (Warner et al., 1998). A recent publication demonstrated that dominant-negative Egr2 mutants actually perturb Sox10 binding at Egr2/Sox10 binding sites in the P_0 intron element thus preventing cooperative Sox10 and wild-type Egr2 mediated myelin gene expression (LeBlanc et al., 2006, 2007). However, these mutations may induce subtly different molecular and cellular phenotypes since they lead to peripheral neuropathies of varying severity. One potential explanation is that the various DNA binding mutants may have different affinities for Sox10 (LeBlanc et al., 2007). Yet, in the case of 3 EGR2 DNA binding

mutants, it has also been shown that the increasing ability to bind DNA also correlates with the increasing severity of peripheral neuropathy that they cause (Warner et al., 1999). In view of the complex spectrum of normal and abnormal functions shown by the Egr2 S382R, D383Y mutant, it will be important for future studies to investigate the functional properties of other EGR2 DNA binding mutants in order elucidate the particular mechanisms by which these mutations lead to peripheral nerve dysfunction.

CHAPTER 6: General Discussion

Since the advent of the unveiling of the double helical structure of DNA (Watson and Crick, 1953) the focus of cell biology has been strongly concentrated on the molecules involved in the control of cellular processes such as proliferation, survival and differentiation. Within the last twenty years much progress has been made in understanding some of the signals and cellular mechanisms involved in many aspects of Schwann cell biology. This knowledge has in turn aided understanding of disease processes in peripheral nerves, when systems do not work as they should. In particular, the discovery of proteins associated with myelinating Schwann cells and some of the transcription factors that control their expression have lead to the identification of many of these molecules as being deficient or mutated in many forms of inherited peripheral neuropathies.

Within this thesis I aimed to identify new roles for factors involved in regulating the differentiation of Schwann cells. I have investigated how cyclic AMP and NRG1 signals and the transcription factor CREB regulate Schwann cell myelin differentiation (Chapter 3). Additionally, I examined the involvement of the transcription factor, c-Jun in Schwann cells in response to nerve injury (Chapter 4). Finally, I observed the functional consequences for Schwann cells of a mutation in the transcription factor Egr-2, which leads to CHN in humans (Chapter 5). A common theme that has developed within the projects described in this thesis is the positive and negative regulation of Schwann cell myelination. In particular, this thesis demonstrates that genes that negatively regulate myelination may also have important roles in controlling the phenotype of Schwann cells after nerve injury.

One of the most surprising findings was that cyclic AMP analogue treatment was insufficient to induce Schwann cell myelin differentiation in cultured mouse Schwann cells whereas it has been known for over twenty years to perform this function in cultured rat Schwann cells. This finding in itself presents intriguing opportunities to investigate why there is such a difference considering the relatively close phylogenetic relationship between rats and mice. In addition it also raises the question of how accurate predictions from studying rodents can be for understanding mechanisms in human cells. This is why the work using human Schwann cells, pioneered by the Bunge laboratory, is essential to identify similarities and differences with work done in rodent Schwann cells or indeed other species (Morrissey et al., 1991). However, the very nature of this species difference allowed me to identify a potential mechanism for how NRG1 signalling might contribute to Schwann cell myelin differentiation. Future work will be able to discern how cyclic AMP modulates NRG1 signalling and identify whether this is an important mechanism *in vivo*.

In addition, I have identified a potential role for the CREB family of transcription factors in regulating Schwann cell myelin differentiation. This finding potentially adds to the list of transcription factors now known to play a role in myelination, which consist of Krox-20 (Egr-2), Oct-6, Sox10 and NFκB (Jessen and Mirsky, 2005). Future investigation will no doubt determine whether CREB or the related transcription factors ATF1 and CREM play a role in Schwann cell differentiation *in vivo*.

Studying the role of c-Jun in Schwann cells, particularly after nerve injury, provided me with a very unique opportunity to open up debate and investigation on relatively unstudied facets of Schwann cell biology, namely the mechanism of

Schwann cell demyelination and the contribution of the Schwann cells to axonal regeneration and neuronal integrity after peripheral nerve injury. The involvement of the Schwann cell in events during Wallerian degeneration and peripheral nerve regeneration have been the subject of conjecture since the time of Cajal though there is a distinct lack of evidence to outline the relative importance of the Schwann cell in these processes. Results in this thesis clearly show that Schwann cells actively respond to nerve injury and this response is required for adequate myelin removal, axonal regeneration, neuronal survival and nerve repair. Thus Schwann cells appear to be key regulators of successful nerve repair and these findings can now be used as a platform to investigate the mechanisms involved in these processes and the relative contribution of c-Jun to these phenotypes.

These results also provide a strong argument to redefine our current perspective of the Schwann cell lineage (Fig.6.1). Many researchers refer to Schwann cells returning to an immature-like phenotype after nerve injury due to re-expression of molecules such as L1, $p75^{NTR}$ and NCAM (Scherer and Salzer, 2001; Jessen and Mirsky, 2005). However, denervated Schwann cells also demonstrate phagocytic/autophagic properties and furthermore these cells express many cytokines to mediate inflammatory responses (see Chapters 1 and 4). In addition, immature Schwann cells express the 04 antigen during development whereas denervated Schwann cells do not express 04 (Mirsky et al., 1990). Denervated Schwann cells have also been shown to express N-cadherin, a marker that is expressed by Schwann cell precursors and only at very low levels on immature Schwann cells (Padilla et al., 1999; Wanner et al., 2006b). These are two examples of the divergence in the phenotype of denervated Schwann cells from that of immature Schwann cells. Furthermore, microarray analysis has also identified that only 47% of genes regulated

after nerve injury are also regulated during development (Bosse et al., 2006). Thus these findings argue that the denervated Schwann cell be identified as phenotypically distinct from the immature Schwann cell.

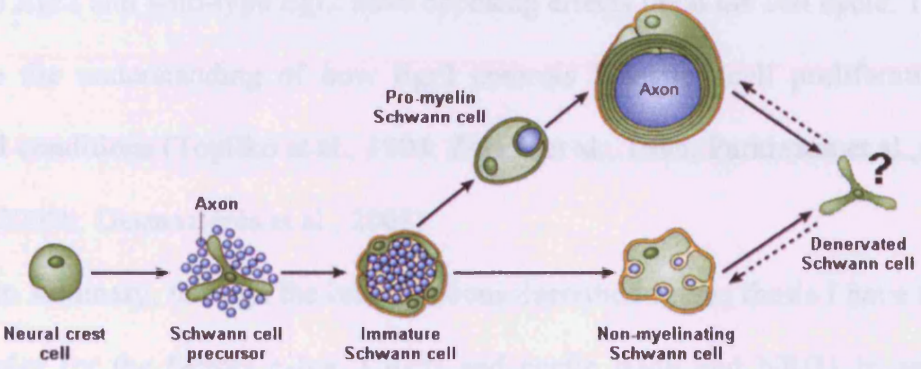

Figure 6.1: The adapted Schwann cell lineage: A case for a new member?

Schematic of the Schwann cell lineage in light of observations of the phenotypic differences between denervated Schwann cells and the rest of the Schwann cell lineage. Dotted arrows demonstrate the ability of denervated Schwann cells to differentiate into myelinating or non-myelinating Schwann cells after associating with regenerating axons during peripheral nerve repair.

Finally, investigating the functional consequences of a mutation in Egr-2 demonstrated that the mutant protein retained some aspects of its wild-type counterpart while it also demonstrated novel aberrant functions, particularly in its ability to induce Schwann cell proliferation whereas wild-type Egr-2 inhibited Schwann cell proliferation. While these observations add to the bank of knowledge regarding the potential mechanisms resulting in the onset of CHN in patients with this mutation (Warner et al., 1998; Warner et al., 1999; Nagarajan et al., 2001; Le et al., 2005a; LeBlanc et al., 2007) they also extend the opportunity to investigate how mutant Egr2 and wild-type Egr2 have opposing effects upon the cell cycle. This could add to the understanding of how Egr2 controls Schwann cell proliferation under normal conditions (Topilko et al., 1994; Zorick et al., 1996; Parkinson et al., 2004; Le et al., 2005b; Desmazières et al., 2008).

In summary, through the investigations described in this thesis I have identified new roles for the factors c-Jun, CREB and cyclic AMP and NRG1 in addition to outlining the functions of a mutant form of Egr-2 in Schwann cells. These projects enabled me to view at first hand the evolving nature of the scientific process and marvel in the beauty of how an unexpected finding can sometimes lead to a completely new perspective on an old idea.

ACKNOWLEDGEMENTS

Firstly, I would like to thank my supervisors, Prof. K. R. Jessen and Prof. R. Mirsky for their all their experience, support and advice during my PhD.

I am particularly indebted to the technical skills of M. Turmaine, M. Rahman and D. Cianter. In addition, I would like to thank Mr. B. Warburton and Mr. M. Lind and everyone at Biological services for their tireless efforts and without which, most of the experiements in this thesis would not have been possible.

My thanks also go to all the current and past members of the lab who have helped me with my work. They include, Dr A. Woodhoo, Dr D.B. Parkinson, Dr M. D'Antonio, Dr A Bhaskaran, Dr S. Sharghi-Namini, Dr G. Wicher, Dr M. Latouche-Hartmann, Ms A. Droggiti, Ms. C. Davis, Mr V. Sahni, Mr D. Wilton, Ms K. Wanek and Mr A. Jayakar.

I thank Prof. G. Raivich, Prof. S.P. Hunt and Prof P. Anderson for their helpful suggestions and use of their equipment. I would also like to thank all those who generously donated reagents and animals for all my experiments.

I am eternally indebted to my parents for their love and their encouragement of everything I do. This thesis is a direct result of all the philosophising carried out at the kitchen table over all those years.

Finally, I would like to thank Olivia for all her love and support, without which this task would have been immeasurably harder.

REFERENCES

Abercrombie, M., Evans, D.H. & Murray, J.G. (1959) Nuclear multiplication and cell migration in degenerating unmyelinated nerves. *J Anat* **93**, 9-14.

Abercrombie, M. & Johnson, M.L. (1946) Quantitative histology of Wallerian degeneration: I. Nuclear population in rabbit sciatic nerve. *J Anat* **80**, 37-50.

Adlkofer, K., Martini, R., Aguzzi, A., Zielasek, J., Toyka, K.V. & Suter, U. (1995) Hypermyelination and demyelinating peripheral neuropathy in Pmp22-deficient mice. *Nat Genet* **11**, 274-280.

Adlkofer, K., Naef, R. & Suter, U. (1997) Analysis of compound heterozygous mice reveals that the Trembler mutation can behave as a gain-of-function allele. *J Neurosci Res* **49**, 671-680.

Ahn, S., Olive, M., Aggarwal, S., Krylov, D., Ginty, D.D. & Vinson, C. (1998) A Dominant-Negative Inhibitor of CREB Reveals that It Is a General Mediator of Stimulus-Dependent Transcription of c-fos. *Mol. Cell. Biol.* **18**, 967-977.

Akagi, K., Sandig, V., Vooijs, M., Van der Valk, M., Giovannini, M., Strauss, M. & Berns, A. (1997) Cre-mediated somatic site-specific recombination in mice. *Nucleic Acids Res* **25**, 1766-1773.

Akassoglou, K., Kombrinck, K.W., Degen, J.L. & Strickland, S. (2000) Tissue plasminogen activator-mediated fibrinolysis protects against axonal degeneration and demyelination after sciatic nerve injury. *J Cell Biol* **149**, 1157-1166.

Akassoglou, K. & Strickland, S. (2002) Nervous system pathology: the fibrin perspective. *Biol Chem* **383**, 37-45.

Akassoglou, K., Yu, W.M., Akpinar, P. & Strickland, S. (2002) Fibrin inhibits peripheral nerve remyelination by regulating Schwann cell differentiation. *Neuron* **33**, 861-875.

Akira, S. & Takeda, K. (2004) Toll-like receptor signalling. *Nat Rev Immunol* **4**, 499-511.

Amici, S.A., Dunn, W.A., Jr., Murphy, A.J., Adams, N.C., Gale, N.W., Valenzuela, D.M., Yancopoulos, G.D. & Notterpek, L. (2006) Peripheral myelin protein 22 is in complex with alpha6beta4 integrin, and its absence alters the Schwann cell basal lamina. *J Neurosci* **26**, 1179-1189.

Anderson, D.J. (1997) Cellular and molecular biology of neural crest cell lineage determination. *Trends Genet* **13**, 276-280.

Anzini, P., Neuberg, D.H., Schachner, M., Nelles, E., Willecke, K., Zielasek, J., Toyka, K.V., Suter, U. & Martini, R. (1997) Structural abnormalities and deficient maintenance of peripheral nerve myelin in mice lacking the gap junction protein connexin 32. *J Neurosci* **17**, 4545-4551.

Araki, T. & Milbrandt, J. (1996) Ninjurin, a novel adhesion molecule, is induced by nerve injury and promotes axonal growth. *Neuron* **17**, 353-361.

Araki, T. & Milbrandt, J. (2000) Ninjurin2, a novel homophilic adhesion molecule, is expressed in mature sensory and enteric neurons and promotes neurite outgrowth. *J Neurosci* **20**, 187-195.

Araki, T., Sasaki, Y. & Milbrandt, J. (2004) Increased nuclear NAD biosynthesis and SIRT1 activation prevent axonal degeneration. *Science* **305**, 1010-1013.

Arroyo, E.J., Bermingham, J.R., Jr., Rosenfeld, M.G. & Scherer, S.S. (1998) Promyelinating Schwann cells express Tst-1/SCIP/Oct-6. *J Neurosci* **18**, 7891-7902.

Arroyo, E.J. & Scherer, S.S. (2000) On the molecular architecture of myelinated fibers. *Histochem Cell Biol* **113**, 1-18.

Asbury, A.K. (1967) Schwann cell proliferation in developing mouse sciatic nerve. A radioautographic study. *J Cell Biol* **34**, 735-743.

Atanasoski, S., Boentert, M., De Ventura, L., Pohl, H., Baranek, C., Beier, K., Young, P., Barbacid, M. & Suter, U. (2008) Postnatal Schwann cell proliferation but not myelination is strictly and uniquely dependent on cyclin-dependent kinase 4 (cdk4). *Mol Cell Neurosci* **37**, 519-527.

Atanasoski, S., Scherer, S.S., Nave, K.-A. & Suter, U. (2002) Proliferation of Schwann cells and regulation of cyclin D1 expression in an animal model of Charcot-Marie-Tooth disease type 1A. *Journal of Neuroscience Research* **67**, 443-449.

Atanasoski, S., Scherer, S.S., Sirkowski, E., Leone, D., Garratt, A.N., Birchmeier, C. & Suter, U. (2006) ErbB2 signaling in Schwann cells is mostly dispensable for maintenance of myelinated peripheral nerves and proliferation of adult Schwann cells after injury. *J Neurosci* **26**, 2124-2131.

Atanasoski, S., Shumas, S., Dickson, C., Scherer, S.S. & Suter, U. (2001) Differential Cyclin D1 Requirements of Proliferating Schwann Cells during Development and after Injury. *Molecular and Cellular Neuroscience* **18**, 581.

Azzedine, H., Bolino, A., Taieb, T., Birouk, N., Di Duca, M., Bouhouche, A., Benamou, S., Mrabet, A., Hammadouche, T., Chkili, T., Gouider, R., Ravazzolo, R., Brice, A., Laporte, J. & LeGuern, E. (2003) Mutations in MTMR13, a new pseudophosphatase homologue of MTMR2 and Sbf1, in two families with an autosomal recessive demyelinating form of Charcot-Marie-Tooth disease associated with early-onset glaucoma. *Am J Hum Genet* **72**, 1141-1153.

Baichwal, R.R., Bigbee, J.W. & DeVries, G.H. (1988) Macrophage-mediated myelin-related mitogenic factor for cultured Schwann cells. *Proc Natl Acad Sci U S A* **85**, 1701-1705.

Bajestan, S.N., Umehara, F., Shirahama, Y., Itoh, K., Sharghi-Namini, S., Jessen, K.R., Mirsky, R. & Osame, M. (2006) Desert hedgehog-patched 2 expression in peripheral nerves during Wallerian degeneration and regeneration. *J Neurobiol* **66**, 243-255.

Balice-Gordon, R.J., Bone, L.J. & Scherer, S.S. (1998) Functional gap junctions in the schwann cell myelin sheath. *J Cell Biol* **142**, 1095-1104.

Banner, L.R. & Patterson, P.H. (1994) Major changes in the expression of the mRNAs for cholinergic differentiation factor/leukemia inhibitory factor and its receptor after injury to adult peripheral nerves and ganglia. *Proc Natl Acad Sci U S A* **91**, 7109-7113.

Barco, A., Alarcon, J.M. & Kandel, E.R. (2002) Expression of Constitutively Active CREB Protein Facilitates the Late Phase of Long-Term Potentiation by Enhancing Synaptic Capture. *Cell* **108**, 689.

Barres, B.A., Jacobson, M.D., Schmid, R., Sendtner, M. & Raff, M.C. (1993) Does oligodendrocyte survival depend on axons? *Curr Biol* **3**, 489-497.

Barton, A.A. (1962) An electron microscope study of degeneration and regeneration of nerve. *Brain* **85**, 799-808.

Bauer, S., Kerr, B.J. & Patterson, P.H. (2007) The neuropoietic cytokine family in development, plasticity, disease and injury. *Nat Rev Neurosci* **8**, 221-232.

Bedi, K.S., Winter, J., Berry, M. & Cohen, J. (1992) Adult Rat Dorsal Root Ganglion Neurons Extend Neurites on Predegenerated But Not on Normal Peripheral Nerves In Vitro. *Eur J Neurosci* **4**, 193-200.

Behrens, A., Sibilia, M., David, J.P., Mohle-Steinlein, U., Tronche, F., Schutz, G. & Wagner, E.F. (2002) Impaired postnatal hepatocyte proliferation and liver regeneration in mice lacking c-jun in the liver. *Embo J* **21**, 1782-1790.

Beirowski, B., Adalbert, R., Wagner, D., Grumme, D.S., Addicks, K., Ribchester, R.R. & Coleman, M.P. (2005) The progressive nature of Wallerian degeneration in wild-type and slow Wallerian degeneration (WldS) nerves. *BMC Neurosci* **6**, 6.

Bellone, E., Di Maria, E., Soriani, S., Varese, A., Doria, L.L., Ajmar, F. & Mandich, P. (1999) A novel mutation (D305V) in the early growth response 2 gene is associated with severe Charcot-Marie-Tooth type 1 disease. *Hum Mutat* **14**, 353-354.

Benbow, U. & Brinckerhoff, C.E. (1997) The AP-1 site and MMP gene regulation: what is all the fuss about? *Matrix Biol* **15**, 519-526.

Bennett, D.L., Boucher, T.J., Armanini, M.P., Poulsen, K.T., Michael, G.J., Priestley, J.V., Phillips, H.S., McMahon, S.B. & Shelton, D.L. (2000) The glial cell line-derived neurotrophic factor family receptor components are differentially regulated within sensory neurons after nerve injury. *J Neurosci* **20**, 427-437.

Bennett, D.L., Michael, G.J., Ramachandran, N., Munson, J.B., Averill, S., Yan, Q., McMahon, S.B. & Priestley, J.V. (1998) A distinct subgroup of small DRG cells express GDNF receptor components and GDNF is protective for these neurons after nerve injury. *J Neurosci* **18**, 3059-3072.

Benninger, Y., Thurnherr, T., Pereira, J.A., Krause, S., Wu, X., Chrostek-Grashoff, A., Herzog, D., Nave, K.A., Franklin, R.J., Meijer, D., Brakebusch, C., Suter, U. & Relvas, J.B. (2007) Essential and distinct roles for cdc42 and rac1 in the regulation of Schwann cell biology during peripheral nervous system development. *J Cell Biol* **177**, 1051-1061.

Berger, P., Niemann, A. & Suter, U. (2006) Schwann cells and the pathogenesis of inherited motor and sensory neuropathies (Charcot-Marie-Tooth disease). *Glia* **54**, 243-257.

Bermingham, J.R., Jr., Scherer, S.S., O'Connell, S., Arroyo, E., Kalla, K.A., Powell, F.L. & Rosenfeld, M.G. (1996) Tst-1/Oct-6/SCIP regulates a unique step in peripheral myelination and is required for normal respiration. *Genes Dev* **10**, 1751-1762.

Bermingham, J.R., Jr., Shearin, H., Pennington, J., O'Moore, J., Jaegle, M., Driegen, S., van Zon, A., Darbas, A., Ozkaynak, E., Ryu, E.J., Milbrandt, J. & Meijer, D. (2006) The claw paw mutation reveals a role for Lgi4 in peripheral nerve development. *Nat Neurosci* **9**, 76-84.

Beuche, W. & Friede, R.L. (1984) The role of non-resident cells in Wallerian degeneration. *J Neurocytol* **13**, 767-796.

Beuche, W. & Friede, R.L. (1986) Myelin phagocytosis in Wallerian degeneration of peripheral nerves depends on silica-sensitive, bg/bg-negative and Fc-positive monocytes. *Brain Res* **378**, 97-106.

Bigbee, J.W., Yoshino, J.E. & DeVries, G.H. (1987) Morphological and proliferative responses of cultured Schwann cells following rapid phagocytosis of a myelin-enriched fraction. *J Neurocytol* **16**, 487-496.

Bixby, J.L., Lilien, J. & Reichardt, L.F. (1988) Identification of the major proteins that promote neuronal process outgrowth on Schwann cells in vitro. *J Cell Biol* **107**, 353-361.

Blanchard, A.D., Sinanan, A., Parmantier, E., Zwart, R., Broos, L., Meijer, D., Meier, C., Jessen, K.R. & Mirsky, R. (1996) Oct-6 (SCIP/Tst-1) is expressed in Schwann cell precursors, embryonic Schwann cells, and postnatal myelinating Schwann cells: comparison with Oct-1, Krox-20, and Pax-3. *J Neurosci Res* **46**, 630-640.

Boerkoel, C.F., Takashima, H., Stankiewicz, P., Garcia, C.A., Leber, S.M., Rhee-Morris, L. & Lupski, J.R. (2001) Periaxin mutations cause recessive Dejerine-Sottas neuropathy. *Am J Hum Genet* **68**, 325-333.

Boivin, A., Pineau, I., Barrette, B., Filali, M., Vallieres, N., Rivest, S. & Lacroix, S. (2007) Toll-like receptor signaling is critical for Wallerian degeneration and functional recovery after peripheral nerve injury. *J Neurosci* **27**, 12565-12576.

Bolin, L.M., Verity, A.N., Silver, J.E., Shooter, E.M. & Abrams, J.S. (1995) Interleukin-6 production by Schwann cells and induction in sciatic nerve injury. *J Neurochem* **64**, 850-858.

Bolino, A., Bolis, A., Previtali, S.C., Dina, G., Bussini, S., Dati, G., Amadio, S., Del Carro, U., Mruk, D.D., Feltri, M.L., Cheng, C.Y., Quattrini, A. & Wrabetz, L. (2004) Disruption of Mtmr2 produces CMT4B1-like neuropathy with myelin outfolding and impaired spermatogenesis. *J Cell Biol* **167**, 711-721.

Bolino, A., Muglia, M., Conforti, F.L., LeGuern, E., Salih, M.A., Georgiou, D.M., Christodoulou, K., Hausmanowa-Petrusewicz, I., Mandich, P., Schenone, A., Gambardella, A., Bono, F., Quattrone, A., Devoto, M. & Monaco, A.P. (2000) Charcot-Marie-Tooth type 4B is caused by mutations in the gene encoding myotubularin-related protein-2. *Nat Genet* **25**, 17-19.

Bolis, A., Coviello, S., Bussini, S., Dina, G., Pardini, C., Previtali, S.C., Malaguti, M., Morana, P., Del Carro, U., Feltri, M.L., Quattrini, A., Wrabetz, L. & Bolino, A. (2005) Loss of Mtmr2 phosphatase in Schwann cells but not in motor neurons causes Charcot-Marie-Tooth type 4B1 neuropathy with myelin outfoldings. *J Neurosci* **25**, 8567-8577.

Bondurand, N., Girard, M., Pingault, V., Lemort, N., Dubourg, O. & Goossens, M. (2001) Human Connexin 32, a gap junction protein altered in the X-linked form of Charcot-Marie-Tooth disease, is directly regulated by the transcription factor SOX10. *Hum Mol Genet* **10**, 2783-2795.

Bonneick, S., Boentert, M., Berger, P., Atanasoski, S., Mantei, N., Wessig, C., Toyka, K.V., Young, P. & Suter, U. (2005) An animal model for Charcot-Marie-Tooth disease type 4B1. *Hum Mol Genet* **14**, 3685-3695.

Borsello, T., Clarke, P.G.H., Hirt, L., Vercelli, A., Repici, M., Schorderet, D.F., Bogousslavsky, J. & Bonny, C. (2003) A peptide inhibitor of c-Jun N-terminal kinase protects against excitotoxicity and cerebral ischemia. *Nat Med* **9**, 1180.

Bos, J.L. (2003) Epac: a new cAMP target and new avenues in cAMP research. *Nat Rev Mol Cell Biol* **4**, 733-738.

Bosse, F., Hasenpusch-Theil, K., Kury, P. & Muller, H.W. (2006) Gene expression profiling reveals that peripheral nerve regeneration is a consequence of both novel injury-dependent and reactivated developmental processes. *J Neurochem* **96**, 1441-1457.

Bottenstein, J.E. & Sato, G.H. (1979) Growth of a rat neuroblastoma cell line in serum-free supplemented medium. *Proc Natl Acad Sci U S A* **76**, 514-517.

Bouldin, T.W., Earnhardt, T.S. & Goines, N.D. (1991) Restoration of blood-nerve barrier in neuropathy is associated with axonal regeneration and remyelination. *J Neuropathol Exp Neurol* **50**, 719-728.

Boyd, J.G. & Gordon, T. (2001) The neurotrophin receptors, trkB and p75, differentially regulate motor axonal regeneration. *J Neurobiol* **49**, 314-325.

Boyd, J.G. & Gordon, T. (2003b) Glial cell line-derived neurotrophic factor and brain-derived neurotrophic factor sustain the axonal regeneration of chronically axotomized motoneurons in vivo. *Exp Neurol* **183**, 610-619.

Boyd, J.G. & Gordon, T. (2003a) Neurotrophic factors and their receptors in axonal regeneration and functional recovery after peripheral nerve injury. *Mol Neurobiol* **27**, 277-324.

Bradley, W.G. & Asbury, A.K. (1970) Duration of synthesis phase in neuilemma cells in mouse sciatic nerve during degeneration. *Exp Neurol* **26**, 275-282.

Bradley, W.G., Jaros, E. & Jenkison, M. (1977) The nodes of Ranvier in the nerves of mice with muscular dystrophy. *J Neuropathol Exp Neurol* **36**, 797-806.

Bradley, W.G. & Jenkison, M. (1973) Abnormalities of peripheral nerves in murine muscular dystrophy. *Journal of the Neurological Sciences* **18**, 227.

Braunewell, K.H., Pesheva, P., McCarthy, J.B., Furcht, L.T., Schmitz, B. & Schachner, M. (1995) Functional involvement of sciatic nerve-derived versican- and decorin-like molecules and other chondroitin sulphate proteoglycans in ECM-mediated cell adhesion and neurite outgrowth. *Eur J Neurosci* 7, 805-814.

Brennan, A., Dean, C.H., Zhang, A.L., Cass, D.T., Mirsky, R. & Jessen, K.R. (2000) Endothelins control the timing of Schwann cell generation in vitro and in vivo. *Dev Biol* **227**, 545-557.

Britsch, S., Goerich, D.E., Riethmacher, D., Peirano, R.I., Rossner, M., Nave, K.A., Birchmeier, C. & Wegner, M. (2001) The transcription factor Sox10 is a key regulator of peripheral glial development. *Genes Dev* **15**, 66-78.

Brockes, J.P., Fields, K.L. & Raff, M.C. (1979) Studies on cultured rat Schwann cells. I. Establishment of purified populations from cultures of peripheral nerve. *Brain Res* **165**, 105-118.

Brown, M.C., Lunn, E.R. & Perry, V.H. (1991) Poor Growth of Mammalian Motor and Sensory Axons Into Intact Proximal Nerve Stumps. *Eur J Neurosci* **3**, 1366-1369.

Brown, M.C., Lunn, E.R. & Perry, V.H. (1992) Consequences of slow Wallerian degeneration for regenerating motor and sensory axons. *J Neurobiol* **23**, 521-536.

Brown, M.C., Perry, V.H., Hunt, S.P. & Lapper, S.R. (1994) Further studies on motor and sensory nerve regeneration in mice with delayed Wallerian degeneration. *Eur J Neurosci* **6**, 420-428.

Bruck, W., Bruck, Y., Maruschak, B. & Friede, R.L. (1995) Mechanisms of macrophage recruitment in Wallerian degeneration. *Acta Neuropathol* **89**, 363-367.

Bruck, W. & Friede, R.L. (1990) Anti-macrophage CR3 antibody blocks myelin phagocytosis by macrophages in vitro. *Acta Neuropathol* **80**, 415-418.

Bruck, W., Huitinga, I. & Dijkstra, C.D. (1996) Liposome-mediated monocyte depletion during wallerian degeneration defines the role of hematogenous phagocytes in myelin removal. *J Neurosci Res* **46**, 477-484.

Bunge, M.B., Williams, A.K. & Wood, P.M. (1982) Neuron-Schwann cell interaction in basal lamina formation. *Dev Biol* **92**, 449-460.

Bunge, R.P., Bunge, M.B. & Bates, M. (1989) Movements of the Schwann cell nucleus implicate progression of the inner (axon-related) Schwann cell process during myelination. *J Cell Biol* **109**, 273-284.

Buonanno, A. & Fischbach, G.D. (2001) Neuregulin and ErbB receptor signaling pathways in the nervous system. *Curr Opin Neurobiol* **11**, 287-296.

Burazin, T.C. & Gundlach, A.L. (1998) Up-regulation of GDNFR-alpha and c-ret mRNA in facial motor neurons following facial nerve injury in the rat. *Brain Res Mol Brain Res* **55**, 331-336.

Burstyn-Cohen, T., Frumkin, A., Xu, Y.T., Scherer, S.S. & Klar, A. (1998) Accumulation of F-spondin in injured peripheral nerve promotes the outgrowth of sensory axons. *J Neurosci* **18**, 8875-8885.

Cafferty, W.B., Gardiner, N.J., Gavazzi, I., Powell, J., McMahon, S.B., Heath, J.K., Munson, J., Cohen, J. & Thompson, S.W. (2001) Leukemia inhibitory factor determines the growth status of injured adult sensory neurons. *J Neurosci* **21**, 7161-7170.

Carroll, S.L., Miller, M.L., Frohnert, P.W., Kim, S.S. & Corbett, J.A. (1997) Expression of neuregulins and their putative receptors, ErbB2 and ErbB3, is induced during Wallerian degeneration. *J Neurosci* **17**, 1642-1659.

Chan, J.R., Cosgaya, J.M., Wu, Y.J. & Shooter, E.M. (2001) Neurotrophins are key mediators of the myelination program in the peripheral nervous system. *Proc Natl Acad Sci U S A* **98**, 14661-14668.

Chan, J.R., Jolicoeur, C., Yamauchi, J., Elliott, J., Fawcett, J.P., Ng, B.K. & Cayouette, M. (2006) The polarity protein Par-3 directly interacts with p75NTR to regulate myelination. *Science* **314**, 832-836.

Chavez, J.C., Almhanna, K. & Berti-Mattera, L.N. (2005) Transient expression of hypoxia-inducible factor-1 alpha and target genes in peripheral nerves from diabetic rats. *Neurosci Lett* **374**, 179-182.

Chavrier, P., Lemaire, P., Revelant, O., Bravo, R. & Charnay, P. (1988) Characterization of a mouse multigene family that encodes zinc finger structures. *Mol. Cell. Biol.* **8**, 1319-1326.

Cheepudomwit, T., Guzelsu, E., Zhou, C., Griffin, J.W. & Hoke, A. (2008) Comparison of cytokine expression profile during Wallerian degeneration of myelinated and unmyelinated peripheral axons. *Neurosci Lett* **430**, 230-235.

Chen, J.K., Yao, L.L. & Jenq, C.B. (1991) Mitogenic response of rat Schwann cells to fibroblast growth factors is potentiated by increased intracellular cyclic AMP levels. *J Neurosci Res* **30**, 321-327.

Chen, S. & Bisby, M.A. (1993a) Impaired motor axon regeneration in the C57BL/Ola mouse. *J Comp Neurol* **333**, 449-454.

Chen, S. & Bisby, M.A. (1993b) Long-term consequences of impaired regeneration on facial motoneurons in the C57BL/Ola mouse. *J Comp Neurol* **335**, 576-585.

Chen, S., Rio, C., Ji, R.R., Dikkes, P., Coggeshall, R.E., Woolf, C.J. & Corfas, G. (2003) Disruption of ErbB receptor signaling in adult non-myelinating Schwann cells causes progressive sensory loss. *Nat Neurosci* **6**, 1186-1193.

Chen, S., Velardez, M.O., Warot, X., Yu, Z.X., Miller, S.J., Cros, D. & Corfas, G. (2006) Neuregulin 1-erbB signaling is necessary for normal myelination and sensory function. *J Neurosci* **26**, 3079-3086.

Chen, Z.L. & Strickland, S. (2003) Laminin gamma1 is critical for Schwann cell differentiation, axon myelination, and regeneration in the peripheral nerve. *J Cell Biol* **163**, 889-899.

Chen, Z.Y., Chai, Y.F., Cao, L., Lu, C.L. & He, C. (2001) Glial cell line-derived neurotrophic factor enhances axonal regeneration following sciatic nerve transection in adult rats. *Brain Res* **902**, 272-276.

Cheng, H.L., Randolph, A., Yee, D., Delafontaine, P., Tennekoon, G. & Feldman, E.L. (1996) Characterization of insulin-like growth factor-I and its receptor and binding proteins in transected nerves and cultured Schwann cells. *J Neurochem* **66**, 525-536.

Citri, A., Skaria, K.B. & Yarden, Y. (2003) The deaf and the dumb: the biology of ErbB-2 and ErbB-3. *Exp Cell Res* **284**, 54-65.

Clark, M.B. & Bunge, M.B. (1989) Cultured Schwann cells assemble normal-appearing basal lamina only when they ensheathe axons. *Dev Biol* **133**, 393-404.

Clemence, A., Mirsky, R. & Jessen, K.R. (1989) Non-myelin-forming Schwann cells proliferate rapidly during Wallerian degeneration in the rat sciatic nerve. *J Neurocytol* **18**, 185-192.

Coggeshall, R.E., Lekan, H.A., Doubell, T.P., Allchorne, A. & Woolf, C.J. (1997) Central changes in primary afferent fibers following peripheral nerve lesions. *Neuroscience* 77, 1115-1122.

Cohen, J.A., Yachnis, A.T., Arai, M., Davis, J.G. & Scherer, S.S. (1992) Expression of the neu proto-oncogene by Schwann cells during peripheral nerve development and Wallerian degeneration. *J Neurosci Res* **31**, 622-634.

Coleman, M. (2005) Axon degeneration mechanisms: commonality amid diversity. *Nat Rev Neurosci* **6**, 889-898.

Coleman, M.P., Conforti, L., Buckmaster, E.A., Tarlton, A., Ewing, R.M., Brown, M.C., Lyon, M.F. & Perry, V.H. (1998) An 85-kb tandem triplication in the slow Wallerian degeneration (Wlds) mouse. *Proc Natl Acad Sci U S A* **95**, 9985-9990.

Colman, D.R., Pedraza, L. & Yoshida, M. (2001) Concepts in myelin sheath evolution. In Jessen, K.R. & Richardson, W.D. (eds) *Glial cell development: basic principles and clinical relevance*, pp. 161-176

Conforti, L., Fang, G., Beirowski, B., Wang, M.S., Sorci, L., Asress, S., Adalbert, R., Silva, A., Bridge, K., Huang, X.P., Magni, G., Glass, J.D. & Coleman, M.P. (2007) NAD(+) and axon degeneration revisited: Nmnat1 cannot substitute for Wld(S) to delay Wallerian degeneration. *Cell Death Differ* **14**, 116-127.

Conforti, L., Tarlton, A., Mack, T.G., Mi, W., Buckmaster, E.A., Wagner, D., Perry, V.H. & Coleman, M.P. (2000) A Ufd2/D4Cole1e chimeric protein and overexpression of Rbp7 in the slow Wallerian degeneration (WldS) mouse. *Proc Natl Acad Sci U S A* **97**, 11377-11382.

Conti, G., Rostami, A., Scarpini, E., Baron, P., Galimberti, D., Bresolin, N., Contri, M., Palumbo, C. & De Pol, A. (2004) Inducible nitric oxide synthase (iNOS) in immune-mediated demyelination and Wallerian degeneration of the rat peripheral nervous system. *Exp Neurol* **187**, 350-358.

Cornbrooks, C.J., Carey, D.J., McDonald, J.A., Timpl, R. & Bunge, R.P. (1983) In vivo and in vitro observations on laminin production by Schwann cells. *Proc Natl Acad Sci U S A* **80**, 3850-3854.

Cosgaya, J.M., Chan, J.R. & Shooter, E.M. (2002) The neurotrophin receptor p75NTR as a positive modulator of myelination. *Science* **298**, 1245-1248.

Court, F.A., Sherman, D.L., Pratt, T., Garry, E.M., Ribchester, R.R., Cottrell, D.F., Fleetwood-Walker, S.M. & Brophy, P.J. (2004) Restricted growth of Schwann cells lacking Cajal bands slows conduction in myelinated nerves. *Nature* **431**, 191-195.

Crang, A.J. & Blakemore, W.F. (1986) Observations on Wallerian degeneration in explant cultures of cat sciatic nerve. *J Neurocytol* **15**, 471-482.

Crawford, A.T., Desai, D., Gokina, P., Basak, S. & Kim, H.A. (2008) E-cadherin expression in postnatal Schwann cells is regulated by the cAMP-dependent protein kinase a pathway. *Glia*.

Crosby, S.D., Veile, R.A., Donis-Keller, H., Baraban, J.M., Bhat, R.V., Simburger, K.S. & Milbrandt, J. (1992) Neural-specific expression, genomic structure, and chromosomal localization of the gene encoding the zinc-finger transcription factor NGFI-C. *Proc Natl Acad Sci U S A* **89**, 6663.

D'Antonio, M., Droggiti, A., Feltri, M.L., Roes, J., Wrabetz, L., Mirsky, R. & Jessen, K.R. (2006a) TGFbeta type II receptor signaling controls Schwann cell death and proliferation in developing nerves. *J Neurosci* **26**, 8417-8427.

D'Antonio, M., Michalovich, D., Paterson, M., Droggiti, A., Woodhoo, A., Mirsky, R. & Jessen, K.R. (2006b) Gene profiling and bioinformatic analysis of Schwann cell embryonic development and myelination. *Glia* **53**, 501-515.

Dahlin, L.B. (1995) Prevention of macrophage invasion impairs regeneration in nerve grafts. *Brain Res* **679**, 274-280.

Dailey, A.T., Avellino, A.M., Benthem, L., Silver, J. & Kliot, M. (1998) Complement depletion reduces macrophage infiltration and activation during Wallerian degeneration and axonal regeneration. *J Neurosci* **18**, 6713-6722.

Daniloff, J.K., Levi, G., Grumet, M., Rieger, F. & Edelman, G.M. (1986) Altered expression of neuronal cell adhesion molecules induced by nerve injury and repair. *J Cell Biol* **103**, 929-945.

Darbas, A., Jaegle, M., Walbeehm, E., van den Burg, H., Driegen, S., Broos, L., Uyl, M., Visser, P., Grosveld, F. & Meijer, D. (2004) Cell autonomy of the mouse claw paw mutation. *Dev Biol* **272**, 470-482.

David, S. & Aguayo, A.J. (1981) Axonal elongation into peripheral nervous system "bridges" after central nervous system injury in adult rats. *Science* **214**, 931-933.

De Felipe, C. & Hunt, S.P. (1994) The differential control of c-jun expression in regenerating sensory neurons and their associated glial cells. *J Neurosci* **14**, 2911-2923.

De, S., Trigueros, M.A., Kalyvas, A. & David, S. (2003) Phospholipase A2 plays an important role in myelin breakdown and phagocytosis during Wallerian degeneration. *Mol Cell Neurosci* **24**, 753-765.

Decker, L., Desmarquet-Trin-Dinh, C., Taillebourg, E., Ghislain, J., Vallat, J.M. & Charnay, P. (2006) Peripheral myelin maintenance is a dynamic process requiring constant Krox20 expression. *J Neurosci* **26**, 9771-9779.

Delague, V., Jacquier, A., Hamadouche, T., Poitelon, Y., Baudot, C., Boccaccio, I., Chouery, E., Chaouch, M., Kassouri, N., Jabbour, R., Grid, D., Megarbane, A., Haase, G. & Levy, N. (2007) Mutations in FGD4 encoding the Rho GDP/GTP exchange factor FRABIN cause autosomal recessive Charcot-Marie-Tooth type 4H. *Am J Hum Genet* **81**, 1-16.

Desmazieres, A., Decker, L., Vallat, J.M., Charnay, P. & Gilardi-Hebenstreit, P. (2008) Disruption of Krox20-Nab interaction in the mouse leads to peripheral neuropathy with biphasic evolution. *J Neurosci* **28**, 5891-5900.

Diamond, J., Coughlin, M., Macintyre, L., Holmes, M. & Visheau, B. (1987) Evidence that endogenous beta nerve growth factor is responsible for the collateral sprouting, but not the regeneration, of nociceptive axons in adult rats. *Proc Natl Acad Sci U S A* **84**, 6596-6600.

Diamond, J., Foerster, A., Holmes, M. & Coughlin, M. (1992a) Sensory nerves in adult rats regenerate and restore sensory function to the skin independently of endogenous NGF. *J Neurosci* **12**, 1467-1476.

Diamond, J., Holmes, M. & Coughlin, M. (1992b) Endogenous NGF and nerve impulses regulate the collateral sprouting of sensory axons in the skin of the adult rat. *J Neurosci* **12**, 1454-1466.

Dickson, K.M., Bergeron, J.J., Shames, I., Colby, J., Nguyen, D.T., Chevet, E., Thomas, D.Y. & Snipes, G.J. (2002) Association of calnexin with mutant peripheral myelin protein-22 ex vivo: a basis for "gain-of-function" ER diseases. *Proc Natl Acad Sci U S A* **99**, 9852-9857.

Diensthuber, M., Ilner, T., Rodt, T., Samii, M., Brandis, A., Lenarz, T. & Stover, T. (2007) Erythropoietin and erythropoietin receptor expression in vestibular schwannoma: potential role in tumor progression. *Otol Neurotol* **28**, 559-565.

Diner, O. (1965) [The Schwann cells during mitosis and their relation to the axons during the development of the sciatic nerve in the rat]. *C R Acad Sci Hebd Seances Acad Sci D* **261**, 1731-1734.

Dong, Z., Brennan, A., Liu, N., Yarden, Y., Lefkowitz, G., Mirsky, R. & Jessen, K.R. (1995) Neu differentiation factor is a neuron-glia signal and regulates survival, proliferation, and maturation of rat Schwann cell precursors. *Neuron* **15**, 585-596.

Dong, Z., Sinanan, A., Parkinson, D., Parmantier, E., Mirsky, R. & Jessen, K.R. (1999) Schwann cell development in embryonic mouse nerves. *J Neurosci Res* **56**, 334-348.

Doyle, G.A., Pierce, R.A. & Parks, W.C. (1997) Transcriptional induction of collagenase-1 in differentiated monocyte-like (U937) cells is regulated by AP-1 and an upstream C/EBP-beta site. *J Biol Chem* **272**, 11840-11849.

Dyck, P.J., Lais, A.C., Giannini, C. & Engelstad, J.K. (1990) Structural alterations of nerve during cuff compression. *Proc Natl Acad Sci U S A* **87**, 9828-9832.

Dytrych, L., Sherman, D.L., Gillespie, C.S. & Brophy, P.J. (1998) Two PDZ domain proteins encoded by the murine periaxin gene are the result of alternative intron retention and are differentially targeted in Schwann cells. *J Biol Chem* **273**, 5794-5800.

Eferl, R., Sibilia, M., Hilberg, F., Fuchsbichler, A., Kufferath, I., Guertl, B., Zenz, R., Wagner, E.F. & Zatloukal, K. (1999) Functions of c-Jun in liver and heart development. *J Cell Biol* **145**, 1049-1061.

Ehrengruber, M.U., Lanzrein, M., Xu, Y., Jasek, M.C., Kantor, D.B., Schuman, E.M., Lester, H.A., Davidson, N. & Conn, P.M. (1998) [27] Recombinant adenovirus-mediated expression in nervous system of genes coding for ion channels and other molecules involved in synaptic function *Methods in Enzymology*. Academic Press, p. 483.

Ehrengruber, M.U., Muhlebach, S.G., Sohrman, S., Leutenegger, C.M., Lester, H.A. & Davidson, N. (2000) Modulation of early growth response (EGR) transcription factor-dependent gene expression by using recombinant adenovirus. *Gene* **258**, 63.

English, A.W., Meador, W. & Carrasco, D.I. (2005) Neurotrophin-4/5 is required for the early growth of regenerating axons in peripheral nerves. *Eur J Neurosci* **21**, 2624-2634.

Eshed, Y., Feinberg, K., Carey, D.J. & Peles, E. (2007) Secreted gliomedin is a perinodal matrix component of peripheral nerves. *J Cell Biol* **177**, 551-562.

Eshed, Y., Feinberg, K., Poliak, S., Sabanay, H., Sarig-Nadir, O., Spiegel, I., Bermingham, J.R., Jr. & Peles, E. (2005) Gliomedin mediates Schwann cell-axon interaction and the molecular assembly of the nodes of Ranvier. *Neuron* **47**, 215-229.

Evan, G.I., Lewis, G.K., Ramsay, G. & Bishop, J.M. (1985) Isolation of monoclonal antibodies specific for human c-myc proto-oncogene product. *Mol Cell Biol* **5**, 3610-3616.

Fallon, J.R. (1985) Neurite guidance by non-neuronal cells in culture: preferential outgrowth of peripheral neurites on glial as compared to nonglial cell surfaces. *J Neurosci* **5**, 3169-3177.

Falls, D.L. (2003) Neuregulins: functions, forms, and signaling strategies. *Exp Cell Res* **284**, 14-30.

Fannon, A.M., Sherman, D.L., Ilyina-Gragerova, G., Brophy, P.J., Friedrich, V.L., Jr. & Colman, D.R. (1995) Novel E-cadherin-mediated adhesion in peripheral nerve: Schwann cell architecture is stabilized by autotypic adherens junctions. *J Cell Biol* **129**, 189-202.

Feltri, M.L., D'Antonio, M., Previtali, S., Fasolini, M., Messing, A. & Wrabetz, L. (1999a) P0-Cre Transgenic Mice for Inactivation of Adhesion Molecules in Schwann Cells. *Ann NY Acad Sci* **883**, 116-123.

Feltri, M.L., D'Antonio, M., Quattrini, A., Numerato, R., Arona, M., Previtali, S., Chiu, S.-Y., Messing, A. & Wrabetz, L. (1999b) A novel P0 glycoprotein transgene activates expression of lacZ in myelin-forming Schwann cells. *European Journal of Neuroscience* **11**, 1577-1586.

Feltri, M.L., Graus Porta, D., Previtali, S.C., Nodari, A., Migliavacca, B., Cassetti, A., Littlewood-Evans, A., Reichardt, L.F., Messing, A., Quattrini, A., Mueller, U. & Wrabetz, L. (2002) Conditional disruption of beta 1 integrin in Schwann cells impedes interactions with axons. *J Cell Biol* **156**, 199-209.

Feltri, M.L. & Wrabetz, L. (2005) Laminins and their receptors in Schwann cells and hereditary neuropathies. *J Peripher Nerv Syst* **10**, 128-143.

Ferguson, T.A. & Muir, D. (2000) MMP-2 and MMP-9 increase the neurite-promoting potential of schwann cell basal laminae and are upregulated in degenerated nerve. *Mol Cell Neurosci* **16**, 157-167.

Fernandes, K.J., Kobayashi, N.R., Jasmin, B.J. & Tetzlaff, W. (1998) Acetylcholinesterase gene expression in axotomized rat facial motoneurons is differentially regulated by neurotrophins: correlation with trkB and trkC mRNA levels and isoforms. *J Neurosci* **18**, 9936-9947.

Fernandez-Valle, C., Bunge, R.P. & Bunge, M.B. (1995) Schwann cells degrade myelin and proliferate in the absence of macrophages: evidence from in vitro studies of Wallerian degeneration. *J Neurocytol* **24**, 667-679.

Fernandez-Valle, C., Gorman, D., Gomez, A.M. & Bunge, M.B. (1997) Actin plays a role in both changes in cell shape and gene-expression associated with Schwann cell myelination. *J Neurosci* **17**, 241-250.

Fernandez-Valle, C., Gwynn, L., Wood, P.M., Carbonetto, S. & Bunge, M.B. (1994) Anti-beta 1 integrin antibody inhibits Schwann cell myelination. *J Neurobiol* **25**, 1207-1226.

Ferri, C.C. & Bisby, M.A. (1999) Improved survival of injured sciatic nerve Schwann cells in mice lacking the p75 receptor. *Neurosci Lett* **272**, 191-194.

ffrench-Constant, C. & Colognato, H. (2004) Integrins: versatile integrators of extracellular signals. *Trends Cell Biol* **14**, 678-686.

Filbin, M.T. (2003) Myelin-associated inhibitors of axonal regeneration in the adult mammalian CNS. *Nat Rev Neurosci* **4**, 703-713.

Flores, A.I., Narayanan, S.P., Morse, E.N., Shick, H.E., Yin, X., Kidd, G., Avila, R.L., Kirschner, D.A. & Macklin, W.B. (2008) Constitutively active Akt induces enhanced myelination in the CNS. *J Neurosci* **28**, 7174-7183.

Foster, E., Robertson, B. & Fried, K. (1994) trkB-like immunoreactivity in rat dorsal root ganglia following sciatic nerve injury. *Brain Res* **659**, 267-271.

Fragoso, G., Robertson, J., Athlan, E., Tam, E., Almazan, G. & Mushynski, W.E. (2003) Inhibition of p38 mitogen-activated protein kinase interferes with cell shape changes and gene expression associated with Schwann cell myelination. *Exp Neurol* **183**, 34-46.

Franz, C.K., Rutishauser, U. & Rafuse, V.F. (2005) Polysialylated neural cell adhesion molecule is necessary for selective targeting of regenerating motor neurons. *J Neurosci* **25**, 2081-2091.

Friede, R.L. & Johnstone, M.A. (1967) Responses of thymidine labeling of nuclei in gray matter and nerve following sciatic transection. *Acta Neuropathol* 7, 218-231.

Friedman, B., Scherer, S.S., Rudge, J.S., Helgren, M., Morrisey, D., McClain, J., Wang, D.Y., Wiegand, S.J., Furth, M.E., Lindsay, R.M. & et al. (1992) Regulation of ciliary neurotrophic factor expression in myelin-related Schwann cells in vivo. *Neuron* **9**, 295-305.

Fukata, Y., Adesnik, H., Iwanaga, T., Bredt, D.S., Nicoll, R.A. & Fukata, M. (2006) Epilepsy-related ligand/receptor complex LGI1 and ADAM22 regulate synaptic transmission. *Science* **313**, 1792-1795.

Funakoshi, H., Frisen, J., Barbany, G., Timmusk, T., Zachrisson, O., Verge, V.M. & Persson, H. (1993) Differential expression of mRNAs for neurotrophins and their receptors after axotomy of the sciatic nerve. *J Cell Biol* **123**, 455-465.

Funakoshi, H., Risling, M., Carlstedt, T., Lendahl, U., Timmusk, T., Metsis, M., Yamamoto, Y. & Ibanez, C.F. (1998) Targeted expression of a multifunctional chimeric neurotrophin in the lesioned sciatic nerve accelerates regeneration of sensory and motor axons. *Proc Natl Acad Sci U S A* **95**, 5269-5274.

Galiano, M., Liu, Z.Q., Kalla, R., Bohatschek, M., Koppius, A., Gschwendtner, A., Xu, S., Werner, A., Kloss, C.U., Jones, L.L., Bluethmann, H. & Raivich, G. (2001) Interleukin-6 (IL6) and cellular response to facial nerve injury: effects on lymphocyte recruitment, early microglial activation and axonal outgrowth in IL6-deficient mice. *Eur J Neurosci* **14**, 327-341.

Gao, X., Daugherty, R.L. & Tourtellotte, W.G. (2007) Regulation of low affinity neurotrophin receptor (p75(NTR)) by early growth response (Egr) transcriptional regulators. *Mol Cell Neurosci* **36**, 501-514.

Gao, Y., Deng, K., Hou, J., Bryson, J.B., Barco, A., Nikulina, E., Spencer, T., Mellado, W., Kandel, E.R. & Filbin, M.T. (2004) Activated CREB is sufficient to overcome inhibitors in myelin and promote spinal axon regeneration in vivo. *Neuron* **44**, 609-621.

Garbay, B., Heape, A.M., Sargueil, F. & Cassagne, C. (2000) Myelin synthesis in the peripheral nervous system. *Prog Neurobiol* **61**, 267-304.

Garratt, A.N., Voiculescu, O., Topilko, P., Charnay, P. & Birchmeier, C. (2000) A dual role of erbB2 in myelination and in expansion of the schwann cell precursor pool. *J Cell Biol* **148**, 1035-1046.

Gatto, C.L., Walker, B.J. & Lambert, S. (2003) Local ERM activation and dynamic growth cones at Schwann cell tips implicated in efficient formation of nodes of Ranvier. *J Cell Biol* **162**, 489-498.

Gavrilovic, J., Brennan, A., Mirsky, R. & Jessen, K.R. (1995) Fibroblast growth factors and insulin growth factors combine to promote survival of rat Schwann cell precursors without induction of DNA synthesis. *Eur J Neurosci* 7, 77-85.

George, E.B., Glass, J.D. & Griffin, J.W. (1995) Axotomy-induced axonal degeneration is mediated by calcium influx through ion-specific channels. *J Neurosci* **15**, 6445-6452.

Ghabriel, M.N. & Allt, G. (1979) The role of Schmidt-Lanterman incisures in Wallerian degeneration. II. An electron microscopic study. *Acta Neuropathol* **48**, 95-103.

Ghazvini, M., Mandemakers, W., Jaegle, M., Piirsoo, M., Driegen, S., Koutsourakis, M., Smit, X., Grosveld, F. & Meijer, D. (2002) A cell type-specific allele of the POU gene Oct-6 reveals Schwann cell autonomous function in nerve development and regeneration. *Embo J* **21**, 4612-4620.

Ghislain, J. & Charnay, P. (2006) Control of myelination in Schwann cells: a Krox20 cis-regulatory element integrates Oct6, Brn2 and Sox10 activities. *EMBO Rep* 7, 52-58.

Ghislain, J., Desmarquet-Trin-Dinh, C., Jaegle, M., Meijer, D., Charnay, P. & Frain, M. (2002) Characterisation of cis-acting sequences reveals a biphasic, axon-dependent regulation of Krox20 during Schwann cell development. *Development* **129**, 155-166.

Giese, K.P., Martini, R., Lemke, G., Soriano, P. & Schachner, M. (1992) Mouse P0 gene disruption leads to hypomyelination, abnormal expression of recognition molecules, and degeneration of myelin and axons. *Cell* **71**, 565-576.

Gillespie, C.S., Sherman, D.L., Blair, G.E. & Brophy, P.J. (1994) Periaxin, a novel protein of myelinating Schwann cells with a possible role in axonal ensheathment. *Neuron* **12**, 497.

Gillespie, C.S., Sherman, D.L., Fleetwood-Walker, S.M., Cottrell, D.F., Tait, S., Garry, E.M., Wallace, V.C., Ure, J., Griffiths, I.R., Smith, A. & Brophy, P.J. (2000) Peripheral demyelination and neuropathic pain behavior in periaxin-deficient mice. *Neuron* **26**, 523-531.

Gillian, A.L. & Svaren, J. (2004) The Ddx20/DP103 dead box protein represses transcriptional activation by Egr2/Krox-20. *J Biol Chem* **279**, 9056-9063.

Glass, J.D., Brushart, T.M., George, E.B. & Griffin, J.W. (1993) Prolonged survival of transected nerve fibres in C57BL/Ola mice is an intrinsic characteristic of the axon. *J Neurocytol* **22**, 311-321.

Gonzalez-Hernandez, T. & Rustioni, A. (1999) Expression of three forms of nitric oxide synthase in peripheral nerve regeneration. *J Neurosci Res* **55**, 198-207.

Gould, R.M., Byrd, A.L. & Barbarese, E. (1995) The number of Schmidt-Lanterman incisures is more than doubled in shiverer PNS myelin sheaths. *J Neurocytol* **24**, 85-98.

Griffin, J.W., Stocks, E.A., Fahnestock, K., Van Praagh, A. & Trapp, B.D. (1990) Schwann cell proliferation following lysolecithin-induced demyelination. *J Neurocytol* **19**, 367-384.

Grinspan, J.B., Marchionni, M.A., Reeves, M., Coulaloglou, M. & Scherer, S.S. (1996) Axonal interactions regulate Schwann cell apoptosis in developing peripheral nerve: neuregulin receptors and the role of neuregulins. *J Neurosci* **16**, 6107-6118.

Grove, M., Komiyama, N.H., Nave, K.A., Grant, S.G., Sherman, D.L. & Brophy, P.J. (2007) FAK is required for axonal sorting by Schwann cells. *J Cell Biol* **176**, 277-282.

Groves, M.J., Schanzer, A., Simpson, A.J., An, S.F., Kuo, L.T. & Scaravilli, F. (2003) Profile of adult rat sensory neuron loss, apoptosis and replacement after sciatic nerve crush. *J Neurocytol* **32**, 113-122.

Groves, M.L., McKeon, R., Werner, E., Nagarsheth, M., Meador, W. & English, A.W. (2005) Axon regeneration in peripheral nerves is enhanced by proteoglycan degradation. *Exp Neurol* **195**, 278-292.

Guertin, A.D., Zhang, D.P., Mak, K.S., Alberta, J.A. & Kim, H.A. (2005) Microanatomy of axon/glial signaling during Wallerian degeneration. *J Neurosci* **25**, 3478-3487.

Guilbot, A., Williams, A., Ravise, N., Verny, C., Brice, A., Sherman, D.L., Brophy, P.J., LeGuern, E., Delague, V., Bareil, C., Megarbane, A. & Claustres, M. (2001) A mutation in periaxin is responsible for CMT4F, an autosomal recessive form of Charcot-Marie-Tooth disease. *Hum Mol Genet* **10**, 415-421.

Guo, W. & Giancotti, F.G. (2004) Integrin signalling during tumour progression. *Nat Rev Mol Cell Biol* **5**, 816-826.

Gutmann, E., Guttman, L., Medawar, P., Young, J.Z. (1942) The rate of regeneration of nerve. *J Exp Biol* **19**, 14-44.

Haines, J.D., Fragoso, G., Hossain, S., Mushynski, W.E. & Almazan, G. (2008) p38 Mitogen-activated protein kinase regulates myelination. *J Mol Neurosci* **35**, 23-33.

Hall, S.M. (1986) The effect of inhibiting Schwann cell mitosis on the re-innervation of acellular autografts in the peripheral nervous system of the mouse. *Neuropathol Appl Neurobiol* **12**, 401-414.

Hall, S.M. (1993) Observations on the progress of Wallerian degeneration in transected peripheral nerves of C57BL/Wld mice in the presence of recruited macrophages. *J Neurocytol* **22**, 480-490.

Hall, S.M. & Gregson, N.A. (1971) The in vivo and ultrastructural effects of injection of lysophosphatidyl choline into myelinated peripheral nerve fibres of the adult mouse. *J Cell Sci* **9**, 769-789.

Harrisingh, M.C. & Lloyd, A.C. (2004) Ras/Raf/ERK signalling and NF1. *Cell Cycle* **3**, 1255-1258.

Harrisingh, M.C., Perez-Nadales, E., Parkinson, D.B., Malcolm, D.S., Mudge, A.W. & Lloyd, A.C. (2004) The Ras/Raf/ERK signalling pathway drives Schwann cell dedifferentiation. *Embo J* **23**, 3061-3071.

Hasselblatt, P., Rath, M., Komnenovic, V., Zatloukal, K. & Wagner, E.F. (2007) Hepatocyte survival in acute hepatitis is due to c-Jun/AP-1-dependent expression of inducible nitric oxide synthase. *Proc Natl Acad Sci U S A* **104**, 17105-17110.

Hayes, T.L., Lindgren, F.T. & Gofman, J.W. (1963) A Quantitative Determination Of The Osmium Tetroxide-Lipoprotein Interaction. *J Cell Biol* **19**, 251-255.

Hayworth, C.R., Moody, S.E., Chodosh, L.A., Krieg, P., Rimer, M. & Thompson, W.J. (2006) Induction of neuregulin signaling in mouse schwann cells in vivo mimics responses to denervation. *J Neurosci* **26**, 6873-6884.

He, T.C., Zhou, S., da Costa, L.T., Yu, J., Kinzler, K.W. & Vogelstein, B. (1998) A simplified system for generating recombinant adenoviruses. *Proc Natl Acad Sci U S A* **95**, 2509-2514.

Heinen, A., Kremer, D., Gottle, P., Kruse, F., Hasse, B., Lehmann, H., Hartung, H.P. & Kury, P. (2008) The cyclin-dependent kinase inhibitor p57kip2 is a negative regulator of Schwann cell differentiation and in vitro myelination. *Proc Natl Acad Sci U S A* **105**, 8748-8753.

Henry, E.W., Eicher, E.M. & Sidman, R.L. (1991) The mouse mutation claw paw: forelimb deformity and delayed myelination throughout the peripheral nervous system. *J Hered* **82**, 287-294.

Heumann, R., Korsching, S., Bandtlow, C. & Thoenen, H. (1987) Changes of nerve growth factor synthesis in nonneuronal cells in response to sciatic nerve transection. *J Cell Biol* **104**, 1623-1631.

Hilberg, F., Aguzzi, A., Howells, N. & Wagner, E.F. (1993) c-jun is essential for normal mouse development and hepatogenesis. *Nature* **365**, 179-181.

Hirata, K., He, J.W., Kuraoka, A., Omata, Y., Hirata, M., Islam, A.T., Noguchi, M. & Kawabuchi, M. (2000) Heme oxygenase1 (HSP-32) is induced in myelin-phagocytosing Schwann cells of injured sciatic nerves in the rat. *Eur J Neurosci* **12**, 4147-4152.

Hirata, K. & Kawabuchi, M. (2002) Myelin phagocytosis by macrophages and nonmacrophages during Wallerian degeneration. *Microsc Res Tech* **57**, 541-547.

Hirata, K., Mitoma, H., Ueno, N., He, J.W. & Kawabuchi, M. (1999) Differential response of macrophage subpopulations to myelin degradation in the injured rat sciatic nerve. *J Neurocytol* **28**, 685-695.

Hirota, H., Kiyama, H., Kishimoto, T. & Taga, T. (1996) Accelerated Nerve Regeneration in Mice by upregulated expression of interleukin (IL) 6 and IL-6 receptor after trauma. *J Exp Med* **183**, 2627-2634.

Ho, W.H., Armanini, M.P., Nuijens, A., Phillips, H.S. & Osheroff, P.L. (1995) Sensory and motor neuron-derived factor. A novel heregulin variant highly expressed in sensory and motor neurons. *J Biol Chem* **270**, 26722.

Hoke, A., Redett, R., Hameed, H., Jari, R., Zhou, C., Li, Z.B., Griffin, J.W. & Brushart, T.M. (2006) Schwann cells express motor and sensory phenotypes that regulate axon regeneration. *J Neurosci* **26**, 9646-9655.

Holtzman, E. & Novikoff, A.B. (1965) Lysomes in the rat sciatic nerve following crush. *J Cell Biol* **27**, 651-669.

Howe, D.G. & McCarthy, K.D. (2000) Retroviral inhibition of cAMP-dependent protein kinase inhibits myelination but not Schwann cell mitosis stimulated by interaction with neurons. *J Neurosci* **20**, 3513-3521.

Hsiao, L.L., Peltonen, J., Jaakkola, S., Gralnick, H. & Uitto, J. (1991) Plasticity of integrin expression by nerve-derived connective tissue cells. Human Schwann cells, perineurial cells, and fibroblasts express markedly different patterns of beta 1 integrins during nerve development, neoplasia, and in vitro. *J Clin Invest* **87**, 811-820.

Hu, X., He, W., Diaconu, C., Tang, X., Kidd, G.J., Macklin, W.B., Trapp, B.D. & Yan, R. (2008) Genetic deletion of BACE1 in mice affects remyelination of sciatic nerves. *Faseb J.*

Huang, E.J. & Reichardt, L.F. (2001) Neurotrophins: roles in neuronal development and function. *Annu Rev Neurosci* **24**, 677-736.

Hughes, P.M., Wells, G.M., Perry, V.H., Brown, M.C. & Miller, K.M. (2002) Comparison of matrix metalloproteinase expression during Wallerian degeneration in the central and peripheral nervous systems. *Neuroscience* **113**, 273-287.

Hunt, D., Hossain-Ibrahim, K., Mason, M.R., Coffin, R.S., Lieberman, A.R., Winterbottom, J. & Anderson, P.N. (2004) ATF3 upregulation in glia during Wallerian degeneration: differential expression in peripheral nerves and CNS white matter. *BMC Neurosci* **5**, 9.

Huxley, C., Passage, E., Manson, A., Putzu, G., Figarella-Branger, D., Pellissier, J.F. & Fontes, M. (1996) Construction of a mouse model of Charcot-Marie-Tooth disease type 1A by pronuclear injection of human YAC DNA. *Hum Mol Genet* **5**, 563-569.

Huxley, C., Passage, E., Robertson, A.M., Youl, B., Huston, S., Manson, A., Saberan-Djoniedi, D., Figarella-Branger, D., Pellissier, J.F., Thomas, P.K. & Fontes, M. (1998) Correlation between varying levels of PMP22 expression and the degree of demyelination and reduction in nerve conduction velocity in transgenic mice. *Hum Mol Genet* **7**, 449-458.

Iacovelli, J., Lopera, J., Bott, M., Baldwin, E., Khaled, A., Uddin, N. & Fernandez-Valle, C. (2007) Serum and forskolin cooperate to promote G1 progression in Schwann cells by differentially regulating cyclin D1, cyclin E1, and p27Kip expression. *Glia* **55**, 1638-1647.

Ide, C., Tohyama, K., Yokota, R., Nitatori, T. & Onodera, S. (1983) Schwann cell basal lamina and nerve regeneration. *Brain Res* **288**, 61-75.

Inoue, K., Shilo, K., Boerkoel, C.F., Crowe, C., Sawady, J., Lupski, J.R. & Agamanolis, D.P. (2002) Congenital hypomyelinating neuropathy, central dysmyelination, and Waardenburg-Hirschsprung disease: phenotypes linked by SOX10 mutation. *Ann Neurol* **52**, 836-842.

Inserra, M.M., Bloch, D.A. & Terris, D.J. (1998) Functional indices for sciatic, peroneal, and posterior tibial nerve lesions in the mouse. *Microsurgery* **18**, 119-124.

Inserra, M.M., Yao, M., Murray, R. & Terris, D.J. (2000) Peripheral nerve regeneration in interleukin 6-deficient mice. *Arch Otolaryngol Head Neck Surg* **126**, 1112-1116.

Ishii, D.N. & Lupien, S.B. (1995) Insulin-like growth factors protect against diabetic neuropathy: effects on sensory nerve regeneration in rats. *J Neurosci Res* **40**, 138-144.

Ito, Y., Yamamoto, M., Li, M., Doyu, M., Tanaka, F., Mutch, T., Mitsuma, T. & Sobue, G. (1998) Differential temporal expression of mRNAs for ciliary neurotrophic factor (CNTF), leukemia inhibitory factor (LIF), interleukin-6 (IL-6), and their receptors (CNTFR alpha, LIFR beta, IL-6R alpha and gp130) in injured peripheral nerves. *Brain Res* **793**, 321-327.

Jaegle, M., Ghazvini, M., Mandemakers, W., Piirsoo, M., Driegen, S., Levavasseur, F., Raghoenath, S., Grosveld, F. & Meijer, D. (2003) The POU proteins Brn-2 and Oct-6 share important functions in Schwann cell development. *Genes Dev* **17**, 1380-1391.

Jaegle, M., Mandemakers, W., Broos, L., Zwart, R., Karis, A., Visser, P., Grosveld, F. & Meijer, D. (1996) The POU factor Oct-6 and Schwann cell differentiation. *Science* **273**, 507-510.

Jang, S.-W., LeBlanc, S.E., Roopra, A., Wrabetz, L. & Svaren, J. (2006) In vivo detection of Egr2 binding to target genes during peripheral nerve myelination. *Journal of Neurochemistry* **98**, 1678-1687.

Jaros, E. & Jenkison, M. (1983) Defective differentiation of peripheral nerves in the dystrophic mouse. *Brain Res* **282**, 231-242.

Jessen, K.R., Brennan, A., Morgan, L., Mirsky, R., Kent, A., Hashimoto, Y. & Gavrilovic, J. (1994) The Schwann cell precursor and its fate: a study of cell death and differentiation during gliogenesis in rat embryonic nerves. *Neuron* **12**, 509-527.

Jessen, K.R. & Mirsky, R. (2005) The origin and development of glial cells in peripheral nerves. *Nat Rev Neurosci* **6**, 671-682.

Jessen, K.R., Mirsky, R. & Morgan, L. (1987a) Axonal signals regulate the differentiation of non-myelin-forming Schwann cells: an immunohistochemical study of galactocerebroside in transected and regenerating nerves. *J Neurosci* 7, 3362-3369.

Jessen, K.R., Mirsky, R. & Morgan, L. (1987b) Myelinated, but not unmyelinated axons, reversibly down-regulate N-CAM in Schwann cells. *J Neurocytol* **16**, 681-688.

Jessen, K.R., Morgan, L., Brammer, M. & Mirsky, R. (1985) Galactocerebroside is expressed by non-myelin-forming Schwann cells in situ. *J Cell Biol* **101**, 1135-1143.

Johnson, R.S., van Lingen, B., Papaioannou, V.E. & Spiegelman, B.M. (1993) A null mutation at the c-jun locus causes embryonic lethality and retarded cell growth in culture. *Genes Dev* 7, 1309-1317.

Joseph, J. (1950) Further studies in changes of nuclear population in degenerating non-myelinated and finely myelinated nerves. *Acta Anat* **9**, 279-288.

Joseph, N.M., Mukouyama, Y.S., Mosher, J.T., Jaegle, M., Crone, S.A., Dormand, E.L., Lee, K.F., Meijer, D., Anderson, D.J. & Morrison, S.J. (2004) Neural crest stem cells undergo multilineage differentiation in developing peripheral nerves to generate endoneurial fibroblasts in addition to Schwann cells. *Development* **131**, 5599-5612.

Jungnickel, J., Claus, P., Gransalke, K., Timmer, M. & Grothe, C. (2004) Targeted disruption of the FGF-2 gene affects the response to peripheral nerve injury. *Mol Cell Neurosci* **25**, 444-452.

Jungnickel, J., Haase, K., Konitzer, J., Timmer, M. & Grothe, C. (2006) Faster nerve regeneration after sciatic nerve injury in mice over-expressing basic fibroblast growth factor. *J Neurobiol* **66**, 940-948.

Keswani, S.C., Buldanlioglu, U., Fischer, A., Reed, N., Polley, M., Liang, H., Zhou, C., Jack, C., Leitz, G.J. & Hoke, A. (2004) A novel endogenous erythropoietin mediated pathway prevents axonal degeneration. *Ann Neurol* **56**, 815-826.

Kiefer, R., Lindholm, D. & Kreutzberg, G.W. (1993) Interleukin-6 and transforming growth factor-beta 1 mRNAs are induced in rat facial nucleus following motoneuron axotomy. *Eur J Neurosci* **5**, 775-781.

Kim, H.A., DeClue, J.E. & Ratner, N. (1997) cAMP-dependent protein kinase A is required for Schwann cell growth: Interactions between the cAMP and neuregulin/tyrosine kinase pathways. *Journal of Neuroscience Research* **49**, 236-247.

Kim, H.A., Pomeroy, S.L., Whoriskey, W., Pawlitzky, I., Benowitz, L.I., Sicinski, P., Stiles, C.D. & Roberts, T.M. (2000) A Developmentally Regulated Switch Directs Regenerative Growth of Schwann Cells through Cyclin D1. *Neuron* **26**, 405.

Kim, H.A., Ratner, N., Roberts, T.M. & Stiles, C.D. (2001) Schwann Cell Proliferative Responses to cAMP and Nf1 Are Mediated by Cyclin D1. *J. Neurosci.* **21**, 1110-1116.

Kirsch, K.H., Korradi, Y. & Johnson, J.P. (1996) Mader: a novel nuclear protein over expressed in human melanomas. *Oncogene* **12**, 963-971.

Kirschner, D.A. & Hollingshead, C.J. (1980) Processing for electron microscopy alters membrane structure and packing in myelin. *J Ultrastruct Res* **73**, 211-232.

Kirschner, D.A. & Sidman, R.L. (1976) X-ray diffraction study of myelin structure in immature and mutant mice. *Biochim Biophys Acta* **448**, 73-87.

Kirschner, L.S., Carney, J.A., Pack, S.D., Taymans, S.E., Giatzakis, C., Cho, Y.S., Cho-Chung, Y.S. & Stratakis, C.A. (2000) Mutations of the gene encoding the protein kinase A type I-alpha regulatory subunit in patients with the Carney complex. *Nat Genet* **26**, 89-92.

Kirschner, L.S., Kusewitt, D.F., Matyakhina, L., Towns, W.H., 2nd, Carney, J.A., Westphal, H. & Stratakis, C.A. (2005) A mouse model for the Carney complex tumor syndrome develops neoplasia in cyclic AMP-responsive tissues. *Cancer Res* **65**, 4506-4514.

Klein, M.A., Moller, J.C., Jones, L.L., Bluethmann, H., Kreutzberg, G.W. & Raivich, G. (1997) Impaired neuroglial activation in interleukin-6 deficient mice. *Glia* **19**, 227-233.

Kleopa, K.A., Yum, S.W. & Scherer, S.S. (2002) Cellular mechanisms of connexin32 mutations associated with CNS manifestations. *J Neurosci Res* **68**, 522-534.

Krekoski, C.A., Neubauer, D., Graham, J.B. & Muir, D. (2002) Metalloproteinase-dependent predegeneration in vitro enhances axonal regeneration within acellular peripheral nerve grafts. *J Neurosci* **22**, 10408-10415.

Kurek, J.B., Austin, L., Cheema, S.S., Bartlett, P.F. & Murphy, M. (1996) Up-regulation of leukaemia inhibitory factor and interleukin-6 in transected sciatic nerve and muscle following denervation. *Neuromuscul Disord* **6**, 105-114.

Kwon, Y.K., Bhattacharyya, A., Alberta, J.A., Giannobile, W.V., Cheon, K., Stiles, C.D. & Pomeroy, S.L. (1997) Activation of ErbB2 during wallerian degeneration of sciatic nerve. *J Neurosci* **17**, 8293-8299.

Langley, J.N. & Anderson, H.K. (1904) On autogenetic regeneration in the nerves of the limbs. *J Physiol* **31**, 418-428.

Larner, A.J., Johnson, A.R. & Keynes, R.J. (1995) Regeneration in the vertebrate central nervous system: phylogeny, ontogeny, and mechanisms. *Biol Rev Camb Philos Soc* **70**, 597-619.

Le Douarin, N., Dulac, C., Dupin, E. & Cameron-Curry, P. (1991) Glial cell lineages in the neural crest. *Glia* **4**, 175-184.

Le, N., Nagarajan, R., Wang, J.Y., Araki, T., Schmidt, R.E. & Milbrandt, J. (2005a) Analysis of congenital hypomyelinating Egr2Lo/Lo nerves identifies Sox2 as an inhibitor of Schwann cell differentiation and myelination. *Proc Natl Acad Sci U S A* **102**, 2596-2601.

Le, N., Nagarajan, R., Wang, J.Y., Svaren, J., LaPash, C., Araki, T., Schmidt, R.E. & Milbrandt, J. (2005b) Nab proteins are essential for peripheral nervous system myelination. *Nat Neurosci* **8**, 932-940.

LeBlanc, S.E., Jang, S.W., Ward, R.M., Wrabetz, L. & Svaren, J. (2006) Direct regulation of myelin protein zero expression by the Egr2 transactivator. *J Biol Chem* **281**, 5453-5460.

LeBlanc, S.E., Srinivasan, R., Ferri, C., Mager, G.M., Gillian-Daniel, A.L., Wrabetz, L. & Svaren, J. (2005) Regulation of cholesterol/lipid biosynthetic genes by Egr2/Krox20 during peripheral nerve myelination. *Journal of Neurochemistry* **93**, 737-748.

LeBlanc, S.E., Ward, R.M. & Svaren, J. (2007) Neuropathy-associated Egr2 mutants disrupt cooperative activation of myelin protein zero by Egr2 and Sox10. *Mol Cell Biol* **27**, 3521-3529.

Lee, H., Jo, E.K., Choi, S.Y., Oh, S.B., Park, K., Kim, J.S. & Lee, S.J. (2006) Necrotic neuronal cells induce inflammatory Schwann cell activation via TLR2 and TLR3: implication in Wallerian degeneration. *Biochem Biophys Res Commun* **350**, 742-747.

Lee, H., Park, C., Cho, I.H., Kim, H.Y., Jo, E.K., Lee, S., Kho, H.S., Choi, S.Y., Oh, S.B., Park, K., Kim, J.S. & Lee, S.J. (2007) Double-stranded RNA induces iNOS gene expression in Schwann cells, sensory neuronal death, and peripheral nerve demyelination. *Glia* **55**, 712-722.

Lee, M., Brennan, A., Blanchard, A., Zoidl, G., Dong, Z., Tabernero, A., Zoidl, C., Dent, M.A., Jessen, K.R. & Mirsky, R. (1997) P0 is constitutively expressed in the rat neural crest and embryonic nerves and is negatively and positively regulated by axons to generate non-myelin-forming and myelin-forming Schwann cells, respectively. *Mol Cell Neurosci* **8**, 336-350.

Lee, M.M., Badache, A. & DeVries, G.H. (1999) Phosphorylation of CREB in axon-induced Schwann cell proliferation. *J Neurosci Res* **55**, 702-712.

Lemke, G. & Chao, M. (1988) Axons regulate Schwann cell expression of the major myelin and NGF receptor genes. *Development* **102**, 499-504.

Levi, A.D., Bunge, R.P., Lofgren, J.A., Meima, L., Hefti, F., Nikolics, K. & Sliwkowski, M.X. (1995) The influence of heregulins on human Schwann cell proliferation. *J Neurosci* **15**, 1329-1340.

Levi-Montalcini, R. & Angeletti, P.U. (1968) Nerve growth factor. *Physiol Rev* **48**, 534-569.

Levy, D., Kubes, P. & Zochodne, D.W. (2001) Delayed peripheral nerve degeneration, regeneration, and pain in mice lacking inducible nitric oxide synthase. *J Neuropathol Exp Neurol* **60**, 411-421.

Li, C., Tropak, M.B., Gerlai, R., Clapoff, S., Abramow-Newerly, W., Trapp, B., Peterson, A. & Roder, J. (1994) Myelination in the absence of myelin-associated glycoprotein. *Nature* **369**, 747-750.

Li, L., Cleary, S., Mandarano, M.A., Long, W., Birchmeier, C. & Jones, F.E. (2002) The breast proto-oncogene, HRGalpha regulates epithelial proliferation and lobuloalveolar development in the mouse mammary gland. *Oncogene* **21**, 4900-4907.

Li, X., Gonias, S.L. & Campana, W.M. (2005) Schwann cells express erythropoietin receptor and represent a major target for Epo in peripheral nerve injury. *Glia* **51**, 254-265.

Liefner, M., Siebert, H., Sachse, T., Michel, U., Kollias, G. & Bruck, W. (2000) The role of TNF-alpha during Wallerian degeneration. *J Neuroimmunol* **108**, 147-152.

Lin, L.F., Doherty, D.H., Lile, J.D., Bektesh, S. & Collins, F. (1993) GDNF: a glial cell line-derived neurotrophic factor for midbrain dopaminergic neurons. *Science* **260**, 1130-1132.

Liu, H.M., Yang, L.H. & Yang, Y.J. (1995) Schwann cell properties: 3. C-fos expression, bFGF production, phagocytosis and proliferation during Wallerian degeneration. *J Neuropathol Exp Neurol* **54**, 487-496.

Liu, T., van Rooijen, N. & Tracey, D.J. (2000) Depletion of macrophages reduces axonal degeneration and hyperalgesia following nerve injury. *Pain* **86**, 25-32.

Ljungberg, C., Novikov, L., Kellerth, J.O., Ebendal, T. & Wiberg, M. (1999) The neurotrophins NGF and NT-3 reduce sensory neuronal loss in adult rat after peripheral nerve lesion. *Neurosci Lett* **262**, 29-32.

Lorenzetto, E., Panteri, R., Marino, R., Keller, F. & Buffelli, M. (2008) Impaired nerve regeneration in reeler mice after peripheral nerve injury. *Eur J Neurosci* **27**, 12-19.

Lowrie, M.B., Lavalette, D. & Davies, C.E. (1994) Time course of motoneurone death after neonatal sciatic nerve crush in the rat. *Dev Neurosci* **16**, 279-284.

Lubinska, L. (1977) Early course of Wallerian degeneration in myelinated fibres of the rat phrenic nerve. *Brain Res* **130**, 47-63.

Lubinska, L. (1982) Patterns of Wallerian degeneration of myelinated fibres in short and long peripheral stumps and in isolated segments of rat phrenic nerve. Interpretation of the role of axoplasmic flow of the trophic factor. *Brain Res* **233**, 227-240.

Luciano, R.L. & Wilson, A.C. (2003) HCF-1 functions as a coactivator for the zinc finger protein Krox20. *J Biol Chem* **278**, 51116-51124.

Ludwin, S.K. (1990a) Oligodendrocyte survival in Wallerian degeneration. *Acta Neuropathol* **80**, 184-191.

Ludwin, S.K. (1990b) Phagocytosis in the rat optic nerve following Wallerian degeneration. *Acta Neuropathol* **80**, 266-273.

Lunn, E.R., Brown, M.C. & Perry, V.H. (1990) The pattern of axonal degeneration in the peripheral nervous system varies with different types of lesion. *Neuroscience* **35**, 157-165.

Lunn, E.R., Perry, V.H., Brown, M.C., Rosen, H. & Gordon, S. (1989) Absence of Wallerian Degeneration does not Hinder Regeneration in Peripheral Nerve. *Eur J Neurosci* **1**, 27-33.

Lupski, J.R., Chance, P. (2005) Hereditary motor and sensory neuropathies involving altered dosage or mutation of PMP22: The CMT1A duplication and HNPP Deletion. In: Dyck, P.J., Thomas, P.K. editors. Peripheral neuropathy. Philadelphia: Elsevier Saunders. pp 1659-1680.

Lyon, M.F., Ogunkolade, B.W., Brown, M.C., Atherton, D.J. & Perry, V.H. (1993) A gene affecting Wallerian nerve degeneration maps distally on mouse chromosome 4. *Proc Natl Acad Sci U S A* **90**, 9717-9720.

Lyons, D.A., Pogoda, H.-M., Voas, M.G., Woods, I.G., Diamond, B., Nix, R., Arana, N., Jacobs, J. & Talbot, W.S. (2005) erbb3 and erbb2 Are Essential for Schwann Cell Migration and Myelination in Zebrafish. *Current Biology* **15**, 513.

Ma, J., Novikov, L.N., Wiberg, M. & Kellerth, J.O. (2001) Delayed loss of spinal motoneurons after peripheral nerve injury in adult rats: a quantitative morphological study. *Exp Brain Res* **139**, 216-223.

MacDonald, J.M., Beach, M.G., Porpiglia, E., Sheehan, A.E., Watts, R.J. & Freeman, M.R. (2006) The Drosophila cell corpse engulfment receptor Draper mediates glial clearance of severed axons. *Neuron* **50**, 869-881.

Macica, C.M., Liang, G., Lankford, K.L. & Broadus, A.E. (2006) Induction of parathyroid hormone-related peptide following peripheral nerve injury: role as a modulator of Schwann cell phenotype. *Glia* **53**, 637-648.

Mack, T.G., Reiner, M., Beirowski, B., Mi, W., Emanuelli, M., Wagner, D., Thomson, D., Gillingwater, T., Court, F., Conforti, L., Fernando, F.S., Tarlton, A., Andressen, C., Addicks, K., Magni, G., Ribchester, R.R., Perry, V.H. & Coleman, M.P. (2001) Wallerian degeneration of injured axons and synapses is delayed by a Ube4b/Nmnat chimeric gene. *Nat Neurosci* **4**, 1199-1206.

Madrid, R.E., Jaros, E., Cullen, M.J. & Bradley, W.G. (1975) Genetically determined defect of Schwann cell basement membrane in dystrophic mouse. *Nature* **257**, 319-321.

Mager, G.M., Ward, R.M., Srinivasan, R., Jang, S.W., Wrabetz, L. & Svaren, J. (2008) Active gene repression by the Egr2.NAB complex during peripheral nerve myelination. *J Biol Chem* **283**, 18187-18197.

Magyar, J.P., Martini, R., Ruelicke, T., Aguzzi, A., Adlkofer, K., Dembic, Z., Zielasek, J., Toyka, K.V. & Suter, U. (1996) Impaired differentiation of Schwann cells in transgenic mice with increased PMP22 gene dosage. *J Neurosci* **16**, 5351-5360.

Mandemakers, W., Zwart, R., Jaegle, M., Walbeehm, E., Visser, P., Grosveld, F. & Meijer, D. (2000) A distal Schwann cell-specific enhancer mediates axonal regulation of the Oct-6 transcription factor during peripheral nerve development and regeneration. *Embo J* **19**, 2992-3003.

Maro, G.S., Vermeren, M., Voiculescu, O., Melton, L., Cohen, J., Charnay, P. & Topilko, P. (2004) Neural crest boundary cap cells constitute a source of neuronal and glial cells of the PNS. *Nat Neurosci* **7**, 930-938.

Marshall, C.J. (1995) Specificity of receptor tyrosine kinase signaling: transient versus sustained extracellular signal-regulated kinase activation. *Cell* **80**, 179-185.

Martin, J.R. & Webster, H.D. (1973) Mitotic Schwann cells in developing nerve: their changes in shape, fine structure, and axon relationships. *Dev Biol* **32**, 417-431.

Martini, R., Bollensen, E. & Schachner, M. (1988) Immunocytological localization of the major peripheral nervous system glycoprotein P0 and the L2/HNK-1 and L3 carbohydrate structures in developing and adult mouse sciatic nerve. *Dev Biol* **129**, 330-338.

Martini, R., Mohajeri, M.H., Kasper, S., Giese, K.P. & Schachner, M. (1995b) Mice doubly deficient in the genes for P0 and myelin basic protein show that both proteins contribute to the formation of the major dense line in peripheral nerve myelin. *J Neurosci* **15**, 4488-4495.

Martini, R. & Schachner, M. (1988) Immunoelectron microscopic localization of neural cell adhesion molecules (L1, N-CAM, and myelin-associated glycoprotein) in regenerating adult mouse sciatic nerve. *J Cell Biol* **106**, 1735-1746.

Martini, R., Schachner, M. & Brushart, T.M. (1994) The L2/HNK-1 carbohydrate is preferentially expressed by previously motor axon-associated Schwann cells in reinnervated peripheral nerves. *J Neurosci* **14**, 7180-7191.

Martini, R., Schachner, M. & Faissner, A. (1990) Enhanced expression of the extracellular matrix molecule J1/tenascin in the regenerating adult mouse sciatic nerve. *J Neurocytol* **19**, 601-616.

Martini, R., Xin, Y., Schmitz, B. & Schachner, M. (1992) The L2/HNK-1 Carbohydrate Epitope is Involved in the Preferential Outgrowth of Motor Neurons on Ventral Roots and Motor Nerves. *Eur J Neurosci* **4**, 628-639.

Martini, R., Zielasek, J., Toyka, K.V., Giese, K.P. & Schachner, M. (1995a) Protein zero (P0)-deficient mice show myelin degeneration in peripheral nerves characteristic of inherited human neuropathies. *Nat Genet* **11**, 281-286.

Masu, Y., Wolf, E., Holtmann, B., Sendtner, M., Brem, G. & Thoenen, H. (1993) Disruption of the CNTF gene results in motor neuron degeneration. *Nature* **365**, 27-32.

Maurel, P., Einheber, S., Galinska, J., Thaker, P., Lam, I., Rubin, M.B., Scherer, S.S., Murakami, Y., Gutmann, D.H. & Salzer, J.L. (2007) Nectin-like proteins mediate axon Schwann cell interactions along the internode and are essential for myelination. *J Cell Biol* **178**, 861-874.

Maurel, P. & Salzer, J.L. (2000) Axonal regulation of Schwann cell proliferation and survival and the initial events of myelination requires PI 3-kinase activity. *J Neurosci* **20**, 4635-4645.

Mayr, B. & Montminy, M. (2001) Transcriptional regulation by the phosphorylation-dependent factor CREB. *Nat Rev Mol Cell Biol* **2**, 599-609.

Meador-Woodruff, J.H., Yoshino, J.E., Bigbee, J.W., Lewis, B.L. & Devries, G.H. (1985) Differential proliferative responses of cultured Schwann cells to axolemma and myelin-enriched fractions. II. Morphological studies. *J Neurocytol* **14**, 619-635.

Meier, C., Parmantier, E., Brennan, A., Mirsky, R. & Jessen, K.R. (1999) Developing Schwann Cells Acquire the Ability to Survive without Axons by Establishing an Autocrine Circuit Involving Insulin-Like Growth Factor, Neurotrophin-3, and Platelet-Derived Growth Factor-BB. *J. Neurosci.* **19**, 3847-3859.

Meisinger, C. & Grothe, C. (1997) Differential regulation of fibroblast growth factor (FGF)-2 and FGF receptor 1 mRNAs and FGF-2 isoforms in spinal ganglia and sciatic nerve after peripheral nerve lesion. *J Neurochem* **68**, 1150-1158.

Melendez-Vasquez, C.V., Rios, J.C., Zanazzi, G., Lambert, S., Bretscher, A. & Salzer, J.L. (2001) Nodes of Ranvier form in association with ezrin-radixin-moesin (ERM)-positive Schwann cell processes. *Proc Natl Acad Sci U S A* **98**, 1235-1240.

Meyer, D. & Birchmeier, C. (1995) Multiple essential functions of neuregulin in development. *Nature* **378**, 386-390.

Meyer, D., Yamaai, T., Garratt, A., Riethmacher-Sonnenberg, E., Kane, D., Theill, L.E. & Birchmeier, C. (1997) Isoform-specific expression and function of neuregulin. *Development* **124**, 3575-3586.

Meyer, M., Matsuoka, I., Wetmore, C., Olson, L. & Thoenen, H. (1992) Enhanced synthesis of brain-derived neurotrophic factor in the lesioned peripheral nerve: different mechanisms are responsible for the regulation of BDNF and NGF mRNA. *J Cell Biol* **119**, 45-54.

Mi, R., Chen, W. & Hoke, A. (2007) Pleiotrophin is a neurotrophic factor for spinal motor neurons. *Proc Natl Acad Sci U S A* **104**, 4664-4669.

Michailov, G.V., Sereda, M.W., Brinkmann, B.G., Fischer, T.M., Haug, B., Birchmeier, C., Role, L., Lai, C., Schwab, M.H. & Nave, K.A. (2004) Axonal neuregulin-1 regulates myelin sheath thickness. *Science* **304**, 700-703.

Mikesova, E., Huhne, K., Rautenstrauss, B., Mazanec, R., Barankova, L., Vyhnalek, M., Horacek, O. & Seeman, P. (2005) Novel EGR2 mutation R359Q is associated with CMT type 1 and progressive scoliosis. *Neuromuscular Disorders* **15**, 764.

Milner, R., Wilby, M., Nishimura, S., Boylen, K., Edwards, G., Fawcett, J., Streuli, C., Pytela, R. & ffrench-Constant, C. (1997) Division of labor of Schwann cell integrins during migration on peripheral nerve extracellular matrix ligands. *Dev Biol* **185**, 215-228.

Mirsky, R., Dubois, C., Morgan, L. & Jessen, K.R. (1990) 04 and A007-sulfatide antibodies bind to embryonic Schwann cells prior to the appearance of galactocerebroside; regulation of the antigen by axon-Schwann cell signals and cyclic AMP. *Development* **109**, 105-116.

Mirsky, R., Woodhoo, A., Parkinson, D.B., Arthur-Farraj, P., Bhaskaran, A. & Jessen, K.R. (2008) Novel signals controlling embryonic Schwann cell development, myelination and dedifferentiation. *J Peripher Nerv Syst* **13**, 122-135.

Mokuno, K., Sobue, G., Reddy, U.R., Wurzer, J., Kreider, B., Hotta, H., Baron, P., Ross, A.H. & Pleasure, D. (1988) Regulation of Schwann cell nerve growth factor receptor by cyclic adenosine 3',5'-monophosphate. *J Neurosci Res* **21**, 465-472.

Molineaux, S.M., Engh, H., de Ferra, F., Hudson, L. & Lazzarini, R.A. (1986) Recombination within the myelin basic protein gene created the dysmyelinating shiverer mouse mutation. *Proc Natl Acad Sci U S A* **83**, 7542-7546.

Monaco, S., Gehrmann, J., Raivich, G. & Kreutzberg, G.W. (1992) MHC-positive, ramified macrophages in the normal and injured rat peripheral nervous system. *J Neurocytol* **21**, 623-634.

Monje, P.V., Bartlett Bunge, M. & Wood, P.M. (2006) Cyclic AMP synergistically enhances neuregulin-dependent ERK and Akt activation and cell cycle progression in Schwann cells. *Glia* **53**, 649-659.

Montag, D., Giese, K.P., Bartsch, U., Martini, R., Lang, Y., Bluthmann, H., Karthigasan, J., Kirschner, D.A., Wintergerst, E.S., Nave, K.A. & et al. (1994) Mice deficient for the myelin-associated glycoprotein show subtle abnormalities in myelin. *Neuron* **13**, 229-246.

Monuki, E.S., Kuhn, R., Weinmaster, G., Trapp, B.D. & Lemke, G. (1990) Expression and activity of the POU transcription factor SCIP. *Science* **249**, 1300-1303.

Monuki, E.S., Weinmaster, G., Kuhn, R. & Lemke, G. (1989) SCIP: a glial POU domain gene regulated by cyclic AMP. *Neuron* **3**, 783-793.

Morgan, L., Jessen, K.R. & Mirsky, R. (1991) The effects of cAMP on differentiation of cultured Schwann cells: progression from an early phenotype (04+) to a myelin phenotype (P0+, GFAP-, N-CAM-, NGF-receptor-) depends on growth inhibition. *J Cell Biol* **112**, 457-467.

Morgan, L., Jessen, K.R. & Mirsky, R. (1994) Negative regulation of the P0 gene in Schwann cells: suppression of P0 mRNA and protein induction in cultured Schwann cells by FGF2 and TGF beta 1, TGF beta 2 and TGF beta 3. *Development* **120**, 1399-1409.

Morgenstern, J.P. & Land, H. (1990) A series of mammalian expression vectors and characterisation of their expression of a reporter gene in stably and transiently transfected cells. *Nucleic Acids Res* **18**, 1068.

Morris, J.K., Lin, W., Hauser, C., Marchuk, Y., Getman, D. & Lee, K.F. (1999) Rescue of the cardiac defect in ErbB2 mutant mice reveals essential roles of ErbB2 in peripheral nervous system development. *Neuron* **23**, 273-283.

Morrissey, T.K., Kleitman, N. & Bunge, R.P. (1991) Isolation and functional characterization of Schwann cells derived from adult peripheral nerve. *J Neurosci* **11**, 2433-2442.

Morrissey, T.K., Levi, A.D., Nuijens, A., Sliwkowski, M.X. & Bunge, R.P. (1995) Axon-induced mitogenesis of human Schwann cells involves heregulin and p185erbB2. *Proc Natl Acad Sci U S A* **92**, 1431-1435.

Mueller, M., Leonhard, C., Wacker, K., Ringelstein, E.B., Okabe, M., Hickey, W.F. & Kiefer, R. (2003) Macrophage response to peripheral nerve injury: the quantitative contribution of resident and hematogenous macrophages. *Lab Invest* **83**, 175-185.

Mueller, M., Wacker, K., Ringelstein, E.B., Hickey, W.F., Imai, Y. & Kiefer, R. (2001) Rapid response of identified resident endoneurial macrophages to nerve injury. *Am J Pathol* **159**, 2187-2197.

Muir, D., Engvall, E., Varon, S. & Manthorpe, M. (1989) Schwannoma cell-derived inhibitor of the neurite-promoting activity of laminin. *J Cell Biol* **109**, 2353-2362.

Murinson, B.B., Archer, D.R., Li, Y. & Griffin, J.W. (2005) Degeneration of myelinated efferent fibers prompts mitosis in Remak Schwann cells of uninjured C-fiber afferents. *J Neurosci* **25**, 1179-1187.

Murphy, P., Topilko, P., Schneider-Maunoury, S., Seitanidou, T., Baron-Van Evercooren, A. & Charnay, P. (1996) The regulation of Krox-20 expression reveals important steps in the control of peripheral glial cell development. *Development* **122**, 2847-2857.

Mutoh, T., Li, M., Yamamoto, M., Mitsuma, T. & Sobue, G. (1998) Differential signaling cascade of MAP kinase and S6 kinase depends on 3',5'-monophosphate concentration in schwann cells: correlation to cellular differentiation and proliferation. *Brain Res* **810**, 274-278.

Myers, R.R., Heckman, H.M., Galbraith, J.A. & Powell, H.C. (1991) Subperineurial demyelination associated with reduced nerve blood flow and oxygen tension after epineurial vascular stripping. *Lab Invest* **65**, 41-50.

Myers, R.R., Sekiguchi, Y., Kikuchi, S., Scott, B., Medicherla, S., Protter, A. & Campana, W.M. (2003) Inhibition of p38 MAP kinase activity enhances axonal regeneration. *Exp Neurol* **184**, 606-614.

Myers, R.R., Yamamoto, T., Yaksh, T.L. & Powell, H.C. (1993) The role of focal nerve ischemia and Wallerian degeneration in peripheral nerve injury producing hyperesthesia. *Anesthesiology* **78**, 308-316.

Nadra, K., Charles, A.S., Medard, J.J., Hendriks, W.T., Han, G.S., Gres, S., Carman, G.M., Saulnier-Blache, J.S., Verheijen, M.H. & Chrast, R. (2008) Phosphatidic acid mediates demyelination in Lpin1 mutant mice. *Genes Dev* **22**, 1647-1661.

Nagarajan, R., Le, N., Mahoney, H., Araki, T. & Milbrandt, J. (2002) Deciphering peripheral nerve myelination by using Schwann cell expression profiling. *Proc Natl Acad Sci U S A* **99**, 8998-9003.

Nagarajan, R., Svaren, J., Le, N., Araki, T., Watson, M. & Milbrandt, J. (2001) EGR2 mutations in inherited neuropathies dominant-negatively inhibit myelin gene expression. *Neuron* **30**, 355-368.

Nakagawa, M., Miyagoe-Suzuki, Y., Ikezoe, K., Miyata, Y., Nonaka, I., Harii, K. & Takeda, S. (2001) Schwann cell myelination occurred without basal lamina formation in laminin alpha2 chain-null mutant (dy3K/dy3K) mice. *Glia* **35**, 101-110.

Namikawa, K., Fukushima, M., Murakami, K., Suzuki, A., Takasawa, S., Okamoto, H. & Kiyama, H. (2005) Expression of Reg/PAP family members during motor nerve regeneration in rat. *Biochem Biophys Res Commun* **332**, 126-134.

Namikawa, K., Okamoto, T., Suzuki, A., Konishi, H. & Kiyama, H. (2006) Pancreatitis-associated protein-III is a novel macrophage chemoattractant implicated in nerve regeneration. *J Neurosci* **26**, 7460-7467.

Nathaniel, E.J. & Pease, D.C. (1963) Collagen And Basement Membrane Formation By Schwann Cells During Nerve Regeneration. *J Ultrastruct Res* **52**, 550-560.

Nave, K.A. (2001) Myelin-specific genes and their mutations in the mouse. In Jessen, K.R. & Richardson, W.D. (eds) *Glial cell development: basic principles and clinical relevance*, pp. 177-208.

Nave, K.A. & Salzer, J.L. (2006) Axonal regulation of myelination by neuregulin 1. *Curr Opin Neurobiol* **16**, 492-500.

Naveilhan, P., ElShamy, W.M. & Ernfors, P. (1997) Differential regulation of mRNAs for GDNF and its receptors Ret and GDNFR alpha after sciatic nerve lesion in the mouse. *Eur J Neurosci* **9**, 1450-1460.

Near, S.L., Whalen, L.R., Miller, J.A. & Ishii, D.N. (1992) Insulin-like growth factor II stimulates motor nerve regeneration. *Proc Natl Acad Sci U S A* **89**, 11716-11720.

Nguyen, Q.T., Sanes, J.R. & Lichtman, J.W. (2002) Pre-existing pathways promote precise projection patterns. *Nat Neurosci* **5**, 861-867.

Nickols, J.C., Valentine, W., Kanwal, S. & Carter, B.D. (2003) Activation of the transcription factor NF-kappaB in Schwann cells is required for peripheral myelin formation. *Nat Neurosci* **6**, 161-167.

Nodari, A., Previtali, S.C., Dati, G., Occhi, S., Court, F.A., Colombelli, C., Zambroni, D., Dina, G., Del Carro, U., Campbell, K.P., Quattrini, A., Wrabetz, L. & Feltri, M.L. (2008) Alpha6beta4 integrin and dystroglycan cooperate to stabilize the myelin sheath. *J Neurosci* **28**, 6714-6719.

Nodari, A., Zambroni, D., Quattrini, A., Court, F.A., D'Urso, A., Recchia, A., Tybulewicz, V.L., Wrabetz, L. & Feltri, M.L. (2007) Beta1 integrin activates Rac1 in Schwann cells to generate radial lamellae during axonal sorting and myelination. *J Cell Biol* **177**, 1063-1075.

Notterpek, L., Ryan, M.C., Tobler, A.R. & Shooter, E.M. (1999) PMP22 accumulation in aggresomes: implications for CMT1A pathology. *Neurobiol Dis* **6**, 450-460.

Numakura, C., Shirahata, E., Yamashita, S., Kanai, M., Kijima, K., Matsuki, T. & Hayasaka, K. (2003) Screening of the early growth response 2 gene in Japanese patients with Charcot-Marie-Tooth disease type 1. *Journal of the Neurological Sciences* **210**, 61.

Oaklander, A.L., Miller, M.S. & Spencer, P.S. (1987) Rapid anterograde spread of premitotic activity along degenerating cat sciatic nerve. *J Neurochem* **48**, 111-114.

Occhi, S., Zambroni, D., Del Carro, U., Amadio, S., Sirkowski, E.E., Scherer, S.S., Campbell, K.P., Moore, S.A., Chen, Z.L., Strickland, S., Di Muzio, A., Uncini, A., Wrabetz, L. & Feltri, M.L. (2005) Both laminin and Schwann cell dystroglycan are necessary for proper clustering of sodium channels at nodes of Ranvier. *J Neurosci* **25**, 9418-9427.

Ogata, T., Iijima, S., Hoshikawa, S., Miura, T., Yamamoto, S., Oda, H., Nakamura, K. & Tanaka, S. (2004) Opposing extracellular signal-regulated kinase and Akt pathways control Schwann cell myelination. *J Neurosci* **24**, 6724-6732.

Olsson, Y. & Sjostrand, J. (1969) Origin of macrophages in Wallerian degereration of peripheral nerves demonstrated autoradiographically. *Exp Neurol* **23**, 102-112.

Owens, G.C. & Bunge, R.P. (1990) Schwann cells depleted of galactocerebroside express myelin-associated glycoprotein and initiate but do not continue the process of myelination. *Glia* **3**, 118-124.

Oya, T., Zhao, Y.L., Takagawa, K., Kawaguchi, M., Shirakawa, K., Yamauchi, T. & Sasahara, M. (2002) Platelet-derived growth factor-b expression induced after rat peripheral nerve injuries. *Glia* **38**, 303-312.

Padilla, F., Marc Mege, R., Sobel, A. & Nicolet, M. (1999) Upregulation and redistribution of cadherins reveal specific glial and muscle cell phenotypes during wallerian degeneration and muscle denervation in the mouse. *J Neurosci Res* **58**, 270-283.

Panteri, R., Mey, J., Zhelyaznik, N., D'Altocolle, A., Del Fa, A., Gangitano, C., Marino, R., Lorenzetto, E., Buffelli, M. & Keller, F. (2006) Reelin is transiently expressed in the peripheral nerve during development and is upregulated following nerve crush. *Mol Cell Neurosci* **32**, 133-142.

Pareyson, D., Taroni, F., Botti, S., Morbin, M., Baratta, S., Lauria, G., Ciano, C. & Sghirlanzoni, A. (2000) Cranial nerve involvement in CMT disease type 1 due to early growth response 2 gene mutation. *Neurology* **54**, 1696-1698.

Parkinson, D.B., Bhaskaran, A., Arthur-Farraj, P., Noon, L.A., Woodhoo, A., Lloyd, A.C., Feltri, M.L., Wrabetz, L., Behrens, A., Mirsky, R. & Jessen, K.R. (2008) c-Jun is a negative regulator of myelination. *J Cell Biol* **181**, 625-637.

Parkinson, D.B., Bhaskaran, A., Droggiti, A., Dickinson, S., D'Antonio, M., Mirsky, R. & Jessen, K.R. (2004) Krox-20 inhibits Jun-NH2-terminal kinase/c-Jun to control Schwann cell proliferation and death. *J Cell Biol* **164**, 385-394.

Parkinson, D.B., Dickinson, S., Bhaskaran, A., Kinsella, M.T., Brophy, P.J., Sherman, D.L., Sharghi-Namini, S., Duran Alonso, M.B., Mirsky, R. & Jessen, K.R. (2003) Regulation of the myelin gene periaxin provides evidence for Krox-20-independent myelin-related signalling in Schwann cells. *Mol Cell Neurosci* **23**, 13-27.

Parkinson, D.B., Dong, Z., Bunting, H., Whitfield, J., Meier, C., Marie, H., Mirsky, R. & Jessen, K.R. (2001) Transforming growth factor beta (TGFbeta) mediates Schwann cell death in vitro and in vivo: examination of c-Jun activation, interactions with survival signals, and the relationship of TGFbeta-mediated death to Schwann cell differentiation. *J Neurosci* **21**, 8572-8585.

Parkinson, D.B., Langner, K., Namini, S.S., Jessen, K.R. & Mirsky, R. (2002) beta-Neuregulin and autocrine mediated survival of Schwann cells requires activity of Ets family transcription factors. *Mol Cell Neurosci* **20**, 154-167.

Paul, J.A. & Gregson, N.A. (1992) An immunohistochemical study of phospholipase A2 in peripheral nerve during Wallerian degeneration. *J Neuroimmunol* **39**, 31-47.

Peirano, R.I., Goerich, D.E., Riethmacher, D. & Wegner, M. (2000) Protein zero gene expression is regulated by the glial transcription factor Sox10. *Mol Cell Biol* **20**, 3198-3209.

Pennuto, M., Tinelli, E., Malaguti, M., Del Carro, U., D'Antonio, M., Ron, D., Quattrini, A., Feltri, M.L. & Wrabetz, L. (2008) Ablation of the UPR-mediator CHOP restores motor function and reduces demyelination in Charcot-Marie-Tooth 1B mice. *Neuron* **57**, 393-405.

Perrin, F.E., Lacroix, S., Aviles-Trigueros, M. & David, S. (2005) Involvement of monocyte chemoattractant protein-1, macrophage inflammatory protein-1alpha and interleukin-1beta in Wallerian degeneration. *Brain* **128**, 854-866.

Perry, V.H., Brown, M.C. & Lunn, E.R. (1991) Very Slow Retrograde and Wallerian Degeneration in the CNS of C57BL/Ola Mice. *Eur J Neurosci* **3**, 102-105.

Perry, V.H., Tsao, J.W., Fearn, S. & Brown, M.C. (1995) Radiation-induced reductions in macrophage recruitment have only slight effects on myelin degeneration in sectioned peripheral nerves of mice. *Eur J Neurosci* 7, 271-280.

Pizzi, M.A. & Crowe, M.J. (2007) Matrix metalloproteinases and proteoglycans in axonal regeneration. *Exp Neurol* **204**, 496-511.

Podratz, J.L., Rodriguez, E. & Windebank, A.J. (2001) Role of the extracellular matrix in myelination of peripheral nerve. *Glia* **35**, 35-40.

Podratz, J.L., Rodriguez, E.H., DiNonno, E.S. & Windebank, A.J. (1998) Myelination by Schwann cells in the absence of extracellular matrix assembly. *Glia* **23**, 383-388.

Poduslo, J.F., Walikonis, R.S., Domec, M.C., Berg, C.T. & Holtz-Heppelmann, C.J. (1995) The second messenger, cyclic AMP, is not sufficient for myelin gene induction in the peripheral nervous system. *J Neurochem* **65**, 149-159.

Pot, C., Simonen, M., Weinmann, O., Schnell, L., Christ, F., Stoeckle, S., Berger, P., Rulicke, T., Suter, U. & Schwab, M.E. (2002) Nogo-A expressed in Schwann cells impairs axonal regeneration after peripheral nerve injury. *J Cell Biol* **159**, 29-35.

Previtali, S.C., Dina, G., Nodari, A., Fasolini, M., Wrabetz, L., Mayer, U., Feltri, M.L. & Quattrini, A. (2003c) Schwann cells synthesize alpha7beta1 integrin which is dispensable for peripheral nerve development and myelination. *Mol Cell Neurosci* **23**, 210-218.

Previtali, S.C., Feltri, M.L., Archelos, J.J., Quattrini, A., Wrabetz, L. & Hartung, H.-P. (2001) Role of integrins in the peripheral nervous system. *Progress in Neurobiology* **64**, 35.

Previtali, S.C., Nodari, A., Taveggia, C., Pardini, C., Dina, G., Villa, A., Wrabetz, L., Quattrini, A. & Feltri, M.L. (2003a) Expression of laminin receptors in schwann cell differentiation: evidence for distinct roles. *J Neurosci* **23**, 5520-5530.

Previtali, S.C., Zerega, B., Sherman, D.L., Brophy, P.J., Dina, G., King, R.H., Salih, M.M., Feltri, L., Quattrini, A., Ravazzolo, R., Wrabetz, L., Monaco, A.P. & Bolino, A. (2003b) Myotubularin-related 2 protein phosphatase and neurofilament light chain protein, both mutated in CMT neuropathies, interact in peripheral nerve. *Hum Mol Genet* **12**, 1713-1723.

Pu, S.F., Zhuang, H.X. & Ishii, D.N. (1995) Differential spatio-temporal expression of the insulin-like growth factor genes in regenerating sciatic nerve. *Brain Res Mol Brain Res* **34**, 18-28.

Raff, M.C., Hornby-Smith, A. & Brockes, J.P. (1978) Cyclic AMP as a mitogenic signal for cultured rat Schwann cells. *Nature* **273**, 672-673.

Rahmatullah, M., Schroering, A., Rothblum, K., Stahl, R.C., Urban, B. & Carey, D.J. (1998) Synergistic regulation of Schwann cell proliferation by heregulin and forskolin. *Mol Cell Biol* **18**, 6245-6252.

Raivich, G., Bohatschek, M., Da Costa, C., Iwata, O., Galiano, M., Hristova, M., Nateri, A.S., Makwana, M., Riera-Sans, L., Wolfer, D.P., Lipp, H.P., Aguzzi, A., Wagner, E.F. & Behrens, A. (2004) The AP-1 transcription factor c-Jun is required for efficient axonal regeneration. *Neuron* **43**, 57-67.

Raivich, G., Graeber, M.B., Gehrmann, J. & Kreutzberg, G.W. (1991a) Transferrin Receptor Expression and Iron Uptake in the Injured and Regenerating Rat Sciatic Nerve. *Eur J Neurosci* **3**, 919-927.

Raivich, G., Hellweg, R. & Kreutzberg, G.W. (1991b) NGF receptor-mediated reduction in axonal NGF uptake and retrograde transport following sciatic nerve injury and during regeneration. *Neuron* 7, 151-164.

Raivich, G. & Makwana, M. (2007) The making of successful axonal regeneration: genes, molecules and signal transduction pathways. *Brain Res Rev* **53**, 287-311.

Ramaglia, V., King, R.H., Nourallah, M., Wolterman, R., de Jonge, R., Ramkema, M., Vigar, M.A., van der Wetering, S., Morgan, B.P., Troost, D. & Baas, F. (2007) The membrane attack complex of the complement system is essential for rapid Wallerian degeneration. *J Neurosci* **27**, 7663-7672.

Ramâon y Cajal, S. & May, R.M. (1928) *Degeneration and regeneration of the nervous system*. Oxford University Press;
Humphrey Milford.

Rangnekar, V.M., Aplin, A.C. & Sukhatme, V.P. (1990) The serum and TPA responsive promoter and intron-exon structure of EGR2, a human early growth response gene encoding a zinc finger protein. *Nucleic Acids Res* **18**, 2749-2757.

Ranscht, B., Clapshaw, P.A., Price, J., Noble, M. & Seifert, W. (1982) Development of oligodendrocytes and Schwann cells studied with a monoclonal antibody against galactocerebroside. *Proc Natl Acad Sci U S A* **79**, 2709-2713.

Ranscht, B., Wood, P.M. & Bunge, R.P. (1987) Inhibition of in vitro peripheral myelin formation by monoclonal anti-galactocerebroside. *J Neurosci* 7, 2936-2947.

Ranvier, L. & Weber, E. (1878) *Leòcons sur l'histologie du systáeme nerveux.* Librairie F. Savy.

Reichert, F., Saada, A. & Rotshenker, S. (1994) Peripheral nerve injury induces Schwann cells to express two macrophage phenotypes: phagocytosis and the galactose-specific lectin MAC-2. *J Neurosci* **14**, 3231-3245.

Riethmacher, D., Sonnenberg-Riethmacher, E., Brinkmann, V., Yamaai, T., Lewin, G.R. & Birchmeier, C. (1997) Severe neuropathies in mice with targeted mutations in the ErbB3 receptor. *Nature* **389**, 725-730.

Roach, A., Boylan, K., Horvath, S., Prusiner, S.B. & Hood, L.E. (1983) Characterization of cloned cDNA representing rat myelin basic protein: absence of expression in brain of shiverer mutant mice. *Cell* **34**, 799-806.

Rocha, S. (2007) Gene regulation under low oxygen: holding your breath for transcription. *Trends Biochem Sci* **32**, 389-397.

Romanes, G.J. (1946) Motor localization and the effects of nerve injury on the ventral horn cells of the spinal cord. *J Anat* **80**, 117-131.

Romine, J.S., Bray, G.M. & Aguayo, A.J. (1976) Schwann cell multiplication after crush injury of unmyelinated fibers. *Arch Neurol* **33**, 49-54.

Rosenbluth, J. (1980) Peripheral myelin in the mouse mutant Shiverer. *J Comp Neurol* **193**, 729-739.

Rougon, G. & Marshak, D.R. (1986) Structural and immunological characterization of the amino-terminal domain of mammalian neural cell adhesion molecules. *J Biol Chem* **261**, 3396-3401.

Rudolph, D., Tafuri, A., Gass, P., Hammerling, G.J., Arnold, B. & Schutz, G. (1998) Impaired fetal T cell development and perinatal lethality in mice lacking the cAMP response element binding protein. *Proc Natl Acad Sci U S A* **95**, 4481-4486.

Rush, R.A., Mayo, R. & Zettler, C. (1995) The regulation of nerve growth factor synthesis and delivery to peripheral neurons. *Pharmacol Ther* **65**, 93-123.

Russo, M.W., Sevetson, B.R. & Milbrandt, J. (1995) Identification of NAB1, a repressor of NGFI-A- and Krox20-mediated transcription. *Proc Natl Acad Sci U S A* **92**, 6873-6877.

Ryan, M.C., Shooter, E.M. & Notterpek, L. (2002) Aggresome formation in neuropathy models based on peripheral myelin protein 22 mutations. *Neurobiol Dis* **10**, 109-118.

Ryu, E.J., Wang, J.Y., Le, N., Baloh, R.H., Gustin, J.A., Schmidt, R.E. & Milbrandt, J. (2007) Misexpression of Pou3f1 results in peripheral nerve hypomyelination and axonal loss. *J Neurosci* **27**, 11552-11559.

Sagane, K., Hayakawa, K., Kai, J., Hirohashi, T., Takahashi, E., Miyamoto, N., Ino, M., Oki, T., Yamazaki, K. & Nagasu, T. (2005) Ataxia and peripheral nerve hypomyelination in ADAM22-deficient mice. *BMC Neurosci* **6**, 33.

Saito, F., Moore, S.A., Barresi, R., Henry, M.D., Messing, A., Ross-Barta, S.E., Cohn, R.D., Williamson, R.A., Sluka, K.A., Sherman, D.L., Brophy, P.J., Schmelzer, J.D., Low, P.A., Wrabetz, L., Feltri, M.L. & Campbell, K.P. (2003) Unique role of dystroglycan in peripheral nerve myelination, nodal structure, and sodium channel stabilization. *Neuron* **38**, 747-758.

Salzer, J.L. & Bunge, R.P. (1980) Studies of Schwann cell proliferation. I. An analysis in tissue culture of proliferation during development, Wallerian degeneration, and direct injury. *J Cell Biol* **84**, 739-752.

Salzer, J.L., Bunge, R.P. & Glaser, L. (1980a) Studies of Schwann cell proliferation. III. Evidence for the surface localization of the neurite mitogen. *J Cell Biol* **84**, 767-778.

Salzer, J.L., Williams, A.K., Glaser, L. & Bunge, R.P. (1980b) Studies of Schwann cell proliferation. II. Characterization of the stimulation and specificity of the response to a neurite membrane fraction. *J Cell Biol* **84**, 753-766.

Scarlato, M., Ara, J., Bannerman, P., Scherer, S. & Pleasure, D. (2003) Induction of neuropilins-1 and -2 and their ligands, Sema3A, Sema3F, and VEGF, during Wallerian degeneration in the peripheral nervous system. *Exp Neurol* **183**, 489-498.

Scarlato, M., Xu, T., Bannerman, P., Beesley, J., Reddy, U.R., Rostami, A., Scherer, S.S. & Pleasure, D. (2001) Axon-Schwann cell interactions regulate the expression of fibroblast growth factor-5 (FGF-5). *J Neurosci Res* **66**, 16-22.

Scherer, S.S., Deschenes, S.M., Xu, Y.T., Grinspan, J.B., Fischbeck, K.H. & Paul, D.L. (1995a) Connexin32 is a myelin-related protein in the PNS and CNS. *J Neurosci* **15**, 8281-8294.

Scherer, S.S. & Easter, S.S., Jr. (1984) Degenerative and regenerative changes in the trochlear nerve of goldfish. *J Neurocytol* **13**, 519-565.

Scherer, S.S. & Salzer, J.L. (2001) Axonal-Schwann cell interactions during peripheral nerve degeneration and regeneration. In Jessen, K.R. & Richardson, W.D. (eds) *Glial cell development: basic principles and clinical relevance*, pp. 299-330

Scherer, S.S., Wang, D.Y., Kuhn, R., Lemke, G., Wrabetz, L. & Kamholz, J. (1994a) Axons regulate Schwann cell expression of the POU transcription factor SCIP. *J Neurosci* **14**, 1930-1942.

Scherer, S.S., Xu, T., Crino, P., Arroyo, E.J. & Gutmann, D.H. (2001) Ezrin, radixin, and moesin are components of Schwann cell microvilli. *J Neurosci Res* **65**, 150-164.

Scherer, S.S., Xu, Y.T., Bannerman, P.G., Sherman, D.L. & Brophy, P.J. (1995b) Periaxin expression in myelinating Schwann cells: modulation by axon-glial interactions and polarized localization during development. *Development* **121**, 4265-4273.

Scherer, S.S., Xu, Y.T., Nelles, E., Fischbeck, K., Willecke, K. & Bone, L.J. (1998) Connexin32-null mice develop demyelinating peripheral neuropathy. *Glia* **24**, 8-20.

Scherer, S.S., Xu, Y.T., Roling, D., Wrabetz, L., Feltri, M.L. & Kamholz, J. (1994b) Expression of growth-associated protein-43 kD in Schwann cells is regulated by axon-Schwann cell interactions and cAMP. *J Neurosci Res* **38**, 575-589.

Schmelzer, J.D., Zochodne, D.W. & Low, P.A. (1989) Ischemic and reperfusion injury of rat peripheral nerve. *Proc Natl Acad Sci U S A* **86**, 1639-1642.

Schneider-Maunoury, S., Topilko, P., Seitandou, T., Levi, G., Cohen-Tannoudji, M., Pournin, S., Babinet, C. & Charnay, P. (1993) Disruption of Krox-20 results in alteration of rhombomeres 3 and 5 in the developing hindbrain. *Cell* **75**, 1199-1214.

Schratzberger, P., Schratzberger, G., Silver, M., Curry, C., Kearney, M., Magner, M., Alroy, J., Adelman, L.S., Weinberg, D.H., Ropper, A.H. & Isner, J.M. (2000) Favorable effect of VEGF gene transfer on ischemic peripheral neuropathy. *Nat Med* **6**, 405-413.

Schreiner, S., Cossais, F., Fischer, K., Scholz, S., Bosl, M.R., Holtmann, B., Sendtner, M. & Wegner, M. (2007) Hypomorphic Sox10 alleles reveal novel protein functions and unravel developmental differences in glial lineages. *Development* **134**, 3271-3281.

Schwab, M.E. & Thoenen, H. (1985) Dissociated neurons regenerate into sciatic but not optic nerve explants in culture irrespective of neurotrophic factors. *J Neurosci* **5**, 2415-2423.

Sebert, M.E. & Shooter, E.M. (1993) Expression of mRNA for neurotrophic factors and their receptors in the rat dorsal root ganglion and sciatic nerve following nerve injury. *J Neurosci Res* **36**, 357-367.

Seilheimer, B. & Schachner, M. (1988) Studies of adhesion molecules mediating interactions between cells of peripheral nervous system indicate a major role for L1 in mediating sensory neuron growth on Schwann cells in culture. *J Cell Biol* **107**, 341-351.

Senderek, J., Bergmann, C., Weber, S., Ketelsen, U.P., Schorle, H., Rudnik-Schoneborn, S., Buttner, R., Buchheim, E. & Zerres, K. (2003) Mutation of the SBF2 gene, encoding a novel member of the myotubularin family, in Charcot-Marie-Tooth neuropathy type 4B2/11p15. *Hum Mol Genet* **12**, 349-356.

Sendtner, M., Gotz, R., Holtmann, B. & Thoenen, H. (1997) Endogenous ciliary neurotrophic factor is a lesion factor for axotomized motoneurons in adult mice. *J Neurosci* **17**, 6999-7006.

Sendtner, M., Kreutzberg, G.W. & Thoenen, H. (1990) Ciliary neurotrophic factor prevents the degeneration of motor neurons after axotomy. *Nature* **345**, 440-441.

Sendtner, M., Stockli, K.A. & Thoenen, H. (1992) Synthesis and localization of ciliary neurotrophic factor in the sciatic nerve of the adult rat after lesion and during regeneration. *J Cell Biol* **118**, 139-148.

Sereda, M., Griffiths, I., Puhlhofer, A., Stewart, H., Rossner, M.J., Zimmerman, F., Magyar, J.P., Schneider, A., Hund, E., Meinck, H.M., Suter, U. & Nave, K.A. (1996) A transgenic rat model of Charcot-Marie-Tooth disease. *Neuron* **16**, 1049-1060.

Shamash, S., Reichert, F. & Rotshenker, S. (2002) The cytokine network of Wallerian degeneration: tumor necrosis factor-alpha, interleukin-1alpha, and interleukin-1beta. *J Neurosci* **22**, 3052-3060.

Shapiro, L., Doyle, J.P., Hensley, P., Colman, D.R. & Hendrickson, W.A. (1996) Crystal structure of the extracellular domain from P0, the major structural protein of peripheral nerve myelin. *Neuron* **17**, 435-449.

Shapiro, L., Fannon, A.M., Kwong, P.D., Thompson, A., Lehmann, M.S., Grubel, G., Legrand, J.F., Als-Nielsen, J., Colman, D.R. & Hendrickson, W.A. (1995) Structural basis of cell-cell adhesion by cadherins. *Nature* **374**, 327-337.

Sharghi-Namini, S., Turmaine, M., Meier, C., Sahni, V., Umehara, F., Jessen, K.R. & Mirsky, R. (2006) The structural and functional integrity of peripheral nerves depends on the glial-derived signal desert hedgehog. *J Neurosci* **26**, 6364-6376.

Shaulian, E. & Karin, M. (2001) AP-1 in cell proliferation and survival. *Oncogene* **20**, 2390-2400.

Shen, A.G., Shi, S.X., Chen, M.L., Qin, J., Gao, S.F. & Cheng, C. (2008) Dynamic Changes of p27(kip1) and Skp2 Expression in Injured Rat Sciatic Nerve. *Cell Mol Neurobiol* **28**, 713-725.

Sherman, D.L. & Brophy, P.J. (2005) Mechanisms of axon ensheathment and myelin growth. *Nat Rev Neurosci* **6**, 683-690.

Sherman, D.L., Fabrizi, C., Gillespie, C.S. & Brophy, P.J. (2001) Specific disruption of a schwann cell dystrophin-related protein complex in a demyelinating neuropathy. *Neuron* **30**, 677-687.

Shubayev, V.I., Angert, M., Dolkas, J., Campana, W.M., Palenscar, K. & Myers, R.R. (2006) TNFalpha-induced MMP-9 promotes macrophage recruitment into injured peripheral nerve. *Mol Cell Neurosci* **31**, 407-415.

Shy, M.E., Shi, Y., Wrabetz, L., Kamholz, J. & Scherer, S.S. (1996) Axon-Schwann cell interactions regulate the expression of c-jun in Schwann cells. *J Neurosci Res* **43**, 511-525.

Siconolfi, L.B. & Seeds, N.W. (2001) Mice lacking tPA, uPA, or plasminogen genes showed delayed functional recovery after sciatic nerve crush. *J Neurosci* **21**, 4348-4355.

Siebert, H., Sachse, A., Kuziel, W.A., Maeda, N. & Bruck, W. (2000) The chemokine receptor CCR2 is involved in macrophage recruitment to the injured peripheral nervous system. *J Neuroimmunol* **110**, 177-185.

Simon, M., Porter, R., Brown, R., Coulton, G.R. & Terenghi, G. (2003) Effect of NT-4 and BDNF delivery to damaged sciatic nerves on phenotypic recovery of fast and slow muscles fibres. *Eur J Neurosci* **18**, 2460-2466.

Soares, H.D., Chen, S.C. & Morgan, J.I. (2001) Differential and prolonged expression of Fos-lacZ and Jun-lacZ in neurons, glia, and muscle following sciatic nerve damage. *Exp Neurol* **167**, 1-14.

Sobue, G. & Pleasure, D. (1984) Schwann cell galactocerebroside induced by derivatives of adenosine 3',5'-monophosphate. *Science* **224**, 72-74.

Sobue, G., Shuman, S. & Pleasure, D. (1986) Schwann cell responses to cyclic AMP: proliferation, change in shape, and appearance of surface galactocerebroside. *Brain Res* **362**, 23-32.

Soilu-Hanninen, M., Ekert, P., Bucci, T., Syroid, D., Bartlett, P.F. & Kilpatrick, T.J. (1999) Nerve growth factor signaling through p75 induces apoptosis in Schwann cells via a Bcl-2-independent pathway. *J Neurosci* **19**, 4828-4838.

Sommer, I. & Schachner, M. (1981) Monoclonal antibodies (O1 to O4) to oligodendrocyte cell surfaces: an immunocytological study in the central nervous system. *Dev Biol* **83**, 311-327.

Son, Y.J. & Thompson, W.J. (1995) Schwann cell processes guide regeneration of peripheral axons. *Neuron* **14**, 125-132.

Son, Y.J., Trachtenberg, J.T. & Thompson, W.J. (1996) Schwann cells induce and guide sprouting and reinnervation of neuromuscular junctions. *Trends Neurosci* **19**, 280-285.

Sonnenberg-Riethmacher, E., Miehe, M., Stolt, C.C., Goerich, D.E., Wegner, M. & Riethmacher, D. (2001) Development and degeneration of dorsal root ganglia in the absence of the HMG-domain transcription factor Sox10. *Mech Dev* **109**, 253-265.

Spiegel, I., Adamsky, K., Eshed, Y., Milo, R., Sabanay, H., Sarig-Nadir, O., Horresh, I., Scherer, S.S., Rasband, M.N. & Peles, E. (2007) A central role for Necl4 (SynCAM4) in Schwann cell-axon interaction and myelination. *Nat Neurosci* **10**, 861-869.

Srinivasan, R., Mager, G.M., Ward, R.M., Mayer, J. & Svaren, J. (2006) NAB2 represses transcription by interacting with the CHD4 subunit of the nucleosome remodeling and deacetylase (NuRD) complex. *J Biol Chem* **281**, 15129-15137.

Stendel, C., Roos, A., Deconinck, T., Pereira, J., Castagner, F., Niemann, A., Kirschner, J., Korinthenberg, R., Ketelsen, U.P., Battaloglu, E., Parman, Y., Nicholson, G., Ouvrier, R., Seeger, J., De Jonghe, P., Weis, J., Kruttgen, A., Rudnik-Schoneborn, S., Bergmann, C., Suter, U., Zerres, K., Timmerman, V., Relvas, J.B. & Senderek, J. (2007) Peripheral nerve demyelination caused by a mutant Rho GTPase guanine nucleotide exchange factor, frabin/FGD4. *Am J Hum Genet* **81**, 158-164.

Stevens, B. & Fields, R.D. (2000) Response of Schwann cells to action potentials in development. *Science* **287**, 2267-2271.

Stevens, B., Ishibashi, T., Chen, J.F. & Fields, R.D. (2004) Adenosine: an activity-dependent axonal signal regulating MAP kinase and proliferation in developing Schwann cells. *Neuron Glia Biol* **1**, 23-34.

Stevens, B., Tanner, S. & Fields, R.D. (1998) Control of myelination by specific patterns of neural impulses. *J Neurosci* **18**, 9303-9311.

Stewart, H.J. (1995) Expression of c-Jun, Jun B, Jun D and cAMP response element binding protein by Schwann cells and their precursors in vivo and in vitro. *Eur J Neurosci* 7, 1366-1375.

Stewart, H.J., Bradke, F., Tabernero, A., Morrell, D., Jessen, K.R. & Mirsky, R. (1996) Regulation of rat Schwann cell Po expression and DNA synthesis by insulin-like growth factors in vitro. *Eur J Neurosci* **8**, 553-564.

Stewart, H.J., Brennan, A., Rahman, M., Zoidl, G., Mitchell, P.J., Jessen, K.R. & Mirsky, R. (2001) Developmental regulation and overexpression of the transcription factor AP-2, a potential regulator of the timing of Schwann cell generation. *Eur J Neurosci* **14**, 363-372.

Stewart, H.J., Eccleston, P.A., Jessen, K.R. & Mirsky, R. (1991) Interaction between cAMP elevation, identified growth factors, and serum components in regulating Schwann cell growth. *J Neurosci Res* **30**, 346-352.

Stewart, H.J., Morgan, L., Jessen, K.R. & Mirsky, R. (1993) Changes in DNA synthesis rate in the Schwann cell lineage in vivo are correlated with the precursor--Schwann cell transition and myelination. *Eur J Neurosci* **5**, 1136-1144.

Stewart, H.J., Turner, D., Jessen, K.R. & Mirsky, R. (1997) Expression and regulation of alpha1beta1 integrin in Schwann cells. *J Neurobiol* **33**, 914-928.

Stirling, C.A. (1975) Abnormalities in Schwann cell sheaths in spinal nerve roots of dystrophic mice. *J Anat* **119**, 169-180.

Stoll, G., Griffin, J.W., Li, C.Y. & Trapp, B.D. (1989b) Wallerian degeneration in the peripheral nervous system: participation of both Schwann cells and macrophages in myelin degradation. *J Neurocytol* **18**, 671-683.

Stoll, G., Jander, S. & Myers, R.R. (2002) Degeneration and regeneration of the peripheral nervous system: from Augustus Waller's observations to neuroinflammation. *J Peripher Nerv Syst* **7**, 13-27.

Stoll, G., Trapp, B.D. & Griffin, J.W. (1989a) Macrophage function during Wallerian degeneration of rat optic nerve: clearance of degenerating myelin and Ia expression. *J Neurosci* **9**, 2327-2335.

Stork, P.J. & Schmitt, J.M. (2002) Crosstalk between cAMP and MAP kinase signaling in the regulation of cell proliferation. *Trends Cell Biol* **12**, 258-266.

Stratakis, C.A., Kirschner, L.S. & Carney, J.A. (2001) Clinical and molecular features of the Carney complex: diagnostic criteria and recommendations for patient evaluation. *J Clin Endocrinol Metab* **86**, 4041-4046.

Subang, M.C. & Richardson, P.M. (2001) Influence of injury and cytokines on synthesis of monocyte chemoattractant protein-1 mRNA in peripheral nervous tissue. *Eur J Neurosci* **13**, 521-528.

Sugiura, S., Lahav, R., Han, J., Kou, S.Y., Banner, L.R., de Pablo, F. & Patterson, P.H. (2000) Leukaemia inhibitory factor is required for normal inflammatory responses to injury in the peripheral and central nervous systems in vivo and is chemotactic for macrophages in vitro. *Eur J Neurosci* **12**, 457-466.

Suter, U. & Scherer, S.S. (2003) Disease mechanisms in inherited neuropathies. *Nat Rev Neurosci* **4**, 714-726.

Svaren, J., Sevetson, B.R., Apel, E.D., Zimonjic, D.B., Popescu, N.C. & Milbrandt, J. (1996) NAB2, a corepressor of NGFI-A (Egr-1) and Krox20, is induced by proliferative and differentiative stimuli. *Mol Cell Biol* **16**, 3545-3553.

Swett, J.E., Torigoe, Y., Elie, V.R., Bourassa, C.M. & Miller, P.G. (1991) Sensory neurons of the rat sciatic nerve. *Exp Neurol* **114**, 82-103.

Swett, J.E., Wikholm, R.P., Blanks, R.H., Swett, A.L. & Conley, L.C. (1986) Motoneurons of the rat sciatic nerve. *Exp Neurol* **93**, 227-252.

Syroid, D.E., Maycox, P.J., Soilu-Hanninen, M., Petratos, S., Bucci, T., Burrola, P., Murray, S., Cheema, S., Lee, K.F., Lemke, G. & Kilpatrick, T.J. (2000) Induction of postnatal schwann cell death by the low-affinity neurotrophin receptor in vitro and after axotomy. *J Neurosci* **20**, 5741-5747.

Syroid, D.E., Maycox, P.R., Burrola, P.G., Liu, N., Wen, D., Lee, K.F., Lemke, G. & Kilpatrick, T.J. (1996) Cell death in the Schwann cell lineage and its regulation by neuregulin. *Proc Natl Acad Sci U S A* **93**, 9229-9234.

Szigeti, K., Wiszniewski, W., Saifi, G.M., Sherman, D.L., Sule, N., Adesina, A.M., Mancias, P., Papasozomenos, S., Miller, G., Keppen, L., Daentl, D., Brophy, P.J. & Lupski, J.R. (2007) Functional, histopathologic and natural history study of neuropathy associated with EGR2 mutations. *Neurogenetics* **8**, 257-262.

Tabernero, A., Stewart, H.J., Jessen, K.R. & Mirsky, R. (1998) The neuron-glia signal beta neuregulin induces sustained CREB phosphorylation on Ser-133 in cultured rat Schwann cells. *Mol Cell Neurosci* **10**, 309-322.

Tandrup, T., Woolf, C.J. & Coggeshall, R.E. (2000) Delayed loss of small dorsal root ganglion cells after transection of the rat sciatic nerve. *J Comp Neurol* **422**, 172-180.

Tapinos, N., Ohnishi, M. & Rambukkana, A. (2006) ErbB2 receptor tyrosine kinase signaling mediates early demyelination induced by leprosy bacilli. *Nat Med* **12**, 961-966.

Tasken, K. & Aandahl, E.M. (2004) Localized effects of cAMP mediated by distinct routes of protein kinase A. *Physiol Rev* **84**, 137-167.

Taskinen, H.S. & Roytta, M. (2000) Increased expression of chemokines (MCP-1, MIP-1alpha, RANTES) after peripheral nerve transection. *J Peripher Nerv Syst* **5**, 75-81.

Taveggia, C., Zanazzi, G., Petrylak, A., Yano, H., Rosenbluth, J., Einheber, S., Xu, X., Esper, R.M., Loeb, J.A., Shrager, P., Chao, M.V., Falls, D.L., Role, L. & Salzer, J.L. (2005) Neuregulin-1 type III determines the ensheathment fate of axons. *Neuron* **47**, 681-694.

Thomas, G.A. (1948) Quantitative histology of Wallerian degeneration: II. Nuclear population in two nerves of different fibre spectrum. *J Anat* **82**, 135-145.

Thompson, S.W., Vernallis, A.B., Heath, J.K. & Priestley, J.V. (1997) Leukaemia inhibitory factor is retrogradely transported by a distinct population of adult rat sensory neurons: co-localization with trkA and other neurochemical markers. *Eur J Neurosci* **9**, 1244-1251.

Tikoo, R., Zanazzi, G., Shiffman, D., Salzer, J. & Chao, M.V. (2000) Cell Cycle Control of Schwann Cell Proliferation: Role of Cyclin-Dependent Kinase-2. *J. Neurosci.* **20**, 4627-4634.

Timmerman, V., De Jonghe, P., Ceuterick, C., De Vriendt, E., Lofgren, A., Nelis, E., Warner, L.E., Lupski, J.R., Martin, J.J. & Van Broeckhoven, C. (1999) Novel missense mutation in the early growth response 2 gene associated with Dejerine-Sottas syndrome phenotype. *Neurology* **52**, 1827-.

Tobler, A.R., Notterpek, L., Naef, R., Taylor, V., Suter, U. & Shooter, E.M. (1999) Transport of Trembler-J mutant peripheral myelin protein 22 is blocked in the intermediate compartment and affects the transport of the wild-type protein by direct interaction. *J Neurosci* **19**, 2027-2036.

Toews, A.D., Barrett, C. & Morell, P. (1998) Monocyte chemoattractant protein 1 is responsible for macrophage recruitment following injury to sciatic nerve. *J Neurosci Res* **53**, 260-267.

Tofaris, G.K., Patterson, P.H., Jessen, K.R. & Mirsky, R. (2002) Denervated Schwann cells attract macrophages by secretion of leukemia inhibitory factor (LIF) and monocyte chemoattractant protein-1 in a process regulated by interleukin-6 and LIF. *J Neurosci* **22**, 6696-6703.

Tolwani, R.J., Cosgaya, J.M., Varma, S., Jacob, R., Kuo, L.E. & Shooter, E.M. (2004) BDNF overexpression produces a long-term increase in myelin formation in the peripheral nervous system. *J Neurosci Res* 77, 662-669.

Tomaselli, K.J., Reichardt, L.F. & Bixby, J.L. (1986) Distinct molecular interactions mediate neuronal process outgrowth on non-neuronal cell surfaces and extracellular matrices. *J Cell Biol* **103**, 2659-2672.

Tona, A., Perides, G., Rahemtulla, F. & Dahl, D. (1993) Extracellular matrix in regenerating rat sciatic nerve: a comparative study on the localization of laminin, hyaluronic acid, and chondroitin sulfate proteoglycans, including versican. *J Histochem Cytochem* **41**, 593-599.

Topilko, P., Levi, G., Merlo, G., Mantero, S., Desmarquet, C., Mancardi, G. & Charnay, P. (1997) Differential regulation of the zinc finger genes Krox-20 and Krox-24 (Egr-1) suggests antagonistic roles in Schwann cells. *J Neurosci Res* **50**, 702-712.

Topilko, P., Schneider-Maunoury, S., Levi, G., Baron-Van Evercooren, A., Chennoufi, A.B.Y., Seitanidou, T., Babinet, C. & Charnay, P. (1994) Krox-20 controls myelination in the peripheral nervous system. *Nature* **371**, 796.

Trachtenberg, J.T. & Thompson, W.J. (1996) Schwann cell apoptosis at developing neuromuscular junctions is regulated by glial growth factor. *Nature* **379**, 174-177.

Traka, M., Dupree, J.L., Popko, B. & Karagogeos, D. (2002) The neuronal adhesion protein TAG-1 is expressed by Schwann cells and oligodendrocytes and is localized to the juxtaparanodal region of myelinated fibers. *J Neurosci* **22**, 3016-3024.

Traka, M., Goutebroze, L., Denisenko, N., Bessa, M., Nifli, A., Havaki, S., Iwakura, Y., Fukamauchi, F., Watanabe, K., Soliven, B., Girault, J.A. & Karagogeos, D. (2003) Association of TAG-1 with Caspr2 is essential for the molecular organization of juxtaparanodal regions of myelinated fibers. *J Cell Biol* **162**, 1161-1172.

Trapp, B.D., Hauer, P. & Lemke, G. (1988) Axonal regulation of myelin protein mRNA levels in actively myelinating Schwann cells. *J Neurosci* **8**, 3515-3521.

Triolo, D., Dina, G., Lorenzetti, I., Malaguti, M., Morana, P., Del Carro, U., Comi, G., Messing, A., Quattrini, A. & Previtali, S.C. (2006) Loss of glial fibrillary acidic protein (GFAP) impairs Schwann cell proliferation and delays nerve regeneration after damage. *J Cell Sci* **119**, 3981-3993.

Trupp, M., Ryden, M., Jornvall, H., Funakoshi, H., Timmusk, T., Arenas, E. & Ibanez, C.F. (1995) Peripheral expression and biological activities of GDNF, a new neurotrophic factor for avian and mammalian peripheral neurons. *J Cell Biol* **130**, 137-148.

Tsujino, H., Mansur, K., Kiryu-Seo, S., Namikawa, K., Kitahara, T., Tanabe, K., Ochi, T. & Kiyama, H. (1999) Discordant expression of c-Ret and glial cell line-derived neurotrophic factor receptor alpha-1 mRNAs in response to motor nerve injury in neonate rats. *Brain Res Mol Brain Res* **70**, 298-303.

Vandenberghe, N., Upadhyaya, M., Gatignol, A., Boutrand, L., Boucherat, M., Chazot, G., Vandenberghe, A., Latour, P. (2002) Frequency of mutations in the early growth response 2 gene associated with peripheral demyelinating neuropathies. *J Med Genet* **39**: e81.

Vargas, M.E. & Barres, B.A. (2007) Why is Wallerian degeneration in the CNS so slow? *Annu Rev Neurosci* **30**, 153-179.

Verheijen, M.H., Chrast, R., Burrola, P. & Lemke, G. (2003) Local regulation of fat metabolism in peripheral nerves. *Genes Dev* **17**, 2450-2464.

Vesque, C. & Charnay, P. (1992) Mapping functional regions of the segment-specific transcription factor Krox-20. *Nucleic Acids Res* **20**, 2485-2492.

Wagner, R. & Myers, R.R. (1996) Endoneurial injection of TNF-alpha produces neuropathic pain behaviors. *Neuroreport* 7, 2897-2901.

Waller, A. (1850) Experiments on the section of the glossopharyngeal and hypoglossal nerves of the frog, and observations on the alterations produced thereby in the structure of their primitive fibres. *Phil Trans R Soc Lond* **140,** 423-429.

Wallquist, W., Patarroyo, M., Thams, S., Carlstedt, T., Stark, B., Cullheim, S. & Hammarberg, H. (2002) Laminin chains in rat and human peripheral nerve: distribution and regulation during development and after axonal injury. *J Comp Neurol* **454**, 284-293.

Wallquist, W., Plantman, S., Thams, S., Thyboll, J., Kortesmaa, J., Lannergren, J., Domogatskaya, A., Ogren, S.O., Risling, M., Hammarberg, H., Tryggvason, K. & Cullheim, S. (2005) Impeded interaction between Schwann cells and axons in the absence of laminin alpha4. *J Neurosci* **25**, 3692-3700.

Wang, G.Y., Hirai, K., Shimada, H., Taji, S. & Zhong, S.Z. (1992) Behavior of axons, Schwann cells and perineurial cells in nerve regeneration within transplanted nerve grafts: effects of anti-laminin and anti-fibronectin antisera. *Brain Res* **583**, 216-226.

Wang, J., Zhai, Q., Chen, Y., Lin, E., Gu, W., McBurney, M.W. & He, Z. (2005) A local mechanism mediates NAD-dependent protection of axon degeneration. *J Cell Biol* **170**, 349-355.

Wang, J.M., Walter, S. & Mantovani, A. (1990) Re-evaluation of the chemotactic activity of tumour necrosis factor for monocytes. *Immunology* **71**, 364-367.

Wang, W.S., Piao, Z.X., Han, M.H., Wang, Q.W. & Piao, Y.J. (2004) [Autophagic effect of Schwann cells in the regeneration of rat sciatic nerves]. *Di Yi Jun Yi Da Xue Xue Bao* **24**, 85-87.

Wanner, I.B., Guerra, N.K., Mahoney, J., Kumar, A., Wood, P.M., Mirsky, R. & Jessen, K.R. (2006b) Role of N-cadherin in Schwann cell precursors of growing nerves. *Glia* **54**, 439-459.

Wanner, I.B., Mahoney, J., Jessen, K.R., Wood, P.M., Bates, M. & Bunge, M.B. (2006a) Invariant mantling of growth cones by Schwann cell precursors characterize growing peripheral nerve fronts. *Glia* **54**, 424-438.

Warburton, E.C., Glover, C.P., Massey, P.V., Wan, H., Johnson, B., Bienemann, A., Deuschle, U., Kew, J.N., Aggleton, J.P., Bashir, Z.I., Uney, J. & Brown, M.W. (2005) cAMP responsive element-binding protein phosphorylation is necessary for perirhinal long-term potentiation and recognition memory. *J Neurosci* **25**, 6296-6303.

Warner, L.E., Mancias, P., Butler, I.J., McDonald, C.M., Keppen, L., Koob, K.G. & Lupski, J.R. (1998) Mutations in the early growth response 2 (EGR2) gene are associated with hereditary myelinopathies. *Nat Genet* **18**, 382.

Warner, L.E., Svaren, J., Milbrandt, J. & Lupski, J.R. (1999) Functional consequences of mutations in the early growth response 2 gene (EGR2) correlate with severity of human myelinopathies. *Hum Mol Genet* **8**, 1245-1251.

Watanabe, T., Hongo, I., Kidokoro, Y. & Okamoto, H. (2005) Functional role of a novel ternary complex comprising SRF and CREB in expression of Krox-20 in early embryos of Xenopus laevis. *Dev Biol* **277**, 508-521.

Watson, J.D. & Crick, F.H. (1953) Molecular structure of nucleic acids; a structure for deoxyribose nucleic acid. *Nature* **171**, 737-738.

Webster, H. & Favilla, J.T. (1984) Development of peripheral nerves. In Dyck, P.J. (ed) *Peripheral neuropathy*. W.B. Saunders Co, pp. 329-359.

Webster, H.D. (1971) The geometry of peripheral myelin sheaths during their formation and growth in rat sciatic nerves. *J Cell Biol* **48**, 348-367.

Webster, H.D., Martin, R. & O'Connell, M.F. (1973) The relationships between interphase Schwann cells and axons before myelination: a quantitative electron microscopic study. *Dev Biol* **32**, 401-416.

Weinberg, H.J. & Spencer, P.S. (1978) The fate of Schwann cells isolated from axonal contact. *J Neurocytol* 7, 555-569.

Werner, A., Willem, M., Jones, L.L., Kreutzberg, G.W., Mayer, U. & Raivich, G. (2000) Impaired axonal regeneration in alpha7 integrin-deficient mice. *J Neurosci* **20**, 1822-1830.

White, F.V., Toews, A.D., Goodrum, J.F., Novicki, D.L., Bouldin, T.W. & Morell, P. (1989) Lipid metabolism during early stages of Wallerian degeneration in the rat sciatic nerve. *J Neurochem* **52**, 1085-1092.

Wigglesworth, V.B. (1957) The use of osmium in the fixation and staining of tissues. *Proc R Soc Lond B Biol Sci* **147**, 185-199.

Willem, M., Garratt, A.N., Novak, B., Citron, M., Kaufmann, S., Rittger, A., DeStrooper, B., Saftig, P., Birchmeier, C. & Haass, C. (2006) Control of peripheral nerve myelination by the beta-secretase BACE1. *Science* **314**, 664-666.

Williams, P.L. & Hall, S.M. (1971) Prolonged in vivo observations of normal peripheral nerve fibres and their acute reactions to crush and deliberate trauma. *J Anat* **108**, 397-408.

Woldeyesus, M.T., Britsch, S., Riethmacher, D., Xu, L., Sonnenberg-Riethmacher, E., Abou-Rebyeh, F., Harvey, R., Caroni, P. & Birchmeier, C. (1999) Peripheral nervous system defects in erbB2 mutants following genetic rescue of heart development. *Genes Dev* **13**, 2538-2548.

Wolpowitz, D., Mason, T.B., Dietrich, P., Mendelsohn, M., Talmage, D.A. & Role, L.W. (2000) Cysteine-rich domain isoforms of the neuregulin-1 gene are required for maintenance of peripheral synapses. *Neuron* **25**, 79-91.

Woodhoo, A., Dean, C.H., Droggiti, A., Mirsky, R. & Jessen, K.R. (2004) The trunk neural crest and its early glial derivatives: a study of survival responses, developmental schedules and autocrine mechanisms. *Mol Cell Neurosci* **25**, 30-41.

Wrabetz, L., D'Antonio, M., Pennuto, M., Dati, G., Tinelli, E., Fratta, P., Previtali, S., Imperiale, D., Zielasek, J., Toyka, K., Avila, R.L., Kirschner, D.A., Messing, A., Feltri, M.L. & Quattrini, A. (2006) Different intracellular pathomechanisms produce diverse Myelin Protein Zero neuropathies in transgenic mice. *J Neurosci* **26**, 2358-2368.

Wrabetz, L., Feltri, M.L., Hanemann, C.O. and Muller, H.W. (2001) The molecular genetics of hereditary demyelinating neuropathies. In Jessen, K.R. & Richardson, W.D. (eds) *Glial cell development: basic principles and clinical relevance*, pp. 331-354

Yamada, H., Komiyama, A. & Suzuki, K. (1995) Schwann cell responses to forskolin and cyclic AMP analogues: comparative study of mouse and rat Schwann cells. *Brain Res* **681**, 97-104.

Yang, D., Bierman, J., Tarumi, Y.S., Zhong, Y.P., Rangwala, R., Proctor, T.M., Miyagoe-Suzuki, Y., Takeda, S., Miner, J.H., Sherman, L.S., Gold, B.G. & Patton, B.L. (2005) Coordinate control of axon defasciculation and myelination by laminin-2 and -8. *J Cell Biol* **168**, 655-666.

Yang, D.P., Zhang, D.P., Mak, K.S., Bonder, D.E., Pomeroy, S.L. & Kim, H.A. (2008) Schwann cell proliferation during Wallerian degeneration is not necessary for regeneration and remyelination of the peripheral nerves: axon-dependent removal of newly generated Schwann cells by apoptosis. *Mol Cell Neurosci* **38**, 80-88.

Yang, X., Kuo, Y., Devay, P., Yu, C. & Role, L. (1998) A cysteine-rich isoform of neuregulin controls the level of expression of neuronal nicotinic receptor channels during synaptogenesis. *Neuron* **20**, 255-270.

Yin, Q., Kemp, G.J., Yu, L.G., Wagstaff, S.C. & Frostick, S.P. (2001) Neurotrophin-4 delivered by fibrin glue promotes peripheral nerve regeneration. *Muscle Nerve* **24**, 345-351.

Yin, X., Crawford, T.O., Griffin, J.W., Tu, P., Lee, V.M., Li, C., Roder, J. & Trapp, B.D. (1998) Myelin-associated glycoprotein is a myelin signal that modulates the caliber of myelinated axons. *J Neurosci* **18**, 1953-1962.

Yin, X., Kidd, G.J., Nave, K.A. & Trapp, B.D. (2008) P0 protein is required for and can induce formation of schmidt-lantermann incisures in myelin internodes. *J Neurosci* **28**, 7068-7073.

Yoon, C., Korade, Z. & Carter, B.D. (2008) Protein kinase A-induced phosphorylation of the p65 subunit of nuclear factor-kappaB promotes Schwann cell differentiation into a myelinating phenotype. *J Neurosci* **28**, 3738-3746.

Yoshihara, T., Kanda, F., Yamamoto, M., Ishihara, H., Misu, K.-i., Hattori, N., Chihara, K. & Sobue, G. (2001) A novel missense mutation in the early growth response 2 gene associated with late-onset Charcot-Marie-Tooth disease type 1. *Journal of the Neurological Sciences* **184**, 149.

Yoshino, J.E., Dinneen, M.P., Lewis, B.L., Meador-Woodruff, J.H. & Devries, G.H. (1984) Differential proliferative responses of cultured Schwann cells to axolemma- and myelin-enriched fractions. I. Biochemical studies. *J Cell Biol* **99**, 2309-2313.

Young, J.Z. (1945) The history of the shape of a nerve. In *Essays on Growth and Form*, presented to D'Arcy W. Thompson. (ed. W.E. Le Gros Clark and P.B. Medawar), pp. 41-93. Oxford: Clarendon.

Yu, W.M., Feltri, M.L., Wrabetz, L., Strickland, S. & Chen, Z.L. (2005) Schwann cell-specific ablation of laminin gamma1 causes apoptosis and prevents proliferation. *J Neurosci* **25**, 4463-4472.

Yum, S.W., Kleopa, K.A., Shumas, S. & Scherer, S.S. (2002) Diverse trafficking abnormalities of connexin32 mutants causing CMTX. *Neurobiol Dis* **11**, 43-52.

Zanazzi, G., Einheber, S., Westreich, R., Hannocks, M.J., Bedell-Hogan, D., Marchionni, M.A. & Salzer, J.L. (2001) Glial growth factor/neuregulin inhibits Schwann cell myelination and induces demyelination. *J Cell Biol* **152**, 1289-1299.

Zhai, Q., Wang, J., Kim, A., Liu, Q., Watts, R., Hoopfer, E., Mitchison, T., Luo, L. & He, Z. (2003) Involvement of the ubiquitin-proteasome system in the early stages of wallerian degeneration. *Neuron* **39**, 217-225.

Zhang, J.Y., Luo, X.G., Xian, C.J., Liu, Z.H. & Zhou, X.F. (2000b) Endogenous BDNF is required for myelination and regeneration of injured sciatic nerve in rodents. *Eur J Neurosci* **12**, 4171-4180.

Zhang, Y., Roslan, R., Lang, D., Schachner, M., Lieberman, A.R. & Anderson, P.N. (2000a) Expression of CHL1 and L1 by neurons and glia following sciatic nerve and dorsal root injury. *Mol Cell Neurosci* **16**, 71-86.

Zhao, Y.L., Takagawa, K., Oya, T., Yang, H.F., Gao, Z.Y., Kawaguchi, M., Ishii, Y., Sasaoka, T., Owada, K., Furuta, I. & Sasahara, M. (2003) Active Src expression is induced after rat peripheral nerve injury. *Glia* **42**, 184-193.

Zhong, J., Dietzel, I.D., Wahle, P., Kopf, M. & Heumann, R. (1999) Sensory impairments and delayed regeneration of sensory axons in interleukin-6-deficient mice. *J Neurosci* **19**, 4305-4313.

Zoidl, G., Blass-Kampmann, S., D'Urso, D., Schmalenbach, C. & Muller, H.W. (1995) Retroviral-mediated gene transfer of the peripheral myelin protein PMP22 in Schwann cells: modulation of cell growth. *Embo J* **14**, 1122-1128.

Zorick, T.S., Syroid, D.E., Brown, A., Gridley, T. & Lemke, G. (1999) Krox-20 controls SCIP expression, cell cycle exit and susceptibility to apoptosis in developing myelinating Schwann cells. *Development* **126**, 1397-1406.

Zuo, J., Hernandez, Y.J. & Muir, D. (1998) Chondroitin sulfate proteoglycan with neurite-inhibiting activity is up-regulated following peripheral nerve injury. *J Neurobiol* **34**, 41-54.

Zuo, J., Neubauer, D., Graham, J., Krekoski, C.A., Ferguson, T.A. & Muir, D. (2002) Regeneration of axons after nerve transection repair is enhanced by degradation of chondroitin sulfate proteoglycan. *Exp Neurol* **176**, 221-228.

APPENDIX I

5X Laemmli Buffer

0.16M Tris pH 6.8

10% SDS

50% glycerol

25% β-Mercaptoethanol

Bromophenol blue

In UPH_20

10X Running Buffer

0.25M Trizma base

1.92M Glycine

1% SDS

In UPH_20

1X Transfer Buffer

48mM Trizma base

40mM Glycine

10% SDS

In UPH_20

10X TBS

0.5M Tris HCl pH 7.4

1.5M NaCl

In UPH_20

APPENDIX II

Primers and PCR conditions for genotyping-

c-jun floxed allele

LoxPCR5: 5'-CTC ATA CCA GTT CGC ACA GGC GGC-3'

LoxPCR6: 5'-CCG CTA GCA CTC ACG TTG GTA GGC-3'

PCR reaction conditions: 1 initial cycle of 2 minutes at 94°C followed by 37 cycles of 40 seconds at 94°C, 40 seconds at 57°C and 1 minute and 30 seconds at 72°C, before a final extension period of 7 minutes at 72°C.

In case of *c-jun*$^{f/f}$ mice, a single band of 350bp resulted from the amplification reaction. In case of *c-jun*$^{f/+}$ mice, two bands of 350bp (floxed) and 300bp (wt) were amplified.

c-jun deleted allele

Flox1: 5'-CTC ATA CCA GTT CGC ACA GGC G-3'

Flox2: 5'-CAG GGC GTT GTG TCA CTG AGC T-3'

PCR reaction conditions: 1 initial cycle of 3 minutes at 94°C followed by 35 cycles of 40 seconds at 94°C, 40 seconds at 57°C and 1 minute at 72°C, before a final extension period of 10 minutes at 72°C.

In the presence of cre recombinase, deletion of *c-jun* was identified by the amplification of a single band of 500bp.

IL-2

IL-2F: 5'-CTA GGC CAC AGA ATT GAA AGA TCT-3'

IL-2R: 5'-GTA GGT GGA AAT TCT AGC ATC ATC C-3'

PCR reaction conditions: 1 initial cycle of 3 minutes at 94°C followed by 35 cycles of 40 seconds at 94°C, 40 seconds at 57°C and 1 minute at 72°C, before a final extension period of 10 minutes at 72°C.

A single band of 300bp was produced by this amplification

P_0 Cre

P_0CreF: 5'-GCT GGC CCA AAT GTT GCT GG-3'

P_0CreR: 5'-CCA CCA CCT CTC CAT TGC AC-3'

PCR reaction conditions: 1 initial cycle of 4 minutes at 94°C followed by 30 cycles of 30 seconds at 94°C, 1 minute at 50°C and 1 minute at 72°C, before a final extension period of 10 minutes at 72°C.

In the presence of cre recombinase a band of 480kb was amplified

Krox-20/LacZ

K20 430C: 5'-ACA TGA CTG GAG AGA AGA GAC CCC T-3'

K20 1233NC: 5'-GCG TTT TGC TGG GCC TGT TAG GGT A-3'

LacZ 1591NC: 5'-TTG GTG TAG ATG GGC GCA TCG TAA C-3'

PCR reaction conditions: 1 initial cycle of 3 minutes at 94°C followed by 40 cycles of 30 seconds at 94°C, 30 seconds at 59°C and 30 seconds at 72°C, before a final extension period of 3 minutes at 72°C.

In case of *Krox-20*$^{+/+}$ mice, a single band of 600bp resulted from the amplification reaction. In case of *Krox-20*$^{+/-}$ mice, two bands of 600bp (wild-type) and 500bp (deleted) were amplified. In case of *Krox-20*$^{-/-}$ mice, one band of 500bp (deleted) was amplified.

APPENDIX III

Buffer B1:

0.1M Tris-HCl

0.15M NaCl

in UPH_20

Buffer B2:

Buffer B1 + 1%heat inactivated goat serum

Buffer B3:

0.1M Tris (pH 9.5)

0.1M NaCl and 50mM $MgCl_2$

in UPH_20

Buffer B4:

Buffer B3 containinig:

3.5mg/ml NBT (Roche Diagnostics, Germany)

3.5mg/ml BCIP (Roche Diagnostics, Germany)

0.24 mg/ml levamisole (Sigma, UK)

Hybridisation Buffer:

1X SALTS

50% formamide (Sigma, UK)

0.1mg/ml yeast total RNA (Invitrogen, UK)

10% w/v dextran sulphate (Fluka chemicals Ltd, Switzerland)

1X Denhart's (Sigma, UK)

in autoclaved UP H_20.

10X SALTS

2M NaCl

50mM EDTA

100mM Tris-Cl (pH 7.5)

50mM $NaH_2PO_4.2H_2O$

50mM Na_2HPO_4

in autoclaved UP H_2O